

TURKISH JOURNAL OF AGRICULTURAL ENGINEERING RESEARCH



VOLUME:5 ISSUE:2 YEAR:2024

TURKAGER

2024



e-ISSN:2717 - 8420

<https://dergipark.org.tr/tr/pub/turkager>



**TURKISH JOURNAL
OF AGRICULTURAL
ENGINEERING
RESEARCH**



TURKAGER

e-ISSN: 2717 - 8420

<https://dergipark.org.tr/tr/pub/turkager>

Turkish Journal of Agricultural Engineering Research
(*Turk J Agr Eng Res, TURKAGER*)

**Volume 5,
Issue 2,
Year 2024**

Indexing / Abstracting

MIAR

EBSCO



CAS Source Index



TURKISH JOURNAL OF AGRICULTURAL ENGINEERING RESEARCH



TURKAGER

e-ISSN: 2717 - 8420

<https://dergipark.org.tr/tr/pub/turkager>

Turkish Journal of Agricultural Engineering Research

(Turk J Agr Eng Res, TURKAGER)

PUBLISHER

Prof. Dr. Ebubekir ALTUNTAŞ

Tokat Gaziosmanpaşa University, TÜRKİYE

ABOUT

Turkish Journal of Agricultural Engineering Research (Turk J Agr Eng Res, TURKAGER) is an international open-access online, and peer double-blind reviewed journal. TURKAGER publishes the original English and Turkish research articles and a very limited number of review articles. There are no page charges for manuscript publishing in this journal. TURKAGER has an open access system and online journal published twice a year in June and December.

Turk J Agr Eng Res (TURKAGER) is a peer double-blind reviewed journal and an interdisciplinary journal concerned with all parts of Agricultural Engineering (Horticulture, Plant Protection, Biosystems Engineering, Field Crops, Agricultural Economics, Soil Science and Plant Nutrition, Aquaculture, Animal Science), Food Science and Technology, Biology, and Environment.

Turkish Journal of Agricultural Engineering Research is indexed/abstracted in Information Matrix for the Analysis of Journals (MIAR), EBSCO, CABI, FSTA (Food Science & Technology Abstracts), CAS Source Index (CASSI).

Turkish Journal of Agricultural Engineering Research is licensed (CC-BY-NC-4.0) under a Creative Commons Attribution 4.0 International License.



TURKISH JOURNAL OF AGRICULTURAL ENGINEERING RESEARCH



TURKAGER

e-ISSN: 2717 - 8420

<https://dergipark.org.tr/tr/pub/turkager>

Turkish Journal of Agricultural Engineering Research (*Turk J Agr Eng Res, TURKAGER*)

EDITORIAL BOARD TEAM

EDITOR-in-CHIEF

Prof. Dr. Ebubekir ALTUNTAŞ / Tokat Gaziosmanpaşa University, TÜRKİYE

ASSISTANT EDITORS

Prof. Dr. Sedat KARAMAN / Tokat Gaziosmanpaşa University, TÜRKİYE
Asst. Prof. Dr. Bahadır ŞİN / Sakarya University of Applied Sciences, TÜRKİYE

TECHNICAL EDITOR

Asst. Prof. Dr. Bahadır ŞİN / Sakarya University of Applied Sciences, TÜRKİYE

LANGUAGE EDITORS

Assoc. Prof. Dr. Gülay KARAHAN / Çankırı Karatekin University, TÜRKİYE
Dr. Manoj Kumar MAHAWAR / ICAR-Central Institute, Res. Cotton Tech., INDIA
Dr. Seyit YAYLA / Universum University, REPUBLIC OF KOSOVO

STATISTICS EDITOR

Asst. Prof. Dr. Lütfi BAYYURT, Tokat Gaziosmanpaşa University, TÜRKİYE
Assoc. Prof. Dr. Yalçın TAHTALI / Tokat Gaziosmanpaşa University, TÜRKİYE

SECRETARIAT

Dr. Burcu AKSÜT Tokat Gaziosmanpaşa University TÜRKİYE
Post Graduate Hamide ERSOY, Tokat Gaziosmanpaşa University, TÜRKİYE
Dr. Esra Nur GÜL, Tokat Gaziosmanpaşa University, TÜRKİYE
Res. Assist. Dr. Ayşe Nida KAYAALP, Muş Alparslan University, TÜRKİYE
Doctoral Emine POLAT, Tokat Gaziosmanpaşa University, TÜRKİYE

(*): The list is based on the surname of the editors in alphabetical order



TURKISH JOURNAL OF AGRICULTURAL ENGINEERING RESEARCH



TURKAGER

e-ISSN: 2717 - 8420

<https://dergipark.org.tr/tr/pub/turkager>

Turkish Journal of Agricultural Engineering Research (*Turk J Agr Eng Res, TURKAGER*)

SECTION EDITORS (*)

- Prof. Dr. Zümrüt AÇIKGÖZ, *Animal Science, Ege University, TÜRKİYE*
Prof. Dr. Bilge Hilal ÇADIRCI EFELİ, *Biology, Tokat Gaziosmanpaşa University, TÜRKİYE*
Assoc. Prof. Dr. Hasan Gökhan DOĞAN, *Agricultural Economics, Kırşehir Ahi Evran University, TÜRKİYE*
Assoc. Prof. Dr. Gülay KARAHAN, *Land Scape and Architecture, Çankırı Karatekin University, TÜRKİYE*
Asst. Prof. Dr. Ayşe ÖLMEZ, *Fisheries Engineering, Tokat Gaziosmanpaşa University, TÜRKİYE*
Asst. Prof. Dr. Mahir ÖZKURT, *Field Crops, Muş Alparslan University, TÜRKİYE*
Prof. Dr. Ahmet ÖZTÜRK, *Horticulture, Ondokuz Mayıs University, TÜRKİYE*
Prof. Dr. Bahadır SAYINCI, *Biosystems Engineering, Bilecik Şeyh Edebali University, TÜRKİYE*
Prof. Dr. Serkan SELİ, *Food Engineering, Cukurova University, TÜRKİYE*
Prof. Dr. Osman SÖNMEZ, *Soil Science and Nutrition, Erciyes University, TÜRKİYE*
Assoc. Prof. Dr. Şerife TOPKAYA, *Plant Protection, Tokat Gaziosmanpaşa University, TÜRKİYE*

ADVISORY BOARD (*)

- Prof. Dr. Şenol AKIN, *Yozgat Bozok University, TÜRKİYE*
Prof. Dr. Omar Ali AL-KHASHMAN, *Al-Hussein Bin Talal University, Ma'an-JORDAN*
Assoc. Prof. Dr. Tewodros AYALEW, *Hawassa University, ETHIOPIA*
Dr. İlkey BARITÇI, *Dicle University, TÜRKİYE*
Assoc. Prof. Dr. Abdullah BEYAZ, *Ankara University, TÜRKİYE*
Assoc. Prof. Dr. Hatem BENTAHHER, *Electromechanical Systems, Sfax University, TUNISIA*
Assoc. Prof. Dr. Özer ÇALIŞ, *Akdeniz University, TÜRKİYE*
Prof. Dr. Ahmet ÇELİK, *Atatürk University, TÜRKİYE*
Prof. Dr. Ashhan DEMİRDÖVEN, *Tokat Gaziosmanpaşa University, TÜRKİYE*
Prof. Dr. Alper DURAK, *Malatya Turgut Ozal University, TÜRKİYE*
Assoc. Prof. Dr. Ramadan ELGAMAL, *Agricultural Engineering, Suez Canal University, EGYPT*
Prof. Dr. Ali İSLAM, *Ordu University, TÜRKİYE*
Prof. Dr. Tomislav JEMRIC, *University of Zagreb, CROATIA*
Assoc. Prof. Dr. Zdzisław KALINIEWICZ, *Uniwersytet Warmińsko-Mazurski, ul. Olsztyn, POLAND*
Dr. Manal H.G. KANAAN, *Middle Technical University, Baghdad, IRAQ*
Assoc. Prof. Dr. Alltane J KRYEZIU, *University of Prishtina, Pristina, REPUBLIC OF KOSOVO*
Assoc. Prof. Dr. Seyed Mehdi NASIRI, *Shiraz University, Shiraz, IRAN*
Assoc. Prof. Dr. Gheorghe Cristian POPESCU, *Pitesti University, ROMANIA*
Dr. Monica POPESCU, *University of Pitesti, ROMANIA*
Prof. Dr. Y. Aris PURWANTO, *IPB University, INDONESIA*
Prof. Dr. Hidayet OĞUZ, *Necmettin Erbakan University, TÜRKİYE*
Prof. Dr. Esen ORUÇ, *Tokat Gaziosmanpaşa University, TÜRKİYE*
Prof. Dr. Mehmet Ali SAKİN, *Tokat Gaziosmanpaşa University, TÜRKİYE*
Prof. Dr. Gordana SEBEK, *University of Montenegro, Podgorica, MONTENEGRO*
Prof. Dr. Feizollah SHAHBAZI, *Lorestan University, Khoram Abad, IRAN*
Prof. Dr. Metin SEZER, *Karamanoğlu Mehmetbey University, TÜRKİYE*
Asst. Prof. Dr. Alaa SUBR, *University of Baghdad, IRAQ*
Specialist Hilary UGURU, *Delta State Polytechnic, Ozoro, Delta State, NIGERIA*

(*): The list is based on the surname of the editors in alphabetical order.



TURKISH JOURNAL OF AGRICULTURAL ENGINEERING RESEARCH



TURKAGER

e-ISSN: 2717 - 8420

<https://dergipark.org.tr/tr/pub/turkager>

Turkish Journal of Agricultural Engineering Research (*Turk J Agr Eng Res, TURKAGER*)

Volume 5, Issue 2, December 31, 2024

No	Articles	Author/s	Pages
Research Article			
1	<u>Development and Performance Evaluation of a Coffee Cherry Size Grading Machine</u>	Tolasa BERHANU , Adesoji OLANIYAN, Habatamu ALEMAYEHU	131-152
2	<u>Performance Evaluation of Two Row Animal Drawn Maize Planter with Fertilizer Applicator</u>	Meseret ABEBE*	153-166
3	<u>Muharrrik Radyal Lastik Çapının Çeki Performansına Etkisi/ Effect on Traction Performance of Driven Radial Tire Diameters</u>	Necmettin Oğuz DEMİR, Kazım ÇARMAN, Ergün ÇITIL*	167-179
4	<u>Duvusal Uvarım Açısından Bitkisel Peyzaj Uygulamalarının İncelenmesi, Malatya Örneği/ Investigation of Planting Landscape Applications in Terms of Sensory Stimulation, Malatya Example</u>	Gamze Öner, SİMA POUYA*	180-198
5	<u>Performance Evaluation of Electric Motor Driven Turmeric Slicing Machine</u>	Amanuel Erchafo ERTEBO*	199-218
6	<u>Investigating the Biomethane Production Potential of Blends of Bovine Manure with Switchgrass (<i>Panicum virgatum</i> L.) and Sugar Beet (<i>Beta vulgaris</i> L.) Foliage</u>	Cevat FİLİKÇİ* , Tamer MARAKOĞLU	219-231
7	<u>Exploring the Potential of Producing Biomass Energy from Agricultural Residues in Chad</u>	Mohamedeltayib Omer Salih EISSA*	232-243
8	<u>Konya İli Ereğli İlçesinde Kırıkhan Yerel Popülasyonu Siyah Havucun Hassas Ekiminde Sıra Üzeri Bitki Dağılım Düzgünlüğü ile Bazı Kalite Kriterlerinin Belirlenmesi/ Determination of Plant Uniformity on rows in Distribution and Certain Quality Criteria in Precision Sowing of Black Carrot in the Kırıkhan Local Population of Konya Province Ereğli District</u>	Haydar HACISEFEROĞULLARI* , Nurhan USLU	244-261
9	<u>Effects of Using Seed Tube on Seed Distribution Uniformity in Single Seed Planters</u>	Mehdi GÜVEN, Nisanur YAKUT, Emrah KUŞ*	262-270
10	<u>Modeling of Thresher Capacity and Fuel Consumption Equations Using Dimensional Analysis for Threshing Operation</u>	Tasfaye Aseffa ABEYE*	271-283
11	<u>Development of a Greenhouse Steam-powered, Self-propelled Soil Sterilization Device</u>	Ahmed Shawky EL-SAYED* , Mohamed Mansour Shalaby REFAAAY, Nermin HUSSEIN, Shereen SAAD,	284-302
12	<u>Air injection in Subsurface Drip Irrigation as an Efficient Method for Zucchini Production</u>	Khaled REFAIE, Wael SULTAN, Mohamed GHONIMY* , Ahmed ALZOHEIRY	303-318



Turkish Journal of
Agricultural
Engineering Research
(Turk J Agr Eng Res)
e-ISSN: 2717-8420



Development and Performance Evaluation of a Coffee Cherry Size Grading Machine

Tolasa BERHANU^{a*} , Adesoji Matthew OLANIYAN^b ,
Habtamu ALEMAYEHU^c 

^aDepartment of Post-Harvest Engineering, Jimma Agricultural Engineering Research Center, Oromia Agricultural Research Institute, Jimma, ETHIOPIA

^bDepartment of Agricultural and Bioresources Engineering, Faculty of Engineering, Federal University Oy-Ekiti, Post Code 370001, Ikole-Ekiti, Ikole-NIGERIA

^cDepartment of Mechanical Engineering, Haramaya Institute of Technology, Haramaya University, ETHIOPIA

ARTICLE INFO: Research Article

Cite this article: Tolasa BERHANU, E-mail: tolasaberhanubenti@gmail.com

Received: 27 May 2024 / Accepted: 18 September 2024 / Published: 31 December 2024

Cite this article: Berhanu, T., Olaniyan, A.M., & Alemayehu, H. (2024). Development and Performance Evaluation of a Coffee Cherry Size Grading Machine. Turkish Journal of Agricultural Engineering Research, 5(2), 131-152. <https://doi.org/10.46592/turkager.1489650>

ABSTRACT

The coffee cherry processing industry traditionally relies on the dry method, involving harvesting, drying, and dehulling. Conventional dehulling machines with fixed drum clearances struggle to handle natural size variations, leading to inefficiencies and increased cherry breakage. To address these challenges, an innovative coffee cherry-size grading machine has been developed, utilizing an inclined oscillating sieve technique powered by a diesel engine through a belt drive. Key components include a feeding hopper, reciprocating grading sieve assembly, support frame, and power transmission system. A comprehensive performance evaluation focused on grading efficiency and capacity, exploring various operational parameters: feed rates (5, 10, 15 kg min⁻¹), sieve angles (7°, 9°, 11°), and speeds (80, 140, 200 rpm). Using a split-split-plot block design for data analysis, the study yielded promising results. Maximum grading efficiency of 88.40% was achieved at 15 kg min⁻¹ feed rate, 8 rpm speed, and 7° sieve angle, with a capacity of 137.11 kg h⁻¹ and 4.96% sieve clogging rate. ANOVA revealed significant influences of operational speed and sieve inclination angle on performance parameters. These findings offer valuable insights for optimizing coffee cherry processing, potentially enhancing efficiency and quality in the industry.

Keywords: Coffee, Dehulling, Eccentric, Grading, Oscillating sieve, Machine



INTRODUCTION

The nonalcoholic stimulating beverage crop, Coffee Arabica, belongs to the Rubiaceae family and the genus *Coffea* ([Alemnew, 2020](#)). This coffee is the backbone of the Ethiopian economy, accounting for 25-30% and 10% of the total foreign currency earnings and the government revenues of the country, respectively ([Adem, 2023](#)). Approximately 200 thousand tons are shipped to the central market in 2023, with the remaining consumed locally ([Gofe Balami *et al.*, 2024](#)).

During the 2018-19 main production season coffee covered 764863.16 ha of land in Ethiopia and yielded almost 500,000 tons, with an average productivity of 0.64 tons per hectare. South Nation Nationalities and Peoples Regional State contributed 30% of the total production ([CSA, 2019](#)).

Coffee quality may be impacted by a variety of factors, including gene type, climate, soil characteristics, and agricultural practices, time of harvest, processing following harvest, grading, packaging, storage, and transporting conditions ([Adugna, 2020](#)). Among these, processing is critical in determining the quality of coffee. Wet or dry methods can be used to prepare coffee, and the intricacy and desired level of quality can vary ([Freitas *et al.*, 2024](#)). Ethiopia uses both sun-drying and wet-processing methods, accounting for 70% and 30% of the country's coffee production, respectively.

The simplest, most affordable, and oldest method is the dry method. It is primarily popular in Brazil and Africa and yields "natural" coffee ([Godwill, 2013](#)). The picked cherries are first cleared of dirt, twigs, and leaves, as well as overripe, damaged, and unripe cherries. This is done manually with a large sieve. Unnecessary berries or other materials that have not been sprayed are collected from the top of the sieve.

Grading is an agricultural processing operation that is undertaken to categorize grains into different grades based on the desired quality parameters for storage, seed preparation, and commercialization or further processing ([Yayock and Ishaya, 2020](#)). An essential value-adding method that raises the market value and processing standards is grading agricultural products according to their size ([Umani and Markson, 2020](#)). Hand grading is costly, and personnel shortages make the process difficult during peak seasons. Human operations can be laborious, inconsistent, and inefficient at times. Farmers are hopeful that appropriate agricultural product grading machinery can assist in alleviating manpower shortages, save time, and enhance the overall quality of items that have been rated ([Mostafa, 2003](#)).

This study addressed the issue at hand and improved the technology used in the processing of micro to medium-sized coffee processing, benefiting all parties involved in the industry like farmers by increasing their income by value adding to their product and by decreasing the breakage losses that occurs during hulling operation. The objective to determine the physical properties of Coffee cherries, to design, manufacture/fabricate and assemble the machine and to test and evaluate the performance of the machine (study the effect of sieve inclination angle, speed of oscillation of the sieve and feeding rate on capacity and efficiency of the machine).

MATERIALS and METHODS

Description of the Study Area

The prototype was manufactured at the Jimma Agricultural Engineering Research Centre workshop. It lies at latitude of 7°40'51.5"N and a longitude of 36°50'38.1"E, and an assessment of the machine's performance was carried out at Goma Woreda.

Determination of Coffee Cherry Properties

The key physical and mechanical properties that influence the design of the grading machine like size, shape, density, friction coefficients, and angle of repose were experimentally determined for coffee Arabica cherries. These are described below:

Geometric mean diameter

Equation (1) can be used to determine the geometric mean diameter (D_g) ([Garnayak, 2008](#)).

$$D_g = \sqrt[3]{LWT} \text{ (cm)} \quad (1)$$

Where; L: length, cm,

W: width, cm,

T: thickness, cm.

Arithmetic mean diameter

The arithmetic mean diameter (D_a) of the bean was calculated using Equation (2) ([Garnayak, 2008](#)).

$$D_a = (LWT)/3, \text{ (cm)} \quad (2)$$

Aspect ratio

The aspect ratio (R_a) of the bean can be calculated using Equation (3) ([Bizimungu *et al.*, 2022](#)).

$$R_a = \frac{W}{L}, \text{ (cm)} \quad (3)$$

Size and shape

The three perpendicular dimensions of 100 randomly selected cherries were measured using digital calipers. The length, width, and thickness gave intermediate (b), major (a), and minor (c) diameters respectively.

Sphericity was calculated using the formula:

$$\phi = \frac{\sqrt[3]{abc}}{a} \quad (4)$$

The shape index was determined as:

$$\text{Shape Index} = \frac{W}{\sqrt{LT}} \quad (5)$$

Bulk density

This indicates the mass per unit volume of the coffee cherries useful for hopper sizing. By adding a sample mass of cherries to a container with a known capacity, it became known,

$$\rho_b = \frac{Ms}{Vc} \left(\frac{kg}{m^3} \right) \quad (6)$$

Where; ρ_b : bulk density,

Ms : total mass of bean in the container, kg,

Vc : volume of the container, m³.

Angle of repose

The angle of repose of the coffee bean was measured by emptying method by using an open-ended cylinder of 15 cm diameter and 30 cm height. The cylinder was placed at the center of a circular plate having a diameter of 70 cm and filled with coffee cherries. The cylinder was raised slowly until it formed a cone on the circular plate. The angle of repose was calculated using Equation (7) ([Karababa, 2006](#)),

$$\theta = \tan^{-1} \frac{2H}{d} \quad (7)$$

Where; θ : Angle of repose, empty or filling (deg.),

H : Height of the cone (cm),

d : Diameter of the cone (cm).

Moisture content

A small sample was oven dried and the moisture percentage determined by using Equation (8),

$$MC(\%) = \frac{(w-d)}{w} * 100 \quad (8)$$

Where; MC : moisture content,

w : weight before drying,

d : weight after drying.

Overall Structure and Design of the Machine**Design consideration**

When designing the machine, it is crucial to evaluate the available alternatives based on several key criteria. The ease of assembly and handling should be a primary consideration, ensuring that the machine can be put together and managed without excessive difficulty. Additionally, the design should prioritize low maintenance requirements and minimal running costs, making it economically viable for long-term use.

Efficiency and durability are equally important factors, as they directly impact the machine's performance and lifespan. The design should also emphasize ease of

operation, allowing users to interact with the machine intuitively and effectively. Lastly, market availability and suitability for operation in rural areas must be taken into account, ensuring that the machine is accessible and practical for its intended users and environments.

Overall structure of the machine

As indicated in Figure 1, the machine consists of the following parts: (i) a feeding hopper; (ii) a grading unit; (iii) a power transmission unit; and (iv) a supporting frame.

Description and design of machine components

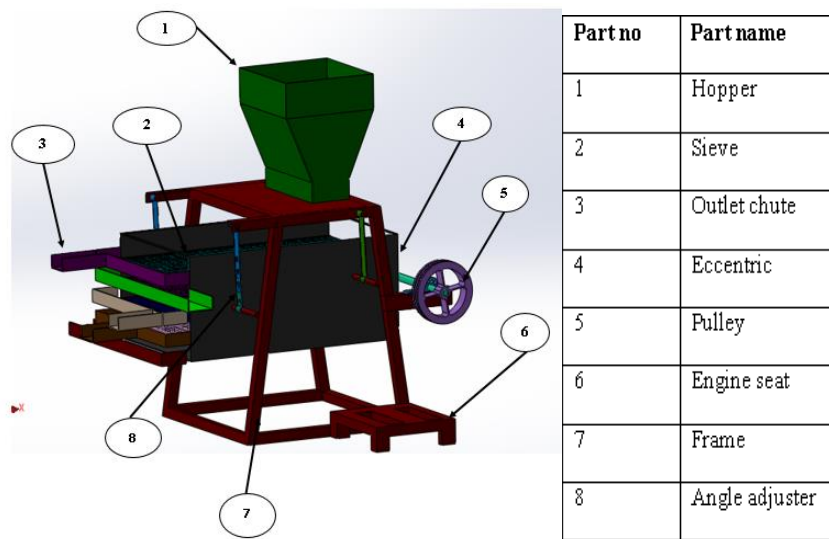


Figure 1. Pictorial view of machine.

Hopper design

This machine is designed to accommodate 20 kg of coffee cherries at a time. According to [Tafa and Olaniyan \(2023\)](#), the actual capacity was estimated in accordance with the requirement that the hopper's capacity be 1% higher than the anticipated capacity.

Then,

$$V_h = 1.1 V_E \quad (9)$$

$$V_E = \frac{W_c}{\rho_d} \quad (10)$$

$$= \frac{20 \text{ kg}}{650 \text{ kg m}^{-3}}; V_E = 0.03 \text{ m}^3$$

Then, $V_h = 1.1 \times 0.03 = 0.033 \text{ m}^3$ this volume of the hopper is needed for our machine. The form of the hopper is trapezoidal. To limit the flow of coffee to the grading equipment, a feed control mechanism was built into the bottom of the hopper. Equation (11) was used to calculate the design hopper's overall volume.

$$V = \frac{1}{2}(a + b) \times h \times L \quad (11)$$

$$V = \frac{1}{2}(0.4 + 0.3) \times 0.35 \times 0.5 ; V = 0.07 \text{ m}^3$$

Where; V_h : Actual volume of hopper

V_E : estimated volume of hopper,

V : volume of hopper, (m^3),

h : height of the hopper, (0.35 m),

a : base width (0.3 m),

b : top width (0.4 m),

L : Length of the hopper (0.55 m).

Frame design

The material used for the frame was mild steel which has a Modulus of Elasticity = 210 GPa, and yield strength, $\sigma_y = 300$ MPa. The ability of a frame structure to support a given load without a sudden change in configuration was assessed by determining its crushing stress and criticality using the equations below ([Khurmi and Gupta, 2005](#)).

$$\sigma_{cr} = \frac{\pi^2 E}{\left(\frac{L_e}{r}\right)^2} \quad (12)$$

$$r^2 = \frac{I}{A} \quad (13)$$

$$P_{cr} = \frac{\pi^2 EI}{L_e^2} \quad (14)$$

By using the standard yield strength and comparing it with a critical load on the frame, we can decide whether the frame is safe or not. Let's determine the specification of the materials utilized for the frame based on the information at hand:

Modulus of elasticity, $E = 210 \text{ GPa} = 210 \times 10^3 \text{ MPa}$,

Yield strength, $\sigma_y = 300 \text{ MPa}$

The actual length of the frame, $L = 1110 \text{ mm}$,

For the frame fixed at both ends equivalent length, L_e was calculated as,

For the frame fixed at both ends equivalent length, L_e was calculated as,

$$L_e = \frac{L}{2} \quad (15)$$

$$= \frac{1110}{2} = 555 \text{ mm}$$

The ratio of equivalent length to the radius of gyration can be determined by,

$$\frac{L_e}{r} = \pi \sqrt{\frac{E}{\sigma_y}} \quad (16)$$

$$= \pi \sqrt{\frac{210 \times 10^3 \text{ MPa}}{300 \text{ MPa}}} = 83.12$$

$$\begin{aligned} \text{The crushing stress is given by, } \sigma_{cr} &= \frac{\pi^2 E}{\left(\frac{L_e}{r}\right)^2} \\ &= \frac{\pi^2 * 210 * 10^3 \text{ MPa}}{83.12^2} = 299.99 \text{ MPa} = 300 \text{ MPa} \end{aligned} \quad (17)$$

The aforementioned outcome indicates the yield strength of the material used to create the frame is equal to the amount of crushing stress. From Equation (16), a radius of gyration can be calculated as:

$$\frac{L_e}{r} = 83.12, L_e = 625 \text{ mm } r = \frac{L_e}{83.12} = \frac{550 \text{ mm}}{83.12} = 6.62 \text{ mm and } r^2 = (6.62 \text{ mm})^2 = 43.80 \text{ mm}^2$$

Also, from the radius of gyration can be calculated the breadth or width of the mild steel pipe material used for the frame as follows:

$$\begin{aligned} r^2 &= \frac{I}{A} \\ &= \frac{bh^3}{12hb} = \frac{h^2}{12}, \text{ then } h^2 = 12 * r^2 = 12 * 43.80 \text{ mm}^2 = 525.6 \text{ mm}^2 \end{aligned} \quad (18)$$

$h = 24.04 \text{ mm}$, for standardizing let take $h = 25 \text{ mm}$.

Assuming thickness = 3mm and depth = 50mm.

The critical load can be determined as:

$$\begin{aligned} P_{cr} &= \frac{\pi^2 EI}{L_e^2} \\ &= \frac{\pi^2 * 210 \left(\frac{bh^3}{12}\right)}{L_e^2} = \frac{\pi^2 * 210 * 10^{11} \left(\frac{25^3 * 50}{12}\right)}{525^2} = 3454.36 * 10^8 \text{ kN} \end{aligned} \quad (19)$$

Hence, critical stress was computed using:

$$\begin{aligned} \sigma_{cr} &= \frac{P_{cr}}{A} \\ &= \frac{P_{cr}}{b * h} = \frac{3,454.36 * 10^8}{50 \text{ mm} * 25 \text{ mm}} = 276.34 \text{ Mpa} \end{aligned} \quad (20)$$

Where; σ_{cr} : Crushing stress (MPa), r : Radius of gyration (mm), L_e : Frame equivalent length, (mm), P_{cr} : The critical load on the frame (kN), I : Polar moment of area for a hollow square shape (mm^4), A : Cross-section area for a hollow square shape (mm^2).

Therefore, when compared to the material's critical stress with yield strength, the estimated critical stress was less than the latter ($\sigma_{cr} < \sigma_y$). According to Euler's theory of buckling, the critical buckling stress for thin columns is frequently lower than the yield stress. As a result, the designed proportions of the frame materials are safe.

Design of the grading unit

The shape of the sieve hole is selected based on the shape index of coffee cherries which is the spherical shape and circular shape was selected since the shape index of the coffee cherries is less than 1.5 and considered as spherical shape. The size of the sieve was selected based on the result of the physical properties of the coffee bean and the diameter of the holes was chosen to be 12 mm, 10 mm, and 8 mm based on the physical characteristics of coffee cherries.

Design of Power Transmission Unit

Shaft selection

For a solid shaft with little or no axial load, the diameter of the shaft was determined using Equation (21) ([Khurmi and Gupta, 2005](#)).

$$d^3 = \frac{16Te}{\pi\tau} [(KbMb)^2 + (KtMt)^2]^{1/2} \quad (21)$$

Where: d : diameter of the shaft, mm,

Mt : torsional moment, N m,

Mb : bending moment, N m,

Kb : combined shock and fatigue factor applied to bending moment,

Te : equivalent twisting moment, N m,

Kt : combined shock and fatigue factor applied to torsional moment,

τ : maximum allowable shear stress, N m⁻¹,

The vertical force acting on the shaft is shown in Figure 2 below.

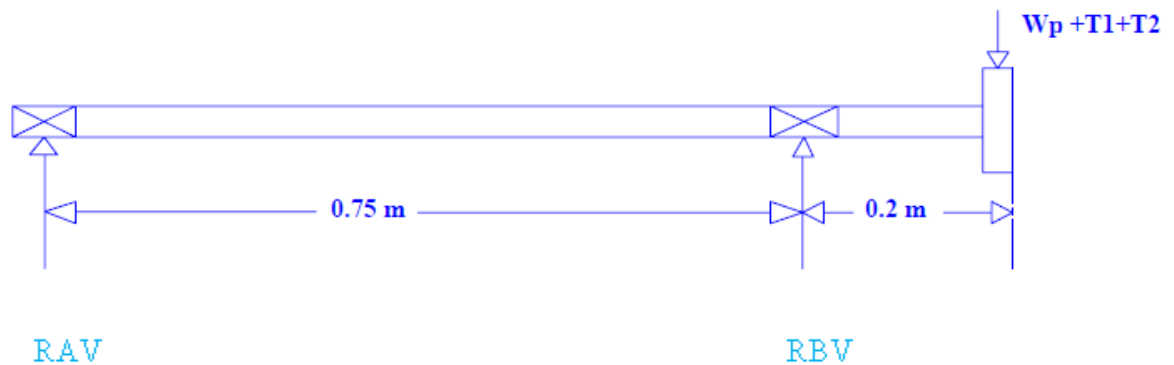


Figure 2. Free body diagram of force acting vertically on shaft.

Then we can find the moment at point A assuming that, the summation of the moment at point A is zero.

$$\sum MA = 0$$

$$RBV(0.75) - (WP + T1 + T2)(0.95) = 0$$

$$= RBV (0.75) - (316.87) (0.95) = RBV (0.75) - 301; RBV (0.75) = 301 \text{ N}$$

$$RBV = 401.37 \text{ N}$$

Then, calculating for moment at B assuming that the summation of moment at B is zero.

$$\sum MB = 0$$

$$RAV(0.75) - (WP + T1 + T2)(0.2) = 0$$

$$= RAV (0.75) - (316.87) (0.2) = RAV (0.75)-163.37; RAV (0.75) = 163.37$$

$$RAV= 84.49 \text{ N}$$

Then, we can calculate Maximum bending moment:

$$BM \text{ at AC} = RAV (0.2) = 401.37(0.2) \text{ N}; BM= 80.27 \text{ N}$$

Horizontal force acting on the shaft was showed in Figure 3 as below.

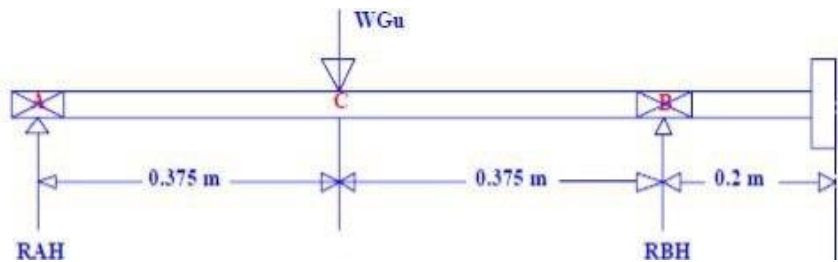


Figure 3. Force acting horizontally on shaft.

Then we can find the moment at point A assuming that, the summation of the moment at A is zero.

$$\sum MA = 0$$

$$RBH(0.75) - (WGU)(0.375) = 0$$

$$= RBH (0.75) - (566.31) (0.375) = RBH (0.75)-212.37; RBH (0.75) = 212.37$$

$$RBH= 283.16 \text{ N}$$

$$\sum MB = 0$$

$$RAH(0.75) - (WGU)(0.375) = 0$$

$$= RAH (0.75) - (566.31) (0.375) = RAH (0.75)-212.37; RAH (0.75) = 212.37$$

$$RAH= 283.16 \text{ N}$$

The maximum bending moment on the shaft was calculated:

$$BM= (283.16) (0.375) = 106.185 \text{ N m}$$

The shear force and bending moment diagram for the shaft was shown in Figure 4 below.

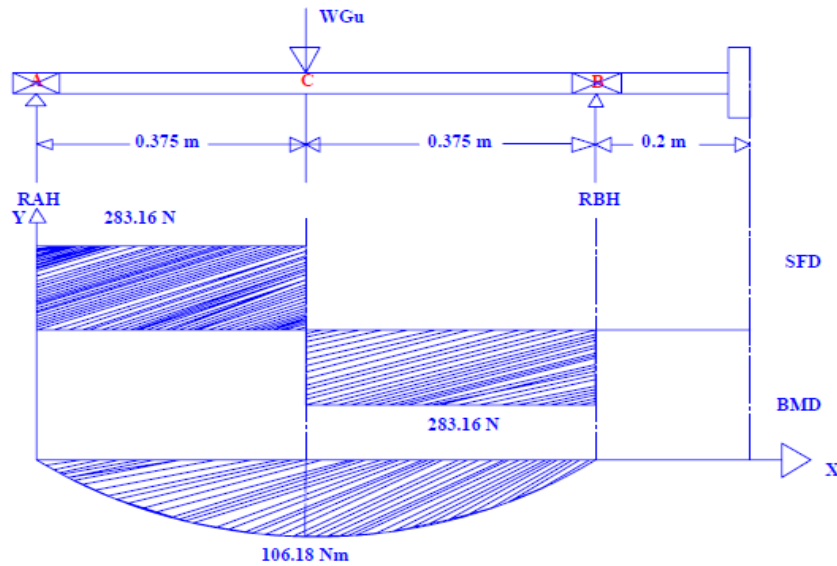


Figure 4. Shear force and bending moment of force acting horizontally on shaft.

The resultant bending moments on the shaft can be calculated using Equation 22.

$$M_b = \sqrt{(M_V)^2 + (M_H)^2} \quad (22)$$

$$= \sqrt{(80.27)^2 + (106.19)^2} = \sqrt{6443.91 + 11275.67} = \sqrt{17719} = 133.15 \text{ N}$$

Where; M_b : Resultant bending moments (N),

M_V : Maximum bending moments on a vertical (N),

M_H : Maximum bending moments on the horizontal (N).

Then we can calculate the diameter of the shaft by using Equation (20) as follow.

$$\begin{aligned} d^3 &= \frac{16}{\pi \tau} \sqrt{(K_b M_b)^2 + (K_t M_t)^2} \\ &= \frac{16}{3.14 * 45} \sqrt{(1.3 * 133.15 * 1000)^2 + (1.2 * 24.53 * 1000)^2} \\ &= 0.11 \sqrt{30828357121} = 0.11 * 175580 \quad d^3 = 19313 \end{aligned}$$

D= 26.83 mm, we can use a 30 mm diameter shaft (Figure 14).

Belt selection

In this design open type v-belt was used. According to [Khurmi and Gupta \(2005\)](#), the nominal pitch length (L) can be determined using Equation (23).

$$L = 2C + \frac{\pi}{2} (D_1 + D_2) + \frac{(D_2 - D_1)^2}{4C} \quad (23)$$

Where; D_1 : Diameter of smaller pulley (mm),

D_2 : Diameter of larger pulley (mm),

C : The center distance between the grading cylinder shaft pulley and the motor pulley (mm).

The least center distance of two pulleys, one acting as the driver and the other as the follower, can be calculated by using Equation (24) ([Khurmi and Gupta, 2005](#)).

$$C = \left(\frac{D_2 + D_1}{2} \right) + D_1 \quad (24)$$

$$= \left(\frac{0.25 + 0.07}{2} \right) + 0.07 = 0.23 \text{ m}$$

The belt length is computed by using Equation (25):

$$L = 2C + \frac{\pi}{2}(D_1 + D_2) + \frac{(D_2 + D_1)^2}{4C} \quad (25)$$

$$= 2 * 0.23 + \frac{\pi}{2}(0.07 + 0.025) + \frac{(0.07 + 0.25)^2}{4 * 0.23}$$

$$= 1.24 + 1.57 (0.32) + 0.11 = 1.24 + 0.5 + 0.11 = 1.85 \text{ m} = 72.83 \text{ inch}$$

Determination of belt tension

Equations (26) and (27) were used to calculate the belt's peripheral velocities (V_1) on the driver pulley, and (V_2) on the driven pulley ([Khurmi and Gupta, 2005](#)).

$$V_1 = \frac{\pi D_1 N_1}{60} \left(1 - \frac{S}{100} \right) \quad (26)$$

$$V_2 = \frac{\pi D_2 N_2}{60} \left(1 - \frac{S}{100} \right) \quad (27)$$

Where: V_1 : The belt's peripheral velocity on the driver pulley (m.s^{-1}), V_2 : The belt's peripheral velocity on the driven pulley (m.s^{-1}), N_1 : Speed of the driver (rpm), N_2 : Speed of the driven (rpm), S : Slip (%) (1° to 2°) ([Khurmi and Gupta 2005](#)).

$$\text{So, } V_1 = \frac{3.14 * 0.07 * 450}{60} \left(1 - \frac{0.015}{100} \right) = 1.63 \text{ m s}^{-1}$$

$$V_2 = \frac{3.14 * 0.25 * 140}{60} \left(1 - \frac{0.015}{100} \right) = 1.8 \text{ m s}^{-1}$$

The following formula was used to calculate the mass of the belt:

$$m = b * t * l * \rho = 0.22 \text{ kg}$$

Where; b : Top width of belt (0.013), M : Mass of the belt, t : Thickness of belt (0.008), l : Length of the belt, ρ : Density of the belt ($\frac{1140 \text{ kg}}{\text{m}^3}$)

The tension on the open belt's two sides was determined using the relationship below ([Khurmi and Gupta, 2005](#)).

$$\frac{T_1 - mv^2}{T_2 - mv^2} = e^{\frac{\mu \theta}{\sin \alpha}} \quad (28)$$

Where; m : Mass of the belt (kg m^{-1}), σ : Maximum allowable stress of the belt (MPa), T_1 : Belt tension on the tight side (N), T_2 : Belt tension on the slack side (N), μ : Friction coefficient between the pulley and the belt (0.43), θ : lap angle on smaller pulley (rad) and groove angle (34°).

Equation 28, can be used to determine the tension on the tight side of a power transmission belt ([Khurmi and Gupta, 2005](#)),

$$T_1 = T_{max} - T_c \quad (29)$$

Where, T_1 : Tension in the tight side (N), T_c and T_{max} : The centrifugal and maximum tension of the belt (N)

The belt's maximum tension (T_{max}), the centrifugal tension (T_c), the belt's bulk relative to its length, and the belt's cross-sectional area are determined by using Equation 30, 31, and 32 ([Khurmi and Gupta, 2005](#)) as follow.

$$T_{max} = A\sigma \quad (30)$$

$$T_c = mv^2 \quad (31)$$

$$A = \frac{(b-x)}{2}t + xt \quad (32)$$

$$\text{Then, } A = \frac{(0.013-0.011)}{2} * 0.008 + (0.011 * 0.008) = 96 \text{ mm}^2$$

$$\text{Then, } T_c = mv^2 = 0.55 \text{ N}$$

$$T_{max} = A\sigma = 96 \text{ mm}^2 * 2.5 \text{ N mm}^{-2} = 240 \text{ N}$$

As a result, the tight side of the belt's tension has been determined by

$$T_1 = T_{max} - T_c \quad (33)$$

$$= (240 - 0.55) \text{ N} = 239.45 \text{ N}$$

Where; A : Belt's cross-sectional area (mm^2), m : Mass per unit length of a belt (kg m^{-1}), σ : Maximum allowable stress of belt ($2500 \text{ N m}^{-2} = 2.5 \text{ N mm}^{-2}$), v : belt speed (mm.s^{-1}), b : Top width of the belt (mm) x : Bottom width of the belt (mm), t : belt thickness (mm) and ρ : Density of Rubber (kg m^{-3}).

The tension on the slack side of the belt,

$$\ln\left(\frac{T_1}{T_2}\right) = \mu * \theta_1 + \operatorname{cosec} \beta \quad (34)$$

$$\ln\left(\frac{239.45 \text{ N}}{T_2}\right) = 0.25 * 2.12 + \operatorname{cosec} 18$$

$$= \frac{239.45}{T_2} = e^{1.715} = \frac{239.45}{T_2} = 5.557 T_2 = 43.089 \text{ N}$$

According to [Khurmi and Gupta \(2005\)](#), torque on a shaft can be determined using Equation (35).

$$T = (T_1 + T_2) * \frac{D_4}{2} \quad (35)$$

$$= (239.45 \text{ N} + 43.09 \text{ N}) * \frac{0.25 \text{ m}}{2} = 24.54 \text{ Nm}$$

The power required to rotate the main shaft was determined by using the Equation (36).

$$P = \frac{2\pi NT}{60} \quad (36)$$

$$= \frac{2 \times 3.14 \times 80 \times 24.54 \text{ Nm}}{60} = 205.48 \text{ watts}$$

Where; P : Power required to rotate the main shaft, T : Torque (Nm), N : Rotational speed (rpm), D_d : Diameter of the driven pulley, T_1 : Tight side tension of the belt, T_2 : Tension slack side of the belt.

Pulley selection

The grading unit's main shaft speed and the prime mover-driven pulley's speed are computed using Equation (37) ([Khurmi and Gupta, 2005](#)).

$$\frac{N_1}{N_2} = \frac{D_2}{D_1} \quad (37)$$

In this design, the pulley is needed to reduce the engine speed which has the highest speed of 700 rpm, medium speed of 500 rpm, and 300 rpm lower speed. The pulleys needed to reduce from the highest engine speed 700 rpm to 200 rpm of shaft speed and the other speed was adjusted by the speed adjuster on the engine. Thus, the driven pulley's diameter was calculated using Equation (34) as follows:

$$\frac{700}{200} = \frac{D_2}{70} \quad D_2 = \frac{700 \times 70}{200} = 245 \text{ mm}$$

Where; N_1 : driven pulley speed (rpm), N_2 : Driver pulley speed (rpm), B : Width of pulley (mm), b : Width of belt (mm), t_1 : rim thickness of the driving pulley (mm) and t_2 : rim thickness of the driven pulley (mm).

Power required

The machine needed the power to rotate the eccentric shaft, run the sieve when the material was on it both horizontally and vertically, and overcome friction. This totaled the power needed for the machine. The power needed to run the sieve was computed using the formula below ([Okunola *et al.*, 2015](#)).

Power required to operate the sieve horizontally;

$$P_1 = \frac{W_s + N + 2 \times X \times \mu}{4500} = \frac{66.7 \text{ kg} + 200 \text{ rpm} + 2 \times 0.09 \text{ m} \times 0.1}{4500} = 0.05 \text{ Hp} = 39.52 \text{ watt}$$

Power required operating the sieve vertically;

$$P_2 = \frac{W_s + N + 2 \times Y}{4500} = \frac{66.7 \text{ kg} + 200 \text{ rpm} + 2 \times 0.02}{4500} = 0.1 \text{ hp} = 74.57 \text{ watt}$$

From Equation 36, we have P_3 205.48 watts. So, we can determine the total power required by using Equation (38) as follows:

$$P = P_1 + P_2 + P_3 \quad (38)$$

$$P = 39.52 + 74.57 + 205.48 = 319.57 \text{ watt}$$

The total power required was calculated as the power required and power loss due to friction (10% of total power):

$$P_T = P + P(0.1) = 319.57 + 319.57(0.1) \quad P_T = 351.53 \text{ watt}$$

Where; W_s : Weight of grading unit with material on it (66.7 kg with material on it), N : Speed (200 rpm), X : Horizontal movement of sieve (diameter of eccentric = 0.09m),

Y : Vertical movement of sieve (maximum angle of sieve 11°), μ : Coefficient of friction of bearing (0.1)

Working Principles of the Machine

The coffee cherries are loaded into the hopper while the main power source is switched on and the machine is operating. The feed regulating is adjusted to the proper position and the engine to the proper speed for optimum performance. Coffee cherries flow under gravity to the grading sieve and fall on the reciprocating screen through the hopper. The horizontal reciprocating motion of the screen causes the materials on it to move towards the front end and the beans that are below the diameter of the hole pass through the hole of the screen to the second level screen which then repeats the first step until the last level sieve and graded was collected through the grain outlet for each sieve level.



Figure 5. Pictorial view of the developed grading machine.

Performance Evaluation

Experimental design

The experimental design was a split-split plot with three replications. Treatments consisted were combinations of three levels of oscillating speed (80 rpm, 140 rpm, and 200 rpm), three levels of feed rate (5 kg min^{-1} , 10 kg min^{-1} , and 15 kg min^{-1} and three levels of inclination of the sieves (7° , 9° , 11°) ([Yayock and Ishaya, 2020](#)). The experiment design was laid as 33 with 3 replications having an entire test run of 81.

Variables and Data Collection

Independent variables

During the evaluation, three independent variables were employed. These were feeding rates (5 , 10 , and 15 kg min^{-1}), the grading unit oscillating speed (80 , 140 , and 200 rpm), and sieve inclination angle (7° , 9° and 11°).

Dependent variables and collected data

Grading efficiency (GE, %)

Grading capacity (kg h^{-1})

Fuel consumption (l kWh^{-1})

Performance indicators

Data were collected through the experiment that was undertaken during testing and, then performance evaluation of the machine was made. The assessment of the performance of the machine followed the method of [Chungcharoen *et al.* \(2019\)](#).

Size grading efficiency (E_w)

$$E_w = \frac{\sum P_g W_i G_i}{Q P_i} \quad (39)$$

Where; P_g : fraction of coffee cherries size I to overall coffee cherries dropped on receipt plate

W_i : fraction of coffee cherries size I at the start of sizing to total coffee cherry at the beginning of sizing

G_i : flow rate of coffee cherry size I (kg h^{-1})

P_i : fraction of size i to total coffee cherries at the beginning of sizing

WC : weight of coffee cherry with a clogging sieve in all sieves (kg)

Wt : total weight of cherry

Capacity of the machine

$$C = \frac{\text{Total output}}{\text{Time taken}} \quad (40)$$

Fuel consumption

Fuel consumption was assessed by refilling the fuel tank after each test run and determining the amount required to refill, recording the time of a test run.

Data Analysis Method

An analysis of variance was performed on the experiment's data using a protocol that was suitable for its design, i.e. oscillating speed as main plot, angle of sieve as subplot, and feed rate as sub-sub plot. The treatment means were different at a 5% level of significance and were separated using LSD. R-statistics 4.1.0 version software was used to analyze the data.

RESULTS AND DISCUSSION

This chapter reports and discusses the findings of the tests done as part of the research study, including the results of the physical and mechanical features. Important physical and mechanical characteristics of coffee cherries were identified in order to build the various components of the grading machine.

Physical and Mechanical Properties of Coffee Cherries

The linear dimensions, geometric mean diameter, arithmetic mean diameter, shape index, surface area, moisture content, bulk density, and unit mass of coffee cherries, as well as their mechanical characteristics, including static friction coefficient and

angle of repose, were determined. Based on their applicability to the design and performance evaluation of the coffee bean grading machine, some of the examined physical and mechanical parameters were taken into consideration.

Major diameter, minor diameter, intermediate diameter, shape index, and sphericity.

In order to determine the size of the hole of the sieve and the physical properties of coffee cherries, major diameter, minor diameter, intermediate diameter, shape index, and sphericity were calculated and considered in the design on the coffee bean grading machine. The result of the determination of coffee physical properties revealed that the coffee cherries have major diameter, minor diameter, intermediate diameter, shape index, and sphericity of 13.44 mm, 8.7 mm, 10.26 mm, 0.9, and 0.77, respectively. Those parameters were used in the design of the size and shape of the sieve of the grading machine. The mean value of the shape index of coffee cherries was 0.98, and this showed that the coffee cherries are spherical in shape. In this regard, the shape of the sieve was selected as spherical.

The measurements of coffee cherry dimensions (major diameter: 13.44 mm, minor diameter: 8.7 mm, intermediate diameter: 10.26 mm) provide a comprehensive understanding of the fruit's size variability. This information is vital for designing sieves that can effectively separate cherries based on size, ensuring proper grading and sorting.

The shape index of 0.9 and sphericity of 0.77 indicate that coffee cherries are not perfectly spherical but close to it. This near-spherical nature is further confirmed by the mean shape index of 0.98. This finding has significant implications for the sieve design, as it justifies the selection of shape for the sieve holes. A circular sieve design aligns well with the natural form of the coffee cherries, potentially improving the efficiency and accuracy of the grading process.

Bulk density and moisture content

When designing the hopper, storage, and grading equipment, bulk density is crucial. The bulk density of the coffee cherries and the moisture of the coffee to be graded were taken into consideration when building the hopper for the grading equipment. Accordingly, the cherries had a bulk density of 650 kg m^{-3} and a moisture content of 12.69%, respectively.

Angle of repose, surface area, arithmetic mean, geometric mean, and aspect ratio of coffee cherries. Thus, these parameters are more important for setting up the coffee grading machine sieve size. The coffee cherry has a mean average of 349.05 m^2 of surface area and 77.38 mm and 10.42 mm of Arithmetic mean and geometric mean respectively.

Coefficient of static and dynamic friction

The roughness of the frictional surface is determined by the coefficient of friction. In line with this, the value of the coefficient of static friction increases with surface roughness. In the experimental test, the coefficients of static friction of coffee cherries were found to be 0.21, 0.29, and 0.37 on surfaces made of galvanized mild steel sheet, mild steel sheet, and plywood, respectively. Similarly, the coefficients of dynamic friction in coffee cherries were found to be 0.34, 0.44, and 0.51 on surfaces made of galvanized mild steel sheet, mild steel sheet, and plywood, respectively.

General design specification of the coffee grading machine

The general specifications of the coffee grading machine describe the functional components such as the feeding hopper, grading mechanism, sieve, shaft, outlet chute, power source, and supporting frame of the machine are listed in Table 1 below.

Table 1. An overview of the coffee grading machine's design specifications.

S/N	Components	Functions	Specifications
	Frame	Serves as the platform for mounting additional	0.9 m, 1.33 m and 1.11 m Height, length, and width respectively
	Hopper	Serve as temporary storage	0.35 m, 0.4 m, 0.55 m Height, width and length respectively
	Grading Unit	To hold grading sieve	0.40 m, 0.95 m, and 0.60 m in Height, length, and width respectively
	Grading Sieve	To grade Coffee cherries into different sizes	0.95 m and 0.60 m, length, and width respectively
	Shaft	To transmit power	0.03 m diameter, 0.95m length
	Outlet chute	To collect graded cherry	0.10 m, 0.70 m, and 0.10 m in Height, length, width respectively
	Pulley	To transmit power	245 mm diameter, 12.5 cm width

Performance evaluation of the machine

The outcomes of the data analysis are summarized in Tables 2 and 3. These comprised of the combination mean values of the performance parameters.

Table 2. The combination effect of operating parameter on capacity, efficiency, sieve clogging, and fuel consumption of machine.

Feed rate (kg min ⁻¹)	Angle (°)	Speed (rpm)	Efficiency (%)	Capacity (kg h ⁻¹)	Clogging (%)	FC (l kWh ⁻¹)
5	7	80	90.40 a	147.12 f	4.86 a	0.60 j
		140	88.47ab	161.36 e	4.37 b	0.70i
		200	86.40ab	1 72.54 c	3.57 c	0.80gh
	9	80	83.21bc	149.10 f	4.18 b	0.61 j
		140	77.87d	161.77 d	3.68 c	0.71i
		200	73.64de	218.27 b	3.24 d	1.00 h
	11	80	78.29cd	191.34 c	3.69 c	0.77 j
		140	73.25de	213.65 b	3.27 d	0.93i
		200	67.66de	277.33 a	2.69 e	1.27 h
10	7	80	89.43 a	139.17 f	4.91 a	0.65 g
		140	88.01ab	157.39 e	4.42 b	0.60 f
		200	87.40ab	177.56 c	3.63 c	0.96 de
	9	80	83.11bc	142.10 f	4.09 b	0.66gh
		140	77.57d	169.77 d	3.68 c	0.64 f
		200	73.84de	228.35 b	3.25 d	1.23 de
	11	80	78.20cd	181.27 c	3.73 c	0.83 h
		140	73.15de	220.37 b	3.23 d	1.12 f
		200	67.76de	278.52 a	2.70 e	1.50 de
15	7	80	90.50 a	137.11 f	4.96 a	0.74 de
		140	88.00ab	151.37 e	4.32 b	0.90 c
		200	86.90ab	175.51 c	3.65 c	1.09 ab
	9	80	83.21bc	146.00 f	4.13 b	0.80 d
		140	78.00d	165.72 d	3.70 c	0.99 c
		200	74.01de	223.26 b	3.22 d	1.38 b
	11	80	78.22cd	181.27 c	3.70 c	0.97 e
		140	73.35de	223.26 b	3.20 d	1.34 c
		200	67.76de	279.32 a	2.66 e	1.75 a
SD			2.65	3.74	0.14	0.05
CV			5.32	2.01	2.01	0.50

Where; SD is standard deviation, CV is coefficient of variance and Mean values with the same letter in a column are not significantly different at 5% level of significance.

Table 3. The main effect of operating parameters is on the capacity, efficiency, sieve clogging, and fuel consumption of the machine.

Parameters		Capacity (kg h ⁻¹)	Efficiency (%)	Sieve clogging (%)	Fuel consumption (l kW h ⁻¹)
Feed rate (kg/min)	5	186.76 ^a	79.93 ^a	3.73 ^a	0.81 ^c
	10	196.16 ^a	79.88 ^a	3.72 ^a	0.99 ^b
	15	198.76 ^a	79.82 ^a	3.68 ^a	1.17 ^a
Sieve inclination angle (°)	7	154.66 ^c	88.42 ^a	4.31 ^a	0.79 ^a
	9	178.33 ^b	78.24 ^b	3.68 ^b	0.91 ^a
	11	227.28 ^a	71.95 ^c	3.13 ^c	1.15 ^a
Oscillating speed (rpm)	80	154.79 ^c	82.84 ^a	4.21 ^a	0.73 ^c
	140	211.11 ^b	79.56 ^b	3.74 ^b	1.09 ^b
	200	225.36 ^a	75.90 ^c	3.18 ^a	1.22 ^a
SD		1.24	0.88	0.04	0.05
CV		2.50	1.77	2.00	2.00

Where, SD is standard deviation, CV is coefficient of variance and Mean values with the same letter in a column are not significantly different at 5% level of significance.

Efficiency of machine

The effect of operation parameters on the grading efficiency of machines was presented in Tables 2 and 3. The result shows that when the oscillating speed of operation increased from 80 rpm to 140 rpm the grading efficiency decreased from 82.84% to 76.56%, whereas it decreased from 76.56% to 75.90% when the oscillating speed increased from 140 rpm to 200 rpm. The grading efficacy decreased from 88.42% to 78.24% and from 78.24% to 71.95% when the sieve inclination angles were increased from 7° to 9° and from 9° to 11°, respectively. This revealed that the greater inclination angle would cause the coffee cherries to move too quickly, and lead to the wrong category of size grading.

The grading efficiency decreased from 79.93% to 78.88% and from 78.88% to 79.82% when feed rates increased from 5 kg min⁻¹ to 10 kg min⁻¹ and from 10 kg min⁻¹ to 15 kg min⁻¹, respectively (Table 3). The analysis of variance (ANOVA) revealed that the inclination angle and oscillating speed had a significant effect ($p < 0.05$) on the grading efficiency. This agrees with the findings of [Chungcharoen et al. \(2019\)](#), who concluded that too much-inclined angle and oscillating speed would lead to excessive movement of coffee cherries, leading to the incorrect size category classification. The combination of feed rate and inclination angle, feed rate and oscillating speed, inclination angle and oscillating speed, and the interaction of inclination, feed rate, and oscillating speed had no significant effect ($p < 0.05$) on the grading efficiency.

Grading capacity of the machine

Main and combined effects of inclination angles, feed rates, and sieve cycles on the grading capacity of the machine

The main and interaction effects of oscillating speed, inclination angle, and feed rate on the grading capacity are shown in Tables 2 and 3. The result revealed that the grading capacity of the machine increased from 154.66 kg h⁻¹ to 178.33 kg h⁻¹ and from 176.33 kg h⁻¹ to 227.28 kg h⁻¹, as the sieve inclination angles increased from 7° to 9° and from 9° to 11°, respectively. Similarly, when the oscillating speed was increased from 80 rpm to 140 rpm the grading capacity increased from 154.79 kg h⁻¹ to 211.11 kg h⁻¹. In addition, it increased from 211.11 kg h⁻¹ to 225.36 kg h⁻¹, as the

oscillating speed increased from 2.33 Hz to 3.33 Hz (Table 5). This happened because the coffee cherries' retention period on the sieves reduced due to increased sieves' inclination angles and sieves' oscillations increase.

The feed rates were also used to evaluate the machine's capacity. Results show that the grading capacity increased from 186.76 kg h⁻¹ to 196.16 kg h⁻¹ and from 196.16 kg h⁻¹ to 198.76 kg h⁻¹ as feed rates increased from 5 kg min⁻¹ to 10 kg min⁻¹ and from 10 kg min⁻¹ to 15 kg min⁻¹, respectively (Table 3).

The machine's highest capacity of 277.32 kg h⁻¹ of grading was recorded at 200 rpm oscillating speed and 11° sieve inclination. While the machine's minimum grading capacity of 137.11 kg h⁻¹ was observed at a feed rate of 15 kg h⁻¹ inclination angle of 7° and at oscillating speed of 80 rpm.

The analysis of variance revealed that, the inclination angle and oscillating speed had a significant effect ($p < 0.05$) on the machine's grading capacity. This result matches with the results of [Ansar *et al.* \(2021\)](#), and [Chungcharoen *et al.* \(2019\)](#) which indicated that the grading capacity of coffee cherries machines is significantly affected by the inclination angle and oscillating speed. Feed rate, the combination of feed rate and inclination angle, feed rate and oscillating speed, inclination angle and oscillating speed and the interaction of inclination, feed rate, and oscillating speed all had no significant effect ($p < 0.05$) on the machine's grading capacity.

The results demonstrate the significant impact of oscillating speed and sieve inclination angle on the coffee grading machine's capacity. As these parameters increased, the grading capacity improved substantially, with the highest capacity of 277.32 kg h⁻¹ achieved at 200 rpm and 11° inclination. This improvement can be attributed to the reduced retention time of coffee cherries on the sieves at higher angles and oscillation speeds. While feed rate also influenced capacity, its effect was less pronounced and not statistically significant. These insights provide valuable guidance for optimizing grading machine design and operation, suggesting that focusing on these two parameters could lead to significant improvements in processing efficiency without the need for increased feed rates.

Fuel consumption

Main and combined effect operating parameters on fuel consumption of the machine. Tables 4 and 5, illustrate the main and combined effects of the inclination angle, feed rate, and speed on fuel consumption. The maximum fuel consumption was 1.75 l kWh⁻¹ at an inclination angle of 11°, feed rate of 15 kg min⁻¹, and speed of 3.33 Hz. On the other hand, the minimum fuel consumption was 0.60 l kWh⁻¹ at 7° inclination angle, feed rate of 5 kg min⁻¹, and oscillating speed of 1.33 Hz.

As shown in Table 3, fuel consumption increases with increasing feed rate and speed. Fuel consumption increased from 0.81 l kWh⁻¹ to 0.99 l kWh⁻¹ and from 0.73 l kWh⁻¹ to 1.09 kWh⁻¹ when the feed rate and oscillating speed were increased from 5 kg min⁻¹ to 10 kg min⁻¹ and from 80 rpm to 140 rpm, respectively. It also increased from 0.99 l kWh⁻¹ to 0.91 l kWh⁻¹ and from 1.09 l kWh⁻¹ to 1.22 l kWh⁻¹ when the feed rate and oscillating speed were increased from 10 kg min⁻¹ to 15 kg min⁻¹ and from 140 rpm to 200 rpm, respectively.

The analysis of variance (ANOVA) revealed that feed rate and speed had a significant effect ($p < 0.05$) on fuel consumption. However, the combination of feed rate and inclination angle, feed rate and speed, inclination angle and speed, and the

interaction of inclination, feed rate, and speed had no significant effect ($p < 0.05$) on fuel consumption.

CONCLUSION

A coffee cherry grading machine was designed and developed taking into consideration the physical and mechanical properties of Coffee Arabica. The machine was fabricated and tested at the Jimma Agricultural Engineering Research Center. From the study, the average measured values of the major diameter, minor diameter, and intermediate diameter of the coffee cherries were found to be 13.44 mm, 7.00 mm, and 10.26 mm, respectively. From the analysis, the shape of the sieve was found to be spherical; its sphericity was 0.77. To fix the size of the hopper, the moisture content and bulk density are critical, and the results of those properties were 650 kg m^{-3} and 12.69%, respectively. The static and dynamic friction coefficients were 0.37 and 0.51 on plywood, 0.29 and 0.44 on mild steel sheet metal, and 0.21 and 0.34 on galvanized metal, respectively. Also, the angle of repose was found to be 35.96. The designed machine was operated with a 3 hp gasoline engine as a power source. The sieve of the grading machine was circular based on the shape index of the coffee cherries and the machine has three sieves. The reciprocating action of the sieve was created by using the eccentric method.

The performance evaluation indicated that the machine's grading efficiency depends on the sieve's inclination angle and the sieve's oscillating speed. In this regard, the grading efficiency decreased when the inclination angle and the oscillating speed increased. The highest grading efficiency was recorded to be 82.84% at an oscillating speed of 80 rpm.

The grading capacity of the machine mainly depended on the inclination angle and oscillating speed of the sieve. The capacity of machine increased with the increase of the inclination angle and oscillating speed. The highest machine capacity of 279.32 kg h^{-1} was recorded at an 11° inclination angle of the sieve, 15 kg min^{-1} feed rate, and 20 rpm.

The lowest value of the sieve clogging recorded was 3.18 % and 3.13 % at an oscillating speed of 200 rpm and 11° inclination angle of the sieve, respectively. Sieve clogging decreased with increasing oscillating speed and inclination angle of the sieve.

In general, the following conclusions can be made:

- The machine has the highest grading capacity when it is operated at 15 kg min^{-1} feed rate, and 11° inclination angle, and a 200 rpm oscillating speed.

- The machine has the highest grading efficiency when it is operated at a 15 kg min^{-1} feed rate, 7° inclination angle, and a 80 rpm oscillating speed.

- The machine has the lowest sieve clogging when operated at a 15 kg min^{-1} feed rate, 11° inclination angle, and 200 rpm oscillating speed.

- The current grading machine has been developed and tested on a small scale. In this regard, the following recommendations are made.

- The grader should be operated at 80 rpm oscillating speed, 15 kg min^{-1} feed rate, and inclination angle of 7° to get high grading efficiency.

- The current machine should be further modified and tested at farmers' level.

- The machine needs to have wheels for easy transportation from place to place.
- The current machine uses a diesel engine better to design it for other alternative sources of energy.
- To make it more versatile, the grading machine should be redesigned with replaceable sieves to grade green coffee bean.

DECLARATION OF COMPETING INTEREST

The authors declare that they have no conflict of interest.

CREDIT AUTHORSHIP CONTRIBUTION STATEMENT

The authors declared that the following contributions are correct.

Tolasa Berhanu: Proposal writing, methodology, manufacturing prototype, writing original draft,

Adesoji Matthew Olaniyan: Advising, review, and editing,

Habtamu Alemayehu: Advising, review, and editing.

ETHICS COMMITTEE DECISION

This article does not require any Ethical Committee Decision.

REFERENCES

- Adem MW (2023). Production, productivity, quality and chemical composition of Ethiopian coffee. *Cogent Food & Agriculture*, 9. <https://doi.org/10.1080/23311932.2023.2196868>
- Adugna BG (2020). Review on coffee production and marketing in Ethiopia. *Journal of Marketing and Consumer Research*, 10(6): 208-213.
- Alemnew S (2020). Factor affecting coffee (*Coffea Arabica* L.) quality and grading methods. *Journal of Natural Sciences Research*, 10(4): 13-20. <https://doi.org/10.7176/JNSR/10-4-02>
- Ansar A, Sukmawaty S, Murad M, Muttalib SA, Putra RH and Abdurrahim (2021). Design and performance test of the coffee bean classifier. *Processes*, 9: 1462. <https://doi.org/10.3390/pr9081462>
- Chungcharoen T, Limmun W, Chanpaka W and Srisang N (2019). *Optimization of sorting efficiency of size grading machine using oscillating sieve with swing along width direction*. MATEC Web of Conferences, 3: 1-4. <https://doi.org/10.1051/mateconf/201929304003>
- Bizimungu G, Houèchénéahouansou R, Semassou, C and Dusabumuremyi JC (2022). Physical and mechanical properties of coffee cherries and beans in Africa: Review and the State of arts. *Food Science and Technology (United States)*, 10(3): 55-74. <https://doi.org/10.13189/fst.2022.100301>
- CSA (2019). Central Statistical Agency (CSA) (2018) The Federal Democratic Republic of Ethiopia central statistical agency agricultural sample survey. Report on Area and Production of Crops. Statistical Bulletin No. 586. Addis Abeba, Ethiopia.
- Freitas VV, Borges LLR, Vidigal MCTR, dos Santos MH and Stringheta PC (2024). Coffee: A comprehensive overview of origin, market, and the quality process. *Trends in Food Science and Technology*, 146. <https://doi.org/10.1016/j.tifs.2024.104411>
- Garnayak DK (2008). Moisture-dependent physical properties of jatropha seed (*Jatropha curcas* L.). *Journal of Industrial Crops and Products*, 27(1): 123-129. <https://doi.org/10.1016/j.indcrop.2007.09.001>
- Godwill E (2013). An assessment of primary processing of coffee berries by small scale coffee growers for quality and price realization in Arumeru district, Arusha Region.
- Gofe Balami K, Ketema M, Goshu A and Author C (2024). *Ethiopian Coffee Export Performance and Diversification Analysis Full Length Research Paper July*. <https://doi.org/10.20372/mwu.iessd.2024.1561>
- Karababa E (2006). Physical properties of popcorn kernels. *Journal of Food Engineering*, 72(1): 100-107. <https://doi.org/10.1016/j.jfoodeng.2004.11.028>

- Khurmi RS and Gupta JK (2005). A textbook of machine design. S.I. Units. *Eurasia Publishing House (PVT) Limited*, New Delhi. (I).
- Mostafa HMSB (2003). *Developing an appropriate system for olive grading*. Unpublished M. Sc. Thesis. Faculty of Agriculture, Moshtohor, Zagazig Univ. Benha Branch.
- Okunola AA, Igbeka JC and Arisoyin AG (2015). Development and evaluation of a cereal cleaner. *Journal of Multidisciplinary Engineering Science and Technology (JMEST)*, 2(6): 3159-3199.
- Tafa W and Olaniyan AM (2023). Design and development of an engine driven onion grading machine. *American Journal of Food Science and Technology*, 2(2): 1-13.
<https://doi.org/10.54536/ajfst.v2i2.1503>
- Umani KC and Markson IE (2020). Development and performance evaluation of a manually operated onions grading machine. *Journal of Agriculture and Food Research*, 2.
<https://doi.org/10.1016/j.jafr.2020.100070>
- Yayock ES and Ishaya J (2020). Development and performance evaluation of a grain grading machine for small and medium scale farmers. *IOSR Journal of Agriculture and Veterinary Science (IOSR-JAVS)*, 13.



Turkish Journal of
Agricultural
Engineering Research
(Turk J Agr Eng Res)
e-ISSN: 2717-8420



Performance Evaluation of a Two Row Animal Drawn Maize Planter with Fertilizer Applicator

Meseret ABEBE^{a*} 

^aEthiopian Institute of Agricultural Research, Melkassa Agricultural Research Center, Adama, ETHIOPIA,

ARTICLE INFO: Research Article

Corresponding Author: Meseret ABEBE, E-mail: mesab04@gmail.com

Received: 21 May 2024 / Accepted: 12 October 2024 / Published: 31 December 2024

Cite this article: Meseret, A. (2024). Performance Evaluation of a Two Row Animal Drawn Maize Planter with Fertilizer Applicator. Turkish Journal of Agricultural Engineering Research, 5(2), 153-166.
<https://doi.org/10.46592/turkager.1487496>

ABSTRACT

In most parts of Ethiopia, planting of maize is done by hand, and it is a tedious, time consuming and less efficient operation. A two-row animal drawn that is cost-effective for farmers, easy to repair, and user friendly was developed and evaluated. The components of the prototype are seed hoppers, fertilizer hoppers, mainframe, seed metering plates, wheels, furrow openers and closers, seed discharge tubes, and handles. The majority of the parts were made of mild steel. In order to optimize the planter's design, the physical properties of maize seeds were taken into account. The parameters used for evaluating the prototype's performance were multiple index, miss-index, precision-index, feed-quality-index, field capacity, field efficiency, planting depth, plant population count, labour cost, and economy. A factorial design was used for the experiment (4x3x3). The result indicated that the percentage of mechanical seed damage, seed sphericity, and seed germination were $1.01 \pm 0.37\%$, $71.56 \pm 7.10\%$ & 94.58 ± 0.21 , respectively. Performance results showed planter's forward speed during operation had a significant effect on the seed's multiple index, miss-index, feed-quality-index and precision-indexes (at $p < 0.05$). Average values of field capacity, field efficiency & depth of planting were 0.21 ha h^{-1} , 86% and $4.61 \pm 0.30 \text{ cm}$, respectively. The performance evaluation results showed that Ethiopian farmers who grow maize would find the prototype planter simple to use, efficient, and economical.

Keywords: Planter design, Row planter, Seed spacing, Field capacity, Field performance

INTRODUCTION

Maize, scientifically named *Zea mays* L., is among the leading crops that is grown in about 170 nations and covers 197 M ha, with significant areas in Asia, Latin America, and Sub-Saharan Africa ([FAOSTAT, 2021](#)). Maize is known for providing both people and livestock with protein and energy, and due to this, it is regarded as a strategic food and feed crop globally ([Erenstein et al., 2022](#)).



Copyright © 2024. This is an Open Access article and is licensed under a Creative Commons Attribution 4.0 International License (CC-BY-NC-4.0) (<https://creativecommons.org/licenses/by-nc/4.0/deed.en>).

Ethiopian farmers primarily cultivate maize for sustenance. Agricultural households consume about 75% of the country's total maize production. The crop currently is the lowest source of calories, supplying 21% of the country's per-person calorie needs ([IFPRI, 2010](#)). Maize is a staple food usually used for preparing beverages locally. In addition, the leaves and stalks are usually used for animal feeding and construction purposes. Maize production is also valuable because the post-harvest waste can be utilized for energy production, enhancing both agricultural and renewable energy sectors in the future ([Ertuğrul *et al.*, 2024](#)).

The level of agricultural mechanization in maize production is on the lower side. The majority of agricultural work is done either manually or with animal-drawn traditional implements ([MOARD, 2010](#); [Kelemu, 2015](#)). Because of the absence of appropriate row planters, farmers primarily use broadcasting to plant maize seeds. The conventional planting/broadcasting method takes a lot of time and scatters seeds unevenly. Maintaining an ideal plant population in the outdoors is therefore challenging.

In Ethiopia, about 60% of farmers cultivate less than 0.90 ha in very fragmented lands ([Rapsomanikis, 2015](#)). However, smallholder farming is responsible for a large proportion of Ethiopian food production. It cultivates more than 90% of the total cropland and provides more than 90% of agricultural output ([Paul and wa Githinji, 2017](#)). Crop yields in the smallholder farms are very low compared to their potential capacity and are also substantially lower (less than 50%) than the yields obtained in experimental farms and research stations ([Taffesse *et al.*, 2013](#)). The gap is especially remarkable for maize, with an average yield of 2.6 t ha⁻¹ compared with the potential yield of 7.8 t ha⁻¹ obtained in on-farm trials ([Central Statistical Agency, 2018](#)). Agricultural mechanization can provide much more efficient work if it can be acquired by farmers with financial power. In fact, the level of agricultural mechanization can be considered as an indicator of the development of the agricultural system ([Ozgunaltay Ertugrul *et al.*, 2019](#)). The smallholder farmers are mostly unable to afford and use the costly planting machines that can provide optimal plant density. These smallholder farmers were unable to afford and use the costly planting machines that established optimal plant density. However, the majority of farmers own animals that can readily be used as power sources for planting activities. Therefore, the development of an animal-powered maize planter is beneficial in terms of affordability, reliability and ease of use.

Melkassa agricultural research center developed a tillage-cum-planter for planting sorghum and maize crops. The planter is pulled by oxen and has two ground engaging wheels where one of them produces the necessary force to drive the seed and fertilizer plates through chain-sprocket drive. The planter was developed to be attached to a ripper so that it can be utilized in conservation agriculture practice. The problem of the planter is that it was mainly developed for conservation agriculture and requires additional draft for ripping the soil ([Abebe, 2017](#)). Another sweeper attached planter was manufactured and distributed by the research center. It is a pair of oxen drawn implement which is designed to place seed and fertilizer in the furrow created by the sweeper. The problem of the machine is its seed and fertilizer metering system. The seed and fertilizer metering are done by the operator himself by swinging a lever, connected to the metering unit. This creates difficulties in achieving uniform seed spacing and seeding rate within the row. Besides, guiding

the draft animals is difficult as the operator must use both of his hands simultaneously for agitating/swinging the metering unit and for exerting a force on the handle of the implement to manipulate the depth of sowing (AIRIC, 1998).

It was the above limitations of the available animal drawn planters that led to the conclusion that a better animal drawn planter should be developed for the poor farmers. The objective of this study was to design, develop and evaluate an animal-drawn maize planter so that the overall efficiency of maize production can be improved.

MATERIALS and METHODS

Study Area

The research was conducted in the Oromia region, Melkassa district, Melkassa agricultural research center, approximately 118 km southeast of the capital, Addis Ababa, Ethiopia. It is located in the great central rift valley at 8° 24' N latitude, 39° 21' E longitude, and altitude of 1466 m above sea level. The area is among the semi-arid regions and has sandy loam soil. The majority of maize crop varieties grow in the area due to its favorable agro-climate.

Prototype Planter

The prototype planter was built at Melkassa agricultural research center workshop and is drawn by draft animals. It plants two rows in a single pass. It consists of two seed hoppers, one fertilizer hopper, four vertical metering plates, two furrow openers, two furrow coverers, mainframe, and two driving wheels.

Laboratory and field tests were carried out to evaluate the prototype planter's performance. The physical properties of maize seeds were measured. Investigations on seed damage, seed rate, and seed spacing were also made. To determine its performance and capacity, the prototype was drawn on a fine-tilled farm field. The farm field was plowed and pulverized by an ard plow.

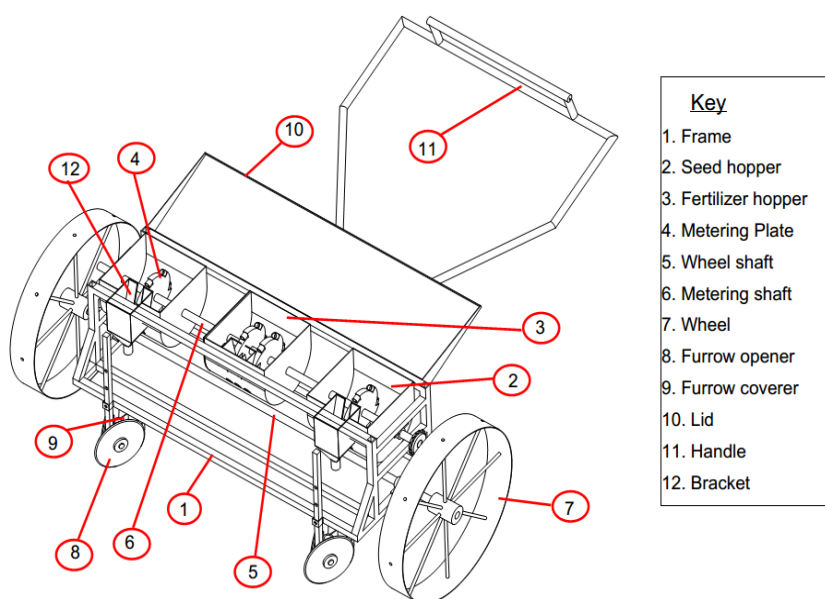


Figure 1. Major parts of the prototype

Performance Evaluation of the Prototype Maize Planter

Laboratory Evaluation

Physical Properties of Maize Seed

The physical properties of maize seeds were determined using three axial dimensions of the seed. The dimensions were length (longest intercept), width (equatorial width perpendicular to L) and thickness (breadth perpendicular to L and W). The dimensions were measured by a manual Vernier-caliper with accuracy of 0.02 mm for randomly selected 100 seeds. Mean dimensions of maize seeds, geometric mean diameter, volume and sphericity and thousand seed weight of grains were calculated using [Mohsenin \(1986\)](#).

Calibration

To calibrate the planter (Figure 1), it was elevated and jacked up to a platform, and a 2.5 kg maize seed was added in each of the two hoppers of the planter. The wheels were marked and rotated to measure the number of revolutions. During the rotation, the discharged seeds were collected in polythene bags. The wheels were then rotated 20 times at 0.5 m s⁻¹ forward speed. The rotation was selected by taking into account the donkey's pulling forward speed in a farm field.

Evaluation of Percent Seed Damage

To examine the performance of the metering rollers, after the 20th revolution, the collected seeds were put and weighed up on a sensitive balance. It was then checked for any visible external breakage. In addition, to examine internal damage, seed samples were randomly picked and tested for germination. The following formula was used to determine percent seed damage:

$$M_d = \frac{S_{nds}}{S_{ns}} \times 100 \quad (1)$$

Where; M_d : percent seed damage,

S_{nds} : number of maize seeds damaged externally,

S_{ns} : number of maize seeds.

Evenness of Seed Spacing

A sand leveled bed that has a 25 cm depth and 2 m width was prepared for the test. The planter was then pulled over the bed at donkey's working forward speed on farmland, i.e., 2.5 km h⁻¹, and furrow openers were lowered to a depth of 5 centimeters. Both the number of seeds and the distance between adjacent seeds were counted and recorded. Three replications were used.

Field Test

Evaluation of Seed Spacing

To evaluate spacing between seeds, the seed hoppers were filled to 25%, 50%, 75%, and 100% loading capacities while the machine was pulled at forward speeds of 1 km h⁻¹, 3 km h⁻¹, and 5 km h⁻¹. The field was carefully prepared using local ard plough. A carefully dug, fine sand covered, leveled, gently packed, and well-watered

soil was used to test the uniformity of seed placement. After each test run, the soil surface was re-leveled, watered, and spacing between dropped seeds was measured by a measuring tape. A guide man and a well-trained donkey were used to operate the planter. Each test runs were replicated thrice over a 10 m distance. The soil type of the test field was sandy loam.

Multiple index, miss index, mean spacing, quality of feed index, and precision in spacing of seed were calculated using measured values. To determine the pattern of dropped seeds and their distribution uniformity in the rows, mean and standard deviation values of spacing were calculated. Equations (2), (3), (4), and (5) were used to calculate seed spacing uniformity ([Kachman and Smith, 1995](#); [Önal and Ertuğrul, 2011](#); [Xiong et al., 2021](#); [Nikolay et al., 2022](#)).

$$MISI(\%) = \frac{n_{III}+n_{IV}+n_V}{N} \times 100 \quad (2)$$

Where; *MISI*: seed miss index,

n_{III}, *n_{IV}*, *n_V*: number of spacings of seed in three different divisions,

n_{III}: spacing having >1.5 Xref (theoretical spacing),

N: total number of spacings.

$$MULI(\%) = \frac{n_I}{N} \times 100 \quad (3)$$

Where; *MULI*: multiple index,

n_I: the number of spacings < 0.5 Xref,

N: total number of spacings.

$$QTFI(\%) = \frac{n_{II}}{N} \times 100 \quad (4)$$

Where; *QTFI*: the quality feed index

n_{II}: number of spacings having a value between 0.5 to 1.5Xref.

N: total number of spacings

$$PREC(\%) = \frac{S_{II}}{X_{ref}} \times 100 \quad (5)$$

Where; *PREC*: the seed precision index,

S_{II}: “n” observations standard deviation in zone II,

X_{ref}: theoretical spacing.

Field Capacity and Field Performance Determination

The field test was carried out on a fallowed rectangular plot having an area of 180 m² (Figure 2). A sandy loam soil having 14.20% moisture content (w.b.), and an ard

plow implement was used for preparing the field. The planting depth of the planter was recorded along the row at three random points spaced 6m meters apart.

According to [Kepner et al. \(1978\)](#), field capacity and efficiency were calculated using parameters such as turning time, effective operation time, and time losses on the field. To assess field efficiency and capacity, a plot having a size of 10 m width and 18 m length was prepared. Forward speed, effective field capacity, and efficiency were calculated as shown in Equation (6), (7) and (8) ([Kepner et al., 1978](#)):

$$V = \frac{D}{t_a} \quad (6)$$

Where; V : forward speed (m s^{-1}),

D : run distance (m),

t_a : the average time of each pass.

$$e = 100 \times \frac{T_e}{T_t} \quad (7)$$

Where; e : the percentage of field efficiency,

T_e : time of operation (effective),

T_t : the total time.

$$C_e = \frac{W_e \times S_{mf} \times e}{10} \quad (8)$$

Where; C_e : field capacity (effective) (ha h^{-1}),

W_e : width of the implement (effective) (m),

S_{mf} : average forward speed (km h^{-1}),

e : field efficiency (decimal).

Statistical Analysis

The experiment was conducted using a split-plot factorial design. Four levels of hopper filling and three levels of planter forward speed represented the main plot and the sub plot, respectively. The experimental design was laid as 4×3 having three replications. As a result, a total test run of 36 (i.e, $4 \times 3 \times 3 = 36$) was used. Analysis of variance (ANOVA) of different performance data was performed using Statistix-8 software. A confidence interval of 95% was utilized to indicate a level of significance. The analysis was done based on the design of experiments ([Gomez and Gomez, 1984](#); [Ertuğrul and Önal, 2006](#); [Fang et al., 2018](#)).



Figure 2. Maize planter prototype and seedling planted by the planter.

RESULTS AND DISCUSSION

Table 1 gives mean values of parameters that express physical properties of maize seed.

Table 1. Physical properties of Melkassa-13 Maize seed.

[1]	Physical properties	[2]	Number of samples	[3]	Mean	[4]	SD
[5]	Length of seed (mm)	[6]	100	[7]	10.30	[8]	1.29
[9]	Thickness of seed (mm)	[10]	100	[11]	4.50	[12]	0.63
[13]	Width of seed (mm)	[14]	100	[15]	8.55	[16]	0.47
[17]	Volume of seed (mm ³)	[18]	100	[19]	206.39	[20]	37.26
[21]	Sphericity of seed (%)	[22]	100	[23]	71.56	[24]	7.10
[25]	Seed geometric diameter (mm)	[26]	100	[27]	7.29	[28]	0.46
[29]	Thousand seed weight (gm)	[30]	1,000	[31]	271	[32]	4.11

SD = Standard deviation

From the results obtained in Table 1, it can be confirmed that the shape of the maize seed was nearly spherical ($71.56 \pm 7.10\%$). Hence, a circular shaped metering cup that accommodates the spherical seeds was developed and utilized.

Performance Evaluation

Evaluation of seed damage

Fifty Melkassa-13 Maize seed samples that passed through seed metering plates were randomly selected and examined for damage. The number of bruised, crushed, or skin removed seeds was examined, and the mean value of seed damage percentage ($1.01 \pm 0.37\%$) was less than the findings obtained by [Oduma *et al.* \(2014\)](#) and [Gupta and Herwanto \(1992\)](#) (2.34% and 3% respectively).

Germination tests conducted at the laboratory as given by [Ertuğrul *et al.* \(2024\)](#) showed that the mean germination percentage was $94.58 \pm 0.21\%$. The variety of seeds used for the test, Melkassa-13, had a mean germination rate of 95%. The quality of the metering roller, friction between seed metering devices and maize seeds, and variability of the seeds can all contribute to the difference. The difference was 0.42% and it showed that the mechanical damage was within the acceptable level.

Seed spacing analysis

Seed miss index

ANOVA showed that the planter's forward speed of operation and its interaction with the level of seed filling significantly affected the planter miss index ($p < 0.05$).

Table 2 indicated the effect of planter forward speed, seed filling level of the hopper, and their combined effect on the percentage of mean miss-index. In addition, figure 4 indicated a relationship between the forward speeds and the mean miss indexes. [Önal and Ertuğrul \(2011\)](#) found that rotational speed of metering units can affect the seed distribution performance of the metering units since the rotational speed is sequentially change with the change of forward speed.

Table 2. Analysis of variance for seed miss index (MISI%).

Source	DF	SS	MS	F	P
REP	2	0.0015	0.0008		
HOPPER	3	2.1823	0.7274	481.10	0.0000
Error REP*HOPPER	6	0.0091	0.0015		
SPEED	2	31.0600	15.5300	11480.1	0.0000
HOPPER*SPEED	6	1.4905	0.2484	183.63	0.0000
Error REP*HOPPER*SPEED	16	0.0216	0.0014		
Total	35	34.7651			

Grand Mean = 4.9475, CV (REP*HOPPER) = 0.79, CV (REP*HOPPER*SPEED) = 0.74, DF = Degree of freedom, SS = Sum of squares, MS = Mean sum of squares, F = F-statistic, P = P-value

The forward speed of operation significantly affected the percentage miss-indexes of seed ($p < 0.05$). As the forward speeds increased from 1 to 5 km h⁻¹, the percentage of seed miss indexes also increased.

Generally, the percent miss index proportionally increased with an increase of forward speed. At a forward speed of 5 km h⁻¹, a maximum miss index percentage value, 6.130, was recorded, whereas at a forward speed of 1 km h⁻¹ a lowest percentage miss index value 3.861, was recorded. The result clearly showed that higher forward speed provides a higher seed miss index value.

Table 2 indicated that the loading level of the seed hopper had a significant effect on the percentage miss index. The seed hopper-loading level and forward speed had a combined significant effect on the percentage seed miss index. Nevertheless, the effect occurred mainly because of variations in forward speeds than the hopper level of the filling. The effect, however, was more attributable to forward speed variations than to hopper fill levels.

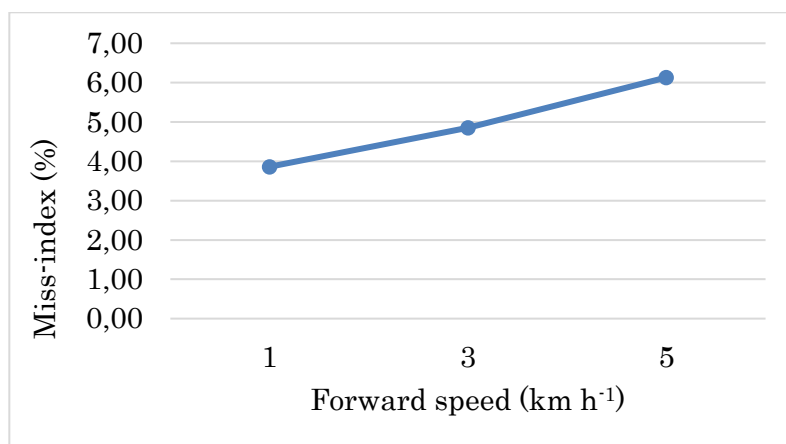


Figure 3. Effect of forward speed on miss index of seed.

Seed multiple index

ANOVA showed that (Table 3) the forward speeds of the prototype planter significantly affected percentage multiple indexes ($p < 0.05$) whereas, the seed hopper loading levels and their interaction with the planter forward speeds didn't significantly affect seed multiple indexes ($p > 0.05$). A similar trend was observed by [Nielsen \(1995\)](#) during performance evaluation of planting speed effects on stand establishment and grain yield of corn.

Table 3. Analysis of variance for seed multiple index (MULI%).

Source	DF	SS	MS	F-Value	P-Value
REP	2	0.0421	0.0211		
HOPPER	3	2.2620	0.7540	69.87	0.0000
Error REP*HOPPER	6	0.0647	0.0108		
SPEED	2	33.9400	16.9700	2793.42	0.0000
HOPPER*SPEED	6	0.2754	0.0459	7.55	0.0006
Error REP*HOPPER*SPEED	16	0.0972	0.0061		
Total	35	36.6815			

Grand Mean = 16.696, CV(REP*HOPPER) = 0.62, CV(REP*HOPPER*SPEED) = 0.4 DF = Degree of freedom, SS = Sum of squares, MS = Mean sum of squares, F = F-statistic, P = P-value

Table 3 indicated the effects of the planter's forward speed, seed filling level of the hopper, and their combined effect on the multiple index. The relationship between the forward speed and percentage of multiple index of the planter was also shown in Figure 5. As indicated from Table 3, the effect of the planter's forward speeds on multiple indexes of seed was significant, whereas the combinational effect of filling levels and planter's forward speeds on the percentage of multiple indexes was not significant.

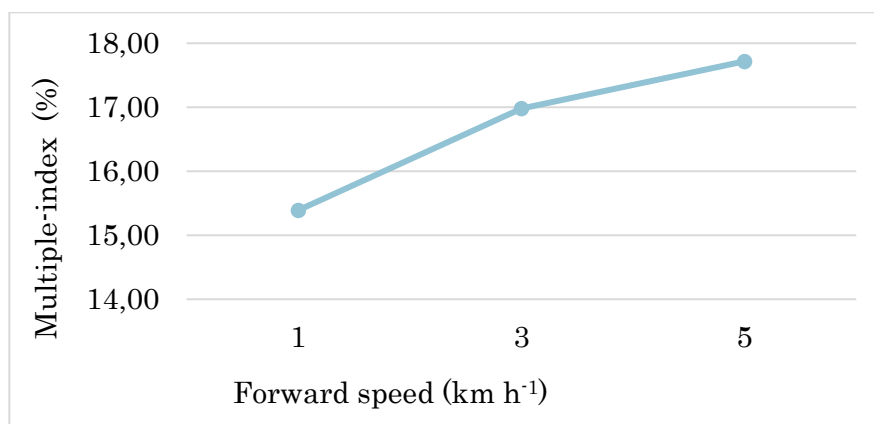


Figure 4. Effects of planter forward speed on seeds multiple index.

At 5 km h⁻¹ forward speed of the planter, the highest percentage of seed multiple index was achieved. On the other hand, 1 km h⁻¹ forward speed of the planter provided the lowest values. As shown from Table 3, the filling levels did not significantly affect the multiple indexes of the seed.

Quality of seed feed index

ANOVA results showed that the planter's forward speeds significantly affected feed-indexes quality ($p < 0.05$). On the other hand, both seed hopper filling levels and interactions between forward speeds and filling levels did not significantly affect the quality of feed index.

The effects of the planter's forward speeds and filling levels on feed-indexes are shown in Table 4. In addition, Figure 3 depicted the relationship between the linear forward speed of the planter and the percentage of feed index quality. At a forward speed of 5 km h⁻¹, forward speed significantly affected the percentage of quality of the seed feed index. However, the seed hopper filling levels did not significantly affect feed-indexes quality. This result indicated that the percentage of feed index quality is detrimentally affected by the forward speed of the prototype planter, which in turn is directly related to the forward speed of a metering plate of the planter (Culpin, 1987; Nielsen, 1995).

Table 4. Analysis of variance for quality of seed feed index (QTFI%).

Source	DF	SS	MS	F	P
REP	2	0.043	0.0214		
HOPPER	3	1.326	0.4419	25.92	0.0008
Error REP*HOPPER	6	0.102	0.0170		
SPEED	2	127.403	63.7016	6891.84	0.0000
HOPPER*SPEED	6	1.781	0.2968	32.11	0.0000
Error REP*HOPPER*SPEED	16	0.148	0.0092		
Total	35	130.803			

Grand Mean = 78.357, CV (REP*HOPPER) = 0.17, CV(REP*HOPPER*SPEED) = 0.12 DF = Degree of freedom, SS = Sum of squares, MS = Mean sum of squares, F = F-statistic, P = P-value

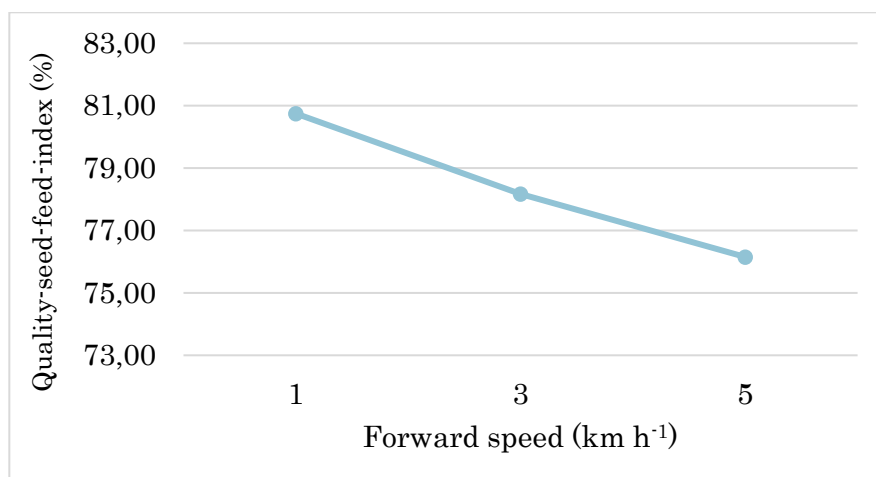


Figure 5. Effects of forward speed of planter on quality of seed feed index.

Seed precision index

ANOVA showed the forward speeds of the planter significantly affected the precision-indexes of seed. However, filling levels and their interaction with forward speeds had no significant effect on seed precision.

The effects of forward speeds and filling levels are shown in Table 5. Figure 7 shows the relationship between the linear forward speed of the planter and the precision index of seed. The analysis results showed planter's forward speeds significantly ($p < 0.05$) affected precision-indexes. However, filling levels did not significantly affect precision-indexes. At 5 km h⁻¹ forward speed, the combination of filling levels and forward speeds significantly affected the precision-indexes.

Table 5. Analysis of variance for seed precision index (PREC%).

Source	DF	SS	MS	F	P
REP	2	0.5162	0.2581		
HOPPER	3	0.5968	0.1989	3.24	0.1028
Error REP*HOPPER	6	0.3687	0.0614		
SPEED	2	27.3037	13.6518	123.43	0.0000
HOPPER*SPEED	6	0.2824	0.0471	0.43	0.8512
Error REP*HOPPER*SPEED	16	1.7697	0.1106		
Total	35	30.8375			

Grand Mean = 15.837, CV(REP*HOPPER) = 1.57, CV(REP*HOPPER*SPEED) = 2.10 DF = Degree of freedom, SS = Sum of squares, MS = Mean sum of squares, F = F-statistic, P = P-value

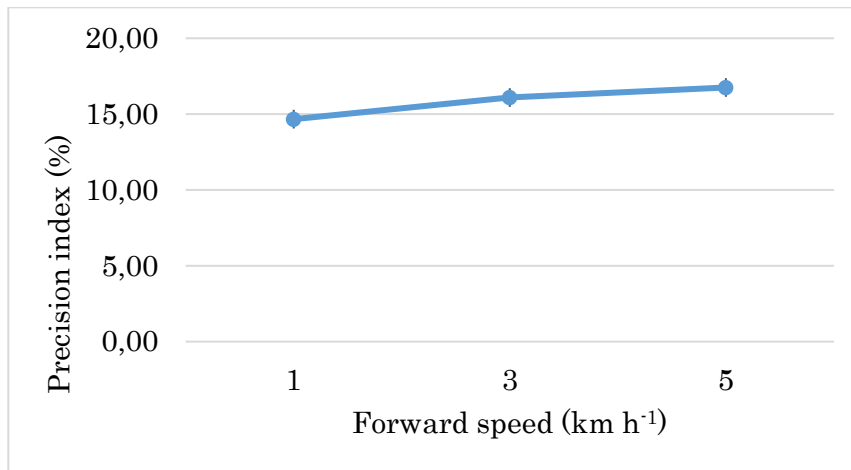


Figure 6. Effects of forward speed on precision index.

At the forward speeds of 1 km h⁻¹, 3 km h⁻¹, and 5 km h⁻¹, the seed precision index percentage values were 14.667, 16.091 and 16.754, respectively. This result obviously showed that spacing variations of over 16% would occur at planter forward speeds of higher than 3 km h⁻¹. In comparison to higher values, lower values of the precision index indicated better performance ([Kachman and Smith, 1995](#)).

Field capacity and efficiency

The machine registered an average field capacity of 0.21 ha h⁻¹, whereas its field efficiency was 86%. [Kepner et al. \(1978\)](#) recommended a field efficiency range of 65-75% for planters, indicating that the planter operates within an acceptable efficiency level.

Depth of Planting

In the field evaluation, a mean depth of seed placement, 4.60±0.30 cm, was achieved. This value is a bit lower than the recommended maize planting depth (5-7 cm). However, the small deviation is in the acceptable range and can easily be adjusted by the furrow opener.

Stand Count

The metering plates were adjusted to drop two seeds per hill to avoid seed misses. For maize, 16 plants were required in a row of 2 meters long, assuming two seeds per hill. After 15 days of planting, a stand count was made. In rows of 2 m length, the average number of maize seedlings was 17.21±1.88. The result indicated that there were few more seedlings than desired; as a result, they should be thinned.

Economic Evaluation

Planting maize with the prototype planter required two people; one person guided the donkey and the other operated the machine. On the other hand, manual planting of maize requires at least three persons for plowing, seed planting and spreading of fertilizer. The time required for planting seeds and spreading fertilizers using the manual method was 26 h ha⁻¹ ([Melesse, 2007](#)). To accomplish the same work using the machine, a single person required only about 4.77 h ha⁻¹. Hence, using the planter, one can reduce the time and labour required for planting by more than eight

folds. It was estimated that the planter will cost 8053.07 Ethiopian Birr (price in USD may be added). Therefore, maize producing small-scale farmers could jointly purchase or rent out and use the planting machine.

CONCLUSION

The evaluated two-row donkey drawn maize planter is a low-cost planter that was developed locally using easily available materials. The technology could be owned and used by small and medium scale maize producing farmers. The machine relieves maize farmers from the planting operation backache. In addition, the machine is user friendly, and requires no special technical skill for operating it. Evaluation of the planter in terms of field capacity, field efficiency, depth of planting, optimum plant population, labour cost, and economics showed acceptable results. The forward speeds of the planter significantly affected the field capacity, field efficiency, seed uniformity, planting depth and related performances of the planter. For an optimum and more precise planting, the planter should be adjusted to a 50% hopper filling level and 1 km h⁻¹ speed. Most importantly, the planter can be used by most Ethiopian smallholder farmers to plant maize seeds efficiently, effectively, and economically.

ACKNOWLEDGEMENT

The author is gratefully acknowledging the infrastructural support received from Melkassa Agricultural Research Center to conduct the research.

DECLARATION OF COMPETING INTEREST

I declare that I have no conflict of interest.

CREDIT AUTHORSHIP CONTRIBUTION STATEMENT

Meseret Abebe: Investigation, methodology, conceptualization, formal analysis, data curation, validation, writing-original draft, review, and editing visualization.

ETHICS COMMITTEE DECISION

This article does not require any Ethical Committee Decision.

REFERENCES

- Abebe F (2017). Performance of animal-drawn, ripper attached maize-cum-fertilizer planter. *Ethiopian journal of Agricultural Science*, 27(3): 9-19.
- AIRIC (1998). Progress Reports. Adama, Ethiopia
- Central Statistical Agency (2018). Report on area and production of major crops. Agricultural Sample Survey 2017/18 (2010 E.C); Central Statistical Agency: Addis Ababa, Ethiopia; Volume 1.

- Culpin C (1987). Farm machinery, 11th edition. *Oxford*, England.
- Erenstein O, Jaleta M, Sonder K, Mottaleb K and Prasanna B (2022). Global maize production, consumption and trade: trends and R&D implications. *Food Security*, 14: 1295-1319. <https://doi.org/10.1007/s12571-022-01288-7>
- Ertuğrul Ö and Önal İ (2006). Çimlendirilmiş susam tohumu ekim tekniği. *Tarım Makinaları Bilimi Dergisi*, 2(2): 125-131.
- Ertuğrul Ö, Daher B, Özgünlaltay Ertuğrul G and Mohtar R (2024). From agricultural waste to energy: Assessing the bioenergy potential of South-Central Texas. *Energies*, 17(4): 802. <https://doi.org/10.3390/en17040802>
- Fang X, Li Y, Nie J, Wang C, Huang K, Zhang Y, She H, Liu X, Ruan R, Yuan X and Yi Z (2018). Effects of nitrogen fertilizer and planting density on the leaf photosynthetic characteristics, agronomic traits and grain yield in common buckwheat (*Fagopyrum esculentum* M.). *Field Crops Research*, 219: 160-168. <https://doi.org/10.1016/j.fcr.2018.02.001>
- FAOStat (2021). Food and Agriculture Organization of the United Nations. Online database, FAO, Rome. <http://www.fao.org/faostat>
- Gomez KA and Gomez AA (1984). Statistical procedures for agricultural research. 2nd Ed. *John Willey & Sons, Inc.* New York, USA.
- Gupta CP and Herwanto T (1992). Design and development of a direct paddy seeder. *Agricultural Mechanization in Asia, Africa and Latin America*, 23(1): 23-27.
- IFPRI (2010). International Food Policy Research Institute. Maize value chain potential in Ethiopia: Constraints and opportunities for enhancing the system. Addis Ababa Ethiopia.
- Kachman SD and Smith JA (1995). Alternative measures of accuracy in plant spacing for planters using single seed metering. *Transaction of the ASAE*, 38(2): 379-387. <https://doi.org/10.13031/2013.27843>
- Kelemu F (2015). Agricultural mechanization in Ethiopian: Experience, Status and Prospects. *Ethiopia Journal of Agricultural Sciences*, 25: 45-60.
- Kepner RA, Bainer R and Barger EL (1978). Principles of farm machinery, 3rd Edition. Inc. *AVI Publishing Company*, Westport, USA.
- Melesse T (2007). *Conservation tillage implements for smallholder farmers in semi-arid Ethiopia*. Unpublished PhD Thesis, Wageningen University. Netherland. <https://doi.org/10.1016/j.still.2008.10.026>
- MOARD (2010). Ministry of Agriculture and Rural Development. Ethiopia's Agricultural Sector Policy and Investment Framework (PIF), 2010-2020, Final Report. Addis Ababa: MOARD.
- Mohsenin NN (1986). Physical properties of plant and animal materials, *Gordon and Breach Science Publishers*, New York: 734. <https://doi.org/10.4324/9781003062325>
- Nielsen RL (1995). Planting forward speed effects on stand establishment and grain yield of corn. *Journal of Production Agriculture*, 8(3): 391-393. <https://doi.org/10.2134/jpa1995.0391>
- Nikolay Z, Nikolay K, Gao X, Li QW, Mi GP and Huang YX (2022). Design and testing of novel seed miss prevention system for single seed precision metering devices. *Computers and Electronics in Agriculture*, 198: 107048. <https://doi.org/10.1016/j.compag.2022.107048>
- Oduma O, Ede JC and Igwe JE (2014). Development and performance evaluation of a manually operated Cow pea precision planter. *International Journal of Engineering and Technology*, 4(12): 693-699.
- Ozgunaltay Ertugrul G, Ertugrul O and Degirmencioglu A (2019). Determination of agricultural mechanization level of Kirsehir province using geographical information systems (GIS). *Comptes rendus de l'Académie bulgare des Sciences*, 72, No 8. <https://doi.org/10.7546/CRABS.2019.08.18>
- Önal İ and Ertuğrul Ö (2011). Seed flow and in-row seed distribution uniformity of the top delivery type fluted roller for onion, carrot and canola seeds. *Journal of Agricultural Sciences*, 17: 10-23.
- Paul M and wa Githinji M (2017). Small farms, smaller plots: Land size, fragmentation, and productivity in Ethiopia. *The Journal of Peasant Studies*, 45(4): 757-775. <https://doi.org/10.1080/03066150.2016.1278365>
- Rapsomanikis G (2015). The economic lives of smallholder farmers; An analysis based on household surveys; Food and Agriculture Organization: Rome, Italy. <https://doi.org/10.13140/RG.2.1.3223.9440>
- Taffesse AS, Dorosh P, Gemessa SA (2013). Crop production in Ethiopia: Regional patterns and trends. *Food and agriculture in Ethiopia: Progress and Policy Challenges*, 97: 53-83.
- Xiong D, Wu M, Xie W, Liu R, and Luo H (2021). Design and experimental study of the general mechanical pneumatic combined seed metering device. *Applied Sciences*, 11(16): 7223. <https://doi.org/10.3390/app11167223>



Turkish Journal of
Agricultural
Engineering Research
(Turk J Agr Eng Res)
e-ISSN: 2717-8420



Effect on Traction Performance of Driven Radial Tire Diameters

Necmettin Oğuz DEMİR^a , Kazım ÇARMAN^b ,
Ergün ÇİTİL^{b*}

^aTAGEM, Patates Araştırma Enstitüsü Müdürlüğü, Niğde, TÜRKİYE

^bSelçuk Üniversitesi Ziraat Fakültesi Tarım Makinaları ve Teknolojileri Mühendisliği Bölümü, Konya, TÜRKİYE

ARTICLE INFO: Research Article

Corresponding Author: Ergün ÇİTİL, E-mail: ecitil@selcuk.edu.tr

Received: 28 August 2024 / Accepted: 15 October 2024 / Published: 31 December 2024

Cite this article: Demir, N.O., Çarman, K., & Çıtlı, E. (2024). Effect on Traction Performance of Driven Radial Tire Diameters. Turkish Journal of Agricultural Engineering Research, 5(2), 167-179.
<https://doi.org/10.46592/turkager.1538787>

ABSTRACT

The main purpose of agricultural tractors, especially in the medium and high power range, is to improve traction. The value of a tractor is measured by the amount of work done according to the cost spent to do the job. The function of forward speed and traction force is traction force. In this study, the effects of three different radial tire sizes and axle loads on traction performance were examined and evaluated with the help of data obtained from the experiments. The trials were conducted on a hard field road. A single wheel test system was used in the trials. Slip, traction force, axle power, net traction ratio and traction efficiency values were obtained as performance values. Depending on the traction force; slip values varied between 1.2% and 19.10%, net traction ratio between 0.14 and 0.8, and traction efficiency between 0.35 and 0.84. According to the results of the variance analysis performed on traction efficiency values, it was found that the effect of wheel tire size and axle load on traction efficiency was significant ($P<0.01$). Tire contact surface area and traction performances increased due to increased tire size and axle load. The effect of axle load on traction performance was greater than tire size.

Keywords: Tire size, Axle load, Skid, Traction efficiency



Muharrik Radyal Lastik Çapının Çeki Performansına Etkisi

MAKALE BİLGİSİ: Araştırma Makalesi

Sorumlu Yazar: Ergün ÇİTİL, E-mail: ecitil@selcuk.edu.tr

Alınış tarihi: 28 Ağustos 2024 / **Kabul tarihi:** 15 Ekim 2024 / **Basım tarihi:** 31 Aralık 2024

ÖZET

Özellikle orta ve yüksek güç aralığındaki tarım traktörlerinin temel amacı çeki geliştirmektir. Bir traktörün değeri, işin yapılması için harcanan maliyete göre yapılan iş miktarıyla ölçülür. İlerleme hızının ve çeki kuvvetinin fonksiyonu çeki gücüdür. Bu çalışmada, çeki performansı üzerine üç farklı radyal lastik ölçüsünün ve aks yükünün etkileri, yapılan deneylerle elde edilen veriler yardımıyla incelenerek değerlendirilmiştir. Denemeler, sert tarla yolu üzerinde yürütülmüştür. Denemelerde tek tekerlek test sistemi kullanılmıştır. Patinaj, çeki gücü, aks gücü, net çeki oranı ve çeki verimliliği değerleri, performans değerleri olarak elde edilmiştir. Çeki kuvvetine bağlı olarak patinaj değerleri %1.2 ile %19.10, net çeki oranı 0.14 ile 0.8 arasında ve çeki verimliliği ise 0.35 ile 0.84 değerleri arasında değişmiştir. Çeki verimliliği değerlerine yapılan varyans analizi sonuçlarına göre tekerlek lastik ölçüsünün ve aks yükünün çeki verimliliği üzerine etkisinin önemli olduğu bulunmuştur ($P<0.01$). Artan lastik ölçüsü ve aks yüküne bağlı olarak lastik temas yüzey alanı ve çeki performansları artmıştır. Çeki performansı üzerine aks yükünün etkisi, lastik ölçüsüne göre daha büyük olmuştur.

Anahtar Kelimeler: Lastik ölçüsü, Aks yükü, Patinaj, Çeki verimliliği

Alıntı için: Demir, N.O., Çarman, K., & Çıtıl, E. (2024). Muharrik Radyal Lastik Çapının Çeki Performansına Etkisi. Turkish Journal of Agricultural Engineering Research, 5(2), 167-179.
<https://doi.org/10.46592/turkager.1538787>

GİRİŞ

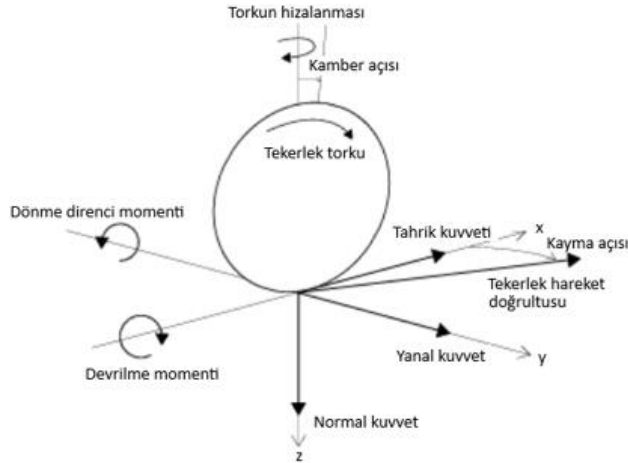
Toprak işlemede çekiş performansının optimizasyonu, yani enerji kaybına neden olan patinajın sınırlandırılması için traktör konfigürasyonunun seçimi birincil öneme sahiptir. Bu durum yakıt tüketimini ve toprak işleme süresini büyük ölçüde etkilemektedir. Lastik boyutları, bir traktörün çeki performansının kontrolünde önemli rol oynayan, kolaylıkla yönetilebilen parametrelerdir (Svendenius, 2007). Lastikler, yol ile araç arasındaki tek arayüz olmalarına ve lastik-zemin arasındaki sürtünmede önemli bir rol oynamalarına rağmen tüketiciler tarafından sıklıkla göz ardı edilmektedir (Grip, 2021).

Traktörler ülkemizdeki mevcut motor mekanik gücünün yaklaşık %10'unu oluşturmaktadır. Traktörlerde çeki kuvvetinin iş makinalarına iletimi, üç nokta askı sistemi ve çeki demiri yardımıyla yapılmaktadır. Çeki kuvveti, iletim sistemlerinde tekerlek ve diğer yürüme organları ile çeki kuvvetine çevrilmektedir. Tekerlekler, traktör ve traktöre farklı bağlantı elemanları ile bağlanan makinaların taşınması, traktörün yol ile arasında sönümleme sağlanması, toprakta tutunmayı artırarak dümenleme etkinliğinin sağlanması gibi görevleri de yapmaktadır (Hassan ve ark., 1987; Wong, 2001).

Lastikler bir araçtaki en önemli çekiş noktasıdır. Traktör lastikleri uygun şekilde optimize edilmezse ihtiyacımızdan daha fazla yakıt tüketimine neden olmaktadır. Uygun lastik seçimi %5 ila %15 aralığında yakıt tasarrufu sağlayabilir. Dikkate alınması gereken faktörler arasında lastik sırt profili, ölçüsü, yük endeksleri, tekli/çiftli/üçlü düzenlemeler ve çalışma hızları yer almaktadır. Uygun olmayan lastikler diğer yakıt verimliliği tedbirlerinin uygulanmasını zorlaştırabilir veya

imkansız hale getirebilir. Daha büyük ölçüdeki lastikler ise ağırlığı dağıtmakta ve daha düşük basınçlarda çalışmayı mümkün kılmaktadır (Svendenius, 2007).

Lastiğe etki eden çok sayıda kuvvet bulunmaktadır (Şekil 1). Boyuna kuvvet F_x ve yanal kuvvet F_y , aracın yol tutuşunu ve kontrolünü etkileyen kuvvetlerdir. Tahrik kuvveti F_x , sürüş veya frenleme sırasında üretilir ve F_y , viraj alma sırasında üretilmektedir. Ayrıca, normal kuvvet F_z , traktör kütlesine göre değişmektedir.



Şekil 1. Lastik üzerinde etkili kuvvet ve momentler (Wong, 2008; Grip, 2021).

Figure 1. Forces and moments acting on the tire (Wong, 2008; Grip, 2021).

Düz bir yüzey üzerinde herhangi bir tahrik torku uygulanmadan serbestçe dönen ve düz bir çizgide giden bir tekerlekte, başlangıç koşulunda sıfıra eşit bir patinajın olduğu kabul edilir. Yuvarlanma direnci nedeniyle, direnci aşmak için bir kuvvet uygulanması gerekir ve bunun sonucunda bir yan kuvvet ve kendiliğinden hizalanan tork gelişir. Yan kuvvet ve kendi kendine hizalanan torkun ortaya çıkması, lastiğin yapısının tamamen simetrik olmamasıyla açıklanabilir (Pacejka, 2006). Tekerlek hareketinin, patinajın sıfıra eşit olduğu başlangıç durumuna göre sapması, ek deformasyonlara ve lastik ile yüzey arasındaki temas alanında patinaja neden olur. Tahrik torku uygulandığında ortaya çıkan patinaj aşağıdaki şekilde tanımlanır (Grip, 2021);

$$S = \frac{R_e \Omega - V_x}{V_x} \quad (1)$$

Burada; S patinajı, V_x tekerleğin merkezinin hız vektörünün boyuna bileşenini, R_e etkin yuvarlanma yarıçapını ve Ω tekerleğin açısal hızını göstermektedir. İlerleme hareketi durumunda patinaj ve çekme kuvveti F_x pozitifdir. Frenleme durumunda ise patinaj negatiftir. Kararlı durum koşulları altında, geliştirilen çeki kuvveti F_x , uygulanan tekerlek torkuyla orantılıdır ve patinaj, çeki kuvvetinin fonksiyonudur. Başlangıçta patinaj, elastik deformasyonların sonucudur ve dolayısıyla çeki kuvveti ve tekerlek torku, patinajla birlikte doğrusal olarak artar. F_x kuvvet ve tekerlek torku arttıkça lastik sırtının bir kısmı patinaja başlar ve patinaj ile çeki kuvveti arasındaki doğrusal ilişki, parabolik hale dönüşür (Wong, 2008).

Araçlar, sürekli bir hıza ulaşmak için meydana getirilen gücün, yaklaşık %25'lik bir bölümünü yuvarlanma direnci için harcarlar. Kaliforniya' da yapılan bir

çalışmada düşük yuvarlanma direncine sahip lastiklerin kullanılması koşulunda yıllık 1.135.623,53 m³ dizel yakıtından (yaklaşık 1 milyar \$) tasarruf sağlanabileceği ortaya konmuştur ([Anonim, 2015](#)).

[Battiato ve Diserens \(2013\)](#) çalışmalarında traktör lastik iç basıncı düştüğünde ve tekerlek aks yükü arttığında traktörün daha yüksek çeki geliştirdiğini saptamışlardır. Yalnızca lastik iç basıncındaki azalma çeki katsayısını, çeki verimliliği ve özgül yakıt tüketimi açısından iyileştirmeler sağlamıştır. Tekerlek aks yükündeki artıştan kaynaklanan tek önemli faydanın, 160 kPa lastik basıncında ve %15'in altındaki patinajda özgül yakıt tüketiminde azalma olduğunu saptamışlardır.

[Serrano ve ark. \(2009\)](#), 59 kW motor gücüne sahip sıvı lastik balastlı ve sıvı lastik balastsız bir traktörün üç farklı lastik iç basıncındaki performansını incelemişlerdir. Lastiklerde sıvı balast kullanımının hektar başına yakıt tüketimini %5-10 oranında artırdığını saptamışlardır. Daha yüksek lastik iç basınçlarının kullanılması, hektar başına yakıt tüketiminde (%10-25) büyük bir artışla birlikte iş başarısında %3-5' lik bir düşüşe neden olduğunu bulmuşlardır. [Smerda ve Cupera \(2010\)](#) tarla koşullarında standart lastik (Ön:14.9 R28; Arka: 18.4 R28) ile yaptıkları çalışmada 170 kPa lastik iç basıncında en yüksek çeki oranına (0.61) ulaşmışlardır. Yüzeye iletilen motor gücü verimliliğinin azalması nedeniyle tekerleklerdeki patinajın %15'i aşmaması gerektiğini önermişlerdir.

Farklı toprak yapısına sahip arazide, radyal ve diagonal iki farklı yapıdaki lastik tekerlekler ve bu yapıdaki tekerlekler ile oluşturulan farklı uygulamaların (arka aksa lastiklerin tek ve çift lastik olarak bağlanması) traktörün performansına etkilerinin incelendiği çalışmada; radyal ve çift lastik tekerleklerin arka aks üzerinde kullanımının bazı avantajlar sağladığı belirlenmiştir. Traktörlerde radyal lastiklerin diagonal lastiklerin yerine kullanılması, traktörün verimini ortalama %3.44 oranında artırmış ve ortalama %3.08 oranında özgül yakıt tüketimini azaltmıştır. Arka aks üzerinde, çift lastik tekerlek kullanılması, traktör verimini ortalama %14.73 oranında artarken, özgül yakıt tüketimi ise ortalama %12.77 oranında azalmıştır ([Sümer ve Sabancı, 2005](#)). [Zoz ve Grisso \(2003\)](#) yaptıkları çeki deneylerinde 520/85R46 radyal lastiğin farklı aks yüklerinin ve iç basıncının, maksimum çeki verimliliği üzerindeki etkilerinin ihmal edilebilir olduğunu bulmuşlardır. Farklı sırt profiline ve çapa sahip iki traktör lastiği üzerinde yapılan çeki testlerinde; benzer yüzeylerde yuvarlanma direncindeki değişime bağlı olarak lastiklerin çeki performansları da değişmiştir. 11.2R24 ölçülerindeki radyal lastik, 31x15.5-15 ölçülerindeki diyagonal lastikten daha yüksek çeki performansı göstermiştir ([Biatczyk ve ark., 2013](#)).

Ülkemizde tarım traktörlerinde kullanılan muharrik lastik çaplarının değişiminin gerek tarla gerekse de laboratuvar koşullarında çeki performansı üzerindeki etkilerini inceleyen sınırlı sayıda ulusal ve uluslararası çalışma bulunmaktadır. Bu çalışmada, sabit lastik kesit genişliğine sahip üç farklı lastik çapının değişen aks yüklerine bağlı olarak çeki performansları saptanmıştır.

MATERYAL ve YÖNTEM

Materyal

Deneylerde üç değişik lastik ölçüsünde 280/70 R16 (R16), 280/70 R18 (R18) ve 280/70 R20 (R20) radyal tip muharrik lastik kullanılmıştır (Çizelge 1). Çalışmada kullanılan lastik ölçüleri, dört tekerleği muharrik traktörlerde ön tekerleklerde ve ülkemizde yaygın olarak kullanımı bulunan bahçe traktörlerinde kullanılmaktadır. Bu çalışmada, “Tek Tekerlek Test Düzeneği” kullanılmıştır (Şekil 2 ve Şekil 3).

Çizelge 1. Deneylerde kullanılan lastiklere ait teknik özellikler.

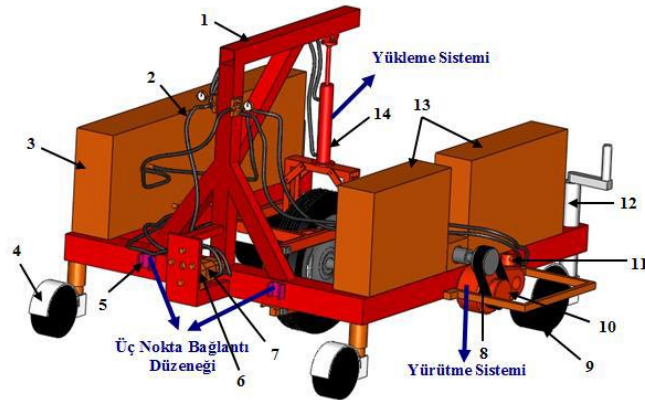
Table 1. Technical specifications of the tires used in the experiments.

Lastik Tipi	Jant Tipi	Statik Dış Çap (mm)	Taşıma Kapasitesi (daN)
280/70 R16	V9	805	1120
280/70 R18	V9	849	1180
280/70 R20	V9	912	1250



Şekil 2. Tek tekerlek test düzeneği.

Figure 2. Single wheel test setup.



1.Yükleme çatısı, 2. Hidrolik geri dönüş hortumları, 3.Hidrolik deposu, 4. Ön destek tekerleği, 5. Üç nokta askı sistemi bağlantı noktası, 6. Dişli pompa, 7. Hidrolik pompa, 8. Zincir, 9.Arka denge tekerleği, 10. Redüktör, 11. Hidrolik motor, 12. Arka denge tekerleği yükseklik ayar kolu, 13. Beton denge ağırlıklar, 14. Hidrolik silindir.

Şekil 3. Tek tekerlek test düzeneği bölümleri (Ekinci, 2011).

Figure 3. Single wheel test setup sections (Ekinci, 2011).

Tek tekerlek test düzeneği üç ana bölümden oluşmaktadır:

1.Çeki bölümü: Testlerde kullanılan düzeneğe hareket veren ve traktörün üç nokta askı düzeneği alt bağlantı noktalarına bağlanan bölümdür.

2.Yürütme sistemi: Traktörün PTO çıkışına bağlanarak çalışan hidrolik pompa ve hareketini bu pompadan alan hidrolik motor ve test düzeneği tekerleğine hareket veren yürütme bölümüdür.

3.Tekerlek aksı yükleme sistemi: Deneylerin yapılması esnasında test tekerleğine dinamik aks yükünün uygulanmasını sağlar. Test düzeneği ana şasisi ile tekerlek çatısı arasına bir hidrolik silindir yerleştirilmiştir.

Tek tekerlek test düzeneği ile yapılan denemelerde, test düzeneğinin ihtiyaç duyduğu kuyruk mili hareketi, frenleyici (çeki arabası) olarak kullanılan New Holland TD90D marka traktörden sağlanmıştır. Ayrıca traktörün park freni üzerindeki kademeler kullanılarak farklı itme (çeki) kuvvetlerindeki değerlerin elde edilmesi sağlanmıştır ([Ekinçi ve ark., 2015](#)).

Yöntem

Denemeler üç farklı aks yükünde (W_1 : 3.5, W_2 : 5.0 ve W_3 : 6.5 kN), sabit lastik iç basıncı (190 kPa) ve ilerleme hızında (5 km h^{-1}) yürütülmüştür. Deneyler, sert tarla yolu koşullarında yürütülmüştür (Şekil 4). Çalışma zemininin özelliklerinin belirlenmesi amacıyla kayma dirençleri ölçülmüştür. Bundan dolayı Stanley London marka ASTM E303 ve BS EN 13036-4:2003 standartlarındaki taşınabilir kayma direnci ölçüm cihazı kullanılmıştır ([Ekinçi ve ark., 2015](#)).



Şekil 4. Sert tarla yolu.

Figure 4. Hard field road.

Denemesi yapılan lastiklerin iz düşüm alanlarını belirlemek amacıyla bütün aks yükleri ve lastik iç basınçlarında, beton zemin üzerinde lastiği zemin ile teması kesilecek kadar kaldırılarak lastiğin belirli bir yüzeyi siyah renge boyanmış ve zemin üzerine sabitlenmiş A3 ebadındaki kağıt üzerine indirilmiştir. Kağıt üzerindeki oluşan iz alanının tam olarak doldurulabilmesi için lastik her seferinde $5-10^\circ$ döndürülerek siyah renge boyanmış farklı bölgelerin kağıt üzerine indirilmesi 4-5 kez tekrar edilmiştir ([Çarman ve Şeflek, 2005](#)). Bilgisayarda UTHSCSA Image Tool Version 3.0 yazılımı kullanılarak, kâğıt üzerinde oluşan temas alanları belirlenmiştir.

Traktör üzerine bağlanabilen, Dickey John DJCMS200 marka hız sensörü kullanılarak gerçek çalışma hızları (V_g) bütün kombinasyonlar için ölçülmüştür. Teorik hızın (V_t) belirlenmesinde ise test tekerleği miline direk bağlanmış olan torkmetre yardımıyla manyetik algılayıcıdan alınan sinyaller ile devir ölçülmüş ve farklı aks yüklerinde tekerleğin çevresi dikkate alınarak hesaplanmıştır. Patinajın belirlenmesinde aşağıdaki eşitlik kullanılmıştır.

$$S = (1 - \frac{V_g}{V_t}) \quad (2)$$

Eşitlikte;

S : Patinaj oranı (%)

V_t : Teorik hız (km h⁻¹)

V_g : Gerçek ilerleme hızı (km h⁻¹)

Çalışmada, itme (çeki) dirençleri (P), tekerlek şasisi ile şasi arasına oynak olarak bağlantısı yapılmış 4 tane tekerlek itme kollarına bağlanmış yük hücreleri yardımıyla ölçülmüştür. Denemeler sırasında DT 80 Datataker marka veri toplayıcı tarafından dört noktadan alınan ÇK değerleri kaydedilmiştir.

Gücün belirlenmesi amacıyla traktör kuyruk miline (PTO) takılan 1800 Nm' lik Datum P7947 marka elektronik torkmetre kullanılmıştır. Torkmetrenin üzerinde gücün belirlenmesi yanında, devir ölçer de bulunmaktadır. Bilgisayarda Datum Electronics TorqueLog 1.0 yazılımı ile torkmetreden alınan sinyallerle her kombinasyon için devir (n), güç ve tork (T) değerleri kaydedilmiştir. Sistemin dışı kutusu verimleri (η_{d1} ve η_{d2} için %98), ve hidrolik pompa verimi (η_{hp}) ve hidrolik motor verimleri (η_{hm}) için %86 olarak dikkate alınmış ve toplam verim $\eta_T = 0.71$ olarak belirlenmiştir (Niemann, 1970; Anonim, 1985).

Aks gücü, devir ($n = 540 \text{ min}^{-1}$) ve tork verilerinden aşağıdaki eşitlik vasıtasıyla hesaplanabilmektedir (Demir, 2014; Ekinci ve ark., 2015).

$$N_a = \frac{T \cdot 0.71 \cdot n}{9550} \quad (3)$$

T : Tork metreden ölçülen tork değeri (Nm)

n : Tekerlek devri (min⁻¹)

Ölçülen çeki direnci ve gerçek çalışma hızları yardımıyla, ayrı ayrı bütün kombinasyonlar için çeki gücü, aşağıdaki eşitlikle hesaplanmıştır (Demir, 2014; Ekinci ve ark., 2015).

$$N_{\text{ç}} = \frac{P \cdot V_g}{1000} \quad (4)$$

$N_{\text{ç}}$: Çeki gücü (kW)

P : Çeki kuvveti (N)

V_g : Traktörün gerçek ilerleme hızıdır (m s⁻¹)

Net çeki oranı (NÇO), lastik tekerleklerle gerçekleştirilen düzenlemelerin performans yönünden değerlendirilmesinde faydalanan etkili bir parametredir. Net çeki oranı aşağıdaki eşitlik yardımıyla hesaplanmıştır (Tiwari ve ark., 2009; Demir, 2014; Ekinci ve ark., 2015).

$$N_{\text{ÇO}} = \frac{P}{W} \quad (5)$$

$N_{\text{ÇO}}$: Net çeki oranı (%)

P : Çeki kuvveti (kN)

W : Aks yükü (kN)

Diğer bir performans parametresi lastik tekerleğin çeki verimliliği (η) aşağıdaki eşitlik yardımıyla hesaplanmıştır (Tiwari ve ark., 2009; Demir, 2014; Ekinci ve ark., 2015).

$$\eta = \frac{N_c}{N_a} \quad (6)$$

η : Çeki verimliliği (-)

N_c : Çeki gücü (kW)

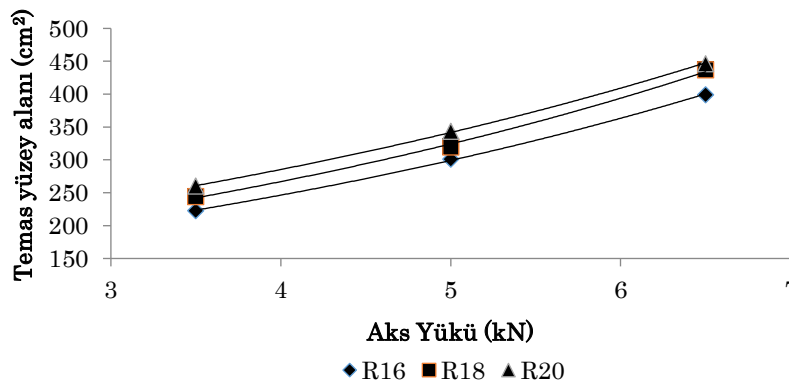
N_a : Aks gücü (kW)

İstatistiksel analizler

Çeki verimliliği üzerine, çalışmada kullanılan muharrik lastik çapı ve aks yükü gibi kontrollü değişkenlerin etkilerini belirlemek için varyans analizi yapılmıştır. Varyans analizi sonuçlarının önemli çıktığında ise LSD testleri yapılmıştır (Düzgüneş ve ark. 1987).

BULGULAR ve TARTIŞMA

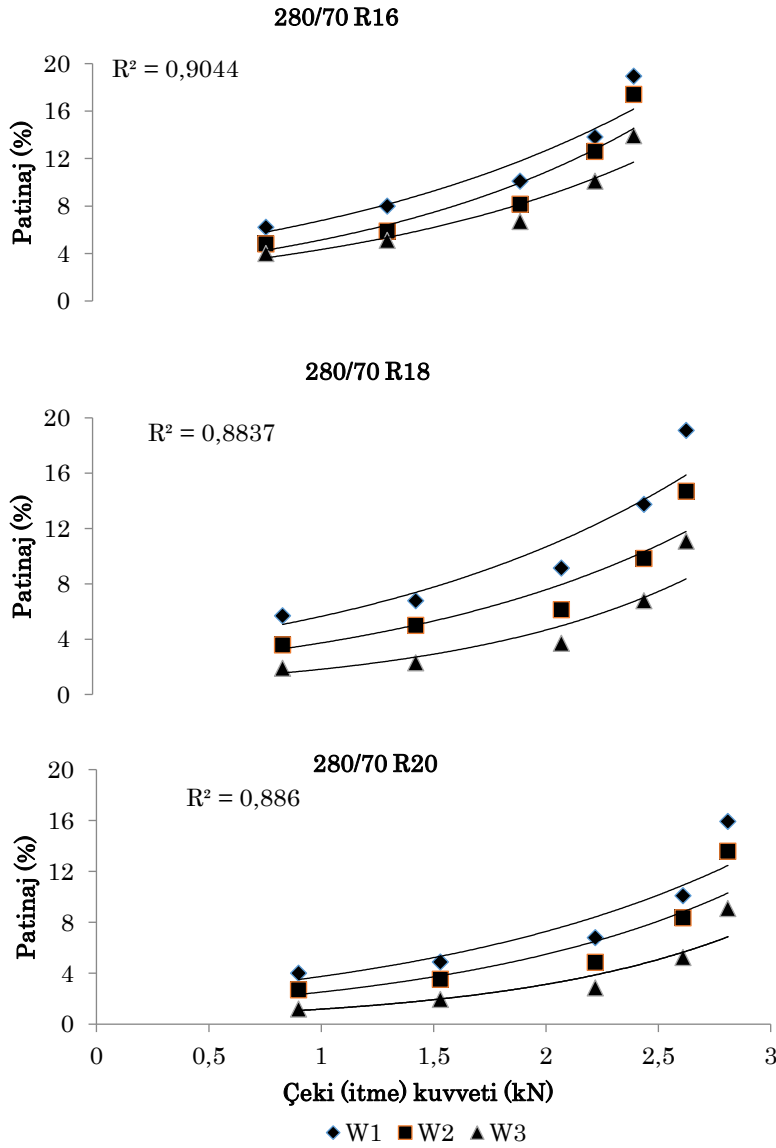
Lastik ile zemin arasındaki tutunmanın bir fonksiyonu olarak çekici tekerleğin oluşturduğu ÇK elde edilmektedir. Sert tarla yolunun kayma direnci, kuru koşullarda 61, ıslak koşulda ise 47 olarak ölçülmüştür. Lastik temas yüzey alanı ile tutunma arasında doğrusal bir ilişki mevcuttur. Lastiklerin değişen lastik aks yükü değerlerinde temas alanları 222.91-446.35 cm² arasında değişmiştir (Şekil 5). Çalışmada, lastik aks yükündeki %85.7'lik bir artış temas alanlarında ortalama %74'lük bir artışa neden olmuştur. Ekinci (2011), 7.50-18 diyagonal ve 7.50 R18 radyal muharrik lastiklerle yaptığı çalışmasında, lastik aks yükündeki %86'lık bir artış iz düşüm alanlarında diyagonal lastiklerde %31, radyal lastiklerde ise %20'lik bir artışa sebep olduğunu saptamıştır. Ekinci ve ark. (2016) 280/70R20 ölçülerindeki radyal lastikte aks yükündeki %67'lik artışın, temas yüzey alanında %84'lik bir artışa neden olduğunu belirlemişlerdir. Elde edilen sonuçlar, literatür değerleri ile benzerlik göstermektedir. Lastik statik çapındaki %13.3'lük bir artış ise, lastik temas alanında ortalama %13.7'lik bir artışa neden olmuştur.



Şekil 5. Aks yüküne bağlı olarak lastik temas yüzey alanındaki değişim.

Figure 5. Change in tire contact surface area depending on axle load.

Çalışmada kontrol edilebilen değişken olan çeki kuvvetine (itme) bağlı olarak patinaj değerleri %1.2 ila %19.10 arasında değişmiştir (Şekil 6). Ortalama patinaj değerleri 3.5 kN'luk aks yükünde %10 iken, 6.5 kN'luk aks yükünde %4.6 azalarak %5.7 olmuştur. Ortalama patinaj, R16 lastik ölçüsünde %9.72 iken, R20 lastik ölçüsünde %34.7 azalarak %6.34 olmuştur. Lastiklerde çap artışıyla birlikte temas yüzey alanları da artış göstermiştir. Temas yüzey alanlarının artması, lastiklerin zemine daha iyi tutunduğu ve patinajın azaldığı anlamına gelmektedir (Smerda ve Cupera, 2010; Ekinci ve ark., 2016).

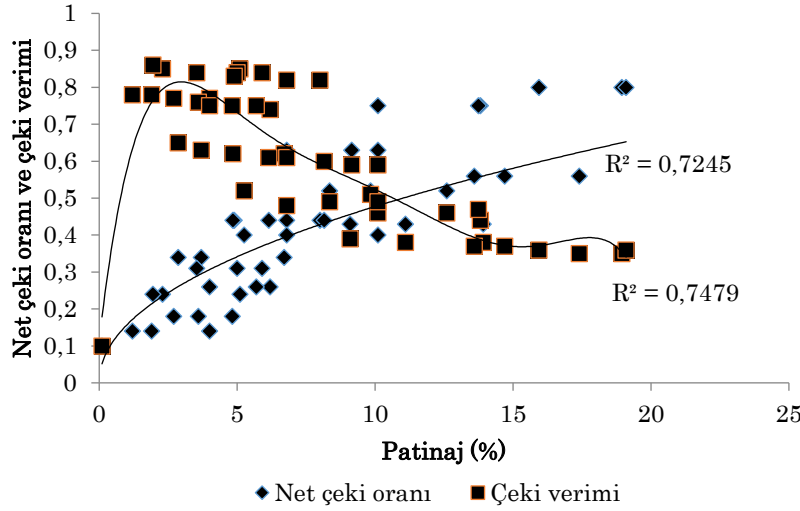


Şekil 6. Çeki kuvvetine (itme) bağlı olarak patinajın değişimi.

Figure 6. Change in slippage depending on traction (push) force.

Lastik ölçüsü ve aks yüküne bağlı olarak net çeki oranı 0.14-0.80 arasında değişirken, çeki verimi değerleri 0.35-0.84 arasında değişmiştir (Şekil 7). Farklı çalışma kombinasyonlarında %4-10 patinaj aralığında maksimum çeki verimine ulaşılmıştır. Maksimum çeki verimlerine karşılık gelen net çeki oranı ise 0.24-0.44 arasında değişmiştir. Elde edilen çeki verimi sonuçları ile yapılan varyans analizi sonuçları çeki verimi üzerinde lastik ölçüsünün ve aks yükünün etkisinin önemli

olduğunu göstermiştir (Çizelge 2). [Ekinci \(2011\)](#) asfalt zeminde aks yükündeki %86'lık bir artışın çeki verimini %2 artırdığını belirtmiştir. Patinaj, çeki verimliliğini maksimuma çıkarmak için dikkate alınması gereken temel parametrelerden biridir. Patinaj, aracın çeki kuvvetine bağlıdır ve çeki arttığında patinajda artar ([Kumar ve ark., 2016](#)). Ölçüleri 7.00-18 olan radyal bir lastiğin çeki performansını farklı çalışma şartları sonucunda elde edilen %5.6-42.0 patinaj oranı değerlerinde çeki kuvveti 1.20-3.35 kN ve çeki verimi ise 0.22-0.74 arasında değişmiştir ([Çarman, 2001](#)).



Şekil 7. Patinaja bağlı olarak net çeki oranı ve çeki veriminin değişimi.

Figure 7. Change in net traction ratio and traction efficiency depending on slippage.

Çizelge 2. Lastik ölçüsü ve aks yükünün çeki verimi üzerine etkisinin varyans analizi ve LSD testi sonuçları.

Table 2. Variance analysis and LSD test results of the effect of tire size and axle load on traction efficiency.

V.K	S.D	K.O	F	Tablo değeri (%1)
Lastik ölçüsü	2	0.001	6.240**	6.010
Aks yükü	2	0.002	20.710**	6.010
AxB	4	0.000	0.25 ns	4.580
Hata	18	0.000		
Genel	26	0.000		

**İstatistiksel olarak %1 seviyesinde önemlidir. (P<0.01)

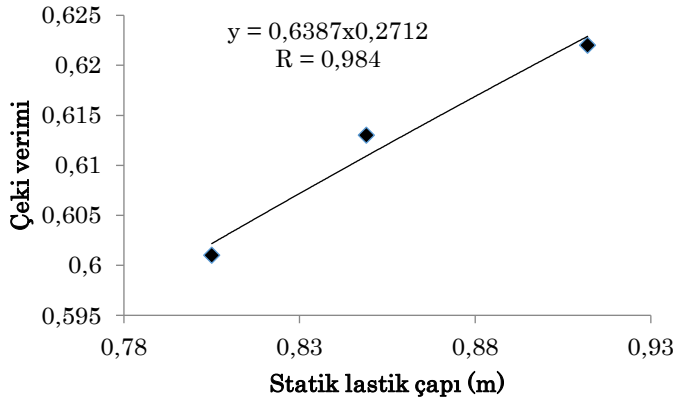
ns: İstatistiksel olarak %1 seviyesinde önemsizdir. (P>0.01)

Lastik ölçüsü	Aks yükü		
(280/70 R16)	0.603a	(3.5 kN)	0.597a
(280/70 R18)	0.615b	(5.0 kN)	0.613b
(280/70 R20)	0.619c	(6.0 kN)	0.627c

LSD(%5)= 0.010

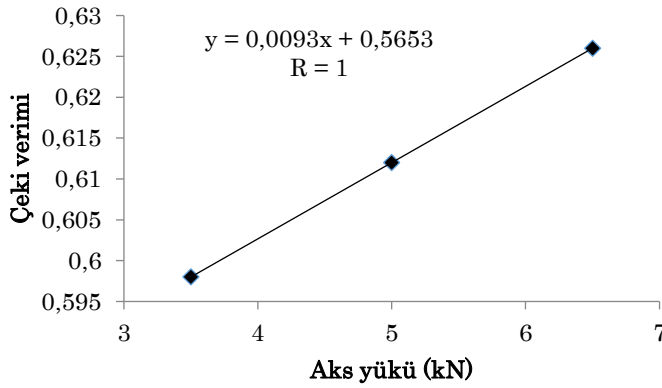
Statik lastik çapındaki %13.3'lük artış çeki veriminde %3.5'lik bir artışa neden olmuştur. Lastik çapı ve çeki verimi arasında üssel bir ilişki olup, ilişkinin korelasyon katsayısı 0.984 olarak elde edilmiştir (Şekil 8). Lastik aks yükündeki %85.7'lik bir artış, çeki veriminde %4.7'lik bir artışa neden olmuştur. Aks yükü ve

çeki verimi arasında doğrusal bir ilişki olup, ilişkinin korelasyon katsayısı 1 olarak elde edilmiştir (Şekil 9).



Şekil 8. Lastik çapı ve çeki verimi arasındaki ilişki.

Figure 8. Relationship between tire diameter and traction efficiency.



Şekil 9. Aks yükü ve çeki verimi arasındaki ilişki.

Figure 9. Relationship between axle load and traction efficiency.

SONUÇ

Çalışmanın sonuçları aşağıdaki gibi özetlenebilir.

- Lastik temas yüzey alanına, lastik çapı ve aks yükü farklı oranlarda etkili olmuştur. Lastik çapının ve aks yükünün artması, temas yüzey alanlarını da artmıştır.

- Sabit itme kuvvetinde R16 W1 kombinasyonunda en büyük, R20 W3 kombinasyonunda ise en düşük patinaj değerleri elde edilmiştir.

- Patinaj değerleri üzerinde aks yükünün etkisinin, lastik çapından daha yüksek olduğu bulunmuştur.

- Farklı çalışma koşullarına bağlı olarak ortalama çeki verimleri %62.4-58.8 arasında elde edilmiştir.

- Çeki verimi üzerinde aks yükünün etkisi istatistiki açıdan önemli iken ($P < 0.01$), lastik çapının etkisi önemsiz bulunmuştur.

- Günümüzde gerek bahçe ve gerekse de tarla tarımında kullanılan traktörlerde, motor gücü tekerlek ölçüsünün uygun seçilememesi motor gücünün verimli kullanılmamasına

diğer bir ifadeyle yakıt tüketiminin artmasına buna bağlı olarak da enerji maliyetinin artmasına neden olabilecektir.

ÇIKAR ÇATIŞMASI

Makale yazarları olarak herhangi bir çıkar çatışması olmadığını beyan ederiz.

YAZAR KATKISI

Necmettin Oğuz DEMİR: Araştırma, metodoloji, kavramsallaştırma, biçimsel analiz ve veri analizi,

Kazım ÇARMAN: Araştırma, metodoloji, kavramsallaştırma, biçimsel analiz, veri analizi, iyileştirme ve doğrulama

Ergün ÇİTİL: Araştırma, metodoloji, yazma - orijinal taslak, inceleme, düzenleme ve görselleştirme

ETİK KURUL KARARI

Bu makale Etik Kurul Kararı gerektirmemektedir.

KAYNAKLAR

- Anonim (1985). Agrartechnik International HTL. Agrartechnische Lehrbriefe. Vogel Verlag Vürzburg.
- Anonim (2015). www.tirekingdom.com/tires/Tire-Rolling-Resistance-Education.j
- Battiato A and Diserens E (2013). Influence of tyre inflation pressure and wheel load on the traction performance of a 65 kW MFWD tractor on a cohesive soil. *Journal of Agricultural Science* 3, 5(8): 197-215. <https://doi.org/10.5539/jas.v5n8p197>
- Biatczyk W, Brennenstul M, Cudzik A and Czarnecki J (2013). Evaluation of changes in traction properties of tyres on selected farming surfaces. Teka. *Commission of Motorization and Energetics in Agriculture*, 13(1): 3-8.
- Çarman K (2001). 7.0-18 Ölçülerindeki bir radyal lastiğin çeki performansı ve enerji tüketiminin belirlenmesi, S.Ü. Araştırma Fonu Proje No:99-021; Konya.
- Çarman K ve Şeflek AY (2005). Lastik defleksiyonu-temas alanı ilişkisinin değerlendirilmesi, *Tarım Makinaları Bilimi Dergisi*, 1(1): 49-54.
- Demir NO (2014). *Tarımda kullanılan bazı muharrik lastiklerin işletme parametrelerinin optimizasyonu*. Selçuk Üniversitesi Fen Bilimleri Enstitüsü Tarım Makineleri A.B.D., Doktora Tezi, Konya.
- Düzgüneş O, Kesici T, Kavuncu O ve Gürbüz F (1987). Araştırma Deneme Metotları (İstatistik Metotları II), *Ankara Üniversitesi Ziraat Fakültesi Yayınları. Yayın No: 1021, Ankara.*
- Ekinci Ş (2011). *Bahçe traktörlerinde kullanılan bazı muharrik lastiklerin yapısal ve işletme özelliklerinin çeki performansına etkisi*. Selçuk Üniversitesi Fen Bilimleri Enstitüsü Tarım Makineleri A.B.D., Doktora Tezi, Konya.
- Ekinci Ş, Çarman K ve Kahramanlı H (2015) Investigation and modeling of the tractive performance of radial tires using off-road vehicles. *Energy*, 93:1953-1963. <https://doi.org/10.1016/j.energy.2015.10.070>
- Ekinci Ş, Çarman K, Taşyürek M and Mirik M (2016). Relationship between deflection and contact area of drive tire. *International Journal of Materials, Mechanics and Manufacturing*, 4(3):179-182. <https://doi.org/10.7763/IJMMM.2016.V4.251>
- Grip M (2021). *Tyre performance estimation during normal driving*. Master of Science Thesis, Department of Electrical Engineering Linköping University.

- Hassan AE, Oakley R, Culshaw D and Dawson JR (1987). Comparison Test of A Forestry and Agriculture Tire. *Transactions of the ASAE*, 30(6): 1562-1568. <https://doi.org/10.13031/2013.30602>
- Kumar AA, Tewari VK and Nare B (2016). Embedded digital draft force and wheel slip indicator for tillage research. *Computers and Electronics in Agriculture*, 127: 38-49. <https://doi.org/10.1016/j.compag.2016.05.010>
- Niemann G (1970). Makine Elemanları Cilt: III. (Çeviri: Hazardın, G., Yurdakonar, S.,) *Matbaa Teknisyenleri Kool. ŞTİ.* İstanbul.
- Pacejka HB (2006). Tyre and Vehicle Dynamics. Butterworth-Heinemann; 2nd Edition.
- Serrano JM, Peça JO, Silva JR and Márquez L (2009). The effect of liquid ballast and tyre inflation pressure on tractor performance. *Biosystems Engineering*, 102: 51-62. <https://doi.org/10.1016/j.biosystemseng.2008.10.001>
- Smerda T and Cupera J (2010). Tire inflation and its influence on drawbar characteristics and performance—Energetic indicators of a tractor set. *Journal of Terramechanics*, 47: 395-400. <https://doi.org/10.1016/j.jterra.2010.02.005>
- Sümer SK and Sabancı A (2005). Effects of different tire configurations on tractor performance. *Turkish Journal of Agriculture and Forestry*, 29: 1-8. <https://journals.tubitak.gov.tr/agriculture/vol29/iss6/5>
- Svendenius J (2007). Tire modeling and friction estimation. PhD thesis, Department of Automatic Control, Lund University.
- Tiwari VK, Pandey KP and Sharma AK (2009). Development of a tyre traction testing facility. *Journal of Terramechanics*, 46: 293-298. <https://doi.org/10.1016/j.jterra.2009.05.004>
- Wong JY (2001). Theory of ground vehicles. *John Wiley & Sons*, Canada.
- Wong JY (2008). Theory of ground vehicles. *Wiley*, 4th edition.
- Zoz FM and Grisso RD (2003). Traction and tractor performance. ASAE distinguished lecture series (Tractor design No. 27). *ASAE Publication* No. 913C0403. St. Joseph, Michigan.



Turkish Journal of
Agricultural
Engineering Research
(Turk J Agr Eng Res)
e-ISSN: 2717-8420



Investigation of Planting Landscape Applications in Terms of Sensory Stimulation, Malatya Example

Gamze ÖNER^a, Sima POUYA^{a*}

^aInonu University, Faculty of Fine Arts and Design, Department of Landscape Architecture, Malatya, TÜRKİYE

ARTICLE INFO: Research Article

Corresponding Author: Sima POUYA, E-mail: sima.pouya@inonu.edu.tr

Received: 05 August 2024 / Accepted: 16 October 2024 / Published: 31 December 2024

To cite: Öner, G., & Pouya, S. (2024). Investigation of Planting Landscape Applications in Terms of Sensory Stimulation, Malatya Example. Turkish Journal of Agricultural Engineering Research, 5(2), 180-198. <https://doi.org/10.46592/turkager.1525288>

ABSTRACT

It is known that plants stimulate the senses of sight, touch, smell and taste. In addition, plants stimulate the sense of sight with their different shapes and colors, the sense of touch with their leaves, the sense of smell with the scents of flowers and fruits, the sense of taste with the fruits and the sense of hearing with the sounds of the leaves. Plants that activate the five senses can create an environment in the form of multi-sensory stimulation that can develop emotional stability and sensitivity in people. Designing with plants has become an important part of the landscape design process in landscape design projects. Plants are used in the discipline of landscape architecture for visual, functional and ecological aspects. However, preliminary studies have shown that the use of plants in designed urban green spaces is weak in the context of sensory stimulation. Designers usually use plants in their designs as shade providers, way markers and so on. In this context, the main objective of this study was to investigate the extent to which plants that stimulate the senses are used in existing urban green spaces and parks. In the study, the landscape applications of the existing parks in the city of Malatya in Turkey were evaluated within the scope of sensory stimulation. The results of this study showed that the plant species used in 4 different recreational areas mainly stimulated the senses of sight and touch and insufficiently stimulated the senses of smell, sound, and taste.

Keywords: Sensory stimulation, Sensory gardens, Senses, Vegetable landscape design



Duyusal Uyarım Açısından Bitkisel Peyzaj Uygulamalarının İncelenmesi, Malatya Örneği

MAKALE BİLGİSİ: Araştırma Makalesi

Sorumlu Yazar: Sima POUYA, E-mail: sima.pouya@inonu.edu.tr

Alınış tarihi: 05 August 2024 / Kabul tarihi: 16 October 2024 / Basım tarihi: 31 December 2024

ÖZET

Bitkilerin görme, dokunma, koku alma ve tat alma duyularının uyardığı bilinmektedir. Ayrıca bitkiler çeşitli şekil ve renkleriyle görme duyusunu, yapraklarına dokunma ile dokunmayı, çiçek ve meyvelerin kokularıyla koku almayı, meyvelerle tat almayı ve yaprakların sesleri ile işitme duyusunu uyandırır. Beş duyuyu harekete geçiren bitkiler, insanlarda duygusal istikrar ve duyarlılığı geliştirebilecek çok duyulu uyarımlar şeklinde bir ortam sağlayabilir. Peyzaj tasarım projelerinde bitkisel tasarım peyzaj tasarım sürecinin önemli bir parçası olmuştur. Peyzaj mimarlığı disiplininde bitkiler görsel, işlevsel ve ekolojik bakımından kullanılmaktadır. Ancak yapılan ön incelemeler tasarlanan kentsel açık ve yeşil alanlarındaki bitkilerin duysal uyarım kapsamında kullanımlarının zayıf olduğu gözlemlenmiştir. Genellikle tasarımcıları bitkisel tasarımlarında bitkileri gölge sağlama, yön gösterme ve bunun gibi amaçlar için kullanmaktadırlar. Bu bağlamda mevcut yapılan kentsel yeşil alanlarda ve parklarda duysal uyarım sağlayan bitki kullanımının ne ölçüde kullanıldığının incelenmesi bu çalışmanın asıl amacı olmuştur. Yapılan çalışma içerisinde Türkiye'nin Malatya kentinde var olan parkların duysal uyarım kapsamında peyzaj uygulamalarının değerlendirilmesi yapılmıştır. Bu çalışmanın sonucu, 4 farklı rekreasyon alanında yapılan bitkisel tasarım incelemelerine göre bu alanlarda kullanılan bitki türlerinin en fazla görme ve dokunma duyusunun uyandırdığını ve koku, ses ve tat duyuların uyandırması anlamında eksiklerin olduğunu açıklamıştır.

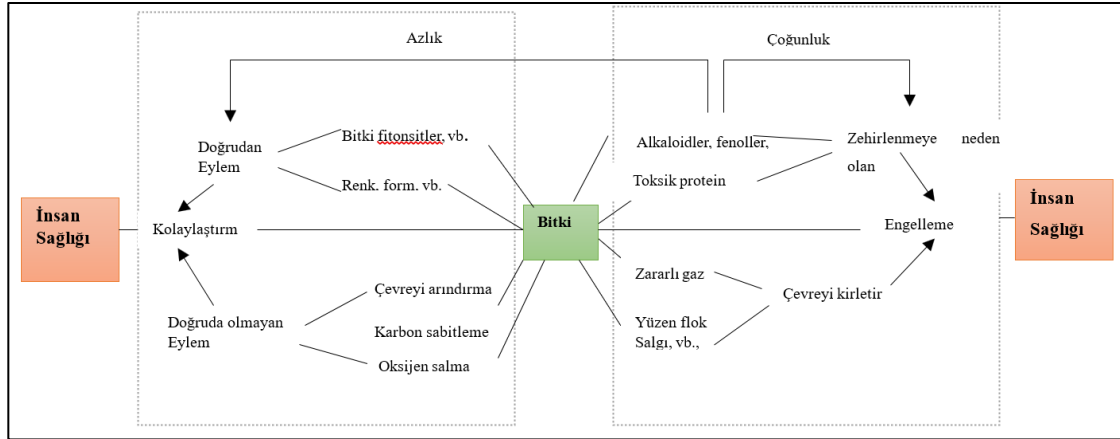
Anahtar Kelimeler: Duyusal uyarım, Duyu bahçeleri, Duyular, Bitkisel peyzaj tasarımı

Alıntı için: Öner, G., & Pouya, S. (2024). Duyusal Uyarım Açısından Bitkisel Peyzaj Uygulamalarının İncelenmesi, Malatya Örneği. Turkish Journal of Agricultural Engineering Research, 5(2), 180-198. <https://doi.org/10.46592/turkager.1525288>

GİRİŞ

Kentsel yeşil alan sistemlerinin önemli bir parçası olarak, kentsel parkları, şehir manzarasını güzelleştirmede ve kentsel ekosistemlerin kalitesini artırmada önemli rol oynamaktadır (Taplin, 2002). Kentsel parklar ve yeşil alanlar, insan kaynaklı bozulmaların neden olduğu ekosistem tahribatını hafifletmek ve genel ekolojik dengeyi korumak için gerekli olan "bir şehrin kalbi" olarak adlandırılır (Chen ve ark., 2018). Yaşlı nüfusunun artması nedeniyle, doğal alanlar ile insan sağlığı arasındaki ilişki kamuoyunda ve akademide giderek daha fazla ilgi görmektedir (Burnett, 1997). Kentsel parkların ve yeşil alanların önemli bir unsuru olarak bitkiler, çevredeki negatif iyonlar üretir ve negatif iyonlar, havadaki toz, küf sporları, bakteriler ve alerjenler gibi partiküllere tutunur ve bunları etkili bir şekilde giderir. Bitkiler oksijen salgılayarak, kirleticileri emerek ve bakteri ve virüslerin büyümesini engelleyerek çevredeki hava kalitesini iyileştirir. Çevre sıcaklığı ve nemi bitkilerin terlemesiyle ayarlanır, konfor seviyesi artar ve çevreyi iyileştirerek dolaylı olarak insan sağlığı etkilenir. Şekil 1'de görüldüğü gibi, bitkiler insan sağlığına faydalı maddeler salgılar. Dahası, renk, morfoloji ve dokudan kaynaklanan pozitif uyarılar insanların fiziksel ve psikolojik durumlarını iyileştirir. İnsanlar üzerinde olumsuz etkisi olan salınan bileşikler arasında glikozitler, alkaloidler, fenoller ve

köklerden, gövdelerden, yaprakçıklardan veya çiçeklerden salınan bazı toksik proteinler bulunur. Bu maddeler alerjilere veya diğer hastalıklara neden olabilir (He ve ark., 2022). Bitkilerin zihinsel durumumuzu şekillendirmede ve zihinsel ve fiziksel hastalık riskini azaltmada temel bir rol oynadığına dair bilimsel kanıtlar artmaktadır. Bitkiler stres hormonu kortizol seviyelerini düşürerek insanlarda depresyon, anksiyete ve ruh hali bozukluğu semptomlarını azaltabilirler, bu da kalp atış hızını düşürebilir ve iyi hissetme halini teşvik edebilir. Bitkilerin canlı, doğal renkleriyle beyni uyatarak yaratıcılığı bile artırabilirler (Cooper Marcus ve Barnes 1995).



Şekil 1. Bitkiler ve insan sağlığı arasındaki ilişkiler (He ve ark., 2022).

Figure 1. Relationships between plants and human health (He et al., 2022).

Doğal alanlarda bulunmak, insanların daha fazla fiziksel aktivite yapmasını sağlar, bu da obeziteyi önemli ölçüde önleyebilir ve kronik tıbbi rahatsızlıkların görülme sıklığını azaltabilir (Liu ve ark., 2017). Dahası, insanların kent parklarında algıladıkları "huzur" ve "sığınak" gibi benzersiz deneyimlerin zihinsel iyileşmeyi önemli ölçüde artırdığı gösterilmiştir. Ayrıca birçok çalışma, yapay çevrenin aksine, doğal ortamların fiziksel güçleri geri kazandırabileceğini öne sürmüştür. Bunlarla birlikte yapılan birçok çalışmada doğal alanların özellikle bitkilerin insanların duyuşsal gelişiminde etkili olduğunu gösterilmiştir (Kaplan, 1973; Minter, 1995).

İnsanlar doğumdan itibaren duyu organları aracılığıyla çevreden çeşitli duyuşsal uyarımları kabul eder ve fiziksel duyuşları geliştirir. Bu tür duyuşsal gelişim, beynin dış çevreyi kabul etmesiyle uygun bir yanıt olarak ifade edilmektedir. Dahası, duyuşlar yorumlama, ilişkilendirme ve bütünleştirme nedeniyle bağlama göre uyarlanabilir davranışlar olarak temsil dilmektedirler (Francis-West ve ark., 2002). Uzmanlar insanların gelişme evrelerinde duyuşları uyatarak olayları ve nesneleri özel olarak görme, duyma, koklama, dokunma, tatma ve hissetme duyuşlarıyla öğretirler. Beş duyuş (görme, koku alma, tat alma, duyma ve dokunma) gözler, burun, dil, kulaklar ve deri tarafından algılanır. Duyuş organları, insanların dış çevreyi anlamalarına ve algılamalarına yardımcı olmak için beyne bilgi iletir. Dahası, beş duyuş dış dünyayla iletişim kurmamız için önemli kanallardır. İnsanların beş duyuşu kendi algısal bedenlerini oluşturur. İnsanlar bu duyuşlar aracılığıyla dış dünyayı anlayabilir, deneyimleyebilir ve ayrıca belirli bir davranış üretebilirler. Bu nedenle, Beş Duyuş Teorisi, doğanın ve çevrenin insanların çok duyuşlu deneyimlerini

oluşturmak ve teşvik etmek için nasıl tasarlanabileceğini anlamak için iyi bir tekniktir (He ve ark., 2022).

Çiçek ve bitkilerin görme, dokunma, koku alma ve tat alma duyularının uyardığı bilinmektedir (Kaplan, 1994). Ayrıca bitkiler çeşitli şekil ve renkleriyle görme duyusunu, yapraklarına dokunma ile dokunmayı, çiçek ve meyvelerin kokularıyla koku almayı, meyvelerle tat almayı ve yaprakların sesleri ile işitme duyusunu uyandırır (Hussein, 2012). Beş duyuyu harekete geçiren bitkiler, insanlarda duygusal istikrar ve duyarlılığı geliştirebilecek çok duyulu uyarımlar şeklinde bir ortam sağlayabilir (Yun ve ark., 2018).

Tüm peyzaj tasarımları beş duyuyu uyabilir, ancak duyu bahçeleri bu konuda daha fazla etkili olmuştur. Bu bahçeler terapötik özelliklere sahip olan ve insanların farklı duyularını uyarak fiziksel ve psikolojik durumlarını olumlu yönde etkileyen alanlar olarak tanımlanabilir. Farklı sağlık iyileştirici işlevlere sahip bitkiler, bilim ve sanatı bütünleştiren bir şekilde ortama dağıtılır ve düzenlenir (Özgüner, 2004). Duyu bahçelerin tasarımında, bitkiler ve diğer tasarım öğeleri beş duyu organı için deneyimler sağlama amacıyla özel olarak tasarlanır (Pouya ve ark., 2024). Örneğin, bitkilerin rengi, görseli, dokusu, biçimi, hareketi, ışığı ve gölgesi görme duyusunu uyarır, aromatik bitkilerin kullanımı koku alma duyusunu uyabilir, yaprakların arasından esen rüzgar, sapsı birbiri vuran veya hışırdayan otlar ses yaratır ve yenilebilir meyvelerden, sebzelerden, otlardan ve baharatlardan faydalanarak tat deneyimi sağlanır ve bazı bitkiler dokunma duyusunu uyandırmak için ve dokusal çeşitlilikleri nedeniyle seçilir ve alanda kullanılır (Ulrich ve Addoms, 1981; Ulrich, 1983; Ulrich ve ark., 1991). Bitkilerin renkliliği ve faydalı uçucu maddeleri insanların fiziksel ve ruhsal sağlığını geliştirebilir. Ancak bazı bitkilerin zararlı maddeler de üretebildiği ve insan sağlığını olumsuz yönde etkileyebildiği dikkat çekmektedir (He ve ark., 2022).

Bitkilerin duysal uyarım bağlamında en önemli özelliği renk olarak tanımlanmıştır. Bitki kompozisyonunda ve mevsimsel değişikliklerinde (sonbahar renklenmesi, ilkbahar renkleri) bitkinin dalları, sürgünleri, meyveleri, çiçekleri, gövde kabuğu, yapraklarında renk etkisi algılanabilir (Karaşah, 2021; Altınçekiç, 2000).

Peyzaj tasarım projelerinde bitkisel tasarım peyzaj tasarım sürecinin önemli bir parçası olmuştur. Peyzaj mimarlığı disiplinde bitkiler görsel, işlevsel ve ekolojik bakımından kullanılmaktadır (Sarı ve Karaşah, 2018). Ancak yapılan ön incelemeler tasarlanan kentsel açık ve yeşil alanlarındaki bitkilerin duysal uyarım kapsamında kullanımlarının zayıf olduğu gözlemlenmiştir. Genellikle tasarımcıları bitkisel tasarımlarında bitkileri gölge sağlama, yön gösterme ve bunun gibi amaçlar için kullanmaktadırlar. Bu bağlamda mevcut yapılan kentsel yeşil alanlarda ve parklarda duysal uyarım sağlayan bitki kullanımının ne ölçüde kullanıldığının incelenmesi bu çalışmanın asıl amacı olmuştur. Yapılan çalışma içerisinde Türkiye'nin Malatya kentinde var olan parkların duysal uyarım kapsamında peyzaj uygulamalarının değerlendirilmesi yapılmıştır.

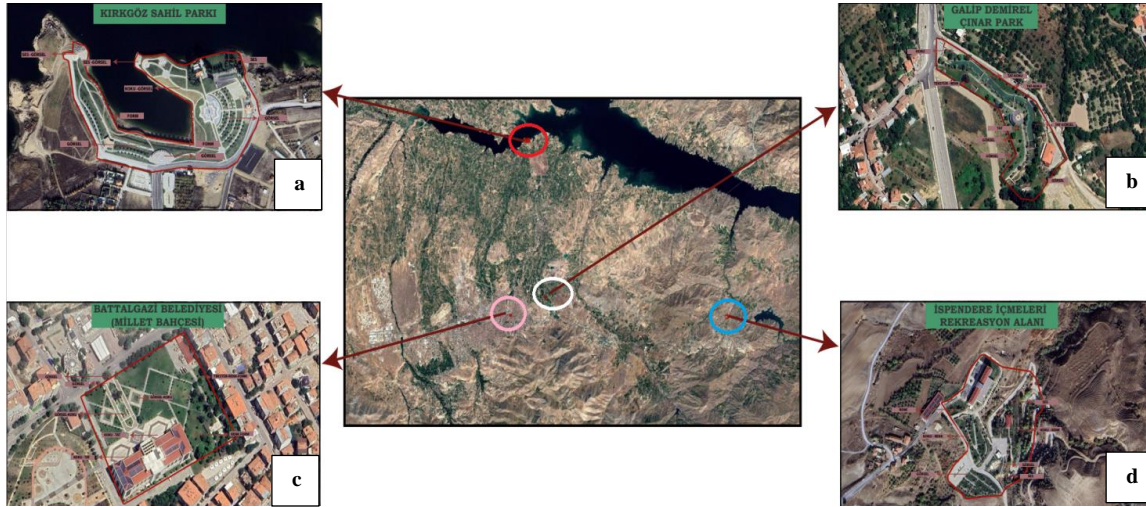
MATERYAL ve YÖNTEM

Malatya İlinin Coğrafi Konumu ve Peyzaj Özellikleri

Malatya, Doğu, Güneydoğu ve Orta Anadolu coğrafyasında bulunan bir ovadır. Yazlar sıcak ve kurak; kışlar ise, çoğu kez yağışlı ve soğuk olan sert iklime sahiptir. Malatya, kuzeyden güneye doğru hafif bir eğimle uzanmaktadır. Malatya'nın yüz ölçümü 12.313 km² olup, 35 54' ve 39 03' kuzey enlemleri ile 38 45' ve 39 08' doğu boylamları arasında kalmaktadır (MGM, 2024).

Malatya il arazisinin 367.253 hektarı (%30)'u ormanlık ve fundalıklarla, 125.156 hektarı (%10)'u ise çayır ve meralarla kaplıdır. Ormanlık alanı %10'dur. İl topraklarının güneyini boydan boya kaplayan batı-doğu doğrultulu Malatya dağlarının batı ucunda Sultansuyu vadisine bakan yamaçlarda akarsu çevreleri orman gibi uzayan kayısı (meyve) bahçeleri ile kaplıdır. Doğu Anadolu'da ortadan kalkmakta olan ibrelilerden kızılıçlılara rastlanmaktadır. Bu kesimde kalın bir toprak tabakası ile meyve ağaçları, söğüt ve kavaklıklar görülmektedir (Coğrafya Dünyası, 2024.).

Bu araştırmanın ana materyali Malatya kenti içinde bulunan önemli olan park ve rekreasyon alanları; Kırkgöz Rekreasyon ve Sahil Parkı, Çınar Park Rekreasyon Alanı, Millet Bahçesi (1. Etap), İspendere Rekreasyon Alanı olmuştur. Bu alanların bitkisel peyzaj tasarımları duysal uyarım açısından incelenmiştir (Şekil 2).



Şekil 2. Araştırmada seçilen alanların konumu. a: Kırkgöz Rekreasyon ve Sahil Parkı, b: Çınar Park Rekreasyon Alanı c: Millet Bahçesi 1. Etap, d: İspendere Rekreasyon Alanı (Google Earth, 2024).

Figure 2. Location of the areas selected in the research a: Kırkgöz Rekreasyon and Coastal Park, b: Çınar Park Rekreasyon Area c: Millet Bahçesi 1. Etap, d: İspendere Rekreasyon Area (Google Earth, 2024).

Yöntem

Bu çalışmada nitel ve nicel araştırma yöntemiyle elde edilen veriler konu kapsamında değerlendirilmiş, konu içeriği ile ilişkili olduğu düşünülen kaynak ve rekreasyon parkları incelenmiş ve bitki listeleri çalışmanın içeriğine dahil edilmiştir. Bu çalışma Malatya' da yer alan 4 adet rekreasyon alanının bitkisel tasarımı duysal uyarım açısından incelenmiştir. Araştırmada seçilen rekreasyon alanlarındaki

mevut bitkilerin duysal etmenler (görme, işitme, koklama, tatma, tekstür ve form) kapsamında alanda doğrudan incelemeler yapılmış ve yerinde analizlerle fotoğraflama yöntemi kullanılmıştır. Alanlarda kullanılan bitkilerin hangi mevsimde hangi duyuya hitap ettiğini araştırmak için mevcut ilgili literatürden yararlanmıştır. Ancak bazı bitki türlerin duysal uyarımı konusundaki bilgisi mevcut literatürde bulunmamıştır ve hangi tür hangi duyuya hitap etme konusundaki eksik veriler yazarların bizzat kendi incelemelerine göre sağlanmıştır.

BULGULAR ve TARTIŞMA

Kırkgöz Sahil Parkı Rekreasyon Alanı

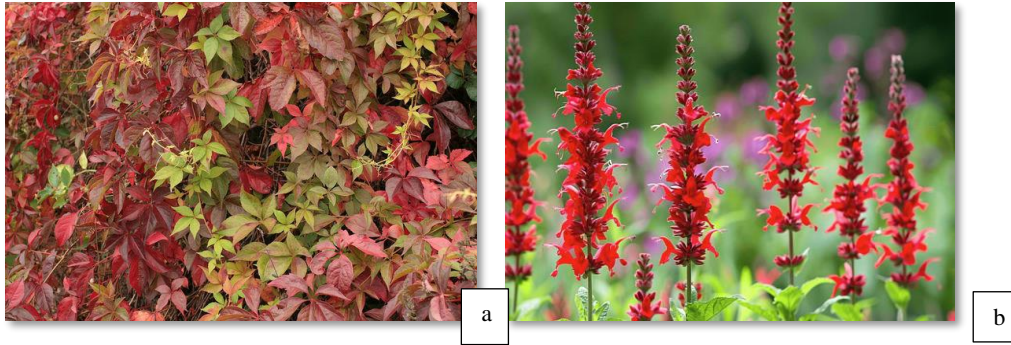
Kırkgöz Rekreasyon ve Sahil Yolu Projesi 150 bin metrekare alana sahiptir. Proje de 2 adet sosyal tesis mevcuttur. İçerisinde; çocuk oyun alanları, otopark alanı, çocuklar için doğa keşif merkezleri, kuş gözlem kulesi, fotoğraf çekme alanları ve ailelerin hem dumanlı hem dumansız piknik yapabilecekleri alanlar mevcuttur. Alanın tarihi dokusuna yönelik ve ismi ile müstesna olan Kırkgöz Köprüsünü simgeleyen giriş kapısı, yer yer bank ve pergolelere motif olarak işlenmiştir (Şekil 3).



Şekil 3. Kırkgöz sahil parkı tasarım projesi (Malatya Battalgazi Belediyesi, 2024).

Figure 3. Kırkgöz coastal park design project (Malatya Battalgazi Municipality, 2024).

Kırkgöz Rekreasyon Alanında yer alan görme-dokunma duysuna hitap eden bitkiler yer almıştır. Ağaç olarak Kırmızı Yapraklı Süs Eriği (*Prunus cerasifera* piss. nigra), Çin Sığılası (*Liquidambar styraciflua formosana*) örnekleri verilir. Çalı Olarak Kırmızı Kadın Tuzluğu (*Berberis thunbergii*), Lavanta (*Lavandula officinalis*), Altuni taflan (*Euonymus japonica aurea*), Gümüşü Taflan (*Euonymus japonica silverking*) Sarmaşık olarak Amerikan Sarmaşığı (*Parthenocissus quinquefolia*), Orman Sarmaşığı (*Hedera helix*) gibi örnekler verilebilir (Şekil 4). Alanda bulunan bitki türlerin hangi duyuya hitap etmesi Çizelge 1’de ve farklı mevsimlerde duysal etkilere sahip bitki türleri Çizelge 2’de açıklanmıştır. Sonuçlar bu alanda tatma ve işitme duysunu uyandıran bitki türlerin az olmasını açıklamıştır.



Şekil 4. Sonbahar aylarında rengini kırmızıya bırakan a: Amerikan Sarmaşığı (*Parthenocissus quinquefolia*) Görme duyusu ve Kırmızı Çiçekli b: Ada Çayı (*Salvia jamensisflammen*) Görmel-Dokunma duyusu.

Figure 4. The sense of sight of a: *Parthenocissus quinquefolia*, which changes its color to red in the autumn months, and the sense of sight-touch of b: *Salvia jamensisflammen*.

Çizelge 1. Kırgöz rekreasyon ve sahil alanında yer alan bitkilerin duyuşal uyarımı açısından incelenmesi.

Table 1. Examination of the plants in Kırgöz recreation and coastal area in terms of sensory stimulation.

Sayı	Latince Adı	Türkçe Adı	Duyusal Uyarımı	Kaynak
1	<i>Acer saccharinum</i>	Şeker Akçaağaç	Görme duyusu	Gülgün ve ark., 2007; Altınçekiç, 2000; Acar ve ark., 2009; Bilgili ve ark., 2014; Acıbuca ve Budak, 2018; Faydaoğlu ve Sürücüoğlu, 2011; Pouya, 2019; Arslan ve ark., 2015; Tilley, 2006; Lambe 1995; Andić ve ark., 2022; Yamauchi ve ark., 2018; Leonard ve Masek, 2014; Akkemik, 2014).
2	<i>Cupressocyparis leylandi goldrider</i>	Şekilli Gold Leylandi	Görme duyusu	
3	<i>Cupressocyparis leylandi spiralle</i>	Şekilli Spiral Formlu Leylandi	Görme duyusu	
4	<i>Cupressus arizonica</i>	Arizona Servisi	Görme duyusu	
5	<i>Cupressocyparis leylandi MultiPompos</i>	Ponpon Leylandi	Görme duyusu	
6	<i>Buxus sempervirens</i>	Top Şimşir	Görme duyusu	
7	<i>Prunus cerasifera piss. “Nigra”</i>	Süs Eriği	Görme-Dokunma duyusu	
8	<i>Lagerstroemia indica</i>	Oya Ağacı	Görme-Dokunma duyusu	
9	<i>Liquidambar styraciflua</i>	Amerikan Sığlası	Görme duyusu	
10	<i>Fraxinus americana autumn applause</i>	Turuncu Dış Budak	Görme duyusu	
11	<i>Liquidambar styraciflua formosana</i>	Çin Sığlası	Görme duyusu	
12	<i>Ligustrum japonica</i>	Kurtbağrı	Görme-Dokunma duyusu	
ÇALILAR , YER ÖRTÜCÜLER ve ÇİÇEKLER				
Sayı	Latince Adı	Türkçe Adı	Duyusal Uyarımı	
1	<i>Jasminum sambac</i>	Arap Yasemini	Koku-Görme duyusu	
2	<i>Lavandula officinalis</i>	Lavanta	Görme-Tat-Koku duyusu	
3	<i>Buxus microphyllafaulkner</i>	Küçük Yapraklı Şimşir	Görme duyusu	
4	<i>Euonymus japonica “Aurea”</i>	Altuni Taflan	Görme-Dokunma duyusu	
5	<i>Weigelia atropurpurea “Nana”</i>	Gelin Tacı	Görme duyusu	
7	<i>Abelia grandiflora</i>	Güzellik Çalısı	Görme duyusu	
8	<i>Berberis thunbergii</i>	Kırmızı Kadın Tuzluğu	Görme-Dokunma duyusu	
9	<i>Cotoneaster microphyllusstra</i>	Dağ Muşmulası	Görme duyusu	
10	<i>Euonymus japonica “Aura”</i>	Altuni Taflan	Görme duyusu	
11	<i>Euonymus japonica silverking</i>	Gümüşü Taflan	Görme duyusu	
12	<i>Euonymus japonica</i>	Yeşil Taflan	Görme duyusu	
13	<i>Euryops pectinatus</i>	Güneş Papatya Çalısı	Koku-Görme duyusu	

14	<i>Gaura lindheimeris</i> pink	Gaura	Görme duyusu
15	<i>Hypericum calycinum</i>	Sarı Kantaron Çiçeği	Koku-Görme-Tat duyusu
16	<i>Rosmarinus officinalis</i>	Biberiye	Tat-Koku duyusu
17	<i>Lonicera caprifolium</i>	Yaylıcı Hanımeli	Koku-Görme duyusu
18	<i>Juniperus sabina</i>	Sabin Ardıcı	Görme duyusu
19	<i>Nandina domestica</i> firepower	Bodur Cennet Bambusu	Görme-Dokunma duyusu
20	<i>Photinia fraseri</i> red robin	Alev Çalısı	Görme duyusu
21	<i>Pyracantha navaho</i>	Bodur Ateş Dikeni	Görme-Dokunma duyusu
22	<i>Salvia jamensis</i> flammen	Kırmızı Çiçekli Adaçayı	Tat-Koku duyusu
23	<i>Teucrium fruticans</i>	Zeytin Çalısı	Dokunma duyusu
24	<i>Viburnum lucidum</i>	Kartopu Çalısı	Görme duyusu
25	<i>Buxus rotundifolia</i>	Yerli Şimşir	Görme duyusu
26	<i>Abelia grandiflora</i> "Nana"	Beyaz Alaca Yapraklı Güzellik Çalısı	Görme-Dokunma duyusu
27	<i>Carex oshimensis</i> 'Evergold'	Altuni Yapraklı Ters	Görme-Dokunma duyusu
28	<i>Photinia nana</i>	Bodur Alev Çalısı	Görme-Dokunma duyusu
29	<i>Parthenocissus quinquefolia</i>	Amerikan Sarmaşığı	Görme duyusu
30	<i>Hedera helix</i>	Orman Sarmaşığı	Görme duyusu
31	<i>Plantago lanceolata</i>	Yumuşak ot	Ses (İşitme duyusu)

Çizelge 2. Kırkgöz sahil parkı ve rekreasyon alanında yer alan bazı bitkilerin mevsimlerine göre duyuşal açıdan incelenmesi.

Table 2. Sensory examination of some plants in Kırkgöz coastal park and recreation area according to seasons.

	Koklama	Tatma	Görme	Dokunma	İşitme	Kaynak
İlkbahar	Gümüşi ıhlamur (<i>Tilia tomentosa</i>) Koku -Görme - Tat duyusu	-	Gelin tacı (<i>Weigelia atropurpurea</i> "Nana") - Görsel duyu	-	Yumuşak ot (<i>Plantago lanceolata</i>) ses duyusu	Gülgün ve ark., 2007; Altınçekiç, 2000; Acar ve ark., 2009; Bilgili ve ark., 2014; Acıbuca ve Budak, 2018; Faydaoğlu ve Sürücüoğlu, 2011; Pouya, 2019;
Yaz	Petunya (<i>Petunia integrifolia</i>) Koku-Görsel duyu	Lavanta (<i>Lavandula officinalis</i>) Tat-Koku duyusu	Rozet Çiçeği (<i>Vinca sp.</i>) Koku-Görsel duyu	Adaçayı (<i>Salvia officinalis</i>)	Yumuşak ot (<i>Plantago lanceolata</i>) ses duyusu	Arslan ve ark., 2015; Tilley, 2006; Lambe 1995; Andić ve ark., 2022; Yamauchi ve ark., 2018; Leonard ve Masek, 2014; Akkemik, 2014
Sonbahar	Biberiye (<i>Rosmarinus officinalis</i>) Koku-Tat Duyusu	-	Amerikan Sarmaşığı (<i>Parthenocissus quinquefolia</i>) Görsel duyu	Konik formulu kurtbağrı (<i>Ligustrum japonicum texanum</i>)	-	
Kış	Limoni servi (<i>Cupressus macrocarpa</i> Goldcrest) Koku-görsel	-	Süs Lahanası (<i>Brassica oleracea</i> var. <i>Acephala</i>) Form-Görsel duyu	Orman sarmağı (<i>Hedera helix</i>) Dokunma duyu	-	

Çınar Park Rekreasyon Alanı

Battalgazi Belediyesi Tarihi Çınar Ağacı Rekreasyon Alanı Projesi, geniş bir alanı kapsayan doğal, tarih ve kültürel alanın korunması amacıyla yapılmış bir çalışmadır. Çevre düzenlemeleri halkın gereksinimleri göz önünde bulundurularak hazırlanmış ve Çınar Parkının içinde bisiklet ve yürüyüş yolları, suni gölet, oturma grupları, çocuk parkı, mesire alanları, bölgede yaşayan medeniyetleri anlatan

rölyeflerle işlenmiş duvarlar yer almaktadır. Bu medeniyet duvarında ilçenin tema yüz etmiş tarihi ve kültürel değerleri duvarlara nakşedilecek böylece insanlara geçmişi ve değerleri hakkında farkındalık kazandırılacak bir mekân olarak tasarlanmıştır ([Malatya Battalgazi Belediyesi, 2024](#)).

Alanda yer alan Petunya (*Petunia integrifolia*), hem renk hem de koku fonksiyonu ile duyulara hitap etmektedir (Şekil 5). Burada 700 yıllık Büyük Çınar (*Platanus orientalis* extra) rivayete göre Battalgazi'nin görseldeki çınar ağacını diktiği bilinir. Bu ağaç tekstür ve form açısından dikkat çekmiştir. Alanda bulunan bitki türlerin hangi duyuya hitap etmesi Çizelge 3'te ve farklı mevsimlerde duyusal etkilere sahip bitki türleri Çizelge 4'te açıklanmıştır. Sonuçlar bu alanda bitki türlerin çoğu görme duyusuna hitap ederken tatma ve işitme duyusunu uyaran bitki türlerin az olması açıklamıştır.

Çizelge 3. Çınar park rekreasyon alanında yer alan bitkilerin duyusal açıdan incelenmesi.

Table 3. Sensory examination of some plants in Çınar park recreation area according to seasons.

Sayı	Latince Adı (Ağaçlar)	Türkçe Adı	Duyusal Uyarımı	Kaynak
1	<i>Platanus orientalis</i>	Çınar	Görme-Dokunma Duyusu	Gülgün ve ark., 2007; Altınçekiç, 2000; Acar ve ark., 2009; Bilgili ve ark., 2014; Acıbuca ve Budak, 2018; Faydaoğlu ve Sürücüoğlu, 2011; Pouya, 2019; Arslan ve ark., 2015; Tilley, 2006; Lambe 1995; Andić ve ark., 2022; Yamauchi ve ark., 2018; Leonard ve Masek, 2014; Akkemik, 2014.
2	<i>Platanus orientalis</i> extra	Büyük Çınar	Görme-Dokunma Duyusu	
3	<i>Prunus ceraciferapisnigra</i>	Kırmızı Yapraklı Süs Eriği	Görme Duyusu	
4	<i>Tilia tomentosa</i>	İhlamur	Koku Duyusu	
5	<i>Ligustrum texanum</i>	Kurtbağrı	Görme Duyusu	
6	<i>Nerium oleander nana</i>	Zakkum	Görme Duyusu	
7	<i>Ligustrum japonicum texanum</i>	Konik Formlu Kurtbağrı	Görme Duyusu	
8	<i>Cupressus macrocarpa</i> Goldcrest	Limon servi şekilli	Görme-Koku Duyusu	
9	<i>Cupressocyparis leylandii spiralle</i>	Leylandi şekilli	Görme Duyusu	
10	<i>Photinia fraseri</i> red robin	Alev ağacı	Görme Duyusu	
11	<i>Prunus laurocerasus</i>	Laz kirazı (Karayemiş)	Görme Duyusu	
12	<i>Acer palmatum</i>	Japon Akçağacı	Görme Duyusu	
13	<i>Betula Pendula</i>	Huş Ağacı	Dokunma-Görme Duyusu	
Sayı	Latince Adı (Çalılar)	Türkçe Adı	Duyusal Uyarımı	
1	<i>Santolina chamaecyparissus</i>	Gri santolina	Dokunma-Görme Duyusu	
2	<i>Rosmarinus officinalis</i>	Biberiye	Tat-Koku Duyusu	
3	<i>Abelia grandiflora</i> "Nana"	Beyaz Alaca Yapraklı Güzellik Çalısı	Görme Duyu	
4	<i>Pyracantha navaho</i>	Bodur Ateş Dikeni	Görme-Dokunma Duyusu	
5	<i>Teucrium fruticans</i>	Zeytin Çalısı	Dokunma Duyusu	
6	<i>Cotoneaster microphyllus</i> stra.	Dağ Muşmulası	Görme Duyusu	
7	<i>Gaura</i>	Gaura	Görme Duyusu	
8	<i>Buxus microphylla</i> faulkner	Küçük Yapraklı Şimşir	Görme duyusu	
9	<i>Euonymus japonica aurea</i>	Altuni Taflan	Görme-Dokunma Duyusu	
10	<i>Viburnum tinus</i>	Defne Yapraklı Kartopu	Görme Duyusu	
11	<i>Jasminum sambac</i>	Arap Yasemini	Koku-Görme Duyusu	
12	<i>Lavandula officinalis</i>	Lavanta	Tat-Koku Duyusu	
13	<i>Berberis thunbergii</i> atropurpurea	Kırmızı KadınTuzluğu	Görme-Dokunma Duyusu	
14	<i>Nandina domestica</i> firepower	Bodur Cennet Bambusu	Görme-Dokunma Duyusu	
15	<i>Weigelia atropurpurea</i> "Nana"	Gelin Tacı	Görme Duyusu	
16	<i>Carex oshimensis</i> 'Evergold'	Altuni Yapraklı Ters Karex	Görme-Dokunma Duyusu	
17	<i>Photinia</i> "Nana"	Bodur Alev Çalısı	Görme-Dokunma Duyusu	
18	<i>Parthenocissus quinquefolia</i>	Amerikan Sarmaşığı	Görme Duyusu	

Çizelge 4. Çınar park rekreasyon alanında yer alan bazı bitkilerin mevsimlerine göre duyuşal açıdan incelenmesi.

Table 4. Sensory examination of plants in Çınar park recreation area.

İlkbahar	Yaz	Sonbahar	Kış	Kaynak
Gelin tacı (<i>Weigelia</i> <i>atropurpurea</i> "Nana")- Görsel duyu	Petunya (<i>Petunia</i> <i>integrifolia</i>) Koku-Görsel duyu	Amerikan Sarmaşığı (<i>Parthenocissus</i> <i>quinquefolia</i>) Görsel duyu	Süs Lahanası (<i>Brassica oleracea</i> var. <i>Acephala</i>) Form-Görsel duyu	Gülgün ve ark., 2007; Altınçekiç, 2000; Acar ve ark., 2009; Bilgili ve ark., 2014; Acıbuca ve Budak, 2018; Faydaoğlu ve Sürücüoğlu, 2011; Pouya, 2019; Arslan ve ark., 2015; Tilley, 2006; Lambe 1995; Andić ve ark., 2022; Yamauchi ve ark., 2018; Leonard ve Masek, 2014; Akkemik, 2014
<i>Gaura lindheimeri</i> - Görsel duyu	Rozet Çiçeği (<i>Vinca</i> sp.) Koku-Görsel duyu	Kırmızı kadın tuzluğu (<i>Berberis thunbergii</i> <i>atropurpurea</i>) Görsel duyu	Konik formlu kurtbağı (<i>Ligustrum japonicum texanum</i>) Görsel duyu	
Altuni yapraklı ters kareks (<i>Carex oshimensis</i> 'Evergold')- Görsel duyu	Lavanta (<i>Lavandula officinalis</i>) Tat-Koku duyusu	Defne yapraklı kartopu (<i>Viburnum tinus</i>) Görsel duyu	Orman sarmağı (<i>Hedera helix</i>) Görsel duyu	
Gümüşü ıhlamur (<i>Tilia tomentosa</i>) Koku-Görsel duyu	Küçük yapraklı şimşir (<i>Buxus microphylla faulkner</i>) Görsel duyu	Biberiye (<i>Rosmarinus officinalis</i>) Koku-Tat Duyusu	Limoni servi (<i>Cupressus macrocarpa</i> Goldcrest) Koku-görsel Duyu	



Şekil 5. Çınar park rekreasyon alanında yer alan mevsimlik çiçeklerden Petunya (*Petunia integrifolia*), görme-koku duyusunu uyandırmaktadır.

Figure 5. *Petunia (Petunia integrifolia)*, seasonal flowers in the Çınar park recreation area, It awakens the sense of sight and smell.

Battalgazi Millet Bahçesi (1. etap)

Çalışma alanı olarak belirtilen Battalgazi Belediyesi Millet Bahçesi (1. etap) Uçbağlar Mahallesi 32.844 m²'lik alana sahiptir. Park içerisinde 2 kütüphane, 1 çay ocağı, 5 adet çardak ve yürüyüş yolları bulunmaktadır (Battalgazi Belediyesi Park İşleri Müdürlüğü).

Battalgazi Belediyesi bahçesinde mevcut bitkisel tasarımda havuz kenarlarında *Rosa* sp. (Gül) kullanılmıştır. Alanın orta kısımlarda *Magnolia grandiflora* (Manolya), *Laurus nobilis pyramidalis* (Piramit defne), *Cupressus arizonica greene* (Mavi servi), *Morus nigra pendula* (Ters dut) *Tilia tomentosa* (Gümüşi ıhlamur), *Lagerstromia indica* (Oya ağacı) ağaçları kullanılmıştır. Açık otopark kısmında *Platanus orientalis* (Çınar ağacı), *Gingo biloba* (Mabet Ağacı) yer alır. Sarmaşık olarak kapalı otoparka girişte *Parthenocissus quinquefolia* (Amerikan sarmaşığı), *Hedera helix* (Kaya sarmaşığı), *Lonicera caprifolium* (Sarılıcı hanımeli) yer almaktadır. Bina girişi sağ ve sol beton saksılıklarda *Diantus sinensis* (Çin karanfili), *Thymus vulgaris* (Kekik), *Lavandula officinalis* (Lavanta), *Cupressocyparis leylandii spiralle* (Spiral formlu leylandi) kullanılmıştır. Alanda bulunan bitki türlerin hangi duyuya hitap etmesi Çizelge 5'te ve farklı mevsimlerde duyusal etkilere sahip bitki türleri Çizelge 6'da açıklanmıştır.

Çizelge 5. Millet bahçesi 1. Etap rekreasyon alanında yer alan bitkilerin duyusal açıdan incelenmesi.

Table 5. Sensory examination of plants in the recreation area of the National Garden Stage 1.

Sayı	Latince Adı	Türkçe Adı	Duyusal Uyarımı	Kaynak
1	<i>Cupressus leylandii</i>	Leylandi pramit	Görme Duyusu	Gülgün ve ark., 2007; Altınçekiç, 2000; Acar ve ark., 2009; Bilgili ve ark., 2014; Acibuca ve Budak, 2018; Faydaoğlu ve Sürücüoğlu, 2011; Pouya, 2019; Arslan ve ark., 2015; Tilley, 2006; Lambe 1995; Andić ve ark., 2022; Yamauchi ve ark., 2018; Leonard ve Masek, 2014; Akkemik, 2014
2	<i>Cupressus sempervirens arizonica glauca</i>	Mavi Leylandi	Görme Duyusu	
3	<i>Acer palmatum</i>	K. Yapraklı akçağaç	Görme Duyusu	
4	<i>Picea Glauca Conica</i>	Konik Ladin	Görme-Dokunma Duyusu	
5	<i>Piceapungens"Glauc"</i>	Mavi Ladin	Görme Duyusu	
6	<i>Cupressus leylandii (spiral ve 3 top karışık)</i>	Leylandi şekilli	Görme Duyusu	
7	<i>Ginko biloba</i>	Çin Mabet Ağacı	Dokunma-Görme Duyusu	
8	<i>Abies nordmanniana</i>	Gökknar	Görme Duyusu	
9	<i>Platanus oientalis</i>	Çınar	Görme Duyusu	
10	<i>Acer platanoides</i>	Çınar yapraklı akçağaç	Görme Duyusu	
11	<i>Catalpa bignonioides "Nana"</i>	Top katalpa	Görme Duyusu	
12	<i>Morus alba pendula</i>	Ters dut	Tat-Görme Duyusu	
13	<i>Magnolia grandiflora</i>	Manolya Pramit	Görme-Koku-Dokunma Duyusu	
14	<i>Flaxinus excelsior</i>	Dişbudak	Görme Duyusu	
15	<i>Laurus nobilis</i>	Defne	Koku-Tat Duyusu	
16	<i>Syringia vulgaris</i>	Leylak	Koku-Görme Duyusu	
17	<i>Tilia tomentosa</i>	Gümüşi ıhlamur	Koku-Tat Duyusu	
18	<i>Picea abies</i>	Batı Ladini	Görme Duyusu	
19	<i>Lagerstromia indica</i>	Oya Ağacı	Görme-Dokunma Duyusu	
20	<i>Cupressus leylandii</i>	Leylandi	Görme Duyusu	
Sayı	Latince Adı	Türkçe Adı	Duyusal Uyarımı	
1	<i>Chamaecyparis lawsoniana elvudi</i>	Elvudi	Görme Duyusu	
2	<i>Gaura lindheimeri</i>	Gaura	Görme Duyusu	
3	<i>Dianthus</i>	Bodur Çin Karanfili	Koku-Görme Duyusu	
4	<i>Rosmarinus officinalis</i>	Kekik	Koku- Tat Duyusu	
5	<i>Erica cernea</i>	Erica	Görme Duyusu	
6	<i>Thuja occidentalis smaragd</i>	Mazı Smargart	Görme Duyusu	
7	<i>Nandina domestica</i>	Cennet Bambusu	Görme Duyusu	
8	<i>Rosa</i> sp. (3-4 yıllık)	Yediveren gül	Koku-Görme Duyusu	
9	<i>Rosa</i> sp. (Peyzaj gülü yayılcı)	Renk Polliyana	Koku-Görme Duyusu	
10	<i>Rosa</i> sp. (Peyzaj gülü yayılcı)	Renk beyaz	Koku -Görme Duyusu	
11	<i>Rosa</i> sp. (Peyzaj gülü yayılcı)	Renk Koyu Pembe	Koku- Görme Duyusu	

12	<i>Rosa</i> sp.(Meyland pembe)	Meyland pembe	Koku-Görme Duyusu
13	<i>Rosa</i> sp.(Meyland kırmızı)	Meyland Kırmızı	Koku-Görme Duyusu
14	<i>Rosa</i> sp.(Peyzaj gülü yayılcı)	Renk Kırmızı	Koku-Görme Duyusu
15	<i>Rosa</i> sp.(Baston Gül)	Renk karışık	Koku-Görme Duyusu
16	<i>Rosa</i> sp.(Sarmaşık gül)	Renk karışık	Koku-Görme Duyusu
17	<i>Berberis thunbergii</i>	Kadın Tuzluğu	Görme Duyusu
18	<i>Buxus rotundifolia</i>	Şimşir	Görme Duyusu
19	<i>Buxus sempervirens</i> (Top)	Osmanlı Şimşiri (Top)	Görme Duyusu
20	<i>Hedera helix</i>	Duvar Sarmaşığı	Görme Duyusu
21	<i>Amphelopsis americana</i>	Amerikan sarmaşığı	Görme Duyusu
22	<i>Photinia serrulata</i>	Alev Çalısı	Görme Duyusu
23	<i>Lonicera japonica</i>	Sarılcı Hanımeli	Koku-Görme Duyusu
24	<i>Pyracantha coccinea</i>	Ateş Dikeni	Görme Duyusu
25	<i>Carex oshimensis</i> 'Everblood'	Altuni Yapraklı Ters	Görme-Dokunma Duyusu
26	<i>Photinia nana</i>	Bodur Alev Çalısı	Görme-Dokunma Duyusu
27	<i>Lavandula officinalis</i>	Lavanta	Tat-Koku Duyusu

Çizelge 6. Millet bahçesi içerisinde yer alan bazı bitkilerin mevsimlerine göre duysal açıdan incelenmesi.

Table 6. Sensory examination of some plants in the public garden according to their seasons.

	Koklama	Tatma	Görme	Dokunma	İşitme	Kaynak
İlkbahar	Sarılcı Hanımeli (<i>Lonicera japonica</i>) Koku Duyusu		<i>Rosa</i> sp.(Baston gül) Görme-Koku	Manolya (<i>Magnolia grandiflora</i>) Dokunma-Görsel-Koku Duyusu	Yumuşak ot (<i>Plantago lanceolata</i>) Ses duyusu	Gülgün ve ark., 2007; Altınçekiç, 2000; Acar ve ark., 2009; Bilgili ve ark., 2014; Acıbuca ve Budak, 2018; Faydaoğlu ve Sürücüoğlu, 2011; Pouya, 2019; Arslan ve ark., 2015; Tilley, 2006; Lambe 1995; Andić ve ark., 2022; Yamauchi ve ark., 2018; Leonard ve Masek, 2014; Akkemik, 2014
Yaz	Gül (<i>Rosa</i> sp.) Koku Duyusu	Ters Dut (<i>Morus alba pendula</i>) Tat-Görme Duyusu	<i>Erica</i> (<i>Erica cernea</i>) Görme Duyusu	Oya Ağacı (<i>Lagerstromia indica</i>) Dokunma-Görsel duyu	Dar yapraklı sinirli ot (<i>Plantago lanceolata</i>) Ses duyusu	
Sonbahar	Biberiye (<i>Rosmarinus officinalis</i>) Koku-Tat Duyusu		Ateş Dikeni (<i>Pyracantha coccinea</i>) Görsel duyu	Çin Mabet Ağacı (<i>Gingo biloba</i>) Dokunma duyusu		
Kış	Mavi Leylandi (<i>Cupressus sempervirens arizonica glauca</i>) Görme – Koku Duyusu	Defne (<i>Laurus nobilis</i>) Tat-Koku-Görme Duyusu	Osmanlı Şimşiri Top (<i>Buxus sempervirens</i>) Görme Duyusu	Konik Ladin (<i>Picea Glauca Conica</i>) Dokunma-Görme Duyusu		

İspendere Şifalı İçmeleri ve Rekreasyon Alanı

Alanda konaklama tesisi, geleneksel ve tamamlayıcı tıp bölümleri, termal havuzlar, hamam, sauna, buhar odası, konferans, toplantı salonları ile de bölge halkı, yerli ve yabancı turistler için bir sağlık turizm merkezi oluşturulmuştur. Mevcut doğal yapı korunarak alanda planlanan şelale, gölet, mesire alanları, bisiklet ve yürüyüş parkurları, çocuk oyun alanları, kafe ve restoranlar ile halkın daha aktif kullanımı amaçlanmıştır. Havza bazlı 500 dekar alanda ağaçlandırma ve sonrasında tabiat parkı yapılması altyapı ve rekreasyon uygulamaları yapılarak, İnönü Üniversitesi Tıp Fakültesi iş birliği ile geleneksel ve tamamlayıcı tıp tedavi ve uygulama merkezi oluşturularak kırsal turizm altyapısı tesis edilmiştir

([Malatya Battalgazi Belediyesi, 2024](#)). Alanda iki adet termal havuz yapılmıştır. Tedaviye gelen vatandaşların konaklama ihtiyacının karşılanması amacıyla 20 oda 40 yataklı konaklama odaları yapılmıştır. 100 dekar alanda yapılan rekreasyon düzenlemeleri ile piknik alanları, oyun grupları, yürüyüş ve bisiklet parkuru alanda yer almaktadır.

Alanda ağaç ve çalı gurubu olarak *Ginkgo biloba* (Çin mabet ağacı), *Abies nordmanniana* (Gökmar), *Prunus cerasifera* piss. Nigra (Kırmızı süs eriği), *Liquidambar styraciflua formosana* (Çin Sığlası), *Cupressus arizonica* (Arizona servisi), *Tilia tomentosa* (Ihlamur), *Ligustrum texanum* (Kurtbağrı), *Lagerstroemia indica* (Oya ağacı), *Liquidambar styraciflua* (Amerikan sığlası), *Betula Pendula* (Huş ağacı), *Cupressocyparis leylandispiralle* (Şekilli spiral formlu leylandi), *Populus tremula* (Titrek kavak), *Buxus sempervirens* (Top şimşir), *Fraxinus americana autumn applause* (Turuncu dış budak) yer almaktadır. Çalı ve yer örtücü olarak *Bambuseae* (Bambu), *Lavandula officinalis* (Lavanta), *Euonymus japonica aurea* (Altuni taflan), *Gaura lindheimerisiskiyou pink* (Gaura), *Cotoneaster microphyllusstra*. (Dağ muşmulası), *Euonymus japonica silverking* (Gümüşü taflan), *Viburnum lucidum* (Kartopu çalısı), *Hypericum calycinum* (Sarı kantaron çiçeği), *Pyracantha navaho* (Bodur ateş diken), *Salvia jamensisflammen* (Kırmızı çiçekli adaçayı), *Teucrium fruticans* (Zeytin çalısı), *Juniperus sabina* (Sabin ardıcı), *Parthenocissus quinquefolia* (Amerikan sarmaşığı), ve *Hedera helix* (Orman sarmaşığı) bulunmaktadır. Alanda bulunan bitki türlerin hangi duyuya hitap etmesi Çizelge 7’de ve farklı mevsimlerde duyuusal etkilere sahip bitki türleri Çizelge 8’de açıklanmıştır.

Çizelge 7. İspendere Şifalı İçmeler ve rekreasyon alanında yer alan bitkilerin duyuusal açıdan incelenmesi.

Table 7. Sensory examination of plants in İspendere Healing Springs and recreation area.

Sayı	LatinceAdı	Türkçe Adı	Duyusal Uyarımı	Kaynak
1	<i>Ginkgo biloba</i>	Çin Mabeta Ağacı	Görme-Dokunma Duyusu	Gülğün ve ark., 2007; Altınçekiç, 2000; Acar ve ark., 2009; Bilgili ve ark., 2014; Acıbuca ve Budak, 2018; Faydaoğlu ve Sürücüoğlu, 2011; Pouya, 2019; Arslan ve ark., 2015; Tilley, 2006;
	<i>Abies nordmanniana</i>	Gökmar	Görme Duyusu	
2	<i>Prunus cerasifera</i> “piss. Nigra”	SüsEriği	Görme Duyusu	
3	<i>Liquidambar styraciflua formosana</i>	Çin Sığlası	Görme Duyusu	
4	<i>Cupressus arizonica</i>	Arizona Servisi	Görme Duyusu	
5	<i>Tilia tomentosa</i>	Ihlamur	Koku Duyusu	
6	<i>Ligustrum texanum</i>	Kurtbağrı	Koku-Dokunma Duyusu	
7	<i>Lagerstroemia indica</i>	Oya Ağacı	Koku-Dokunma Duyusu	
8	<i>Liquidambar styraciflua</i>	Amerikan Sığlası	Görme Duyusu	
9	<i>Acer palmatum</i>	Japon Akçağacı	Görme Duyusu	
10	<i>Betula pendula</i>	Huş Ağacı	Görme-Dokunma Duyusu	
11	<i>Cupressocyparis leylandi goldrider</i>	Şekilli Gold Leylandi	Görme Duyusu	
12	<i>Cupressocyparis leylandi spiralle</i>	Şekilli Spiral Formlu Leylandi	Görme Duyusu	
13	<i>Populus tremula</i>	Titrek Kavak	İşitme Duyusu	
14	<i>Buxus sempervirens</i>	Top Şimşir	Görme Duyusu	
15	<i>Ligustrum japonica</i>	Kurtbağrı	Görme-Dokunma Duyusu	
16	<i>Fraxinus americana autumn applause</i>	Turuncu Dışbudak	Görme Duyusu	
ÇALILAR, YER ÖRTÜCÜLER ve ÇİÇEKLER				
Sayı	Latince Adı	Türkçe Adı	Duyusal Uyarımı	
1	<i>Bambuseae</i>	Bambu	İşitme Duyusu	
2	<i>Lavandula officinalis</i>	Lavanta	Tat-Koku Duyusu	

3	<i>Buxus microphylla</i> faulkner	Küçük Yapraklı Şimşir	Görme Duyusu	Lambe 1995; Andić ve ark., 2022; Yamauchi ve ark., 2018; Leonard ve Masek, 2014; Akkemik, 2014
4	<i>Euonymus japonica</i> “Aura”	Altuni Taflan	Görme-Dokunma Duyusu	
5	<i>Euryopspectinatus</i>	Güneş Papatya Çalısı	Koku-Görme Duyusu	
7	<i>Gaura lindheimeri</i> siskiyou pink	Gaura	Görme Duyusu	
8	<i>Berberis thunbergii</i>	Kırmızı Kadın Tuzluğu	Görme-Dokunma Duyusu	
9	<i>Cotoneaster microphyllus</i> stra.	Dağ Muşmulası	Görme Duyusu	
10	<i>Euonymus japonica</i> “Aura”	Altuni Taflan	Görme Duyusu	
11	<i>Euonymus japonica</i> silverking	Gümüşi Taflan	Görme Duyusu	
12	<i>Euonymus japonicus</i>	Yeşil Taflan	Görme Duyusu	
13	<i>Viburnum lucidum</i>	Kartopu Çalısı	Görme Duyusu	
14	<i>Buxus rotundifolia</i>	Yerli Şimşir	Görme Duyusu	
15	<i>Hypericum calycinum</i>	Sarı Kantaron Çiçeği	Koku-Tat-Görme Duyusu	
16	<i>Rosmarinus officinalis</i>	Biberiye	Tat-Koku Duyusu	
17	<i>Nandina domestica</i> firepower	Bodur Cennet Bambusu	Görme Duyusu	
18	<i>Photinia fraseri</i> red robin	Alev Çalısı	Görme-Dokunma Duyusu	
19	<i>Pyracantha navaho</i>	Bodur Ateş Dikeni	Görme –Dokunma Duyusu	
20	<i>Salvia jamensis</i> flammen	Kırmızı Çiçekli Adaçayı	Tat-Koku Duyusu	
21	<i>Teucrium fruticans</i>	Zeytin Çalısı	Dokunma-Görme Duyusu	
22	<i>Lonicera caprifolium</i>	Yayılcı Hammeli	Koku-Görme Duyusu	
23	<i>Juniperus sabina</i>	Sabin Ardıcı	Görme Duyusu	
24	<i>Carex oshimensis</i> 'Evergold'	Altuni Yapraklı Ters Kareks	Görme-Dokunma Duyusu	
25	<i>Photinia</i> “Nana”	Bodur Alev Çalısı	Görme-Dokunma Duyusu	
26	<i>Parthenocissus quinquefolia</i>	Amerikan Sarmaşığı	Görme Duyusu	
27	<i>Hedera helix</i>	Orman Sarmaşığı	Görme Duyusu	

Çizelge 8. İspendere rekreasyon alanında yer alan bazı bitkilerin mevsimlerine göre duysal açıdan incelenmesi.

Table 8. Sensory examination of some plants in İspendere recreation area according to seasons.

	Koklama	Tatma	Görme	Dokunma	İşitme	Kaynak
İlkbahar	Güneş Papatya Çalısı (<i>Euryops pectinatus</i>) Koku-görme Duyusu	Sarı Kantaron Çiçeği (<i>Hypericum calycinum</i>) Tat-Koku-Görme	Kartopu Çalısı (<i>Viburnum lucidum</i>) Görme-Dokunma duyusu	-	Yumuşak ot (<i>Plantago lanceolata</i>) ses duyusu	Gülgün ve ark., 2007; Altınçekiç, 2000; Acar ve ark., 2009; Bilgili ve ark., 2014; Acıbuca ve Budak, 2018; Faydaoğlu ve Sürücüoğlu, 2011; Pouya, 2019; Arslan ve ark., 2015; Tilley, 2006; Lambe 1995; Andić ve ark., 2022; Yamauchi ve ark., 2018; Leonard ve Masek, 2014; Akkemik, 2014
Yaz	Petunya (<i>Petunia integrifolia</i>) Koku-Görsel duyu	Lavanta (<i>Lavandula officinalis</i>) Tat-Koku duyusu	Yerli Şimşir (<i>Buxus rotundifolia</i>) Görme Duyusu	Adaçayı (<i>Salvia officinalis</i>)	Titrek Kavak (<i>Populus tremula</i>) İşitme Duyusu	
Sonbahar	Biberiye (<i>Rosmarinus officinalis</i>) Koku-Tat Duyusu	-	Kızaran cennet bambusu (<i>Nandina domestica</i> firepower) Görme Duyusu	Konik formlu kurtbağrı (<i>Ligustrum japonicum texanum</i>)	Bambu (<i>Bambuseae</i>) İşitme Duyusu	
Kış	-	-	Gökmar (<i>Abies nordmannian</i>) Görme Duyusu	Sabin Ardıcı (<i>Juniperus sabina</i>) Dokunma Duyusu	-	

İspendere rekreasyon alanında çeşitli alanlardan drone görüntüleri çekilmiştir. Ayak havuzu kenarı Güller (*Rosa* sp.) koku-görme duyusu Lavanta (*Lavandula officinalis*) koku-tat-görme duyusu, Biberiye (*Rosmarinus officinalis*) koku-tat duyusu hakimdir (Şekil 6).



Şekil 6. İspendere şifalı içmeler ve rekreasyon alanına ait resim ([Battalgazi Belediyesi Basın Müdürlüğü, 2024](#)).

Figure 6. Photo of the İspendere healing springs and recreation area ([Battalgazi Municipality Press Office, 2024](#)).

Bu çalışmanın sonucu, 4 farklı rekreasyon alanında yapılan bitkisel tasarım incelemelerine göre bu alanlarda kullanılan bitki türlerin en fazla görme ve dokunma duyusunun uyandırdığını ve koku, ses ve tat duyuların uyandırması anlamında eksiklerin olduğunu açıklamıştır (Şekil 7).

	GÖRME	DOKUNMA	KOKU	SES	TAT
KIRKGÖZ SAHİL PARKI	41	9	7	2	4
GALİP DEMİREL ÇINAR PARK	30	10	5	1	2
MİLLET BAĞÇESİ (BELEDİYE ÖNÜ)	33	5	16	1	8
İSPENDERE İÇMELERİ REKREASYON ALANI	25	7	18	4	7

Şekil 7. Araştırma alanlarının bitkisel tasarım konusunda duysal uyarm açısından değerlendirilmesi.

Figure 7. Evaluation of research areas in terms of sensory stimulation in plant design.

SONUÇ

Peyzaj tasarım projelerinde bitkisel tasarım peyzaj tasarım sürecinin önemli bir parçası olmuştur. Peyzaj mimarlığı disiplininde bitkiler görsel, işlevsel ve ekolojik bakımından kullanılmaktadır. Ancak yapılan ön incelmeler tasarlanan kentsel açık ve yeşil alanlarındaki bitkilerin duysal uyarm kapsamında kullanımlarının zayıf olduğu gözlemlenmiştir. Genellikle tasarımcıları bitkisel tasarımlarında bitkileri gölge sağlama, yön gösterme ve bunun gibi amaçlar için kullanılmaktadırlar. Bu bağlamda mevcut yapılan kentsel yeşil alanlarda ve parklarda duysal uyarm

sağlayan bitki kullanımının ne ölçüde kullanıldığının incelenmesi bu çalışmanın asıl amacı olmuştur. Yapılan çalışma içerisinde Türkiye'nin Malatya kentinde var olan parkların duysal uyarım kapsamında peyzaj uygulamalarının değerlendirilmesi yapılmıştır.

Bu çalışmada 4 farklı rekreasyon alanında alanda incelemeler yapılmış ve kullanılan bitki türlerin hangi duyuyu uyandırdığı konusunda mevcut literatüre başvurulmuştur. Ancak bazı bitki türlerin duysal uyarımı konusundaki bilgisi mevcut literatürde bulunmamıştır ve hangi tür hangi duyuya hitap etme konusundaki eksik veriler yazarların bizzat kendi incelemelerine göre sağlanmıştır. Elde edilen sonuçlara göre Malatya'da bulunan Kırkgöz Sahil parkında çok çeşitli ağaç ve çalı türleri yer almaktadır. Bu alanda sayısal olarak (41 adet bitki türü) en fazla görme duyusuna hitap etmiştir. Yaz aylarında alanın sağ kısmında Lavanta (*Lavandula officinalis*) bahçesi koku-tat-görme duyusuna, Adaçayı (*Salvia officinalis*) tat-koku-dokunma duyusuna hitap etmektedir. Çalışma alanında ses duyusu olarak Yumuşak ot (*Plantago lanceolata*), Bambu (*Bambusoideae*) bulunmaktadır. İlkbahar aylarında koku-tat duyusuna hâkim Gümüşi ıhlamur (*Tilia tomentosa*) yer alır. Sonbahar aylarında Amerikan sarmaşığı (*Parthenocissus quinquefolia*) görme duyusuna, Biberiye (*Rosmarinus officinalis*) koku-tat duyusuna uyarım yapmaktadır. Kış mevsiminde Orman sarmaşığı (*Hedera helix*) hem görsel hem de dokunma duyusunu harekete geçirir. Tıbbi aromatik bitkilerin az olması dikkat çekmektedir. Alana Çınar (*Platanus orientalis*), Kırmızı yapraklı akçaağaç (*Acer rubrum*) görsel anlamda dikkat çekmiştir. Özellikle kış mevsiminde duysal bitkilerin az olması açıklanmıştır. Bu doğrultuda alanda Kurtbağrı (*Ligustrum vulgare*), Kara Çam (*Pinus nigra*), Piramidal mazı (*Thuja orientalis pyramidalis*) dikilmesi önerilmiştir.

Malatya'da bulunan Galip Demirel Çınar parkı adını aldığı 700 yıllık Büyük çınar (*Platanus orientalis*) dokunma-görme duyusuna hitap etmektedir. İlkbahar aylarında ıhlamur (*Tilia tomentosa*) koku-tat duyusunu, Şekilli leylandi (*Cupressocypariss leylandii* "Spiralle") görme duyusunu uyandırmaktadır.

Yaz aylarında Arap yasemini (*Jasminum sambac*) koku duyusunu, Lavanta (*Lavandula officinalis*) tat-koku duyusunu, Zakkum (*Nerium oleander* "Nana") görme duyusunu insanlara hissettirir. Sonbahar mevsiminde Biberiye (*Rosmarinus officinalis*) koku-tat duyusu, Bodur alev çalısı (*Photinia fraseri* "Nana") görme duyusu, Zeytin çalısı (*Teucrium fruticans*) dokunma duyusunu çağrıştırır. Kış mevsiminde Süs lahanası (*Brassica oleracea* var. *Acephala*) görme duyusu, Huş ağacı (*Betula pendula*) dokunma duyusuna hakimdir. Alanda işitme ve tat duyusuna hitap eden bitki türü oldukça az olmuştur. Su kenarlarında Salkım söğüt (*Salix babylonica*) ağacı dikilmesi ses duyusunun arttırılmasını sağlayacaktır. Alanda tıbbi aromatik bitkiler ve meyve ağaçları dikilmesi önerilmektedir.

Çalışma alanı olarak Battalgazi Belediyesi Millet Bahçesi incelendiğinde tatma duyusunun diğer parklara göre fazla olduğu gözlemlenir. Alanda Ayva ağacı (*Cydonia oblonga* Mill.), Ters dut (*Morus nigra* "Pendula"), Defne (*Laurus nobilis*), Kekik (*Thymus* sp.), Biberiye (*Rosmarinus officinalis*) bulunmaktadır. Havuz kenarında yer alan yedi veren güller (*Rosa* sp.), Baston güller koku ve görme duyusuna hitap etmektedir. Dokunma duyusu için olarak Manolya, Mabet Ağacı (*Ginkgo biloba*) yer almıştır. İlkbahar aylarında Sarılcı hanımeli (*Lonicera japonica*) koku duyusunu, yaz aylarında Oya ağacı (*Lagerstromia indica*) dokunma-görme

duyusunu, sonbahar aylarında Biberiye (*Rosmarinus officinalis*) koku-tat duyusu, Ateş dikenini (*Pyracantha coccinea*) görsel duyusunu hissettirir.

Çalışma alanı olarak İspendere rekreasyon alanında yapılan bitkisel tasarım incelemesi neticesinde en fazla ses duyusu bu parkta yer alır. Alanda Titrek kavak (*Populus tremula*), Yumuşak ot (*Plantago lanceolata*), Bambu (*Bambusoideae*), Salkım söğüt (*Salix babylonica*) ses duyusuna hitap etmektedir. İlkbahar aylarında Güneş papatya çalısı (*Euryops pectinatus*) koku-görme duyusu, Sarı kantaron (*Hypericum calycinum*) tat-koku-görme duyusuna, Kartopu çalısı (*Viburnum lucidum*) görme-dokunma duyusuna, yaz mevsiminde Petunya (*Petunia integrifolia*) koku-görme duyusu, Lavanta (*Lavandula officinalis*) tat-koku duyusunu ve kış mevsiminde Göknar (*Abies nordmanniana*) görme duyusu, Sabin ardıcı (*Juniperus sabina*) dokunma-görme duyusunu çağrıştırır. Alanda Kuşburnu (*Rosa canina*), Gülhatmi (*Alcea apterocarpa*) Yabani kişniş (*Bifora radianis*) ve Rezene (*Foeniculum vulgare*) tat duyusu için kullanılabilir. Bu çalışmanın sonucu, mevcut rekreasyon alanlarında kullanılan bitki türlerinin en fazla görme ve dokunma duyusunun uyandırdığını ve koku, ses ve tat duyuların uyandırması anlamında eksiklerin olduğunu açıklamıştır.

Türkiye’de bitki çeşidi anlamında oldukça zengin bir ülke bilinmektedir. Ancak buna rağmen yapılan kentsel park ve açık yeşil alanlarda bitki çeşitliliği az olmuştur. Yapılacak olan yeni projelerde bitkilerin duyusal uyarım özelliklerini göz önüne alınarak bitki türlerinin seçimi yapılmalı ve seçilen türlerinin eşit olarak tüm beş duyuya hitap etmesine dikkat edilmelidir.

ÇIKAR ÇATIŞMASI

Makale yazarları olarak herhangi bir çıkar çatışması olmadığını beyan ederiz.

YAZAR KATKISI

Gamze ÖNER: Biçimsel analiz, Yazma - orijinal taslak, Metodoloji

Sima POUYA: Araştırma, İnceleme ve Düzenleme, Doğrulama.

ETİK KURUL KARARI

Bu makale Etik Kurul Kararı gerektirmemektedir.

KAYNAKLAR

- Acar C, Demirbaş E, Dinçer P ve Acar H (2009). Anlamsal farklılaşım tekniğinin bitki kompozisyonu örneklerinde değerlendirilmesi. *Turkish Journal of Forestry*, 4(1): 15-28.
- Acıbuca V ve Budak D B (2018). Dünya’da ve Türkiye’de tıbbi ve aromatik bitkilerin yeri ve önemi. *Çukurova Tarım ve Gıda Bilimleri Dergisi*, 33(1): 37-44.
- Akkemik Ü (2014). Türkiye’nin doğal egzotik ağaç ve çalıları angiospermiler 1.2.Ciltler, T.C. Orman ve Su İşler Bakanlığı Orman genel Müdürlüğü, Ankara.
- Altınçekiç H (2000). Peyzaj mimarlığında renk ve önemi. *Journal of the Faculty of Forestry Istanbul University*, 50(2): 59-78.

- Andić B, Šorgo A, Cvjetićanin S, Maričić M ve Stešević D (2022). Multisensory Identification of Characteristics of Reproductive Plant-Parts by People with Blindness or People with Ultra-Low-Vision. *Exceptionality*, 30(5): 310-323. <https://doi.org/10.1080/09362835.2021.1938055>
- Arslan N, Baydar H, Kızıl S, Karık Ü, Şekeroğlu N ve Gümüşçü A (2015). Tıbbi aromatik bitkiler üretiminde değişimler ve yeni arayışlar. Türkiye Ziraat Mühendisliği VIII. Teknik Kongresi, 12, 16. Battalgazi Belediyesi Basın Müdürlüğü, (2024). <https://www.battalgazi.bel.tr/author/battalgazi-basin/> (02.11.2024).
- Bilgili B, Aytas İ, Çorbacı Ö ve Alp Ş (2014). İlkbaharda çiçek açan bazı bitki türlerinin Çankırı koşullarında çiçeklenme zamanlarının belirlenmesi. *Türk Tarım ve Doğa Bilimleri Dergisi*, 1(3): 338-347.
- Burnett JD (1997). Therapeutic effects of landscape architecture. In Health Care Design, ed. Marberry, Sara O. New York: John Wiley and Sons, USA.
- Chen BX, Qi XH and Qiu ZM (2018). Recreational use of urban forest parks: A case study in Fuzhou National Forest Park, China. *Journal of Forest Research*, 23(3): 183-189.
- Cografya Dünyası, 2024. <https://www.cografya.gen.tr/tr/malatya/iklim.html> (10.06.2024)
- Cooper Marcus C ve Barnes M (1995). Gardens in healthcare facilities: Uses, Therapeutic benefits, and design recommendations, The center for health design, University of California at Berkeley, Inc. CA, 7-9.
- Faydaoğlu E ve Sürücüoğlu M S (2011). Geçmişten günümüze tıbbi ve aromatik bitkilerin kullanılması ve ekonomik önemi. *Kastamonu University Journal of Forestry Faculty*, 11(1): 52-67.
- Francis-West PH, Ladher RK ve Schoenwolf GC (2002). Development of the sensory organs. *Science progress*, 85(2): 151-173.
- Google Earth (2024). <https://earth.google.com/web/> (10.06.2024)
- Gülgün B, Atıl AG, Sayman M ve Yörük İ (2007). Peyzaj Mimarlığı çalışmalarında kullanılan bazı önemli akuatik bitkiler ve kullanım ilkeleri. *Ege Üniversitesi Ziraat Fakültesi Dergisi*, 44(1): 177-188.
- He M, Wang Y, Wang WJ ve Xie Z (2022). Therapeutic plant landscape design of urban forest parks based on the five senses theory: A case study of Stanley Park in Canada. *International Journal of Geoheritage and Parks*, 10(1): 97-112. <https://doi.org/10.1016/j.ijgeop.2022.02.004>
- Hussein H (2012). Experiencing and engaging attributes in a sensory garden as part of a multi-sensory environment. *Journal of Special Needs Education*, 2: 38-50.
- Kaplan R (1973). Some psychological benefits of gardening. *Environment and Behavior*, 5(2): 145-152. <https://doi.org/10.1177/001391657300500202>.
- Kaplan RS (1994). Management accounting (1984-1994): Development of new practice and theory. *Management Accounting Research*, 5(3-4): 247-260. <https://doi.org/10.1006/mare.1994.1015>
- Karashaş B (2021). Bitkilendirme tasarımında renk özellikleri dolayısıyla değerlendirilebilecek tıbbi ve aromatik bitkiler üzerine bir araştırma. *Turkish Journal of Forest Science*, 5(2): 536-550.
- Lambe L (1995). Gardening: A multisensory experience. In making leisure provision for people with profound learning and multiple disabilities (pp. 113-130). Boston, MA: Springer US.
- Leonard AS ve Masek P (2014). Multisensory integration of colors and scents: insights from bees and flowers. *Journal of Comparative Physiology A*, 200: 463-474.
- Liu H, Li F, Li J ve Zhang Y (2017). The relationships between urban parks, residents' physical activity, and mental health benefits: A case study from Beijing, China. *Journal of Environmental Management*, 190: 223-230. <https://doi.org/10.1016/j.jenvman.2016.12.058>.
- Malatya Battalgazi Belediyesi (2024). <https://www.battalgazi.bel.tr/category/projeler/> (02.11.2024).
- MGM (2024) T.C. Çevre, Şehircilik ve İklim Değişikliği Bakanlığı Meteoroloji Genel Müdürlüğü. <https://www.mgm.gov.tr/Veridegerlendirme/il-ve-ilceler-istatistik.aspx?m=MALATYA>
- Minter S (1995). The Healing Garden, *Eddison Sadd Editions*, London, England.
- Özgüner H (2004). Doğal peyzajın insanların psikolojik ve fiziksel sağlığı üzerine etkileri. *Turkish Journal of Forestry*, 5(2): 97-107.
- Pouya S (2019). Rekreasyon alanlarında bitkisel tasarım yaklaşımı, Malatya kenti örneği. *The Journal of Academic Social Science*, 7(96): 162-184.
- Pouya S, Bayındır E ve Pouya S (2024). Sensory garden design proposal for children with autism spectrum disorder. *Support for Learning*, 39(1): 44-57. <https://doi.org/10.1111/1467-9604.12466>.
- Sarı D ve Karashaş B (2018). Bitkilendirme tasarımı öğeleri, ilkeleri ve yaklaşımlarının peyzaj tasarımı uygulamalarında tercih edilirliliği üzerine bir araştırma. *Megaron*, 13(3): 470-479.

- Taplin DH (2002). *Art, nature, and people: Landscape values of an urban park* (Master's thesis). City University of New York, New York.
- Tilley C (2006). The sensory dimensions of gardening. *The Senses and Society*, 1(3): 311-330.
- Ulrich RS (1983). Aesthetic and affective response to natural environment. In behavior and the natural environment (pp. 85-125). Boston, MA: *Springer* US.
- Ulrich RS and Addoms DL (1981). Psychological and recreational benefits of a residential park. *Journal of Leisure Research*, 13: 43-65. <https://doi.org/10.1080/00222216.1981.11969466>
- Ulrich RS, Simons RF, Losito BD, Fiorito E, Miles MA and Zelson M (1991). Stress recovery during exposure to natural and urban environments. *Journal of Environmental Psychology*, 11(3): 201-230. [https://doi.org/10.1016/S0272-4944\(05\)80184-7](https://doi.org/10.1016/S0272-4944(05)80184-7).
- Yamauchi T, Seo JH and Sungkajun A (2018). Interactive plants: Multisensory visual-tactile interaction enhances emotional experience. *Mathematics*, 6 (11): 225. <https://doi.org/10.3390/math6110225>
- Yun HS, Yun, SY ve Choi BJ (2018). Effects of horticultural activities designed to stimulate five senses on the sensory development of children. *Journal of People, Plants, and Environment*, 21(5): 369-378. <https://doi.org/10.11628/ksppe.2018.21.5.369>



Turkish Journal of
Agricultural
Engineering Research
(Turk J Agr Eng Res)
e-ISSN: 2717-8420



Performance Evaluation of Electric Motor Driven Turmeric Slicing Machine

Amanuel Erchafo ERTEBO^{a*} 

^aDepartment of Agricultural Engineering Research Process, Melkassa Agricultural Research Center, P.O.Box 436, Adama, ETHIOPIA

ARTICLE INFO: Research Article

Corresponding Author: Amanuel Erchafo ERTEBO, E-mail: amanbaaman40@gmail.com

Received: 30 July 2024 / **Accepted:** 18 October 2024 / **Published:** 31 December 2024

Cite this article: Ertebo, A.E. (2024). Performance evaluation of Electric Motor Driven Turmeric Slicing Machine. Turkish Journal of Agricultural Engineering Research, 5(2), 199-218.
<https://doi.org/10.46592/turkager.1525100>

ABSTRACT

This study investigated the performance of an electric motor driven turmeric rhizome slicer machine. The physical properties of turmeric rhizome such as geometric mean diameter, arithmetic mean diameter, square mean diameter, equivalent diameter, aspect ratio, sphericity, shape factor, bulk density, porosity, coefficient of friction, and angle of repose were studied. According to the determination results, these parameters were found to be 23.9 mm, 30.3 mm, 45.3 mm, 33.2 mm, 0.33, 0.4, 1.8, 336 kg m⁻³, 81.7%, and 28.4°, respectively. It was observed during the test that the machine slices the rhizomes of turmeric into slices with a desired thickness range of 1.5 to 2 mm. According to findings, at 500 rpm rotor speed and 10 kg min⁻¹ feeding rates, the maximum slicing capacity of 824.7 kg h⁻¹ was recorded; at 300 rpm rotor speed and 15 kg min⁻¹ feeding rates, the minimum slicing capacity was recorded. At 500 rpm of rotor speed and 15 kg min⁻¹ of feeding rate, a maximum slicing efficiency of 97.4% was found, while at 300 rpm and 10 kg min⁻¹ feeding rate, a minimum slicing efficiency of 93.9% was noted. From test results, at 500 rpm rotor speed and feed rates of 15 kg min⁻¹, the minimum material loss was recorded as 4.06%, while at 300 rpm rotor speed and 10 kg min⁻¹ feed rate, the maximum material loss was recorded as 7.6%. This turmeric slicing machine is highly recommendable because the machine's performance for slicing the rhizome of turmeric was very impressive based on the test results.

Keywords: Turmeric slicer, Slicing capacity, Slicing efficiency, Material loss, Rotor speeds

INTRODUCTION

Turmeric (*Curcuma longa* L.) is a spice crop produced in tropical and subtropical regions which is typically utilized for both culinary and medicinal targets. Turmeric is a perennial herbaceous crop belonging to the tuberous rhizomes with members of ginger (Shi, 2020). It is a rich, golden-orange spice that enhances food's color, flavor,



Copyright © 2024. This is an Open Access article and is licensed under a Creative Commons Attribution 4.0 International License (CC-BY-NC-4.0) (<https://creativecommons.org/licenses/by-nc/4.0/deed.en>).

and nutritional value. Nearly one billion peoples' worldwide utilize turmeric as a spice ([Polshettiwar et al., 2022](#)). An estimated 1,100,000 tons of turmeric are produced worldwide each year ([Nair, 2023](#)).

Turmeric rhizome is a source of income for many Ethiopians which supports a large number of people in ways of life. As a key component of the regional sauce *Alicha Wot*, Ethiopian homemakers consider turmeric, or "Ird" in the Amharic language, one of the greatest flavorful spices. Turmeric is one spice that is produced primarily in Ethiopia by smallholder subsistence farmers in the country's southwest and southeast, regions ([Hordofa and Tolossa, 2020](#)). The output, production, and coverage of land of turmeric spices in Ethiopia were 3.95 tons per hectare, 3962.03 metric tons, and 1002.2 hectares, respectively ([Deribe, 2021](#)).

Turmeric rhizomes are harvested and then processed through some post-harvest steps, including slicing, boiling, drying, and polishing to create enduring commodities before being used ([Girma and Mohammedsani, 2021](#)).

Problems associated with turmeric slicing using conventional methods include their irregularity, which can lead to uneven drying or infected dry slices. In Ethiopia, the most time-consuming, tedious, and laborious method of processing turmeric is the conventional method of slicing it. This method has a limited output per time and requires a large number of workers to do the job. ([Hailemariam et al., 2023](#)). A major obstacle for producers of turmeric is the lack of mechanical turmeric processing technologies in the areas where turmeric is grown ([Muogbo et al., 2017](#)). Because of this, producers of turmeric reduced the size of the spice using hand instruments like hand knives and stationary curing units. However, this tool can cause harm to the operator's fingers and produce an uneven product that after processing has poor final quality due to variations in size, shape, or thickness. Due to a lack of turmeric processing technologies, Ethiopian farmers who grow turmeric often neglect to follow the crucial steps and avoid the most fundamental and crucial steps of curing, peeling, slicing, boiling, and polishing turmeric ([Hailemichael et al., 2016](#)).

Currently, turmeric is produced nationally by farmers, large private farms, massive investment projects, and small business owners, indicating a high demand for turmeric-slicing machines in Ethiopia ([Hordofa and Tolossa, 2020](#)). Turmeric crops have to be sliced using a slicing machine because of the increasing demand for processed turmeric for a variety of applications. As technology develops, it gets increasingly significant to slice turmeric using a slicer machine. The main purposes of slicing turmeric with a slicing machine are to achieve uniform drying, reduce the drying time, improve quality of products, and decrease the final moisture content in the small pieces of rhizomes without compromising the product's appearance.

Consequently, this study aimed to evaluate the performance of the motorized fresh turmeric rhizome slicing machine in order to minimize the technological gap in turmeric slicing in turmeric growing areas of Ethiopia, avail the turmeric slicer machine for future intervention, and generate information regarding the slicer machine's effectiveness for beneficiaries. The study also aimed to replace the conventional slicing of turmeric with a machine, which would slice the spice more quickly and with higher quality while reducing labour intensive tasks.

MATERIALS and METHODS

Study area

Evaluating the performance of the turmeric slicing machine was carried out in southwestern parts of Ethiopia, Tepi National Spices Research Center is situated 579 km from Ethiopia's capital, A.A. The site is located with a latitude of 7°3' N and a longitude of 35°0' E with an altitude of 1200 m above sea level.

Description of slicer machine

The turmeric rhizome slicing machine was powered by a three-horsepower (3 hp) variable electric motor which rotates at a constant rotor speed of 1500 rpm. The machine mainly consists of a feeding table, hopper, cylindrical disc, cutting blade, blade holder, outlet, frame, shaft, and power transmission units. The slicing unit was made up of a cylindrical stainless steel sheet metal. Its slicing mechanism could be based on a cutting blade when the actual slicing operation takes place on it. Turmeric slicing machine is easy to use, less complicated to operate and it has only one or two people to control the whole process. Due to its simple operating mechanism, this turmeric slicing machine was an excellent choice for farmers who produce turmeric. The machine was capable of slicing at a uniform dimension, was fast enough, lasted longer in use with high efficiency, and was portable and affordable for small-scale farmers, businessmen and individuals.

Materials

Experimental materials

The sample of turmeric (Figure 1) was obtained from the southwestern parts of Ethiopia, Tepi National Spices Research Center or Tepi Agricultural Research Center experimental field for calculating properties as well as detailed tests on the turmeric slicing machine. The materials used in the experiment were turmeric rhizomes of the Tepi-1 (Bonga 51/71) variety. This variety should be selected because of its availability and its well-known for its high production capacity in the Tepi area and other growing areas of southern Ethiopia.



Figure 1. *Turmeric rhizome for experiment.*

Measuring instruments

The multiple measurements on the fresh turmeric rhizome have been implemented. The lengths of the turmeric rhizomes were determined with the aid of a pocket meter, this measuring pocket meter can measure a minimum length up to 0.5 cm, therefore, its sensitivity is 0.5 cm. The turmeric rhizomes' diameter was taken by the caliper with its 0.01 mm accuracy; the sensitivity of the caliper is 0.02 mm which means that the smallest measurement that can be read using this instrument is 0.02 mm. A mass of turmeric rhizomes was taken by using weight balances. The sensitivity of a digital weighing balance is 1 mg with a model of YP150001; this means that a weight of at least 1.0 mg is needed to move the pointer over one scale and the smallest weight that the scale can measure. The stopwatch was utilized for recording slicing time when testing a slicer. The machine's rotor speed was measured using a contact type of tachometer. The machine was started, and the speed was adjusted to 300 rpm, 400 rpm, and 500 rpm by using a tachometer.

Methods

Determination of physical properties of turmeric rhizomes

Determining different properties for agricultural produce is essential for designing agricultural machinery and the improvement of processes for harvesting, handling, postharvest operations, and storage ([Obaia and Ibrahim, 2015](#)). The properties of fresh turmeric rhizomes are useful for the design of turmeric processing equipment, handling and storage. Determining the characteristics of those products is important to designing machines and processes conveying, for designing feed hoppers and metering mechanisms. Food products like turmeric are often characterized based on their physical dimension (length, width, thickness) and density since these properties are utilized for processing ([Ramos *et al.*, 2021](#)).

While determining the physical characteristics like thickness, lengths, breadth, arithmetic diameters, geometric diameters, square diameters, equivalent mean diameter, sphericity, aspect ratio, unit volume, surface area, shape factor, bulk and true density, porosity, angle of repose, and moisture contents for turmeric rhizome random choices were carried out 100, 80, 50, 33, 36, 34, 30, 35, 27, 38, 40, 25, 100, 60, 35, 46, and 54 respectively. As a consequence, the following physical characteristics have been investigated:

Turmeric rhizome's axial dimensions

Fresh turmeric rhizomes were randomly selected for measuring the axial dimensions such as lengths, breadth as well as thickness.

Geometric mean diameter

A diameter was an important measurement criterion and was expressed as the cub root of three axes of the mother rhizome using the major length (l), breadth (b) and diameter (d). It's the mean value for turmeric mother rhizome is ascertained by applying Equation 1 ([Dhineshkumar and Anandakumar, 2016](#)).

$$GMD = \sqrt[3]{l \times b \times d} \quad (1)$$

Where, GMD is the geometric means diameters, l is the major length (mm), b is the breadth (mm), and d is the diameter (mm).

Arithmetic mean diameter

The arithmetic mean diameter of turmeric mother rhizome samples was determined using the formula (Dhineshkumar and Anandakumar, 2016) in Equation 2.

$$AMD = \frac{(l+b+d)}{3} \quad (2)$$

Where, AMD is the arithmetic mean diameter (mm), l is the major length (mm), b is the breadth (mm), and d is the diameter (mm).

Square mean diameter

The square mean diameter of turmeric mother rhizome samples was determined using the formula (Dhineshkumar and Anandakumar, 2016) in Equation 3.

$$SMD = \sqrt[3]{lb + bd \times dl} \quad (3)$$

Where, SMD is the square mean diameter (mm), l is the major length (mm), b is the breadth (mm), and d is the diameter (mm).

Equivalent diameter

The equivalent mean diameter of turmeric mother rhizome samples was determined using the formula (Dhineshkumar and Anandakumar, 2016) in Equation 4.

$$EQD = \frac{(GMD+AMD+SMD)}{3} \quad (4)$$

Where, EQD is the equivalent mean diameter (mm), GMD is the geometric mean diameter, AMD is the arithmetic mean diameter (mm), and SMD is the square mean diameter (mm).

Sphericity

Sphericity of turmeric mother rhizome samples was determined using the formula by (Ramos *et al.*, 2021) given in Equation 5.

$$\Phi = \frac{\sqrt[3]{lbd}}{l} \quad (5)$$

Where, Φ is the sphericity (mm) l is the major length (mm), b is the breadth (mm), and d is the diameter (mm).

Unit volume and surface area

The unit volume (V) and surface area (S) can be estimated by applying the Equations 6 and 7 (Ramos *et al.*, 2021).

$$S = \frac{(\pi Bl^2)}{2l-B} \quad (6)$$

$$V = \frac{(\pi B^2 l^2)}{6(2l-B)} \quad (7)$$

Where, B is the cub root of breadth (mm) and l is the major length (mm).

Shape factor (\ddot{e})

It can be determined using Equation 8 ([Ramos et al., 2021](#)).

$$\ddot{e} = \frac{(D)}{C} \quad (8)$$

Where, C is the unit volume per cubic breadth (mm) and D is the area per six times cubic breadth (mm).

Bulk density

The mass-to-volume proportion of the turmeric in a container was used to calculate bulk density. Rhizomes were filled in a measuring cylinder as well as mass of rhizomes was estimated. The bulk density of the rhizomes was estimated by applying Equation 9 ([Rajkumar et al., 2021](#)).

$$\rho_B = \frac{\text{Mass of rhizome}}{\text{Volume of rhizomes}} \quad (9)$$

Where, ρ_B is the bulk density.

True density

The true density of fresh turmeric rhizomes was determined by the platform scale method. The known sample of fresh turmeric rhizome was taken and then immersed in a toluene. True density can be calculated using the following formula ([Rajkumar et al., 2021](#)) given in Equation 10.

$$T_D = \frac{\text{Mass of rhizome}}{\text{True Volume of rhizomes}} \quad (10)$$

Where, T_D is the true density.

Porosity and aspect ratio

The mother rhizome of turmeric's porosity has been estimated by dividing its volume in voids by its percentages. It can be determined by the expression as reported by [Ramos et al. \(2021\)](#) as given in Equations 11 and 12.

$$n = \frac{T_D - \rho_B}{T_D} \times 100 \quad (11)$$

$$Ar = \frac{b}{l} \times 100 \quad (12)$$

Where, T_D is the true density, ρ_B is the bulk density, b is the breadth (mm) and l is the major length (mm).

Moisture content

The moisture content for turmeric rhizomes was determined using the standard oven drying method. The weighed samples were subjected to remove moisture at $105 \pm 2^\circ\text{C}$

for 24 hours ([AOAC, 2000](#)). Moisture contents can be estimated utilizing Equation 13.

$$MC (wb)\% = \frac{W_1 - W_2}{W_1} \times 100 \quad (13)$$

Where, W_1 is the initial mass (g), W_2 is the final mass (g) and MC is the moisture content of the turmeric rhizome.

Angle of repose

The angle of the repose was calculated by the formula given in Equation 14 ([Rajkumar et al., 2021](#)).

$$Angle (\theta) = \tan^{-1} \frac{H}{D/2} \quad (14)$$

Where, θ is the angle of repose in ($^\circ$), H is the height of the heap in (cm), and D is the diameter of the heap in (cm).

Coefficient of friction

Coefficients of friction for turmeric rhizome concerning various materials like aluminum, mild steel, as well as wood, were obtained through techniques stated by ([Rajkumar et al., 2021](#)).

Test procedures

The samples of turmeric rhizomes were weighed, and each sample was fed to the machine through the hopper at a constant feed rate while the blade ran at various predetermined rotor speeds. The rhizomes were cleaned and washed manually to remove adhering soil, hairs and extraneous matter. The fed materials were pushed by the hand into the cutting disc against the stationary blade and were sliced into the desired thickness. The time taken to slice was recorded. The slicer was started, and the rotor speed was adjusted to 300, 400, and 500 rpm by using a speed regulator. The rotor speeds were chosen for testing the slicer performance on turmeric rhizome ([Murumkar et al., 2016a](#)). To evaluate the performance of the slicer machine, a total of 225 kg of fresh turmeric rhizome free from deterioration, scuffs, scratches, and damage could have been used for the entirety of the experiment.

Evaluation of the slicing machine

The evaluation had been executed at a turmeric slicer at three chosen rotor speeds with a fixed cutting clearance (2 mm) after weighing the test sample of the turmeric rhizome. Evaluating the slicer machine (Figure 2) was conducted by considering the slicing capacity, slicing, efficiency, material loss, and slicing time. The test parameters such as slicing capacity, slicing, efficiency, material loss, and percentage of scattered turmeric rhizomes were investigated using the following formulas by ([Khurmi and Gupta \(2005\)](#)).

$$Slicing\ capacity\ (kg\ h^{-1}) = \frac{Ws}{T} \quad (15)$$

$$\text{Slicing efficiency (\%)} = \frac{Q_o - Q_b}{Q_o} \times 100 \quad (16)$$

$$\text{Material loss} = \frac{Q_i - Q_o}{Q_i} \times 100 \quad (17)$$

$$\text{Percentage of scattered} = \frac{W_s - W_{sc}}{W_s} \times 100 \quad (18)$$

Where, W_s is the weight of sliced turmeric in kilogram, T is the time taken to slice turmeric in hours, Q_o is the weight of turmeric collected in kilogram, Q_i is the weight of turmeric feed in kilogram, Q_b is the weight of a non-uniform slice in kilogram and W_{sc} is the weight of scattered.



Figure 2. Slicer during testing.

Cost estimation

The cost of operation for the slicing machine was estimated by calculating the material cost of the machine. Estimation of hourly operational costs of the slicer was based on the capital cost of the slicer, interest on capital, depreciation, cost of repairs and maintenance, electric costs, labor cost, tax and insurance. According to [Lazarus \(2008\)](#), the annual fixed and variable costs were calculated as follows:

$$D = \frac{C - S}{L \times H} \quad (19)$$

$$I = \frac{C \times S}{2} \times \frac{i}{H} \quad (20)$$

$$RM = 2.5\% \times C \quad (21)$$

$$W = \frac{LW}{H} \quad (22)$$

Where, D is the depreciation (EB h^{-1}), C is the capital investments of slicer, S is the salvage values, L is the life of a machine in hours, I is the interest on capital (EB h^{-1}), i is the interest, RM is the repair and maintenance cost, W is the wages (EB h^{-1}), LW is the labor wage, and H is the working hours.

Statistical data analysis

The factorial design was employed in the experiment, and the three levels of rotor speed with two feeding rate levels were taken as treatments. The slicer rotor speeds were also taken into consideration as the main factor. There were eighteen experimental units in each of the three replicates of the experiments. Data analysis was done using Statistix 8 software and SPSS Statistics 23 software was used for generating graphs. The significant relationship in variables was indicated by using the ninety-five per cent confidence interval. The mean separation between treatment means was conducted by least significance difference (LSD) at a 5% level. Using a methodology suitable for the experiment's design, an analysis of variance was implemented in the data.

RESULTS AND DISCUSSION

Physical Properties of Turmeric Rhizome

Geometric properties of rhizome

The average of axial dimensions, geometric, gravimetric, and frictional properties of the Tepi-1 (Bonga. 51/71) variety of turmeric rhizome samples were determined, as given in (Table 1). Based on the results the turmeric rhizomes ranged in length from 17.4 to 112.8 mm, width from 10.6 to 25.6 mm, and thickness from 8.2 to 19 mm, in that order. It was determined that the length, width, and thickness had respective mean values of 59.8 mm, 17 mm, and 14 mm. The standard deviation was computed to be 22.8, 3.3, and 2.7. The results showed that the diameter of the geometric mean varied from 12.8 mm to 35.7 mm. 23.9 mm and 5.3 were determined as mean values as well as standard deviations, correspondingly. The arithmetic mean diameter varied from 13.1 to 51 mm. The mean values and standard deviations were determined to be 30.3 mm and 8.8.

The diameter of the square mean varied from 22.4 to 70.5 mm. After computation, mean values as well as standard deviations came out to be 45.3 mm and 10.9 mm. The equivalent mean diameter ranged from 16.1mm to 52.3 mm. Also, mean values as well as standard deviations were 33.2 mm and 8.3 mm, respectively.

Turmeric rhizome aspect ratios ranged from 0.28 to 0.4. The calculated mean value also has standard deviations obtained at 0.33 and 0.06, respectively. The rhizomes of turmeric had a sphericity ranging from 0.27 to 0.73, through mean as well as standard deviations of 0.4 and 0.1, correspondingly. The unit volume and surface area of turmeric rhizome were found in the range from 4.6×10^5 to 5.5×10^8 mm³ and 436 to 390.2 mm². The average values of unit volume and surface area were estimated to be 8.5×10^7 mm³ and 1725.6 mm² with standard deviations of 1.2×10^8 mm³ and 809.6 mm², while mean also standard deviations for the shape factor of the turmeric rhizomes were found to be 1.8 and 0.2, respectively, ranging from 1.56 to 1.9. A similar trend was reported by [\(Thul et al., 2022\)](#).

Gravimetric and frictional properties of turmeric rhizome

According to the findings (Table 1), the bulk density of the fresh turmeric rhizomes ranged from 294 to 378 kg m³, while this density's mean and standard deviation were determined to be 356 kg m³ and 42. The fresh turmeric rhizomes were found to have

a true density between 1373 and 1381 kg m³ which had mean values of 1378 kg m³ and a standard deviation of 4.4. The porosity of the rhizome of turmeric ranged from 78% to 86.9%. The porosity was computed to have a mean of 81.7% and a standard deviation of 4.6. The fresh turmeric rhizomes had an angle of repose that varied from 26.6° to 31.2°, a mean of 28.4° and a standard deviation of 2.5. Results revealed that the fresh turmeric rhizome's mean moisture contents were obtained at 48% on a wet basis through standard deviations of 1.5. This moisture content ranged from 46.3% to 49.1%. The static coefficient of friction on sheet metal, wood, and rubber surfaces for turmeric rhizome was found in the average of 0.54, 0.78, and 0.84 with standard deviations of 0.11, 0.17, and 0.08, respectively.

Table 1. *Physical characteristics of turmeric rhizome.*

Properties	Mean value	Standard deviation (SD)	Mean±SD	Maximum value	Minimum value	Coefficient of variation (CV)
Length (mm)	59.8	22.8	59.8±22.8	112.8	17.4	38.0
Width (mm)	17.0	3.3	17±3.3	25.6	10.6	19.7
Thickness (mm)	14.0	2.7	14±2.7	19.0	8.2	19.3
Geometric mean diameter (mm)	23.9	5.3	23.9±5.3	35.7	12.8	22.3
Arithmetic mean diameter (mm)	30.3	8.8	30.3±8.8	51.0	13.1	28.9
Square mean diameter (mm)	45.3	10.9	54.3 ±10.9	70.3	22.4	24.3
Equivalent diameter (mm)	33.2	8.3	33.2 ± 8.3	52.3	16.1	25.0
Aspect ratio	0.33	0.06	0.3± 0.06	0.4	0.28	18.9
Sphericity	0.4	0.1	0.43 ±0.1	0.73	0.27	24.4
Unit volume (mm ³)	8.5E+07	1.2E+08	8.5e ⁷ ± 1.2e ⁸	5.5E+08	455635	40.29
Surface area (mm ²)	1725.6	809.6	1725.6 ±809.6	3903.2	436.0	46.9
Shape factor	1.8	0.2	1.8± 0.2	1.9	1.56	10.1
Bulk density (kg m ⁻³)	336	42	336± 42	378	294	12.5
True density (kg m ⁻³)	1378	4.4	1378 ± 4.4	1381	1373	0.3
Porosity (%)	81.7	4.6	81. ± 4.6	86.9	78	5.7
Angle of repose (°)	28.4	2.5	28.4±2.5	31.2	26.6	8.7
Moisture content (%)	48.0	1.5	48±1.5	49.1	46.3	3.2
Coefficient of friction (sheet metal)	0.54	0.11	0.54±0.11	0.64	0.4	20.8
Coefficient of friction (wood)	0.78	0.17	0.78±0.17	0.95	0.6	21.7
Coefficient of friction (rubber)	0.84	0.08	0.84±0.08	0.92	0.76	9.5

The findings demonstrated that when the moisture content of the fresh turmeric rhizome was increased, slicing performed more effectively. The test revealed that the

rhizome's moisture content was the most crucial factor in maintaining the turmeric rhizome's ability to be sliced. Moisture content of the produce determines the shelf life and the keeping quality of the turmeric. [Singh et al. \(2018\)](#) have suggested that the drying of fresh turmeric to a safe limit of moisture content about 10% for milling and 6% for storage. The angle of repose is important in design and construction of the material handling system ([Shirsat et al., 2018](#)). The obtained angle of repose showed that a slight inclination was required at the slicer feeding inlet for the rhizome to be fed simultaneously on the slicer machine. Studying the physical characteristics of the fresh turmeric rhizome was highly advantageous for primary processing machinery as well as post-harvest handling and testing equipment.

Also, from this study it was observed that the determination of engineering properties of fresh turmeric rhizomes is useful for design of turmeric processing equipment's, handling and storage. The engineering property investigated in this study was the most important properties which mainly considered in the design of the machine components. It gives the proper guidelines to an engineer and designer for designing the machines that will be suitable for processing of agricultural materials ([Shirsat et al., 2018](#)). The properties of turmeric rhizomes such as axial dimensions, geometric mean diameter, arithmetic mean diameter, sphericity, bulk density, true density, porosity, angle of repose, volume and surface area were studied. The same trend was stated by [Thul et al. \(2022\)](#). This study finding related with previous research findings conducted by [Ramos et al. \(2021\)](#). Similar findings were reported by [Mishra and Kulkarni \(2019\)](#) for physical properties of turmeric rhizome.

Evaluation of the slicer

The slicer's performance was assessed at three different rotor speed settings and two different feeding rate settings at mean moisture contents of 48% at the wet basis for fresh turmeric rhizome (Tepi-1 (Bonga 51/71)) concerning slicing capacity, slicing efficiency, material loss, slicing time, and percentage of scattered. After the machine had completed slicing turmeric, weight measurements were made for the whole sliced turmeric, the scattered turmeric rhizome, the weight uniform slice, the weight non-uniform slice, and the slicing time. During the test, it was noted that the machine slices the rhizomes of turmeric into slices with a desired thickness range of 1.5 to 2 mm. The machine's performance for slicing the rhizome of turmeric was very impressive based on the test results. [Devarshi et al. \(2023\)](#) noted a similar observation. The previous studies in the literature relating to slicing machines for turmeric crops were reported by [Navyashree et al. \(2024\)](#); and [Adeleke et al. \(2021\)](#). This finding was comparable with the findings stated by [Katanga \(2022\)](#).

Slicing capacity

Univariate analysis of variances for impacts in feed rates, rotor speeds, and their combination on the slicer machine's slicing capacity has been shown in Table 2. In accordance with the findings, analysis of variances revealed that impacts in rotor speeds, feed rates, and their interaction were significant at 5% due to the values for p being smaller than 0.05. The results suggested that feed rates, rotor speeds, and their interaction all had an impact on a machine's ability to slice. The observations for significance effects were in agreement with the findings of earlier researchers by

[Adeleke et al. \(2021\)](#). For root crop slicers, a similar trend was noted by [Abubakar et al. \(2019\)](#). The same funding pattern for a turmeric-slicing machine was reported by [Agbetoye and Balogun \(2009\)](#).

Table 2. Univariate analysis of variance for slicing capacity.

Sources	DF	SS	MS	F	P	
Replication	2	5.1	2.5			
Rotor speed	2	27374.6	13687.3	319.3	0.0000	*
Feeding rate	1	459.9	459.9	10.7	0.0084	*
S×F	2	588.6	294.3	6.87	0.0133	*
Error	10	428.7	42.9			
Total	17	28856.8				

* = significant, ** = non significant, $P < 0.05$, significant at 5 % level, $P > 0.05$, non-significant at 5% level.

The machine's mean slicing capacity varied from 714.9 kg h⁻¹ to 824.7 kg h⁻¹, as can be seen in Figure 3. The slicing capacity increased from 714.9 kg h⁻¹ to 824.7 kg h⁻¹ as the rotor speeds increased from 300 rpm to 500 rpm. When rotor speeds increased, the slicer's capacity headed to increase, but feed rates caused it to decrease. According to this finding, the slicing capacity was inversely correlated with the feed rates of the turmeric rhizome and directly correlated with the rotor speeds.

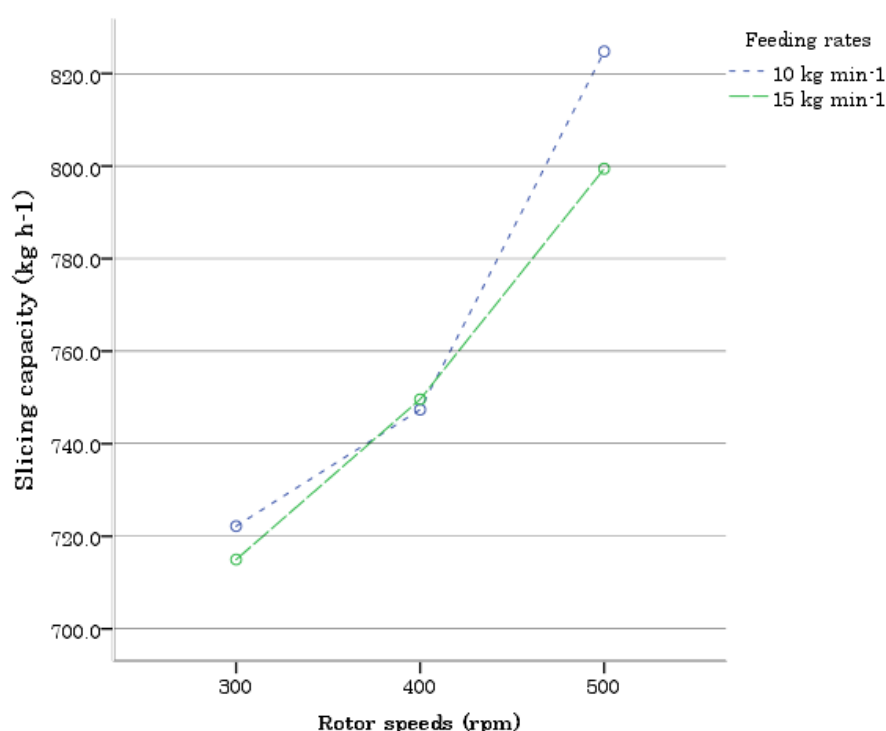


Figure 3. Impact of rotor speed and feed rate on slicing capacity.

According to findings, at 500 rpm rotor speed and 10 kg min⁻¹ feeding rates, the maximum slicing capacity of 824.7 kg h⁻¹ was recorded; at 300 rpm rotor speed and 15 kg min⁻¹ feeding rates, the minimum slicing capacity was recorded.

The slicing capacity obtained in this study was higher compared to the value of 130.67 kg h⁻¹ reported by [Devarshi et al. \(2023\)](#). [Tanimola et al. \(2019\)](#) stated the

slicing capacity of 34.3 kg h⁻¹ when slicing turmeric with a turmeric slicer. In comparison, [Murumkar *et al.* \(2016a\)](#) reported an average slicing capacity of 250 kg h⁻¹ when testing the performance of a motor-operated slicer. [Agbetoye and Balogun \(2009\)](#) stated an output of 42.9 kg h⁻¹ when testing an electric motor-powered slicer machine.

Slicing efficiency

Univariate analysis of variances for impacts in feed rates, rotor speeds, and their combination on the slicer machine's slicing efficiency has been shown in Table 3. The analysis of variances suggested that an impact of rotor speeds and feed rates were significant at 5% levels because of the values for p being lesser than 0.05 but their interaction impacts were non-significant (P>0.05). Depending on the result, the machine slicing efficiency was influenced by feed rates and rotor speeds excluding their relative interactions. The significant effects observations related with the previous researchers' findings by [Adeleke *et al.* \(2021\)](#). For root crop slicers, a similar trend was noted by [Abubakar *et al.* \(2019\)](#). The same funding pattern for a turmeric-slicing machine was reported by [Agbetoye and Balogun \(2009\)](#).

Table 3. Univariate analysis of variance for slicing efficiency.

Sources	DF	SS	MS	F	P	
Replication	2	0.0268	0.0134			
Rotor speed	2	31.7815	15.8908	19.34	0.0004	*
Feeding rate	1	4.3611	4.361	5.31	0.0440	*
S×F	2	3.8988	1.9494	2.37	0.1435	**
Error	10	8.2169	0.8217			
Total	17	48.2852				

* = significant, ** = non significant, P < 0.05, significant at 5 % level, P>0.05, non-significant at 5% level.

In accordance with the test's result, it revealed that a slicer's mean slicing efficiency varied from 93.9% to 97.4%, as indicated in Figure 4. The slicing efficiency rose from 93.9% to 97.4% as rotor speeds increased from 300 rpm to 500 rpm. The machine's slicing efficiency looked after to rise as rotor speeds and feeding rates increased. This indicates a direct correlation between the rotor speeds and feeding rates of the experimental material and the slicing efficiency.

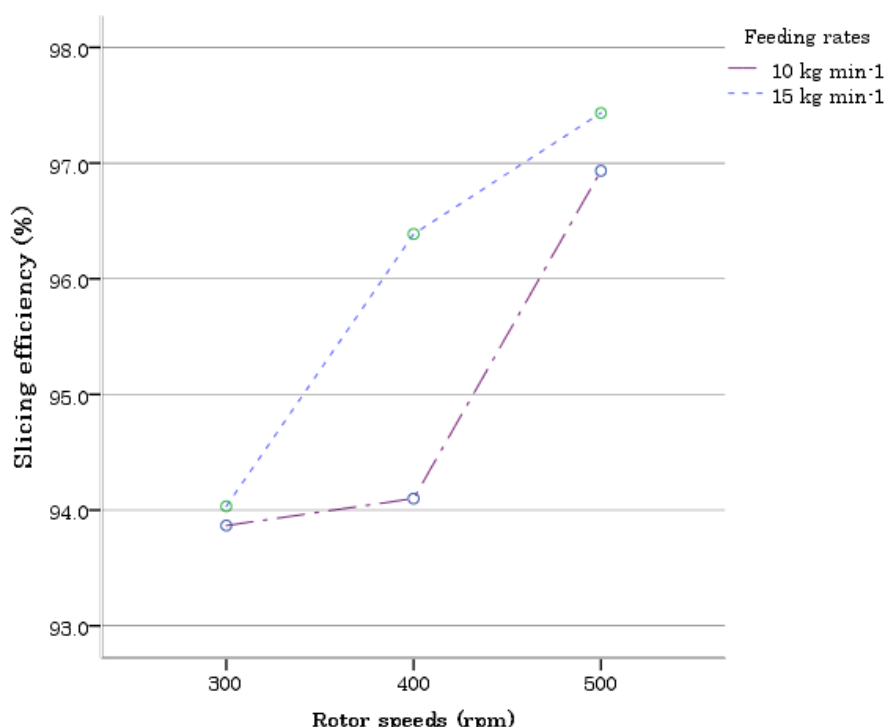


Figure 4. Impact of rotor speed and feed rate on slicing efficiency.

At 500 rpm of rotor speed and 15 kg min⁻¹ of feeding rate, a maximum slicing efficiency of 97.4% was found, while at 300 rpm and 10 kg min⁻¹ feeding rate, a minimum slicing efficiency of 93.9% was noted. The slicing efficiency obtained in this study was higher compared to the value of 94.07% reported by [Devarshi et al. \(2023\)](#). [Tanimola et al. \(2019\)](#) reported a machine efficiency of 59.8% while assessing turmeric slicer. In comparison, [Murumkar et al. \(2016b\)](#) reported an efficiency of 94.7% while assessing a motor-operated slicer. [Agbetoye and Balogun \(2009\)](#) reported a machine efficiency of 71% while assessing the slicer machine.

Material loss

Univariate analysis of variances for impacts in rotor speeds, feed rates, and their combination on the slicer machine's material loss has been shown in Table 4. In accordance with the findings, analysis of variances revealed that impact of rotor speeds and feed rates was significant at the five percent significance level due to the values for p being smaller than 0.05 but their interaction impact was non-significant which means the result obtained was greater than 0.05 ($P > 0.05$). The findings showed that, when their interactions were taken out of consideration, feed rates and rotor speeds had an impact on a machine's material loss. A comparable pattern for root crop slicers was observed by [Abubakar et al. \(2019\)](#). The same funding pattern for a turmeric-slicing machine is reported by [Agbetoye and Balogun \(2009\)](#). The significant effects observations related with the previous researchers' findings by [Adeleke et al. \(2021\)](#).

Table 4. Univariate analysis of variance for material loss.

Sources	DF	SS	MS	F	P	
Replication	2	0.0304	0.0152			
Rotor speed	2	31.6437	15.8219	19.3	0.0004	*
Feeding rate	1	4.4402	4.4402	5.42	0.0422	*
S×F	2	3.9184	1.9592	2.39	0.1417	**
Error	10	8.1947	0.8195			
Total	17	48.2274				

* = significant, ** = non significant, $P < 0.05$, significant at 5 % level, $P > 0.05$, non-significant at 5% level.

From the test result, a machine's mean material loss varied between 4.06% and 7.6%, as Figure 5 illustrates. The material loss dropped from 7.6% to 4.06% as the rotor speeds increased from 300 rpm to 500 rpm. As rotor speeds and feed rates increased, the machine's material loss looked after to decrease as well. This indicates that the rotor speeds and feed rates of the experimental material had a negative correlation with the material loss. A similar trend for slicers were stated by [Murumkar *et al.* \(2016a\)](#). The loss of the sliced rhizome occurred due to the lack of cover in front of the circular disc which caused the dropping of the slice far from the machine outlet.

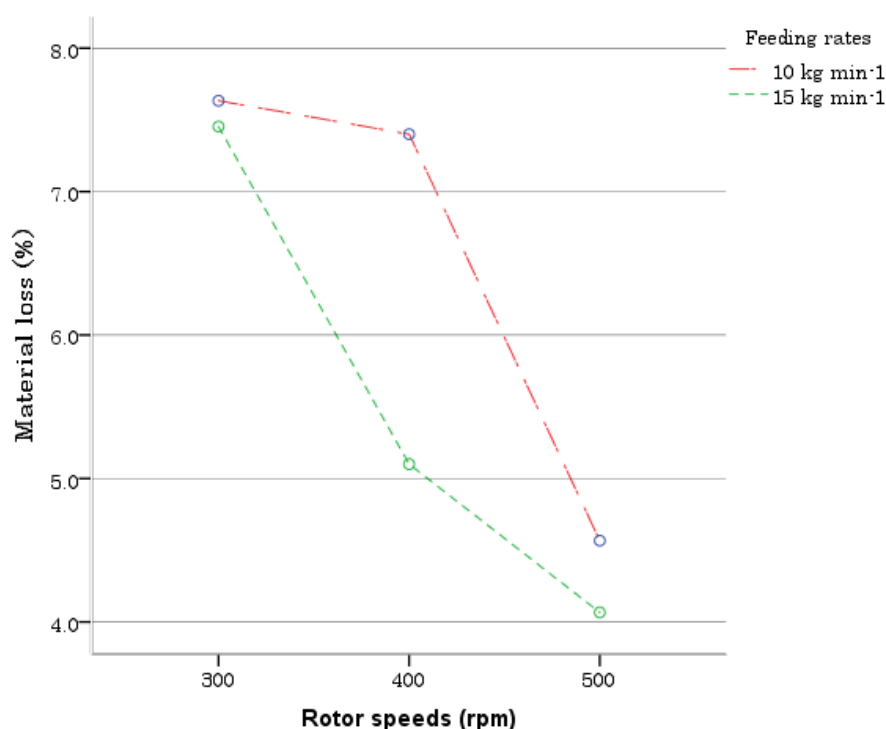


Figure 5. Impact of rotor speed and feed rate on material loss.

From test results, at 500 rpm rotor speed and feed rates of 15 kg min⁻¹, the minimum material loss was recorded as 4.06%, while at 300 rpm rotor speed and 10 kg min⁻¹ feed rate, the maximum material loss was recorded as 7.6%. This rotor speed was given that, in comparison to the other rotor speeds, the 500 rpm rotor speed had a minimal loss. The minimum percentage of loss recorded in this study was lower than the 7.3% reported by [Tanimola *et al.* \(2019\)](#). In comparison, [Murumkar *et al.* \(2016b\)](#) reported a percentage loss of 4.58% when slicing turmeric with a turmeric

slicer. [Agbetoye and Balogun \(2009\)](#) reported a loss of 8.7% while evaluating a slicer machine.

Slicing time

Univariate analysis of variance for impacts in rotor speeds, feed rates, and their combination on the slicer machine's slicing time has been shown in Table 5. Accordance with the analysis, an analysis of variances suggested that impacts in rotor speeds and feed rates were significant at 5% levels as a result of the values for p smaller than 0.05 however, their interaction impact was non-significant ($P > 0.05$). Based on the result, the machine slicing time was affected by feed rates and rotor speeds but was not affected by their impact interactions. A similar trend for root crop slicers was reported by [Murumkar et al. \(2016a\)](#). Comparable pattern for root crop slicers were observed by [Abubakar et al. \(2019\)](#). The same funding pattern for a turmeric-slicing machine was reported by [Agbetoye and Balogun \(2009\)](#).

Table 5. Univariate analysis of variance for slicing time.

Sources	DF	SS	MS	F	P	
Replication	2	0.4	0.2			
Rotor speed	2	1690.8	845.4	122.7	0.0000	*
Feeding rate	1	11250	11250	1633	0.0000	*
S×F	2	26.3	13.2	1.91	0.198	**
Error	10	68.9	6.9			
Total	17	13036.4				

* = significant, ** = non significant, $P < 0.05$, significant at 5 % level, $P > 0.05$, non-significant at 5% level.

It was noted that a machine's mean slicing time varied between 161 sec and 235 sec when fed at 10 kg min^{-1} with 500 rpm rotor speeds and at 15 kg min^{-1} with 300 rpm rotor speeds, as Figure 6 illustrates. In particular, the findings showed that the machine's slicing time had a tendency to decrease as rotor speeds increased and feed rates decreased. This is since higher rotor speeds performed more rapidly than smaller rotor speeds, meaning that the slicing time was oppositely correlated with rotor speed however closely associated with the feed rate of turmeric rhizome.

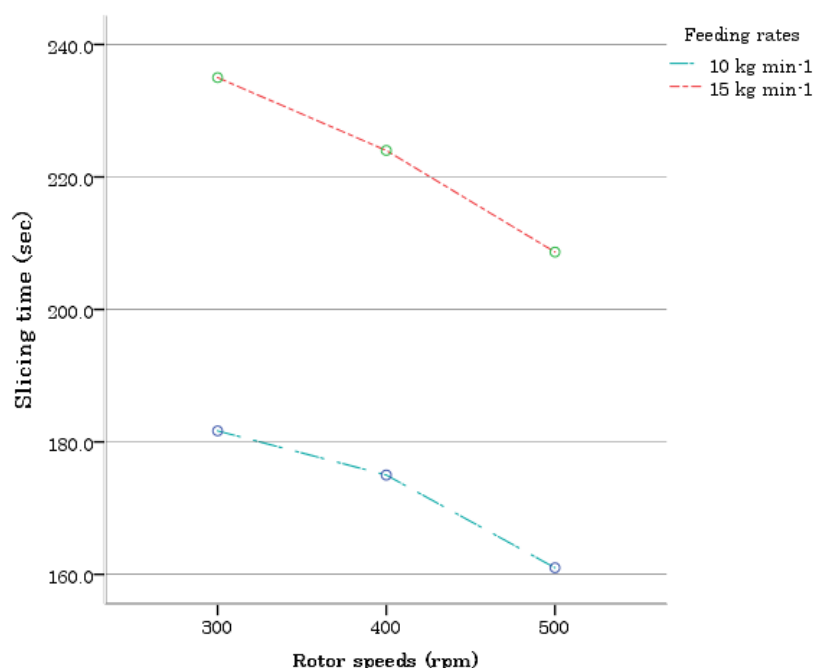


Figure 6. Impact of rotor speed and feed rate on slicing time

The rotor speeds of 500 rpm besides a feeding rate with 10 kg min⁻¹ resulted in a minimum slicing time of 161 sec, while the rotor speeds of 300 rpm besides a feeding rate with 15 kg min⁻¹ resulted in a maximum slicing time of 235 sec based on test results. Slicing time was reduced from 235 seconds to 161 seconds with higher rotor speeds of 300 rpm to 500 rpm.

Comparisons test of dependent variables for treatments

The LSD all pairwise comparison tests for slicing capacity, slicing efficiency, and material loss were carried out for each treatment as given below in Table 6 then this analysis was subjected to LSD all pairwise comparison tests for dependent variables for three levels of rotor speeds and two levels of feed rates to know significant differences among treatment means. So, LSD all pairwise comparison tests showed (Table 6) that there were four groups (a, b, etc.) whose treatment means were not significantly different from one another at the 5% level.

Table 6. Mean separation of variables for treatments.

No.	Treatments	Rotor speeds (rpm)	Feed rate (kg min ⁻¹)	Capacity (kg h ⁻¹)	Efficiency (%)	Material loss (%)
1	S1F1	300	10	722.19 ^d	93.867 ^b	7.6333 ^a
2	S1F2	300	15	714.97 ^d	94.033 ^b	7.4533 ^a
3	S2F1	400	10	747.37 ^c	94.1 ^b	7.4 ^a
4	S2F2	400	15	749.60 ^c	96.387 ^a	5.1 ^b
5	S3F1	500	10	824.77 ^a	96.933 ^a	4.566 ^b
6	S3F2	500	15	799.43 ^b	97.433 ^a	4.06 ^b
7	Grand mean			759.72	95.5	6.04
8	CV			0.86	0.95	15

S = Speeds, F = feed rate, CV = Coefficient of variation

Cost estimation

The costs of various parts as well as additional expenses were computed for estimating the costs associated with motorized turmeric-slicing machine. By applying farm machinery cost estimation techniques, depreciation, interest on capital, electric costs, wages, lubricant costs, repair and maintenance costs, tax, and insurance have been estimated as 6.4, 5.2, 0.93, 25, 0.51, 1.8, and 0.49 ETB h⁻¹, respectively. The turmeric slicer for slicing fresh turmeric rhizomes was found to have production costs of 56,324 Ethiopian birr. The motorized turmeric slicer machine was predicted to return for itself in a duration of ten to eleven months, or ten plus six months. The same pattern of cost estimation for root crop slicer was reported by [Kunta \(2018\)](#). A similar trend for root crop slicers was reported by [Singh \(2016\)](#). A comparable relation for root crop slicers was observed by [Katanga \(2022\)](#).

CONCLUSION

The turmeric slicer's evaluation was assessed at three different rotor speed settings and two different feeding rate settings at mean moisture contents of 48% at the wet basis for fresh turmeric rhizome Tepi-1 (Bonga 51/71) variety. The slicer underwent evaluation in terms of material loss, slicing efficiency, and slicing capacity. Studies revealed that understanding the physical characteristics of the turmeric rhizome was crucial for post-harvest tasks like material handling, testing, and processing. According to determination results, geometric mean diameter, arithmetic mean diameter, square mean diameter, equivalent diameter, aspect ratio, sphericity, shape factor, bulk density, porosity, coefficient of friction, and angle of repose were found to be 23.9 mm, 30.3 mm, 45.3 mm, 33.2 mm, 0.33, 0.4, 1.8, 336 kg m⁻³, 81.7%, and 28.4°, respectively. The results of the evaluations showed that as rotor speeds raised from 300 rpm to 500 rpm, the slicing capacity rose from 714.9 kg h⁻¹ to 824.7 kg h⁻¹, the slicing efficiency rose from 93.9% to 97.4%, and the material loss reduced from 7.6% to 4.06%. According to the results, the slicer machine's performance indicators were affected by rotor speeds and feed rates but were not affected by their interactions except slicing capacity.

DECLARATION OF COMPETING INTEREST

The author declares that there is no conflict of interest.

CREDIT AUTHORSHIP CONTRIBUTION STATEMENT

The author declared that the following contributions is correct.

Amanuel Erchafo Ertebo: Investigation, methodology, conceptualization, formal analysis, data curation, validation, writing-original draft, review, editing, and visualization etc.

ETHICS COMMITTEE DECISION

This article does not require any Ethical Committee Decision.

REFERENCES

- Abubakar I, Yusuf DD, Muhammed US, Zakariyah A, Agunsoye JK, Habiba KA and Bashir ZU (2019). Performance evaluation of a portable ginger slicing machine. *Journal of Engineering Research and Reports*, 5(3): 1-8. <https://doi.org/10.9734/jerr/2019/v5i316925>
- Adeleke O, Ojekanmi O and Seidu I (2021). Development and performance evaluation of a quadcopter. *International Journal of Advanced Engineering and Management*, 3 (September): 1116.
- Agbetoye LAS and Balogun A (2009). Design and performance evaluation of a multi-crop slicing machine. 5th International Technical Symposium on Food Processing, Monitoring Technology in Bioprocesses and Food Quality Management, February, 622-640. <https://doi.org/10.51244/IJRSI>
- AOAC (2000). Association of Official Analytical Chemists, Official Method of Analysis, 15th Ed., Washington, DC and Arlington, VA: c2000.
- Deribe H (2021). Spices production in Ethiopia: A review. *Agricultural Reviews*, 7: 11-17. <https://doi.org/10.18805/ag.rf-218>
- Devarshi AP, Shirsat BS, Sawant AA and Dhande KG (2023). Design and development of fresh turmeric rhizome slicer. *TPI International Journal*, 12(10): 267-272.
- Dhineshkumar V and Anandakumar S (2016). Physical and engineering properties of turmeric rhizome. *Journal of Food Research and Technology*, 4(1): 30-34.
- Girma H and Mohammedsani Z (2021). Pre- and post-harvest practices influencing yield and quality of turmeric (*Curcuma longa* L.) in Southwestern Ethiopia: A review. *African Journal of Agricultural Research*, 17(8): 1096-1105. <https://doi.org/10.5897/ajar2020.15409>
- Hailemariam MM, Abera S and Neme G (2023). Effects of processing methods on the quality of turmeric (*Curcuma longa* L.). Haramaya University.
- Hailemichael G, Kiflew H and Mitiku H (2016). Spices Research Achievements, Challenges and Future Prospects in Ethiopia. 4 (January), 9-17. <https://doi.org/10.14662/ARJASR2015.061>
- Hordofa TS and Tolossa TT (2020). Cultivation and postharvest handling practices affecting yield and quality of major spices crops in Ethiopia: A review. *Cogent Food and Agriculture*, 6(1): 1788896. <https://doi.org/10.1080/23311932.2020.1788896>
- Katanga J (2022). Design and fabrication of an engine operated turmeric grinding machine. Busitema University.
- Khurmi RS and Gupta JK (2005). A textbook of machine design. S. Chand Publishing.
- Kunta N (2018). Techno-economic analysis of extraction curcumin from turmeric.
- Lazarus WF (2008). Estimating farm machinery repair costs. Extension Economist, University of Minnesota, 8.
- Mishra AK and Kulkarni SD (2009). Engineering properties of Turmeric Rhizome (*Curcuma longa* L.). *Agricultural Engineering Today*, 33(2): 26-31.
- Muogbo PC, Gbabo A, Nwakuba NR and Ejechi ME (2017). *Status and prospects for mechanization of turmeric production and postharvest operations in Nigeria*. Nigerian Institution of Agricultural Engineers (NIAE). Conference: 18th International Conference.
- Murumkar RP, Borkar PA, Bhoyar SM, Rajput MR, Dorkar AR and Rathod PK (2016a). Performance evaluation of PDKV turmeric slicer for slicing of ginger. *Journal of Ready To Eat Food*, 3(1): 6-12.
- Murumkar RP, Borkar PA, Bhoyar SM, Rathod PK. and Dorkar AR (2016b). Testing of turmeric slicer for potato slicing. *International Journal of Advanced Research*, 4(10): 701-709. <https://doi.org/10.21474/ijar01/1847>
- Nair KPP (2013). The agronomy and economy of turmeric and ginger: the invaluable medicinal spice crops. *Newnes*, p. 544.
- Navyashree BM, Vedamurthy KB, Vaishnavi and Venkataramana MN (2024). Economic analysis of cost and returns in turmeric production and processing in the Chamarajanagar district of Karnataka, India. *Journal of Scientific Research and Reports*, 30(5): 570-579. <https://doi.org/10.9734/jsrr/2024/v30i51973>
- Obaia A and Ibrahim MM (2015). Physical and aerodynamic properties of some agricultural crops. *Journal of Agricultural Research*, 93(5): 577.

- Polshettiwar SA, Sawant DH, Abhale NB, Chavan NB, Baheti AM, Wani MS, Tagalpallewar AA, Deshmukh CD and Polshettiwar A P (2022). Review on regulation of herbal products used as a medicine across the globe: A case study on turmeric - golden medicine. *Biomedical and Pharmacology Journal*, 15(3): 1227-1237. <https://doi.org/10.13005/bpj/2458>
- Rajkumar P, Ganapathy S and Amirtham D (2021). Comparative study on engineering properties of the selected turmeric varieties (Prathibha & Erode local). *Journal of Pharmacognosy and Phytochemistry*, 10(1): 1870-1873.
- Ramos J, Santiago M, Barreto R, Talaro NM and Cullat J (2021). Determination of the physical and mechanical properties of turmeric (*Curcuma longa* L.). *Philippine Journal of Agricultural and Biosystems Engineering*, 17(1): 27-38. <https://doi.org/10.48196/017.01.2021.03>
- Shi S (2020). Assessment of turmeric processing and its production. 8-15.
- Singh TP (2016). Farm machinery. *PHI Learning Pvt. Ltd.*
- Shirsat BS, Patel S, Borkar PA and Bakane PH (2018). Physical properties of fresh ginger (*Zingiber officinale*) rhizomes. *Multilogic in Science*, 8: 304-307.
- Tanimola OA, Odunukan R and Bankole YO (2019). Development of a turmeric slicing machine. *International Journal of Sciences & Applied Research*, 6(11): 15-23. <https://www.ijisar.in/Admin/pdf/development-of-a-turmeric-slicing-machine.pdf>
- Thul PP, Shirsat BS and Sawant AA (2022). Studies on engineering properties of fresh turmeric (*Curcuma longa* L.) rhizomes. *The Pharma Innovation Journal*, 11(9): 2587-2590.



Turkish Journal of
Agricultural
Engineering Research
(Turk J Agr Eng Res)
e-ISSN: 2717-8420



Investigating the Potential of Biomethane Production from Blends of Cattle Waste with Switchgrass (*Panicum virgatum* L.) and Sugar Beet (*Beta vulgaris* L.) Foliage

Cevat FİLİKÇİ^{a*} , Tamer MARAKOĞLU^b 

^aKırşehir Ahi Evran University, Çiçekdağı Vocational School, Department of Crop and Animal Production, Kırşehir, TURKEY

^bSelçuk University, Faculty of Agriculture, Department of Agricultural Machinery and Technology Engineering, Konya, TURKEY

ARTICLE INFO: Research Article

Corresponding Author: Cevat FİLİKÇİ, E-mail: cevat.filikci@ahievran.edu.tr

Received: 30 August 2024 / Accepted: 01 November 2024 / Published: 31 December 2024

Cite this article: Filikci, C., & Marakoğlu, T. (2024). Investigating the Potential of Biomethane Production from Blends of Cattle Waste With Switchgrass (*Panicum virgatum* L.) and Sugar Beet (*Beta vulgaris* L.) Foliage. Turkish Journal of Agricultural Engineering Research, 5(2), 219-231. <https://doi.org/10.46592/turkager.1540939>

ABSTRACT

The research aimed to evaluate the biomethane (CH_4) content of biogas generated from various combinations of cattle waste (CW), three different varieties of Switchgrass (SG) (*Panicum virgatum* L.) plants (Kanlow (SG1), Shawne (SG2), Alamo (SG3), and sugar beet (*Beta Vulgaris* L.) leaves (BL). A laboratory-scale biomethane application setup was established to determine the biomethane potential. Three different experimental designs were implemented as the 1st application group, 2nd application group, and 3rd application group within the research framework. Biogas produced in the setup was stored using valves and balloons under optimal storage conditions. The Optima Biogas - Portable Biogas Analyzer device was employed to analyze the biomethane content of biogas samples from the materials and mixtures in the application groups. Biogas values were recorded, and glass reactor-specific methane production values were calculated. The highest glass reactor-specific methane production value was found to be $7.28 \text{ m}^3 \text{CH}_4 \text{ m}^{-3} \text{Reactor day}$ in the CW (50%)-SG (20%)-BL (30%) mixture. The components of the biogas produced from the treatment groups were identified, and the highest CH_4 (biomethane) yield was obtained from BL (beet leaves) at 58.86% in materials and from the CW-BL mixture at 53.76% in mixtures. Biomethane yields of the materials in other mixtures ranged from 53.42% to 43.12%.

Keywords: Biomethane, Biogas, Switchgrass, Sugar Beet Leaf, Biomass



INTRODUCTION

The energy demand is on the rise due to technological advancements both globally and locally. Consequently, there has been a shift towards various energy sources, especially recently. The inadequacy of exhaustible energy sources like oil, natural gas, and coal, along with their detrimental environmental impact, has prompted this change. However, there is a growing inclination towards renewable energy sources, which offer different and sustainable methods of energy production. Developed nations are actively diversifying their energy sources and exploring alternatives to reduce their reliance on specific energy types. Biofuels have emerged as a significant and rapidly expanding alternative energy source ([Eser *et al.*, 2007](#)).

Despite the significant potential of agricultural and animal wastes, they are currently not being utilized effectively. Wastes are either incinerated or disposed of in nature, with only a small portion being used as fertilizer after being left in open areas for extended periods. Animal wastes are not being properly managed, leading to uncontrolled discharge into agricultural areas, pastures, open spaces, and waterways, resulting in soil pollution and detrimental effects on both human and environmental health, including strong odors and increased mosquito populations during summer ([Avcıoğlu, 2011](#)).

In our country, the regulation on the control of solid wastes, which came into effect in 1991, outlines various methods and criteria related to the subject with certain limitations. Among these methods is the decomposition of organic wastes by aerobic microorganisms. This process results in the production of methane gas, also known as biogas ([Yaldız, 2004](#)).

Türkiye is negatively affected by the fact that 92% of our oil needs are met through imports and our economy is dependent on imports. This is a problem for all countries that are at risk in terms of energy security.

In the context of sustainable energy development, there is growing interest in agriculture-based biofuels such as biodiesel, bioethanol, biomass, and biogas on a global scale. Among 37 plant species in the USA, switchgrass has been identified as a key candidate due to its potential as a feed source and its significant bioenergy capacity. Switchgrass is highly favored for its ability to produce high net energy per unit area, its cost-effective cultivation, low ash content, efficient water utilization, adaptability to diverse environments, ease of seed production, and its capacity for carbon storage in the soil ([Samson and Omielan, 1992](#); [Sanderson *et al.*, 1996](#); [Christian and Elbersen, 1998](#)).

The key to successful Switchgrass cultivation lies in nurturing healthy plants. Therefore, it is crucial to focus on mechanization, soil preparation, and sowing techniques. Drawing on insights from past projects in our region, we aim to develop a system that optimizes the use of existing agricultural tools and machinery for the cultivation and establishment of this plant ([Soylu *et al.*, 2010](#)).

In the research project titled "*Adaptation of Switchgrass (*Panicum virgatum* L.), Creating Adaptation Maps, Determining Mechanization Characteristics, Energy Balance Sheet, and Biogas Production from Bioethanol Wastes*" with reference number 114O941 from TÜBİTAK. It was determined that the Kanlow variety of Switchgrass displayed the most favorable results for green biomass and dry grass in the Karapınar district of Konya province. However, in the Haymana district of

Ankara province, the Cave in Rock, Shawnee, and Shelter varieties showed promise for green biomass, while the Kanlow variety was found promising for dry herbage yield. Additionally, the Alamo variety was recommended for green biomass and hay yield at the Simav location. Although Switchgrass is a current plant that attracts attention for biofuel production all over the world, it is not sufficiently recognized in our country. If its cultivation is realized on a producer basis, it will provide significant gains in terms of energy production as it is an energy source in the coming years (Soylu *et al.*, 2010).

Sugar beet is an important agricultural crop with economic potential attributable to its high yield capacity. From literature sources, sugar beet yields range from 40 to 90 t ha⁻¹ and beyond (Ungai and Győri, 2007).

In a study conducted by Pospišil *et al.* (2006), the production of 42 sugar beet hybrids was investigated. The results revealed a wide range of yields, varying from 61 t ha⁻¹ to an exceptional high of 101.54 t ha⁻¹.

Annual weather conditions significantly influence the yield and technological quality of sugar beet, as demonstrated by Pospišil *et al.* (1999) when identical sugar beet varieties were utilized throughout the years of research.

In the context of sugar beet by-products, in addition to primary sugar production, sugar beet energy by-processing includes dry or wet sugar beet pulp, molasses, saturation sludge and approximately 60% of the green mass of sugar beet leaves. Previously used as cattle feed, the leaves and heads are now used as green manure on arable land. Given the global energy crisis, sugar beet is increasingly seen as a suitable energy crop for biofuel production (Szakál *et al.*, 2007). Sugar beet production in Turkey reached 18.9 million tons in 2023. Consequently, 756 thousand tons of sugar beet-derived agricultural waste was generated. The energy equivalent value of this agricultural waste is quantified as 265,881.2 TOE year⁻¹ (Anonymous, 2023). In this context, it is anticipated that the utilization of agricultural wastes from sugar beet as a substrate in biogas production will yield significant energy gains.

This research aimed to evaluate the biomethane potential of biogas produced from various combinations of cattle waste (CW), three different switchgrass (*Panicum virgatum* L.) varieties (SG1 (Kanlow), SG2 (Shawnee), SG3 (Alamo)) and sugar beet leaves (BL).

MATERIALS and METHODS

Material

Organic Materials Used in Biogas Production

The switchgrass varieties Kanlow, Shawnee, and Alamo were acquired from Konya Selçuk University, Faculty of Agriculture, Department of Field Crops. The switchgrass samples were finely ground and stored under optimal conditions. Similarly, sugar beet leaf samples used in biogas production studies were sourced from various regions in Konya province and stored under optimal conditions.

Establishment of Application Setup and Determination of Application Pattern to Determine Biogas Potential

In order to assess the biogas potential, the experimental setup illustrated in Figure 1 was utilized. The setup comprised a glass jar, a 10x7 polyurethane hose (Blue) with a length of 10 meters, 5 10 mm hose inlet ball valves, 5 pneumatic tees, and 20 1/4 - 10 pneumatic rotary elbows.

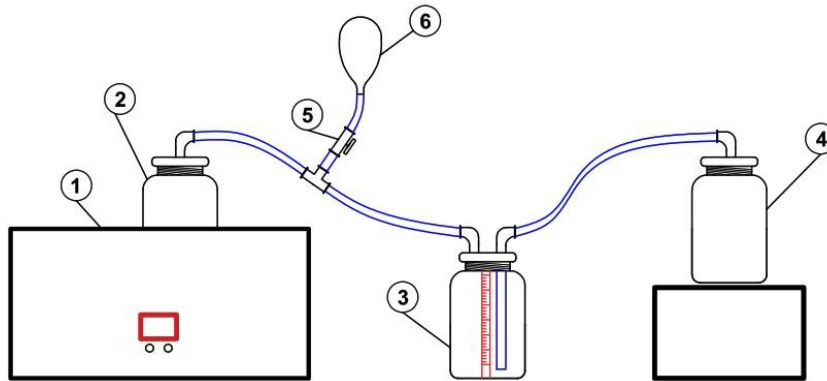


Figure 1. Application setup (1. Water Bath Device, 2. Reactor (Glass Jar), 3. Acidified Water (Gas Outlet), 4. Water Inlet, 5. Gas Sampling Valve, 6. Gas Storage Balloon).

In the context of this research, an application design was developed, consisting of three application groups: the 1st application group, the 2nd application group, and the 3rd application group. The implementation design can be found in Figure 2.

1 st Application					2 nd Application				3 rd Application		
CW	SG1 (Karlow)	SG2 (Shawne)	SG3 (Alamo)	BL	CW-SG1	CW-SG2	CW-SG3	CW-BL	CW(%50)- SG(%25)-BL(%25)	CW(%50)- SG(%30)-BL(%20)	CW(%50)-SG(%20)-BL(%30)

Figure 2. Application design.

Instruments and Devices Used in Experiments

Water bath devices

JSR - JSIB-22T Series Circulating Water Bath device and BW-10H Heating Bath (11.5L) device were used to maintain the reactor operating temperature as mesophilic (37 ± 1) in the biogas setup. The BW-10H Heating Bath (11.5L) represents an economically viable solution for maintaining optimal temperature control in laboratory settings. This digital water bath exhibits remarkable temperature stability, making it a dependable choice for scientific and research applications.

Precision balance

Weighing of the samples and mixtures prepared to be used in the determination of biogas potentials was carried out with the help of “Denver Instrument” brand precision measuring balance with a maximum capacity and sensitivity of 0.1 mg and 210 g, respectively.

pH measurement paper

The pH 0-14 pH indicator strip, universal indicator MColorpHast pH paper, was employed to ascertain the pH levels of the substances and combinations within the experimental groups during the treatment process.

OPTIMA Biogas - Portable Biogas Analyzer

The biomethane content of biogas samples collected from the materials and mixtures in the treatment groups was determined using the Optima Biogas - Portable Biogas Analyzer device.

Method

Performing Basic Characterization Analyses

We conducted basic characterization analyses (dry matter, organic matter) to determine the quantities of energy crops such as switchgrass, sugar beet leaves, and cattle wastes to add to the experimental setup. This setup was established to measure biogas yield and achieve the desired solids amount in the reactor (refer to Table 1).

Table 1. Analysis of Basic Characterization (dry matter, organic matter).

Sample Name	Organic Matter (%)	Sample (g)	Oven Dry (g)	Dry Matter (%)
SG-1 (Kanlow)	6.92	4.6506	4.3286	93.08
SG-2 (Aloma)	6.42	3.1603	2.9573	93.58
SG-3 (Shelter)	6.30	3.7667	3.5295	93.70
Sugar Beet Leaf	85.71	20.4167	2.9174	14.29
Cattle Waste	90.12	14.8338	1.4657	9.88

Determination of Mixture Ratios Used in Applications

It is essential to maintain specific reactor conditions to optimize the fermentation of bacteria in an anaerobic environment for the production of biogas and methane.

Achieving the ideal dry matter level in the feed materials is crucial for this process ([Von Mitzlaff, 1988](#); [Nagamani and Ramasamy, 1999](#)). Research indicates that biogas production is most efficient when the total dry matter content of the feed materials falls within the range of 6-13% ([Šarapatka, 1993](#)).

The Department of Soil Science and Plant Nutrition at the Faculty of Agriculture, Selçuk University, conducted comprehensive analyses to determine the dry matter ratio and optimized different mixing ratios of three Switchgrass varieties and beet leaf samples with constant cattle waste samples.

Determination of Biomethane Potential (BMP)

Please take note of the following information: In our experiments, we used 1000 ml glass jar bottles as reactors to determine the biomethane potential. The experimental setup was positioned in a secluded area to shield it from sunlight. The reactors were operated under mesophilic conditions at $37\pm^{\circ}\text{C}$. To maintain a constant temperature, we utilized a JSR - JSIB-22T Series circulating water bath device and a BW-10H heating bath (11.5l) device. To measure the biogas produced in the reactors, we connected two glass jars using pneumatic sealing elements, and the water displacement principle was employed. The first glass jar, connected to the reactor, was filled with water acidified with sulfuric acid (H_2SO_4) to a pH of less than 2, and then sealed ([Durgut, 2020](#)).

The volumes were determined by drawing on the glass jars from the SolidWorks program on the PC, and the volumes corresponding to each mm length were determined and added to the glass jars for readings. In order to measure the gas content of the gas between the reactor and the glass jar filled with acidified water, a valve was added to the connection line between the two glass jars. At the end of the experiments, the gas collected by means of the valve was removed from the gas containment flask and the gas content was determined. In order to determine the amount of biogas released as a result of the experiments, measurements were made with the help of scales added on glass jars filled with water and recorded in computer environment.

At the end of the gas outputs, the gases collected in the balloons by means of the valve were preserved and the biogas contents were realized with the help of the measuring device.

Biogas Collection for Measurement of the Amount of Biogas Produced and Determination of Biogas Content

Daily readings were made with the help of the volume scale created to measure the amount of biogas produced in the anaerobic reactor by anaerobic fermentation of Switchgrass and beet leaves. The detected biogas values were recorded in computer environment. In the experimental setup, biogas storage was provided with the help of valves and balloons and biogas compositions (CH_4 (%), H_2S (ppm), CO_2 (%), O_2 (%), N_2 (%)) were determined.

Determination of Specific Biomethane Production Values of Materials

Biomethane production values were calculated for each sample as a result of the analysis to determine the amount of biogas and its components. During the calculation, the temperature at which the experiment was conducted, the

temperature at which the biogas yield measurement was determined and the effect of the empty volume inside the glass reactor were taken into account. The following Equation 1 was used to determine the specific biomethane production values (Onursal, 2016).

$$\text{mL CH}_4 = \left[\frac{V_r \cdot |M_2 - M_1|}{100} * \frac{273,15}{T_1 + 273,15} \right] * \left[\frac{V_g \cdot |M_2 - M_1| * 0,5}{100} * \frac{273,15}{T_1 + 273,15} \right] \quad (1)$$

V_r : Void volume inside the biomethane reactor, (mL),

M_1 : Biomethane value before measurement, (%),

M_2 : Measurement day biomethane value, (%).

Where; 273,15: Kelvin, T_1 is the temperature of the biomethane at which the measurement was made and 36°C was taken, T_2 is the temperature of the biogas amount at which the measurement was made and 25°C and V_g is the amount of biogas (mL) used in the formula.

Glass Reactor Specific Methane Production

The amount of methane production per glass reactor volume for one day is expressed as specific methane production. The glass reactor specific methane production amount was calculated through the Equation 2 below (Onursal, 2016).

$$R_{\text{grm}} = \frac{V_g}{V_r} \quad (2)$$

R_{grm} : Glass reactor specific methane production value ($\text{m}^3\text{CH}_4 \text{ m}^{-3} \text{ glass reactor day}$),

V_g : Amount of methane produced during one day (m^3CH_4),

V_r : Total volume of the glass reactor (m^3).

Statistical Evaluation of Biomethane Values

The biomethane values obtained as a result of the trials were analyzed with the analysis of variance test to determine whether there was a significant difference between the materials in the statistical package program. LSD results were used to show that there was a relevant comparison among the materials.

RESULTS AND DISCUSSION

Material and Mixtures Potential Production of Methane

The actual methane production amount of the materials in the experiments was 5916.35 mL CH_4 in the mixture of CW (50%) - SG (20%) - BL (30%). The overall amount of original methane yield of the materials obtained during the 1st, 2nd and 3rd treatments (mL) is presented in Table 2.

Table 2. Original methane production values of materials (mL).

Material	CH ₄ (mL)
CW	2844.29
SG1	1594.29
SG2	618.25
SG3	667.63
BL	1744.2
CW-BL	327.52
CW-SG1	574.54
CW-SG2	96.59
CW-SG3	160.71
CW(%50)- SG(%25)-BL(%25)	442.03
CW(%50)- SG(%30)-BL(%20)	1887.25
CW(%50)- SG(%20)-BL(%30)	5916.35

Glass Reactor Original Methane Production Values

Reactor related methane produced by using a particular formula. After the calculation, it was determined that the highest reactor-specific methane production value was 7.28 m³CH₄ m⁻³ reactor day for the CW (50%)-SG (20%)-BL (30%) mixture. You can refer to Table 3 for the specific methane production values of all materials and mixtures in the experimental groups.

Table 3. Glass reactor specific methane production values (m³CH₄ m⁻³) glass reactor day).

Material	R _{özü} (m ³ CH ₄ m ⁻³ Glass Reactor day)
CW	3.50
SG1	1.97
SG2	0.76
SG3	0.82
BL	2.15
CW-BL	0.40
CW-SG1	0.71
CW-SG2	0.12
CW-SG3	0.2
CW(%50)- SG(%25)-BL(%25)	0.54
CW(%50)- SG(%30)-BL(%20)	2.32
CW(%50)- SG(%20)-BL(%30)	7.28

In their study, [Jin *et al.* \(2012\)](#) investigated the effect of semi-feeding and continuous anaerobic reactors on the yield of pearl Switchgrass and municipal wastewater biomasses at the laboratory level. They found that the unique methane production value was found in finely Switchgrass, 2%-loaded pearl Switchgrass from the October harvest (0.317 m³ CH₄ kg⁻¹ pearl Switchgrass and 0.359 317 m³ CH₄ kg VKM⁻¹).

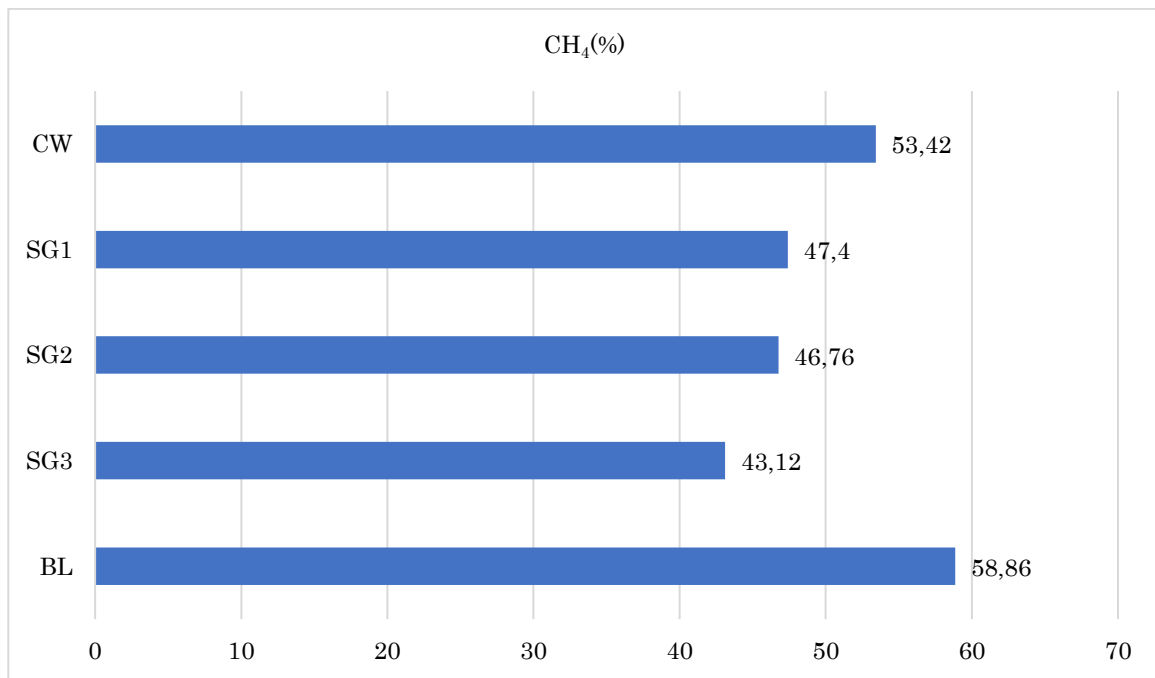
Components of Biogas Produced from Materials and Mixtures

The components of the biogas produced from the treatment groups were determined and the highest CH₄ (methane) yield was determined as 58.86% in BL (beet leaves) and 53.76% in BHA-BL mixture. Methane yields of other mixtures and materials in the treatments varied between 53.22% and 43.12% (Table 4).

Table 4. Components of biogas produced from materials.

Material	CH ₄ (%)	H ₂ S (ppm)	CO ₂ (%)	O ₂ (%)	N ₂ (%)
CW	53.42	12	15.6	11.36	19.61
SG1	47.4	6	20.5	6.85	25.25
SG2	46.76	5	21.26	6.81	25.17
SG3	43.12	5	23.25	6.83	26.8
BL	58.86	9	16.85	7.36	24.92
CW-BL	49.78	9	16.48	7.26	26.18
CW-SG1	48.43	8	16.62	7.16	27.79
CW-SG2	44.86	7	16.06	6.98	32.1
CW-SG3	53.76	10	16.37	9.19	20.68
CW(%50)- SG(%25)-BL(%25)	51.74	9	16.85	7.49	23.92
CW(%50)- SG(%30)-BL(%20)	50.86	9	16.85	7.36	24.92
CW(%50)- SG(%20)-BL(%30)	53.22	10	16.68	8.27	21.84

In Treatment 1, the highest biomethane yield was determined in BL with 58.86%. Among the other materials, CW, SG1, SG2 and SG3 yielded 53.42%, 47.4%, 46.76% and 43.12%, respectively (Figure 3). In their study, [Sheets *et al.* \(2015\)](#) also looked at the effect of dry matter ratio on methane yield from switchgrass plants in mixtures with hot. In biomethane production, the highest biomethane yields of 13% and 22% were obtained under mesophilic conditions in the reactor operating as solid fermentation.

**Figure 3.** 1st Application biomethane yield values (%).

In the 2nd treatment, the highest biomethane yield was determined in CW-BL with 53.76%. Among the other materials, CW-SG1, CW-SG2 and CW-SG3 yielded 49.78%, 48.43% and 44.86%, respectively (Figure 4).

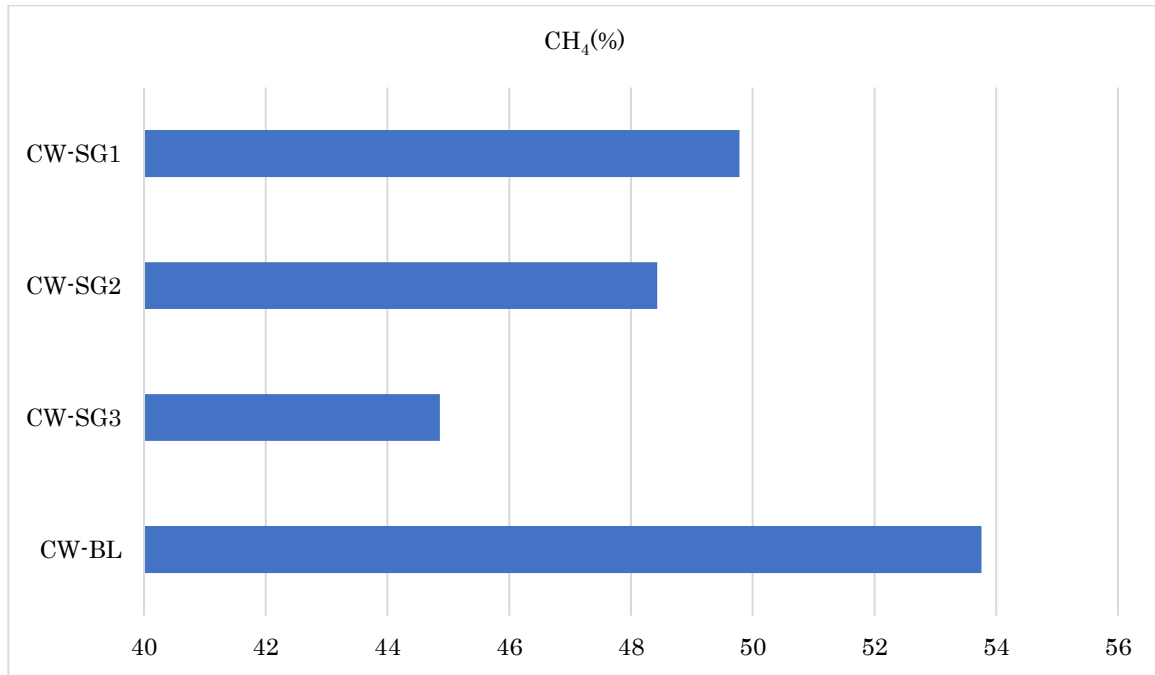


Figure 4. 2nd Application biomethane yield values (%).

In the 3rd treatment, the highest biomethane yield was found in the mixture of CW (50%)-SG (20%)-BL (30%) with 53.22%. Among the other materials, it was determined as 51.74% in CW (50%)-SG (25%)-BL (25%) mixture and 50.86% in CW (50%)-SG (30%)-BL (20%) mixture, respectively (Figure 5). Ciggin (2016), in his study, mixed switchgrass with process sludge. According to the results of the experiment, the highest methane yield was found in the mixture of 0.4-0.6 ratio. In their study, [Liew *et al.* \(2012\)](#) investigated methane production from corn cobs, wheat straw, garden waste and leaves by anaerobic fermentation. The highest methane yield of 81.2 L kgVKM⁻¹ was observed in corn cobs, followed by wheat straw (66.9 L kgVKM⁻¹), leaves (55.4 L kgVKM⁻¹), and garden waste (40.8 L kgVKM⁻¹).

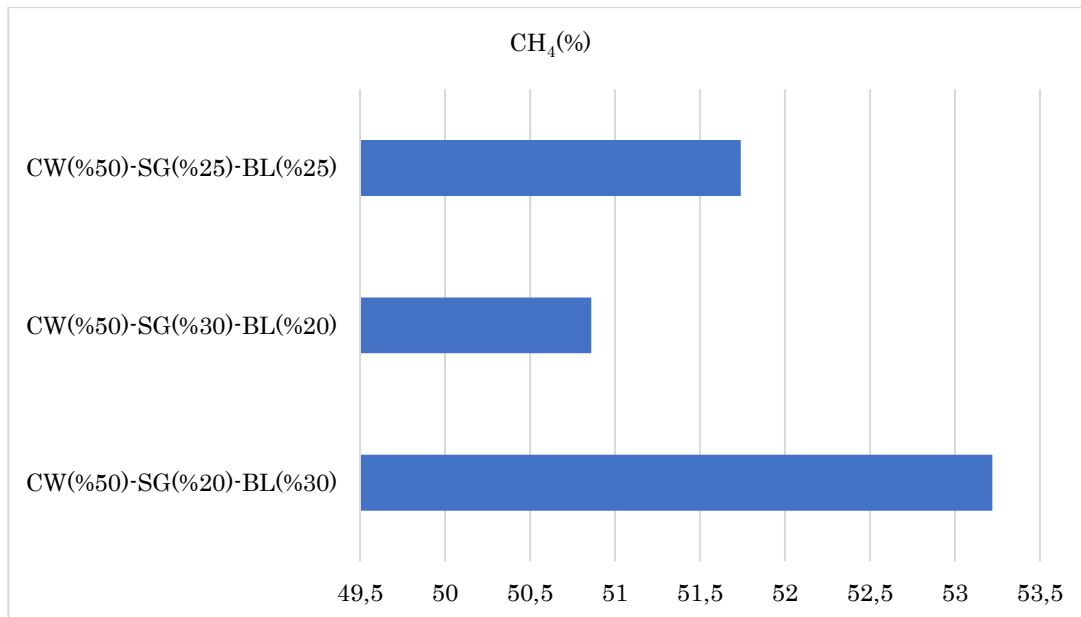


Figure 5. 3rd Application group biomethane yield values (%).

Evaluation of Statistical Analysis

Variance analysis was performed for the treatments and biomethane ratios were found to be significant at $p < 0.05$ level in variance analysis (Table 5). LSD test was performed on these significant values (Table 6).

Table 5. Analysis of variance results.

Application	Average Biogas Yield (ml/gDM)	Standard Deviation	Standard Deviation Square (Variance)	Minimum	Maximum
CW-SG1	49.16	0.82	0.67	48.2	49.78
CW-BL	52.49	1.28	1.63	51.2	53.76
CW-(50%) - SG (25%) - BL (25%)	50.48	1.37	1.88	49	51.74
CW- (50%) - SG (30%) - BL(20%)	48.92	1.78	3.17	47.3	50.86
CW- (50%) - SG 2(0%) - BL(30%)	52.00	1.28	1.63	50.7	53.22

Table 6. LSD test results.

Material	N	Standard Error Mean	Mean ⁽¹⁾
CW-SG1	4	0.48676	52.48 _A
CW-BL	4	0.73904	52,006 _A
CW-(50%) - SG (25%) - BL (25%)	3	0.79858	50.48 _{AB}
CW- (50%) - SG (30%) - BL(20%)	3	1.04006	49.16 _B
CW- (50%) - SG 2(0%)- BL(30%)	3	0.72896	48.92 _B

⁽¹⁾ The difference between the means shown with different lowercase letters in the same column is statistically significant (A, B: $p < 0.05$, LSD= 2.454).

When the table obtained according to the LSD results is examined, the highest yield was obtained in the BHA-SG1 mixture and the lowest biomethane yield was obtained in the CW (50%) - SG (20%) - BL (30%) mixtures.

CONCLUSION

The fact that our country is foreign-dependent in terms of energy supply makes renewable energy sources an important issue. In our research on the Switchgrass plant as part of the TÜBİTAK project, we examined mechanization criteria for the first time. We discovered that by combining the sugar beet plant, abundant in Konya and its surrounding areas, with cattle waste, we could determine the biogas yield. During the study, we calculated the reactor based methane productivity using a specific formula. The highest reactor based methane production value obtained was $7.28 \text{ m}^3\text{CH}_4 \text{ m}^{-3} \text{Reactor day}$ for the CW (50%)- SG (20%)-BL (30%) mix.

The components of the biogas produced from the trial groups were determined and the highest CH_4 (methane) yield was determined as 58.86% in BL (beet leaves) in materials and 53.76% in CW-BL mixture in mixtures. Methane yields of other mixtures and materials of the experimental groups varied between 53.22% and 43.12%.

Agricultural and livestock mechanization plays a significant role in our economy today. However, the majority of the energy requirements for agricultural operations are currently met using non-renewable energy sources. The utilization of biogas, which is environmentally friendly and helps reduce production inputs, is becoming increasingly important for meeting energy needs in agricultural operations. Biogas can be produced from animal manure, various energy crops, and agricultural waste, offering the potential to enhance operational efficiency and decrease carbon dioxide (CO₂) emissions, thus mitigating environmental impact. As a result of the applications, high biomethane rates were obtained in BL mixtures. Beet leaves can be considered as an important waste in terms of agricultural waste in our country within the framework of production area and product obtained. Beet leaves generated from sugar beet agriculture, especially in Konya province and its surroundings, are used in some animal feed, but 100% disposal cannot be ensured. The huge biomass formed by beet leaves can be converted into biogas energy as a result of anaerobic fermentation and recovery can be achieved.

DECLARATION OF COMPETING INTEREST

We declare that we have no conflict of interest.

ACKNOWLEDGEMENT

This study was summarized from a part of the PhD Thesis titled “*Investigation of biogas yield of some vegetable and animal wastes and Switchgrass (Panicum virgatum L.) mixtures*”.

CREDIT AUTHORSHIP CONTRIBUTION STATEMENT

The authors declared that the following contributions are correct.

Cevat FİLİKCI: Investigation, methodology, conceptualization, validation, writing - original draft, visualization,

Tamer MARAKOĞLU: Formal analysis, data curation, validation, review, and editing.

ETHICS COMMITTEE DECISION

This article does not require any Ethical Committee Decision.

REFERENCES

- Anonymous (2023). Beet production, TUIK Data. <https://www.tuik.gov.tr/>
- Avcıoğlu AO (2011). Renewable energies of agricultural origin: Biofuels, *Nobel Academic Publishing*.
- Ayhan A (2013). *A Research on determining the amount of biogas that can be produced by mesophilic fermentation from cattle manure and corn silage at different mixing ratios*. Doctoral dissertation, Bursa Uludag University (Turkey), 28740461.

- Christian D and Elbersen H (1998). Prospects of using *Panicum virgatum* (switchgrass) as a biomass energy crop. N. ElBassam (Ed.), 257-263.
- Durgut FT (2020). *Fabrication of a prototype biogas reactor for experimental purposes and evaluation of its performance in different biomass mixtures and media*. Tekirdağ Namık Kemal Üniversitesi, Fen Bilimleri Enstitüsü, Biyosistem Mühendisliği A.B.D. Doktora Tezi, s. 84, Tekirdağ.
- Eser V, Sarsu F and Altunkaya M (2007). *Current status and future of plants used in biofuel production*. Biofuels and Biofuel Technologies Symposium, 51, 61.
- Filikci C (2018). Determination of mechanization characteristics in Switchgrass cultivation, Institute of Science and Technology. *Selcuk Journal of Agriculture and Food Sciences*, 31(3): 111-115. <https://doi.org/10.15316/SJAfS.2017.42>
- Jin G, Bierma T and Walker P (2012). Biogas production from switchgrass under experimental conditions simulating US digester operations. *Journal of Environmental Science and Health, Part A*, 47(3): 470-478. <https://doi.org/10.1080/10934529.2012.646150>
- Liew LN, Shi J and Li Y (2012). Methane production from solid-state anaerobic digestion of lignocellulosic biomass. *Biomass and Bioenergy*, 46: 125-132. <https://doi.org/10.1016/j.biombioe.2012.09.014>
- Nagamani B and Ramasamy K (1999). Biogas production technology: An Indian perspective. *Current Science*, 44-55. <https://www.jstor.org/stable/24102913>
- Onursal E (2016). *Optimization and economic analysis of effective factors in biogas production from rose processing wastes*. Süleyman Demirel University Institute of Science and Technology Doctoral dissertation.
- Pospišil M, Mustapić Z, Pospišil A, Tot I and Salaj M (1999). Ispitivanje gospodarskih svojstava novih hibrida šećerne repe. *Sjemenarstvo*, 16(5): 403-413. <https://hrcak.srce.hr/168112>
- Pospišil M, Pospišil A, Mustapić Z, Butorac J, Tot I and Žeravica A (2006). Proizvodne vrijednosti istraživanih hibrida šećerne repe. *Poljoprivreda*, 12(1): 16-21. <https://hrcak.srce.hr/5567>
- Samson RA and Omielan JA (1992). *Switchgrass: A potential biomass energy crop for ethanol production*. The Thirteenth North American Prairie conference, Windsor, Ontario.
- Sanderson MA, Reed R, McLaughlin S, Wulschleger SD, Conger BV, Parrish D, Wolf D, Taliaferro C, Hopkins A and Ocumpaugh W (1996). Switchgrass as a sustainable bioenergy crop. *Bioresource Technology*, 56(1): 83-93. [https://doi.org/10.1016/0960-8524\(95\)00176-X](https://doi.org/10.1016/0960-8524(95)00176-X)
- Šarapatka B (1993). A study of biogas production during anaerobic fermentation of farmyard manure. *Biomass and Bioenergy*, 5(5): 387-393. [https://doi.org/10.1016/0961-9534\(93\)90018-Y](https://doi.org/10.1016/0961-9534(93)90018-Y)
- Sheets JP, Ge X and Li Y (2015). Effect of limited air exposure and comparative performance between thermophilic and mesophilic solid-state anaerobic digestion of switchgrass. *Bioresource technology*, 180: 296-303. <https://doi.org/10.1016/j.biortech.2015.01.011>
- Soylu S, Sade B, Ögüt H, Akınerdem F, Babaoğlu M, Ada R, Eryılmaz T, Öztürk Ö and Oğuz H (2010). Investigation of cultivation possibilities of Switchgrass (*Panicum virgatum* L.) as an alternative biofuel and silage crop for Turkey. TÜBITAK, TOVAG-107 O, 161.
- Szakál P, Schmidt R, Lesny J, Kalocsai R and Barkóczi M (2007). Quality parameters of wheat. Bio ethanol versus bread? *Cereal Research Communications*, 35: 1137-1140. <https://doi.org/10.1556/CRC.35.2007.2.243>
- Ungai D and Győri Z (2007). Possibility of increasing sugar yield by foliar treatments for crop production sustainability. *Cereal Research Communications*, 35: 1241-1244. <https://doi.org/10.1556/CRC.35.2007.2.269>
- Von Mitzlaff K (1988). Engines for biogas. *Deutsche Zentrum für Entwicklungstechnologien*.
- Yaldız O (2004). Biogas Technologies Textbook.



Turkish Journal of
Agricultural
Engineering Research
(Turk J Agr Eng Res)
e-ISSN: 2717-8420



Exploring the Potential of Producing Biomass Energy from Agricultural Residues in Chad

Mohamedeltayib Omer Salih EISSA^{a*}

^aDepartment of Agricultural Engineering, Faculty of Engineering, University of Bahri, Khartoum Bahri, SUDAN

ARTICLE INFO: Research Article

Corresponding Author: Mohamedeltayib Omer Salih EISSA, E-mail: mohammeddl123@gmail.com

Received: 08 September 2024 / **Accepted:** 14 November 2024 / **Published:** 31 December 2024

Cite this article: Eissa, M.O.S. (2024). Exploring the potential of producing biomass energy from agricultural residues in Chad. Turkish Journal of Agricultural Engineering Research, 5(2), 232-243.
<https://doi.org/10.46592/turkager.1545563>

ABSTRACT

This study investigates the potential for generating biomass energy from agricultural residues in Chad. Biomass energy, derived from organic materials, is a renewable and sustainable energy source that can significantly contribute to the energy needs of many countries. In Chad, a country with a predominantly agrarian economy, agricultural residues present a promising opportunity for biomass energy production. The biomass energy production from agricultural residues in Chad holds significant potential to contribute to the country's energy needs while promoting sustainable development. The country possesses abundant agricultural resources, with substantial residues remaining after harvest, including sorghum stalks, maize stalks, millet straw, and rice straw, often underutilized. These residues can be converted into biofuels like biogas through anaerobic digestion or burned directly to produce heat and electricity. Using data from the Food and Agriculture Organization Statistical Database of the United Nations (FAOSTAT) for 2021, the annual production of agricultural residues was quantified, and their energy potential was calculated based on the residue-to-product ratio and the calorific values of specific residues. The major crops contributing to the total residue amount in Chad are sorghum (56.50%), rice (17.72%), maize (13.31%), millet (6.70%), and dry beans (5.37%). The total amount of agricultural residues in Chad, including annual crop residues, was calculated to be about 18.1 kilotons (kt). The study reveals that the total energy potential of these residues is approximately 252.5 terajoules (TJ) for the 2021 production period in Chad.

Keywords: Renewable energy, Biofuel, Electricity, Heating value, Energy potential

INTRODUCTION

Chad, situated in Central Africa, is a landlocked country located between 7° and 24° north latitude and 13° and 24° east longitude. It shares borders with Libya to the north, Sudan to the east, the Central African Republic to the south, and Cameroon, Niger, and Nigeria to the west. Notably, it shares Lake Chad with these western neighbors ([Soulouknga et al., 2020](#)). The rapid population growth in developing



Copyright © 2024. This is an Open Access article and is licensed under a Creative Commons Attribution 4.0 International License (CC-BY-NC-4.0) (<https://creativecommons.org/licenses/by-nc/4.0/deed.en>).

countries, coupled with limited access to electricity, particularly in remote or rural areas, presents significant challenges for energy production ([Jahangiri et al., 2019](#)). Energy plays a crucial role in economic development, with a clear correlation between energy consumption and living standards ([Demirel et al., 2019](#)). Every nation's economic growth is closely tied to its electricity infrastructure and availability. Electricity has become a central element of daily life in the modern world, influencing various sectors and activities essential for economic development ([Kriga et al., 2023](#)). Energy sources can be divided into three categories: fossil fuels, renewable sources, and nuclear sources ([Eissa et al., 2024](#)). Renewable energy sources are readily available, inexhaustible, and mostly environmentally clean, making them a sustainable option for meeting energy needs ([Kelly et al., 2023](#)).

Conversely, the depletion of fossil fuels and the imperative to mitigate greenhouse gas (GHG) emissions have intensified the pursuit of alternative energy sources, particularly in many developing nations where energy poverty remains a significant concern. The increasing global worry about climate change and its impacts has led to a heightened focus on renewable energy as the cornerstone of a dependable and eco-friendly energy provision system ([Kidmo et al., 2022](#)). Researchers worldwide have explored the potential of harnessing renewable energy for electricity generation due to the adverse environmental impacts of fossil fuels ([Soulouknga et al., 2020](#)).

According to the United States Energy Information Administration projections, global energy consumption is expected to surge by 50% by the year 2050, following the current trajectory ([Djimtoingar et al., 2022](#)). Between 1993 and 2005, energy consumption in Chad increased from 200 koe (kilo of oil equivalent) to 292 koe. Wood fuels, including wood and charcoal, dominate energy consumption, accounting for 90% of the total, while conventional energy sources such as petroleum products and electricity contribute only 10%. Wood fuels are predominantly used for cooking in households (88%), while kerosene lamps are the primary source of lighting, utilized by 69% of households ([Medjo Nouadje et al., 2024](#)).

Chad currently needs to grapple with an electricity supply deficit, low rates of electricity access, and notably high costs per kilowatt-hour. These challenges stem from heavy reliance on fossil fuels, limited interconnection with neighboring countries, and insufficient integration of renewable energies into electricity generation ([Medjo Nouadje et al., 2024](#)). Making electricity accessible in Chad is crucial from a socio-economic standpoint because much of the population still struggles to obtain reliable access ([Soulouknga et al., 2023](#)). In Chad, only 8% of the population has access to electricity, highlighting a substantial disparity between rural (1%) and urban (20%) areas. Chad ranks among the countries with the lowest electricity access rates globally ([Soulouknga et al., 2022](#)). Over two-thirds of Africa's population, approximately 621 million people, lack access to electrical energy ([Jahangiri et al., 2019](#)). Approximately 775 million people worldwide are estimated to lack access to electricity ([Verhoeven and Pouget-abadie, 2024](#)).

Biomass energy includes agricultural residues, household waste, fuelwood, animal waste, and other fuels derived from biological sources ([Karaca, 2017](#)). Biomass resources are globally recognized as sustainable alternative energy sources due to their widespread availability, renewable nature, and carbon-neutral characteristics ([Djimtoingar et al., 2022](#)). It's important to note that Chad, possesses substantial renewable energy potential, including wind, solar, and biomass resources

([Ali et al., 2024](#)). It is imperative that appropriate resource allocation policies are implemented, particularly in relation to water, energy and food resources, in order to facilitate sustainable development ([Degirmencioglu et al., 2019](#)). The successful utilization of biomass for energy contributes to the increasing ratio of renewable energy generation, particularly in the context of electricity generation. Biomass energy represents one of numerous clean sources of energy, offering carbon-neutral electricity and heat generation ([Ertuğrul et al., 2024](#)).

This study aims to explore the potential of producing biomass energy from agricultural residues in Chad. This includes assessing the availability and types of agricultural residues and evaluating the feasibility and efficiency of converting these residues into biomass energy. The study seeks to provide a comprehensive understanding of how biomass energy production from agricultural residues could contribute to Chad's energy security, rural development, and environmental sustainability.

MATERIALS and METHODS

Agricultural Lands in Chad

In Chad, agriculture is carried out on two distinct types of land: dunes during the rainy season and wadis during the dry season. Both men and women participate in agricultural activities, which serve as the primary food source for households ([Narem, 2024](#)). Agriculture in Chad contributes 40% to the GDP and 80% to exports while employing 80% of the workforce. However, farmers need more access to essential services, knowledge, and technology needed for productivity improvements. Furthermore, inadequate access to rural financial services prevents poor farmers from diversifying their income sources or increasing productivity ([Senn, 2024](#)). Various factors across different scales and intensities influence agricultural systems in Sub-Saharan Africa. These systems operate within dynamic political and socioeconomic contexts, experiencing frequent transformations. Moreover, they heavily rely on unstable environmental conditions ([Nilsson and Uvo, 2020](#)). Due to Chad's challenging climatic conditions and the impact of its unstable political environment, engaging in agricultural activities is already a significant struggle for the population ([Su and Amrit, 2024](#)).

Assessment of Biomass Energy in Chad

Biomass can be transformed into energy, which can then be utilized to generate electricity and provide heating. This is an alternative to traditional cooking fuels, particularly in rural regions where access to conventional energy sources is limited ([Ghanem et al., 2024](#)). Biomass is Chad's main energy source primarily used for cooking and heating in rural and peri-urban areas. The most common forms of biomass are firewood, charcoal, and agricultural residues. The primary challenges in utilizing biomass for energy production are the logistics of collection and transportation, and its seasonal availability. These factors can lead to significant variability in biomass supply, making it an unreliable source for energy applications ([Karaca, 2017](#)).

Most of the population relies on traditional biomass for energy, leading to significant deforestation and environmental degradation. Chad has low electricity

access, especially in rural areas. Biomass energy fills the gap where modern energy infrastructure is lacking.

Chad has a significant agricultural sector, producing residues that can be utilized for energy production. This includes crop residues from maize (corn), millet, sorghum, rice, etc... Utilizing local biomass resources can enhance energy security and reduce dependency on imported fossil fuels ([Boyacı et al., 2021](#)).

Biomass energy projects can create jobs and improve livelihoods in rural areas. Properly managed biomass energy can reduce deforestation, soil erosion, and greenhouse gas emissions. Biomass energy helps to manage agricultural and animal waste, turning potential pollutants into energy.

Calculation of the available amount of agricultural residues in Chad

The quantity of agricultural residues produced annually by crops in Chad, expressed in tons of dry material, was assessed using agricultural production data from the Food and Agriculture Organization Statistical Database of the United Nations (FAOSTAT) in 2021. The annual overall potential of agricultural residues was calculated using the residue-to-product ratio.

The residual net potential was evaluated by considering the availability of residues, which refers to the unutilized and entirely wasted portion of the residues. The attainable potential of agricultural wastes in Chad was calculated using Equation (1) ([Karaca, 2015](#)).

$$(AAR)_i = (ACP)_i \times (RPR)_i \times (A)_i \quad (1)$$

Where; $(AAR)_i$ is the available amount of agricultural residues of i^{th} crop in ton, $(ACP)_i$ is the amount of crop production in tons, $(RPR)_i$ is the residue-to product ratio of the i^{th} crop, and $(A)_i$ is the availability of residues.

Table 1. Data regarding the residue to product ratio, availability and calorific value of various field crop residues ([Karaca, 2015](#); [Karaca, 2017](#); [Karaca et al., 2017](#); [Demirel et al., 2019](#)).

FC	R	RPR	A(%)	LHV (MJ kg ⁻¹)
Beans, dry	Stalk	0.016	40	19.4
Maize (corn)	Stalk	0.011	60	17.95
Millet	Straw	0.013	15	12.39
Potatoes	Stalk	0.003	60	18.61
Rice	Straw	0.022	60	14.92
Sorghum	Stalk	0.019	60	12.38
Wheat	Straw	0.014	15	18.2

FC: Field Crops, R: Residues RPR: Ratio of Residue to Product, A: Availability, LHV; Lower Heating Value (MJ kg⁻¹)

Agricultural residues include materials left behind in fields after operations. Agricultural residues are an abundant and underutilized resource in Chad. These residues, often left to decompose in fields or burned, represent a significant opportunity for biomass energy production. The primary agricultural residues in Chad include stalks and straw from beans, maize (corn) millet, potatoes, rice, sorghum, and wheat. These materials have high energy content and can be converted

into bioenergy through various technologies. While some residues are repurposed for domestic uses like heating, animal feed, and bedding, most residues from industrial agricultural production often remain untouched in the fields. These residues include cotton stalks, maize stalks, sunflower stalks, cereal straws, and similar materials.

Determination of the energy potential in Chad

To determine the energy potential of residues, the calorific values of specific agricultural residues, as derived from the analyses presented in (Table 1), were multiplied by the available residue amounts, following Equation (2) (Demirel *et al.*, 2019).

$$(EP)_i = (AAR)_i \times (LHV)_i \quad (2)$$

Where, $(EP)_i$ the energy potential of agricultural residues of i^{th} crop in $GJ\ kg^{-1}$, $(AAR)_i$ is the available amount of agricultural residues of i^{th} crop in tons, and $(LHV)_i$ lower heating value of air dry residues of i^{th} crop in $MJ\ Kg^{-1}$.

The flowchart below describes the process that can be used to calculate the total energy potential in Chad. This step-by-step representation (Figure 1) ensures clarity and consistency in calculating the energy potential of biomass in Chad.

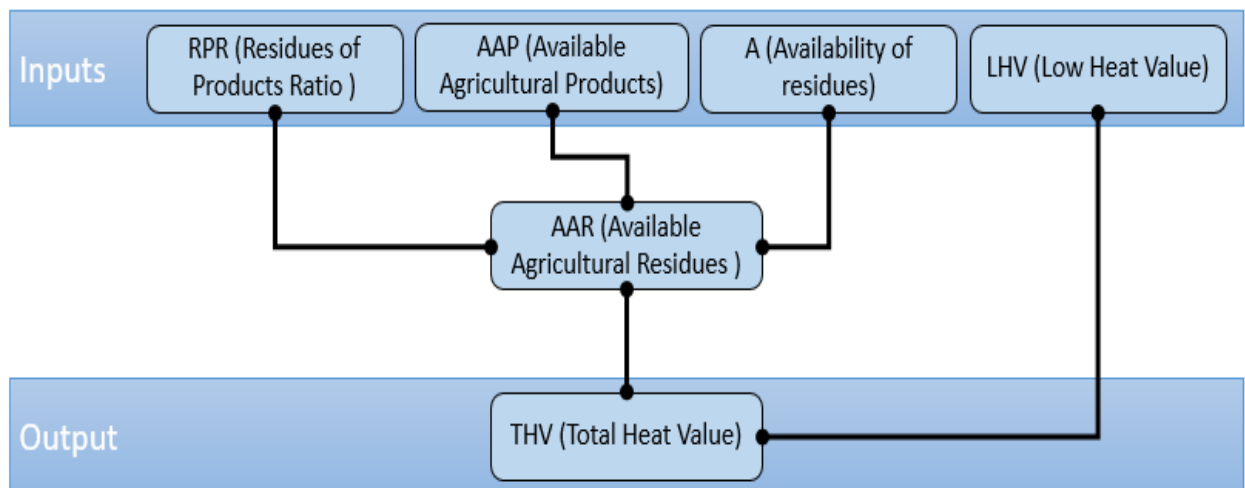


Figure 1. A flowchart for calculating the total heat value (energy potential).

RESULTS AND DISCUSSION

Chad produces significant crop residues from staple crops like beans, maize, millet, potatoes, rice, sorghum, and wheat. These residues include stalks and straws.

Table 2. Total agricultural production and crop residues in Chad, based on data from (FAOSTAT, 2021).

FC	ACP (Ton)	R	TPR (Ton)
Beans, dry	151696.4	Stalk	2457.3
Maize (corn)	364630.7	Stalk	4089.2
Millet	621367.3	Straw	7998.2
Potatoes	36314.9	Stalk	119.6
Rice	242646.7	Straw	5395.4
Sorghum	895778	Stalk	17837.7
Wheat	1539.5	Straw	21.1
Total	2313973.5	Residues	37918.5

FC; Field crops, ACP; Amount of Crop Production (tons), R; Residues TPR; Total Potential of Residues (tons)

Table 2 provides an overview of Chad's agricultural production, and the estimated quantities of crop residues generated annually, based on data from FAOSTAT (2021). By systematically presenting production and residue data, Table 2 serves as a foundation for energy resource assessments, agricultural policy planning, and biomass utilization projects in Chad.

The energy content of crop residues varies but is generally high enough to make them a viable source of biomass energy. The combined energy potential from all agricultural residues in Chad is substantial, indicating a strong potential for biomass energy production.

Table 3. Total energy potential and the corresponding quantity of available agricultural residues in Chad.

FC	R	AAR (Ton)	(EP) (GJ kg ⁻¹)
Beans, dry	Stalk	970.9	18835.5
Maize (corn)	Stalk	2406.6	43198.5
Millet	Straw	1211.7	15012.9
Potatoes	Stalk	65.4	1217.1
Rice	Straw	3202.9	47787.3
Sorghum	Stalk	10211.9	126423.3
Wheat	Straw	3.2	58.2
Total	Residues	18072.6	252532.8

FC; Field crops, R; Residues AAR; Amount of Crop Residues (tons), EP; Energy Potential (GJ kg⁻¹)

Chad has abundant raw materials for energy production from agricultural residues. The total energy potential of agricultural residues was estimated at around 252.5 TJ for the 2021 production period in Chad. There are some studies below performed to determine energy potential from agricultural residues in different countries; Demirel *et al.* (2019) in a study carried out in Sudan, calculated the biomass energy from Agricultural residues, for the production period of 2016; the total calorific value of agricultural residues amounted to around 154 petajoules (PJ), which is substantially higher than Chad's figure. There's a notable difference in the total energy potential of agricultural residues between Chad and Sudan. This suggests that Sudan had a significantly larger amount of agricultural residue energy potential than Chad. In a study conducted by Eissa *et al.* (2024), assessed the energy potential in Libya and found that the total energy potential of agricultural residues for the 2021 production season was approximately 17.7 TJ, which is less than that in

Chad. In a study by [Karaca *et al.* \(2017\)](#), they examined the energy potential of agricultural residues in Turkey's Black Sea Region, they estimated that, for the 2016 production period, the total calorific value of these residues was about 33.60 PJ per year, which is larger than that in Chad. In a study conducted by [Ghanem *et al.* \(2024\)](#), researchers evaluated Syria's energy potential and found that, for the 2016 production season, the total calorific value of agricultural residues from field and orchard crops was approximately 68,904 Btu which is greater than the total calorific value in Chad.

The difference in energy potential among these countries could be influenced by various factors such as agricultural practices, crop types, land availability, and biomass utilization efficiency. Also, thermal efficiency of a biomass-based power plant, which is 35%, is an important factor to be considered before the utilization decisions ([Sun *et al.*, 2014](#)). Understanding these differences can provide insights into optimizing biomass energy production and utilization in different countries. This estimate provides a quantitative foundation for understanding the capacity of Chad to produce biomass energy from agricultural waste materials. This energy can enhance energy security, support rural development, and contribute to environmental sustainability. (Table 3) displays the heating value of agricultural residues for each product.

Biomass energy conversion technologies, such as direct combustion, gasification, and anaerobic digestion, have varying efficiencies. The choice of technology and its efficiency will significantly impact on the usable energy derived from these residues. While these technologies are available, their adoption in Chad is currently limited. Small-scale biogas plants exist, but there is significant potential for expansion. Utilizing agricultural residues for energy production can have positive environmental impacts. It can reduce the need for fossil fuels, thereby lowering greenhouse gas emissions. Moreover, proper management of agricultural residues can prevent open burning, which causes air pollution and health problems.

The practical implementation of biomass energy production in Chad hinges on several factors. First and foremost is the availability of infrastructure for collecting, processing, and converting agricultural residues into usable energy. This includes facilities for biomass collection, transportation networks, and conversion plants. Economic factors also play a vital role; the cost of collecting and processing agricultural residues must be weighed against the market price of the energy produced. Additionally, government policies, subsidies, and incentives for renewable energy projects can significantly influence the economic viability of biomass energy production.

The total amount of agricultural residues in Chad, including annual crop residues, was calculated to be about 18.1 kt. The agricultural residues considered in this study typically include crop residues like straw and stalks from major crops such as beans, maize, millet, potatoes, rice, sorghum, and wheat. The quantity and energy content of these residues are critical in determining the overall energy potential.

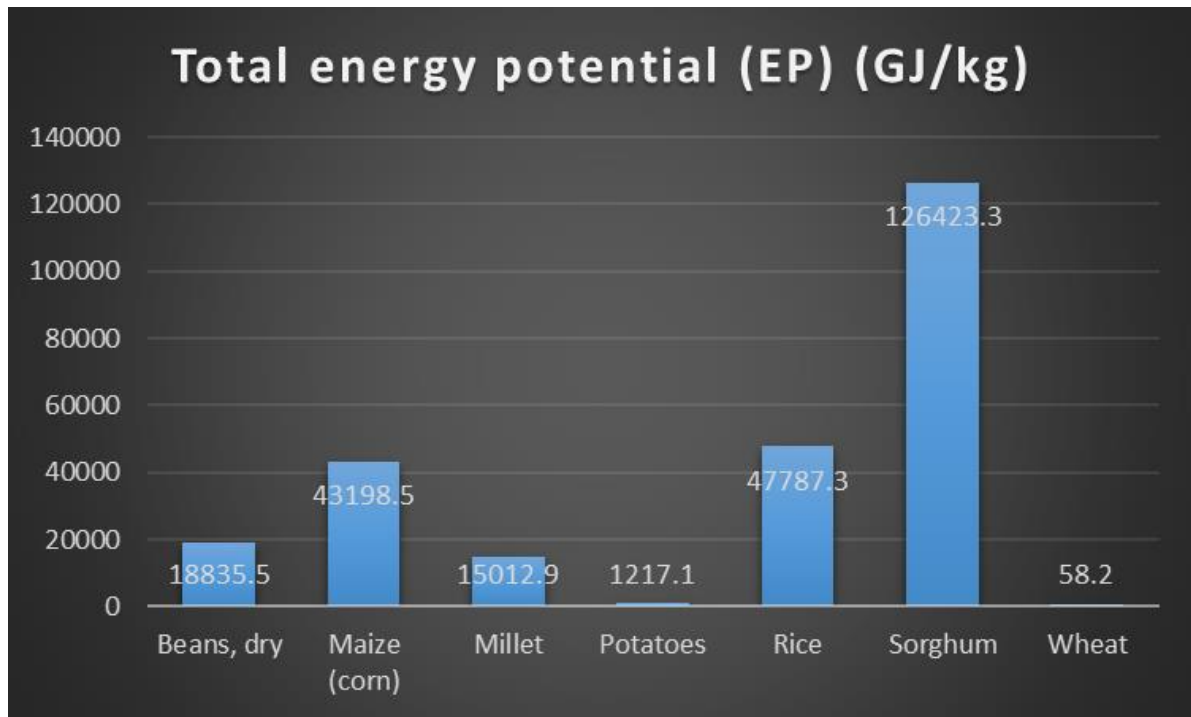


Figure 2. The amount of energy potential for agricultural residues.

Figure 2 represents the amount of energy potential for agricultural residues in Chad. This bar chart visually represents the energy potential of various crop residues, emphasizing their contribution to biomass energy production. From this figure, we can see that Chad has a sufficient amount of agricultural residues to produce biomass energy, especially the residues from sorghum.

The major crops contributing to the total residue amount in Chad are sorghum (56.50%), rice (17.72%), maize (13.31%), millet (6.70%), and beans (5.37%).

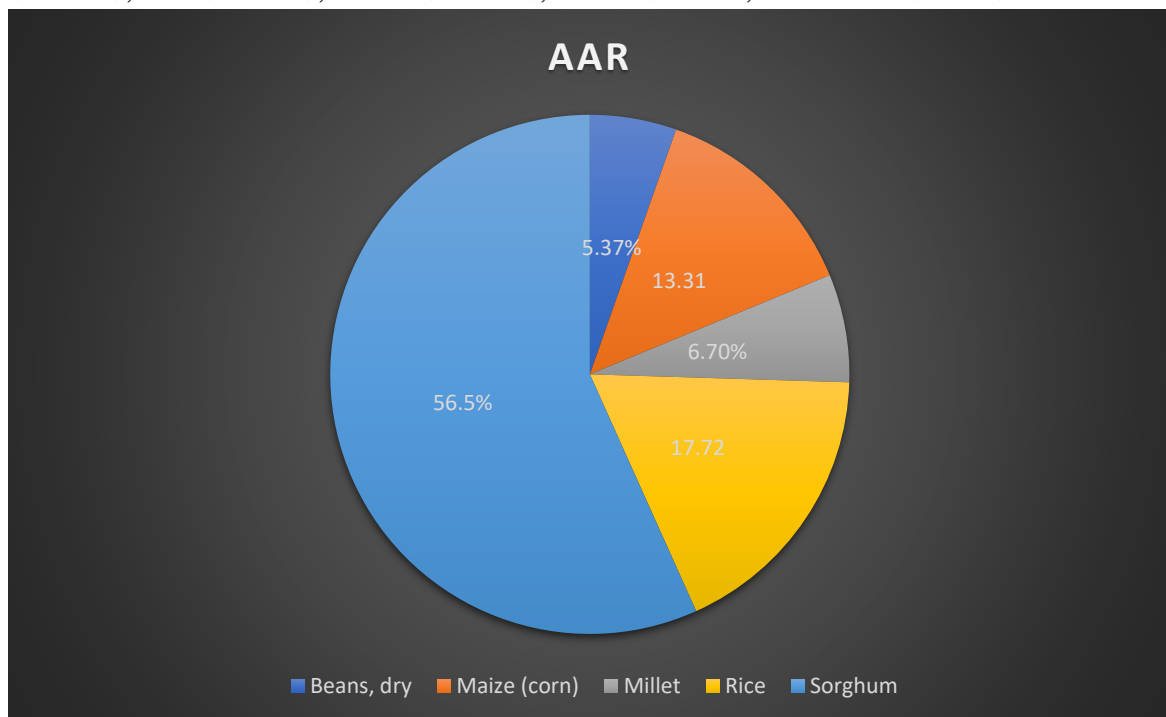


Figure 3. Amount of agricultural residues in Chad.

Figure 3 illustrates the total amount of agricultural residues generated annually in Chad, categorized by crop type. This data is critical for assessing the availability of biomass resources and their potential applications in energy production or sustainable agricultural practices.

CONCLUSION

This study aims to investigate the potential for generating biomass energy from agricultural residues in Chad. Chad has abundant agricultural residues, presenting a promising opportunity for biomass energy generation. Harnessing this potential could enhance energy security, promote sustainable agricultural practices, and contribute to the country's overall economic development. Further research and investment in appropriate technologies and infrastructure are essential to realize the complete potential. Utilizing agricultural residues for energy production can provide several benefits, including reducing greenhouse gas emissions, promoting rural development, and diversifying energy sources.

Biomass energy has significant potential to contribute to Chad's energy mix, particularly in rural areas where other forms of energy are scarce. Developing biomass energy aligns with Chad's renewable energy goals and can help reduce dependence on imported fuels. By leveraging data from the Food and Agriculture Organization Statistical Database of the United Nations (FAOSTAT) for 2021, the quantity and energy potential of these residues were assessed. The study examines the calorific values of specific agricultural residues and calculates the total heating value, highlighting the feasibility of converting these residues into a viable energy source. For the 2021 production period in Chad, the total heating value of agricultural residues was estimated to be approximately 252.5 TJ. With the right policies, infrastructure, and community engagement, Chad can make strides in developing a sustainable and economically viable biomass energy sector.

There are potential challenges that need to be addressed. These include the seasonal availability of agricultural residues, storage issues, and the possible competition with other uses of residues. Additionally, the initial capital investment required for setting up biomass energy plants can be a barrier, particularly in developing regions. A supportive policy and regulatory framework are crucial. Governments can play a key role by enacting policies that promote biomass energy, providing subsidies for technology adoption, and ensuring a stable market for the energy produced. Additionally, regulations to manage the sustainable use of agricultural residues can help in maintaining a balance between energy production and other agricultural needs.

Recommendations for Biomass Energy Development

1. Promote sustainable harvesting and reforestation programs to ensure a continuous supply of biomass.
2. Develop a systematic approach to catalogue and quantify the types and amounts of agricultural residues available across different regions in Chad. This data will be crucial for planning and optimizing biomass energy production.

3. Conduct awareness campaigns and train farmers and local communities on the benefits and methods of utilizing agricultural residues for biomass energy. This will enhance community participation and support for biomass projects.
4. Invest in efficient biomass technologies, such as improved cookstoves and biogas digesters, to enhance energy efficiency and reduce health impacts.
5. Develop capacity-building programs to educate communities on sustainable biomass use and management.
6. Establish supportive policies and incentives for biomass energy development, including subsidies for improved technologies and support for research and development.
7. Encourage public-private partnerships to mobilize resources and expertise for biomass energy projects.
8. Integrate biomass energy into the broader national energy strategy, ensuring it complements other renewable energy sources and contributes to overall energy goals.

DECLARATION OF COMPETING INTEREST

I declare that I have no conflict of interest.

CREDIT AUTHORSHIP CONTRIBUTION STATEMENT

The author declared that the following contributions is correct.

Mohamedeltayib Omer Salih EISSA: The author would like to declare that he solely developed all the sections in this manuscript.

ETHICS COMMITTEE DECISION

This article does not require any Ethical Committee Decision.

REFERENCES

- Ali AR, Nediguina MK, Kriga A, Gouajio MJ, Adile AD, Kenmogne F and Tahir AM (2024). Mathematical prediction of electrical solar energy based on solar data for two main cities of Chad: Mongo in the Centre and Pala in the South of Chad. *Journal of Energy, Environmental & Chemical Engineering*, 9(1): 33-45. <https://doi.org/10.11648/j.jeece.20240901.14>
- Boyacı S, Ertugrul O and Ertuğrul GÖ (2021). Kırşehir ilinin örtü altı domates yetiştiriciliğinde bitkisel artık kaynaklı enerji potansiyelinin mekânsal olarak değerlendirilmesi. *Mustafa Kemal Üniversitesi Tarım Bilimleri Dergisi*, 26(3): 600-609.
- Degirmencioglu A, Mohtar RH, Daher BT, Ozgunaltay-Ertugrul G and Ertugrul O (2019). Assessing the sustainability of crop production in the Gediz Basin, Turkey: a water, energy, and food nexus approach. *Fresenius Environmental Bulletin*, 28(4): 2511-2522.
- Demirel B, Alp G, Gürdil K and Gadalla O (2019). Biomass energy potential from agricultural production in Sudan. *Erciyes Tarım ve Hayvan Bilimleri Dergisi ETHABD*, 2(2): 35-38.
- Djimtoingar SS, Derkyi NSA, Kuranchie FA and Sarquah K (2022). Anaerobic digestion of calotropis procera for biogas production in arid and semi-arid regions: A case study of Chad. *Cogent Engineering*, 9(1). <https://doi.org/10.1080/23311916.2022.2143042>

- Eissa MOS, Gürdil GAK, Ghanem L and Demirel B (2024). *Biomass Energy Potential from Agricultural Production in Libya. Tarım Makinaları Bilimi Dergisi*, 20(2): 61-71.
- Ertuğrul Ö, Daher B, Özgünaltay Ertuğrul G and Mohtar R (2024). From agricultural waste to energy: Assessing the bioenergy potential of South-Central Texas. *Energies*, 17(4): 802.
- FAOSTAT (2021). Access date 2024(May). <https://www.fao.org/faostat/en/#data/GCF>
- Ghanem L, Gürdil GAK, Omer Salih Eissa M, and Demirel B (2024). Determining and mapping biomass energy potential from agricultural residues in Syria. *Black Sea Journal of Agriculture*, 7(4): 391-398. <https://doi.org/10.47115/bsagriculture.1479266>
- Jahangiri M, Soulouknga MH, Bardei FK, Shamsabadi AA, Akinlabi ET, Sichilalu SM and Mostafaeipour A (2019). Techno-econo-environmental optimal operation of grid-wind-solar electricity generation with hydrogen storage system for domestic scale, case study in Chad. *International Journal of Hydrogen Energy*, 44(54): 28613-28628. <https://doi.org/10.1016/j.ijhydene.2019.09.130>
- Karaca C (2015). Mapping of energy potential through annual crop residues in Turkey. *International Journal of Agricultural and Biological Engineering*, 8(2): 104-109. <https://doi.org/10.3965/j.ijabe.20150802.1587>
- Karaca C (2017). *Determining and mapping agricultural biomass energy potential in Samsun Province of Turkey*. ICOEST 3rd International Conference on Environmental Science and Technology, October, 190-194.
- Karaca C, Gürdil GAK, and Öztürk HH. (2017). The biomass energy potential from agricultural production in the Black Sea Region of Turkey. In *ICOEST 3rd International Conference on Environmental Science and Technology*, 184-189, 19-23 October, Budapest, Hungary.
- Kelly E, Astrid B, Nouadje M, Hermann R, Djiela T, Tiam P and Tchuen G (2023). Off grid PV / Diesel / Wind / Batteries energy system options for the electrification of isolated regions of Chad. *Heliyon*, 9(October 2022). <https://doi.org/10.1016/j.heliyon.2023.e13906>
- Kidmo DK, Bogno B, Ngohe Ekam PS, Nisso N and Aillerie M (2022). Hydropower generation potential and prospective scenarios for sustainable electricity supply for the period 2022-2042: A case study of the NIN zone of Cameroon. *Energy Reports*, 8(May): 123-136. <https://doi.org/10.1016/j.egyr.2022.06.090>
- Kriga A, Désiré A, Abanda A, Adile AD, Dari YD and Kenmogne F (2023). Forecast of the electrical energy demand of N'Djamena, Chad, based on the statistical method. *World Journal of Advanced Research and Reviews*, 17(1): 762-768. <https://doi.org/10.30574/wjarr.2023.17.1.0073>
- Medjo Nouadje BA, Kelly E, Tonsie Djiela RH, Tiam Kapen P, Tchuen G and Tchinda R (2024). Chad's wind energy potential: an assessment of Weibull parameters using thirteen numerical methods for a sustainable development. *International Journal of Ambient Energy*, 45(1). <https://doi.org/10.1080/01430750.2023.2276119>
- Narem BKJ (2024). Food Insecurity in the Sahel Strip and Permanent Food Assistance in Chad: Analysis from Bahr El Gazal Province. *Journal of Innovation in Education and Social Research*, 2(2), 21-30. Retrieved from <https://journals.proindex.uz/index.php/jiesr/article/view/582>
- Nilsson E and Uvo C (2020). Nonlinear dynamics in agricultural systems in Chad. *African Geographical Review*, 39(1): 1-27. <https://doi.org/10.1080/19376812.2018.1485585>
- Senn RH (2024). Chad. <https://www.ifad.org/en/web/operations/w/country/chad>
- Soulouknga MH, Oyedepo SO, Doka SY and Kofane TC (2020). Evaluation of the cost of producing wind-generated electricity in Chad. *International Journal of Energy and Environmental Engineering*, 11(2): 275-287. <https://doi.org/10.1007/s40095-019-00335-y>
- Soulouknga MH, Dandoussou A and Djongyang N (2022). Empirical Models for the Evaluation of Global Solar Radiation for the Site of Abeche in the Province of Ouadda in Chad. *Smart Grid and Renewable Energy*, 13(10): 223-234. <https://doi.org/10.4236/sgre.2022.1310014>
- Soulouknga MH, Pishkar I, Kidmo DK and Jahangiri M (2023). Estimation and mapping of the global component of solar radiation and wind power density over Chad. *Journal of Simulation and Analysis of Novel Technologies in Mechanical Engineering*, 15(1): 39-49.
- Su Y and Amrit C (2024). A predictive model for analysing Chad's food security. *Journal of Decision Systems*, 00(00), 1-16. <https://doi.org/10.1080/12460125.2024.2354596>
- Sun J, Sun D, and Guo S. (2014). Evaluation on the efficiency of biomass power generation industry in China. *The Scientific World Journal*, 2014(1): 831372.

Verhoeven BH and Pouget-abadie T (2024). Oil and the Politics of Energy Access in Chad.
https://www.energypolicy.columbia.edu/wp-content/uploads/2024/02/Oil-and-energy-access-in-Chad-Commentary_CGEP_012224.pdf



Turkish Journal of
Agricultural
Engineering Research
(Turk J Agr Eng Res)
e-ISSN: 2717-8420



Determination of Plant Uniformity on rows in Distribution and Certain Quality Criteria in Precision Sowing of Black Carrot in the Kırıkhan Local Population of Konya Province Ereğli District

Haydar HACISEFEROĞULLARI^a,* Nurhan USLU^b

^aDepartment of Agricultural Machinery and Technologies Engineering, Faculty of Agriculture, Selcuk University, 42075, Konya, TÜRKİYE

^bDepartment of Food Engineering, Faculty of Agriculture, Selcuk University, 42075 Konya, TÜRKİYE

ARTICLE INFO: Research Article

Corresponding Author: Haydar HACISEFEROĞULLARI, E-mail: hhsefer@selcuk.edu.tr

Received: 16 September 2024 / Accepted: 29 November 2024 / Published: 31 December 2024

Cite this article: Haciseferoğulları, H., & Uslu, N. (2024). Determination of Plant Uniformity on Rows in Distribution and Certain Quality Criteria in Precision Sowing of Black Carrot in the Kırıkhan Local Population of Konya Province Ereğli District. Turkish Journal of Agricultural Engineering Research, 5(2), 244-261. <https://doi.org/10.46592/turkager.1550931>

ABSTRACT

In Türkiye, black carrot is cultivated in the Ereğli and Karapınar districts of Konya and the Kırıkhan district of Hatay. It is used both as a fresh vegetable and in the production of highly fermented beverages. In this study, the seeds of the Kırıkhan local population were sowing in a different location, Konya's Ereğli district. As a result of the sowing process, the study aimed to evaluate the on-row seed distribution uniformity, as well as the diameter, mass, length, and branching rates of black carrots, along with their color and certain food analysis results. The sowing was done on ridges in three narrow rows (75 mm) using a vacuum type of pneumatic precision vegetable seeder at a forward speed 2.16 km h⁻¹. The experiments were conducted in a randomized block design (2x3) with three replications, at three different nominal planting distances (22.30 mm, 49.08 mm, and 67.22 mm). According to the results, coefficient of variation of plant distribution on the row, number of plants per unit area, average carrot diameter, average carrot mass and average carrot length values were found to be between 63.79% and 79.12%, 20.56 to 105.11 plants.m⁻², 25.91 to 47.03 mm, 57.73 to 223.40 g and 202.2 to 315.1 mm, respectively. According to the food analysis results, the black carrots produced with both seed types had the following values: Brix ranged from 7.37% to 8.10%, pH from 5.47 to 5.61, antioxidant activity from 78.20% to 80.32%, and total phenolic content ranged from 629.1 to 803.7 mg GAE (100 g)⁻¹. As a result of the study, it can be recommended to use bare and calibrated seeds at the Z₂ (49 mm) planting distance based on food analysis results.

Keywords: Plant number, Plant distribution on the row, Black carrot, Quality criteria

Konya İli Ereğli İlçesinde Kırıkhan Yerel Popülasyonu Siyah Havucun Hassas Ekiminde Sıra Üzeri Bitki Dağılım Düzensizliği ile Bazı Kalite Kriterlerinin Belirlenmesi

MAKALE BİLGİSİ: Araştırma Makalesi

Sorumlu Yazar: Haydar HACISEFEROĞULLARI, E-mail: hhsefer@selcuk.edu.tr

Alınış tarihi: 16 Eylül 2024 / **Kabul tarihi:** 29 Kasım 2024 / **Basım tarihi:** 31 Aralık 2024

Alıntı için: Haciseferoğulları, H., & Uslu, N. (2024). Konya İli Ereğli İlçesinde Kırıkhan Yerel Popülasyonu Siyah Havucun Hassas Ekiminde Sıra Üzeri Bitki Dağılım Düzensizliği ile Bazı Kalite Kriterlerinin Belirlenmesi. Turkish Journal of Agricultural Engineering Research, 5(2), 244-261. <https://doi.org/10.46592/turkager.1550931>

ÖZET

Türkiye’de, Konya’nın Ereğli ve Karapınar ilçeleri ile Hatay İlinin Kırıkhan ilçesinde siyah havuç üretimi yapılmakta, taze sebze olarak ve yüksek oranda fermente edilmiş içecek üretiminde kullanılmaktadır. Bu araştırmada, Kırıkhan yerel popülasyonu tohumların farklı lokasyon olan Konya Ereğli ilçesinde ekimi yapılmıştır. Ekim işlemi sonucunda, sıra üzeri tohum dağılım düzensizliği, siyah havuçların çap, kütle, uzunluk ve çatallanma oranları ile renk ve bazı gıda analiz sonuçlarının değerlendirilmesi amaçlanmıştır. Ekim işlemi sırta üç dar sıra (75 mm) olarak vakumlu tip pnömatik hassas sebze ekim makinesi ile 2.16 km h⁻¹ ilerleme hızında gerçekleştirilmiştir. Denemeler, üç farklı anma ekim mesafesinde (22.30 mm, 49.08 mm ve 67.22 mm), tesadüf blokları deneme desenine göre (2x3) üç tekerrürlü olarak yürütülmüştür. Araştırma sonuçlarına göre her iki tohumda bitki dağılımının varyasyon katsayısı değerleri, birim alandaki bitki sayısı, ortalama havuç çapı, ortalama havuç kütlesi ve ortalama havuç boyu değerleri sırasıyla, %63.79 ile %79.12, 20.56 ile 105.11 bit.m⁻², 25.91 ile 47.03 mm, 57.73 ile 223.40 g, 202.2 ile 315.1 mm ve %2.22 ile %12.87 arasında bulunmuştur. Gıda analiz sonuçlarına göre her iki tohumla üretilen siyah havuçların briks, pH, antioksidan aktivitesi ve toplam fenolik miktarları sırasıyla %7.37 ile %8.10, 5.47 ile 5.61, %78.20 ile %80.32 ve 629.1 ile 803.7 mg GAE (100 g)⁻¹ arasında belirlenmiştir. Araştırma sonucunda, çıplak ve kalibre edilmiş tohumlarla Z₂ (49 mm) ekim mesafesinde ekim yapılması gıda analiz sonuçlarına göre önerilebilir.

Anahtar Kelimeler: Bitki sayısı, Sıra üzeri dağılım düzensizliği, Siyah havuç, Kalite kriterleri

GİRİŞ

Siyah veya mor havuç (*Daucus carota* ssp. *sativus* var. *Atrorubens* Alef.) koyu mor bir renge sahiptir. Koyu pigment antosiyaninler, sebzeye antioksidan özellikleri katar ve β-karoten seviyeleri ise genellikle turuncu havuçlardan daha yüksektir (Chhetri ve ark., 2022).

Siyah havuç, insan sağlığına faydalı birkaç element içerdiğinden insan beslenmesinde önemli bir bileşendir (Kaur ve ark., 2023). Antosiyanin olarak bilinen flavonoid kimyasalları, havuçların mor veya siyah renk tonuyla ilgilidir. Koyu renkte olan hemen hemen tüm yiyeceklerde antosiyaninler bulunur. Antosiyaninler renklendirici özelliklerinin yanı sıra nörolojik hastalıkları, kardiyovasküler hastalıkları, kanseri, diyabeti, iltihabı ve diğer birçok hastalığı önlemeye yardımcı olan güçlü bir antioksidan aktivite sergiledikleri, kanser tedavisinde etkili olduğu, kan damarlarını gevşettiği ve kan damarı duvarlarını kaplayan endotel hücrelerinin bütünlüğünü koruduğu bildirilmektedir (Yousuf ve ark., 2016).

Tüketicilerin, sentetik katkı maddelerine alternatif olarak, doğal renklendiricilere olan talepleri artmaktadır. Siyah havuç, işleme koşullarına ve depolamaya karşı yüksek

1 stabilitesi nedeniyle gıda renklendiricisi olarak en çok kullanılan antosiyanin kaynakları
2 arasındadır ([Purkiewicz ve ark., 2020](#)).

3 Ereğli ve Kırıkhan popülasyonu siyah havuçların coğrafi işaret belgeleri alınmıştır
4 ([Anonim, 2017](#); [Anonim, 2022](#)). Konya'nın Ereğli ve Karapınar ilçelerinde siyah havuç
5 üretimi yapan tarımsal işletmelerin %5.4'ünün sadece Kırıkhan popülasyonu, %64.8'nin
6 ise Ereğli ve Kırıkhan popülasyonu ile hibrit siyah tohumları kullanarak, siyah havuç
7 üretimi yaptıkları bildirilmektedir ([Yılmaz, 2019](#)). Aynı zamanda bölgede, Kırıkhan yerel
8 popülasyon siyah havucun, tohumluk üretimi de yapılmaktadır.

9 Yerel ortamlarda, yerel genotiplerin üretimlerinin yapıldığı bilinmektedir. Aynı
10 zamanda bunların fitokimyasal özelliklerini incelemek, değerlendirmek ve genetik açılımı
11 önlemek önemlidir. Yerel ırkları korumak ve hedeflenen özelliklerini ticari çeşitlere
12 aktarmak için ıslah programlarına almak gerekmektedir ([Blando ve ark., 2021](#)). Bu yerel
13 popülasyonlar gıda güvenliği için önemli bir kaynaktır. Üretim bölgelerinde çiftçiler için
14 önemli bir gelir kaynağı olup, aynı zamanda endüstriyel kalkınmayı da teşvik etmektedir
15 ([Saranraj ve ark., 2019](#)).

16 Hatay'ın Kırıkhan ilçesinde, ağustos ayı başında siyah havucun ekimi yapılmakta,
17 aralık ayında hasadı başlayıp, nisan ayı sonuna kadar devam etmektedir. Havuç
18 yetiştiriciliğinde yüksek kalite ve verim elde etmek için kumlu topraklar tercih
19 edilmektedir ([Sermenli, 2012](#)). Havuç verimini ve kimyasal bileşimini belirleyen temel
20 faktörlerin, genotip, yetiştirme mevsimi ve yöntemi olduğu bildirilmektedir
21 ([Seljasen ve ark., 2012](#)).

22 Havuç üretiminin yapıldığı ekolojinin, bitkinin biyokimyasal reaksiyonlarını etkilediği
23 ve bu reaksiyonlara, iklim özellikleri ile toprak faktörlerinin yanı sıra bitki örtüsü ve
24 bitkilerin sıra üzeri mesafesinin de önemli rolü olduğu bildirilmektedir. Sıra üzeri
25 mesafenin azalmasıyla, fenolik madde üretimini yönlendiren biyokimyasal reaksiyonların
26 olumsuz olarak etkilendiği ve yine havuçların sekonder metabolit sentezinin de negatif
27 olarak etkilenebileceği işaret edilmektedir ([Kotecha ve ark., 1998](#)).

28 Siyah havucun ekimi ile sınırlı sayıda araştırma bulunmaktadır.
29 [Önal ve Ertuğrul \(2011\)](#), oluklu makaralı ekici düzen ile gerçekleştirdikleri
30 çalışmalarında havuç tohumunda sıra üzeri mesafeleri artırdıkça sıra üzeri dağılım
31 düzgünlüğünün iyilik kriteri ve varyasyon faktörü değerlerine bağlı olarak arttığını tespit
32 etmişlerdir. [Ornek ve ark. \(2018\)](#), bin dane ağırlığı 1.64 g ve laboratuvar çimlenme oranı
33 %91 olan çıplak Ereğli popülasyonu siyah havuç tohumları ile yaptıkları araştırmada,
34 46.50 mm sıra üzeri mesafede ve 0.84 m s⁻¹ ilerleme hızında, tarla çıkış değerlerini
35 ortalama olarak %49.17 olarak belirlemişlerdir. [Bülbül ve Haciseferoğulları \(2017\)](#),
36 değişik tipteki baskı tekerleriyle 2015 yılında yaptıkları ekimde kaplanmamış siyah
37 tohumlarının varyasyon katsayısı değerlerini, yatay rotovator ile hazırlanan tohum
38 yatağında %78.28 ile %113.25 arasında elde edildiğini bildirmektedirler.

39 Bu araştırmada, Ereğli ilçesinde dar sıra aralıklı vakumlu pnömatik hassas sebze ekim
40 makinesi kullanılarak, Kırıkhan popülasyonu tohumların ekimi yapılmıştır. Böylece
41 farklı lokasyonda ve farklı mevsimlerde üretimi yapılmış, ekim işleminde kalibre edilmiş
42 çıplak ve kaplanmış Kırıkhan popülasyonu tohumlar kullanılmıştır. Bu yerel genotipin
43 farklı bir ekolojide üretimi yapılarak, ana bitki dağılım düzgünlüğü ve bazı havuç kalite
44 kriterlerine etkisi değerlendirilmiştir.

MATERYAL ve YÖNTEM

Araştırma, Ereğli ilçesi Kuzukuyu mahallesinde yürütülmüştür. Toprağın tekstür sınıfı tınlı-kum olup, bünyesi %4 kil, %10 silt ve %86 kumdan oluşmaktadır. Toprak kuvvetli alkali sınıfında (pH 8.96) bulunmakta, kireç içeriği %39.2 ve organik madde içeriği ise %1.31 olarak belirlenmiştir. Siyah havucun üretim sezonu boyunca aylık sıcaklık verileri Çizelge 1’de verilmiştir.

Çizelge 1. Aylık maksimum ve minimum sıcaklık verileri (Anonim, 2020).

Table 1. Monthly maximum and minimum temperature data (Anonymous, 2020).

Aylar	Günlük maksimum sıcaklık (°C)	Günlük minimum sıcaklık (°C)
Haziran	28.4	13.1
Temmuz	32.3	16.7
Ağustos	31.4	14.8
Eylül	30.7	14.2
Ekim	26.1	9.1
Kasım	12.7	0.6

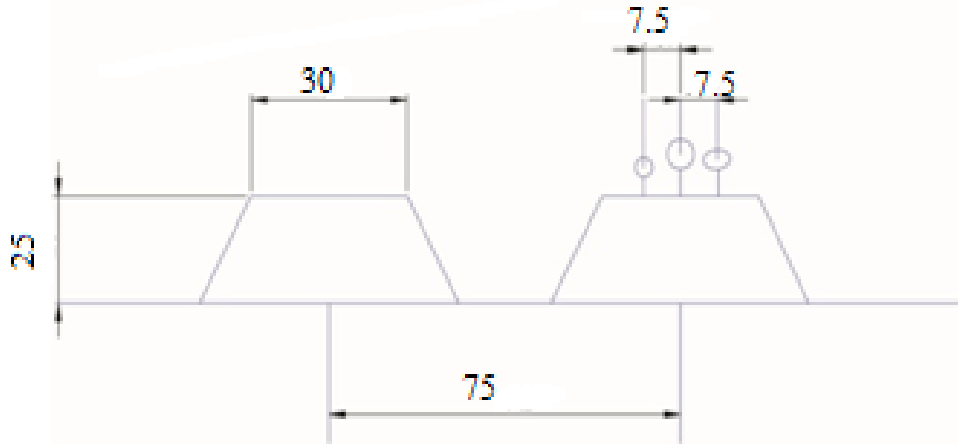
Denemelerde, Kırıkhan popülasyonu siyah havuç tohumları kullanılmıştır. Bu tohumların kalibrasyonu yapılmıştır. Araştırmada kullanılan çıplak (T_1) ve kaplanmış (T_2) standart siyah havuç tohumlarının küresellik, bin tohum kütlesi ve çimlenme oranları sırasıyla %44.37 - %55.34, 2.18 g - 6.53 g ve %84.25 - %77.85’dir.

Üç farklı anma ekim mesafesinde ($Z_1=22.30$ mm, $Z_2=49.08$ mm ve $Z_3=67.22$ mm) “Tesadüf Blokları Deneme Desenine” göre (2x3) üç tekerrürlü olarak ekim işlemi yapılmıştır. Parsellerin ölçüleri 150 m x 2.8 m (350 m²) olup, parseller arasında boşluk bırakılmamıştır. Araştırmada, yerli olarak üretimi yapılan vakumlu tip yüksek hassasiyetli pnömatik hassas sebze ekim makinesi kullanılmıştır (Şekil 1).



Şekil 1. Vakumlu tip pnömatik hassas sebze ekim makinesinin ve ekici diskin görünüşü.
Figure 1. The view of the vacuum-type pneumatic precision vegetable sowing machine and the seeding disc.

Pnömatik hassas ekim makinesinin önünde sac, arkasında lastik ve ortasında ise üçlü dar lastik baskı tekerleri kullanılmıştır. Ekici diskin dış çapı 235 mm ve kalınlığı ise 0.25 mm'dir. Ekici diskte üç sıra halinde 96'şar adet delik bulunmakta olup, delik eksenlerinin çapları üst sıradan başlayarak sırasıyla 210, 185 ve 155 mm'dir (Şekil 1). Kalibre edilmiş Hatay genotipi çıplak siyah havuç tohumlarının ekiminde delik çapı 0.7 mm ve kaplanmış tohumlar için ise delik çapı 1.2 mm olan ekici diskler kullanılmıştır. Ekim işlemi sırta yapılmış olup, sırt ölçüleri Şekil 2'de verilmiştir. Sırt üzerindeki sıra aralığı 7.5 cm olup, üç dar sıraya ekim işlemi gerçekleştirilmiştir. Ekim işlemi, ekim makinesinin 2.16 km h⁻¹ ilerleme hızında yapılmıştır.



Şekil 2. Ekim sırtının şematik görünüşü ve ölçüleri (cm).

Figure 2. Schematic view of sowing ridge and dimensions (cm).

Araştırmada, parsellere uygulanan tüm işlemler Çizelge 2'de verilmiştir. Çizelge incelendiğinde farklı metotlarla 6 defa gübreleme ve 24 kez yağmurlama sulama işlemi yapıldığı görülmektedir. Toprak kulaklı pulluk ile sürülmüş, dik rotovator ile tohum yatağı hazırlanmış ve sırt yapma makinesi ile ekim sırtları oluşturularak ekim işlemi gerçekleştirilmiştir. Siyah havucun üretimi boyunca biri gübreli olmak üzere 2 defa ara çapa işlemi yapılmıştır. Deneme alanının sulama suyu, derin kuyudan sağlanmıştır. Deneme alanına kurulan, yağmurlama sulama sisteminde başlık ve lateral aralığı 10x10 m şeklinde düzenlenmiş ve başlıklarının ortalama hızı ise 18 mm h⁻¹ olarak ölçülmüştür. Yağmurlama sulama sisteminde 5-4.2 mm meme çapı olan başlıklar kullanılmıştır.

Çizelge 2. Uygulanan tarımsal ve sulama işlemleri.**Table 2.** *Applied implement and irrigation practices applied in trials.*

Tarih	Uygulanan tarımsal işlemler
04.06.2020	Kulaklı pulluk ile sürüm
05.06.2020	Santrifüj gübre dağıtması ile 50 kg da ⁻¹ gübre normunda DAP)*
05.06.2020	Tohum yatağının dik rotovatorle işlenmesi
06.06.2020	Sırt yapma ile ekim sırtlarının oluşturulması
06.06.2020	Ekim işlemi
07.06.2020	1. Yağmurlama sulama sistemi ile sulama (90 mm)
09.06.2020	2. Yağmurlama sulama sistemi ile sulama (54 mm)
12.06.2020	3. Yağmurlama sulama sistemi ile sulama (54 mm)
17.06.2020	4. Yağmurlama sulama sistemi ile sulama (36 mm)
20.06.2020	5. Yağmurlama sulama sistemi ile sulama (36 mm)
25.06.2020	6. Yağmurlama sulama sistemi ile sulama (54 mm)
30.06.2020	7. Yağmurlama sulama sistemi ile sulama (54 mm)
03.07.2020	8. Yağmurlama sulama sistemi ile sulama (54 mm)
07.07.2020	9. Yağmurlama sulama sistemi ile sulama (108 mm)
12.07.2020	Gübreli ara çapa, ÜRE 20 kg da ^{-1**}
12.07.2020	10. Yağmurlama sulama sistemi ile sulama (108 mm)
20.07.2020	11. Yağmurlama sulama sistemi ile sulama (108 mm)
28.07.2020	12. Yağmurlama sulama sistemi ile sulama (108 mm), MAF 5 kg da ^{-1***}
06.08.2020	Gübresiz ara çapalama
06.08.2020	13. Yağmurlama sulama sistemi ile sulama (108 mm)
15.08.2020	14. Yağmurlama sulama sistemi ile sulama (126 mm)
22.08.2020	15. Yağmurlama sulama sistemi ile sulama (126 mm), MAF 5 kg da ⁻¹
29.08.2020	16. Yağmurlama sulama sistemi ile sulama (144 mm)
05.09.2020	17. Yağmurlama sulama sistemi ile sulama (144 mm)
14.09.2020	18. Yağmurlama sulama sistemi ile sulama (144 mm), MAF 5 kg da ⁻¹
23.09.2020	19. Yağmurlama sulama sistemi ile sulama (144 mm), MAF 5 kg da ⁻¹
04.10.2020	20. Yağmurlama sulama sistemi ile sulama (126 mm)
11.10.2020	21. Yağmurlama sulama sistemi ile sulama (126 mm)
19.10.2020	22. Yağmurlama sulama sistemi ile sulama (108 mm)
27.10.2020	23. Yağmurlama sulama sistemi ile sulama (108 mm)
05.11.2020	24. Yağmurlama sulama sistemi ile sulama (108 mm)
07.11.2020	Söküm

*DAP (Diamonyum Fosfat 18.46.0), azot (N) %18, fosfor pentaoksit (P₂O₅) %46**ÜRE (Üre 46 N), üre azotu (N-NH₂) %46***MAF (Monoamonyum Fosfat 12.61.0), amonyak azotu %12 (N-NH₄) ve suda çözünür fosfor (P₂O₅) %61)

Ana bitki dağılım düzgünlüğü ISO-7256/2 standardına göre belirlemiştir (ISO, 1984). Ana dağılımın, ortalama sıra üzeri bitki mesafesi ve varyasyon katsayısı değerleri aşağıdaki formüller kullanılarak hesaplanmıştır (Lei ve ark., 2021).

$$Z_{ort} = \frac{1}{n} \sum_{i=1}^n X_i \quad (i=1. 2. 3. n) \quad (1)$$

$$S = \left\{ \sum_{i=1}^n [(X_i - \bar{X})^2] / (n-1) \right\}^{\frac{1}{2}} \quad (2)$$

$$CV = \frac{S}{Z_{ort}} 100 \quad (3)$$

- Z_{ort} : n sayıdaki sıra üzeri ekim mesafelerinin ortalaması (mm)
 n : Ölçüm sayısı
 x_i : Ölçülen her bir sıra üzeri bitki aralığı (mm)
 \bar{x} : Ortalama sıra üzeri ekim mesafesi (mm)
 S : Standart sapma
 CV : Varyasyon katsayısı (%)

Hasattaki siyah havuç sayısı ve çatallanma oranı değerlerini bulmak için parsellerden rastgele seçilen 1.33 m (1 m²) uzunluğundaki sırtta bulunan bitkiler sökülüştür. Sökülen bitkiler ile çatallanan siyah havuçlar sayılıp, kaydedilmiştir.

TS 1193 standardı dikkate alınarak siyah havuçlar, ekstra sınıfa göre değerlendirilmiştir. Bu sınıfa giren en büyük havuç çapının 25 ile 45 mm ve kütlelerinin ise 50-200 g arasında olması gerekmektedir (TSE, 2007). Siyah havuçların, hasat sonrası ölçümlerinde, bu aralıklara giren havuç çap ve kütle değerlerinin yüzde (%) oranları ile uzunluk değerleri belirlenmiştir.

Siyah havuç sularının renk ölçümleri L* (parlaklık), a* (+ kırmızı, - yeşil) ve b* (+ sarı, - mavi) renk değerleri CIE Lab renk skalasına göre yapılmıştır (Hunt ve ark., 1991). Ölçülen L*, a* ve b* değerlerinden, aşağıdaki eşitlikler kullanılarak Chroma (C) ve Hue (h°) değerleri hesaplanmıştır.

$$C=(a^{*2}+b^{*2})^{1/2} \quad (4)$$

$$h^{\circ}=\arctan\left(\frac{b^{*}}{a^{*}}\right) \quad (5)$$

Siyah havuçların nem analizi (AOAC, 2000) ve suda çözünür kuru madde miktarı el refraktometresi ile havuç sularının pH'sı doğrudan cam elektrotlu pH metre kullanılarak ölçülmüştür (Cemeroğlu, 2013). Siyah havuç örneklerinde ekstraksiyon işlemi, Chihoub ve ark. (2019)'a göre yapılmıştır. 0.5 g siyah havuç suyu 20 ml çözücüyle (metanol:su, 80:20, v/v) karıştırılmıştır. Karışım, oda sıcaklığında 1 saat çalkalamalı su banyosunda bekletilmiş ve filtre (Whatman No:1) edilerek analizlerde kullanılmıştır.

Toplam fenolik maddenin belirlenmesinde, fenolik maddelerin Folin-Ciocalteu çözeltisi fosfomolibdik-fosfotungistik çözeltisine indirgenerek mavi bir kompleks oluşturması ve bu mavi rengin kolorimetrik olarak ölçülmesi prensibine dayanmaktadır (Alper Özdemir, 2001; Abdullakasim ve ark., 2007). Elde edilen sonuçlar, gallik asit eşdeğeri (GAE) olarak verilmiştir. Antioksidan aktivitesi ise DPPH (1.1-difenil-2-pikril-hidrazil) yöntemi kullanılarak tespit edilmiştir (Brand-Williams ve ark., 1995).

Elde edilen tüm verilerin istatistiksel olarak değerlendirilmesinde tesadüf blokları deneme deseni kullanılmıştır (Düzgüneş ve ark., 1983). İstatistiksel analiz için MINITAB'ın GLM (ANOVA) prosedürü kullanılmıştır. Ortalamalar arasındaki anlamlı farklılıkları belirlemek için Tukey testi uygulanmış ve ortalamaların anlamlılık düzeyi 0.05 olarak kabul edilmiştir.

BULGULAR ve TARTIŞMA

Konya'nın Ereğli İlçesinde, Kırıkhan popülasyonu siyah havucun 2020 yılında ekimi ve üretimi yapılmıştır. Araştırma sonucunda elde edilen ana bitki dağılım düzgünlüğü ve birim alandaki bitki sayıları Çizelge 3'te verilmiştir.

Çizelge 3'ün incelenmesiyle, tarla koşullarında elde edilen sıra üzeri ekim mesafelerinde artış görülmüştür. Anma ekim mesafelerine bağlı olarak ($Z_1=22.30$, $Z_2=49.08$ ve $Z_3=67.22$ mm) tarla koşullarında çıplak kalibre tohumda sırasıyla ortalama 44.24 mm, 62.75 mm ve 103.53 mm, kaplanmış tohumda ise 55.67 mm, 84.41 mm ve 107.95 mm sıra üzeri bitki mesafeleri elde edilmiştir. Başka bir ifadeyle bitkiler arası mesafeler, sıra üzeri mesafelerin yükselmesine bağlı olarak çıplak tohumda sırasıyla 1.98, 1.28 ve 1.54 kat, kaplı tohumda ise 2.50, 1.72 ve 1.61 kat daha fazla bulunmuştur. [Bülbül \(2017\)](#), Ereğli yerel popülasyonu kalibre edilmemiş çıplak siyah havuç tohumlarıyla, 2015 yılında yaptığı ekimde, farklı baskı tekerleriyle, dik ile yatay rotavatorle hazırlanmış tohum yatağında ve 2.38 cm, 4.65 cm ile 6.78 sıra üzeri mesafelerde, artış oranlarını sırasıyla, 3.18 ile 4.81 kat, 2.42 ile 3.13 kat ve 1.80 ile 3.10 arasında değiştiğini bildirmektedir. Araştırmada elde edilen sıra üzeri mesafelerdeki artış oranlarının düşük olması, tohumların kalibre edilmesinden kaynaklanmaktadır.

Çizelge 3. Çıplak ve kaplanmış tohumlar ile üretilen Kırıkhan popülasyonu siyah havuç bitkisinin ana dağılım düzgünlüğü ile bitki sayısı.

Table 3. The main distribution uniformity and plant count of the Kırıkhan population black carrot plants produced with bare and coated seeds.

		Z_{avg} (mm)	VK (%)	Bitki sayısı (bitki.m ⁻²)
Tohum	T ₁	69.51	75.78 _a	59.79 _a
	T ₂	82.68	69.59 _b	43.56 _b
	SHO		1.644	2.455
	P-değeri		0.021	0.001
Sıra üzeri mesafe	Z ₁	48.95	77.02 _a	87.89 _a
	Z ₂	73.58	73.38 _{ab}	39.24 _b
	Z ₃	105.74	67.65 _b	27.89 _c
	SHO		2.014	3.007
	P-değeri		0.020	0.000
Tohum x Sıra üzeri	T ₁ x Z ₁	44.24	79.12	105.11 _a
	T ₁ x Z ₂	62.75	76.70	39.04 _c
	T ₁ x Z ₃	103.53	71.50	35.22 _c
	T ₂ x Z ₁	55.67	74.92	70.67 _b
	T ₂ x Z ₂	84.41	70.06	39.44 _c
	T ₂ x Z ₃	107.95	63.79	20.56 _c
	SHO		2.848	4.352
	P-değeri		0.822	0.005

a, b, c Bir sütündeki farklı üst simgelere sahip ortalamalar istatistiki olarak farklılık gösterir ($p<0.05$), SHO standart hata ortalaması, T₁ kalibre edilmiş çıplak tohum, T₂ kaplı tohum, Z₁, Z₂ ve Z₃ sıra üzeri ekim mesafeleri,

Ana bitki dağılım düzgünlüğünü ifade eden varyasyon katsayısı değerleri, sıra üzeri anma ekim mesafelerindeki artışa bağlı olarak sırasıyla kaplanmış tohumda %79.12, %76.70 ve %71.50, kaplı tohumda ise %74.92, %70.06 ve %63.79 olarak bulunmuş ve azalma eğilimi göstermiştir. Bunun nedeni sıra üzeri ekim mesafesinin artışına bağlı olarak ekim makinesinin transmisyon oranının düşmesinden, diğer bir deyişle ekici diskin çevre hızının azalmasından kaynaklanmıştır ([Önal, 1987](#)). Tohum ve sıra üzeri ekim mesafesi parametreleri istatistiksel olarak anlamlı bulunmuş, kalibre çıplak ve kaplı tohumda ortalama varyasyon katsayısı değerleri sırasıyla %75.78 ve %69.59 olarak, sıra üzeri ekim mesafelerinin ortalamaları ise sırasıyla %77.02, %73.38 ve %67.65 olarak tespit edilmiştir. Tohum ve sıra üzeri ekim mesafesi interaksiyonu ise istatistiksel olarak anlamlı bulunmamıştır. Ereğli bölgesinde kalibre edilmiş ve kaplanmış Kırıkhan popülasyonu siyah havuç tohumları ile yapılan araştırmada, benzer sonuçlar elde edilmiş olup, 2.36, 4.92 ve 6.71 cm'lik sıra üzeri ekim mesafelerinde tarla koşullarında sıra üzeri bitki

dağılım düzgünlüğünü ifade eden varyasyon katsayısı değerleri, çıplak kalibre tohumda %77.83, %85.71 ve %70.89 olarak, kaplanmış tohumda ise %70.95, %66.67 ve %64.24 olarak belirlemiştir ([Sadetaş Önal, 2023](#)).

Birim alandaki (m^2) bitki sayıları, sıra üzeri ekim mesafelerine bağlı olarak, çıplak tohumda sırasıyla 105.11, 39.04 ve 35.22 bitki. m^{-2} , kaplı tohumda ise 70.67, 39.44, ve 20.56 bitki. m^{-2} olarak bulunmuştur. Tüm parametreler istatistiksel olarak önemli bulunmuş olup, her iki tohumun Z_1 anma ekim mesafesi dışında, diğer sıra üzeri ekim mesafelerinde elde edilen bitki sayısı değerleri arasında istatistiksel olarak anlamlı bir farklılık bulunmamıştır. Bölgede, Ereğli popülasyonu için metrekarede 60-90 adet bitki olması istenmektedir. Ancak bu sayının sadece Z_1 ekim mesafesinde elde edildiği görülmektedir. [Bülbül \(2017\)](#), dik rotovatorle hazırlanan tohum yatağında ortalama 27.26 bitki. m^{-2} , [Yalçın Dokumacı \(2021\)](#) ise ekici diskte üç sıra ve 96'şar delik bulunan ekim tekniğinde ortalama 42.64 bitki. m^{-2} elde edildiğini bildirmektedir.

Siyah havuç örneklerinin ölçümleri sonucu elde edilen kütle, çap, uzunluk ve çatallanma oranları Çizelge 4'te verilmiştir. Siyah havuçların en büyük çap değerleri 25.91 mm ile 47.03 mm arasında bir değişim göstermiştir. Seçilen parametreler ($p>0.01$) ve interaksyonu ($p>0.05$) istatistiksel olarak anlamlı bulunmuş, en yüksek çap değeri 47.03 mm ile T_2Z_3 kombinasyonunda elde edilmiştir. Kırıkhan yerel popülasyonu siyah havuçların çap değerlerinin 29.8 ile 34.7 mm arasında bir değişim gösterdiği ([Anonim, 2022](#)), araştırmada ise T_1Z_1 , T_1Z_3 , T_2Z_2 ve T_2Z_3 kombinasyonlarında elde edilen havuç çap değerlerinin bu sınırların dışında olduğu belirlenmiştir. [Bıyıktaş \(2018\)](#), yaptığı araştırmada Kırıkhan popülasyonu siyah havuçların ortalama çap değerini 32.06 mm olarak elde etmiştir. Bu en büyük çap değeri, araştırmada elde edilen çıplak (33.85 mm) ve kaplı tohumda (39.23 mm) elde edilen ortalamalardan daha düşük bulunmuştur.

Çizelge 4. Kırıkhan popülasyonu siyah havuçların bazı fiziksel özellikleri ve dağılımı (%).

Table 4. Some physical properties and distribution (%) of black carrots in Kırıkhan population.

		Ort. çap	Havuç çap aralığının dağılımı (%)			Ort. kütle	Havuç kütlesi dağılımı (%)			Ort. uzunluk	Çatallanma oranı
		(mm)	<24.99	25- 45	>45.01	(g)	<49.99	50- 200	>200.01	mm	(%)
Tohum	T ₁	33.85 _b	27.39 _a	53.41	19.20 _b	120.13 _b	29.46 _a	52.36	18.17 _b	246.8 _a	7.43
	T ₂	39.23 _a	11.62 _b	55.22	33.16 _a	162.44 _a	14.26 _b	55.11	30.63 _a	284.0 _b	8.69
	SHO	0.5661	1.912	2.745	2.091	6.11	1.624	2.355	1.880	7.959	1.594
	P-değeri	0.000	0.000	0.650	0.000	0.000	0.000	0.422	0.001	0.006	0.585
Sıra üzeri mesafe	Z ₁	29.47 _c	34.45 _a	54.53 _{ab}	10.01 _c	86.15 _c	40.27 _a	50.90 _b	8.83 _c	217.4 _a	6.06
	Z ₂	36.54 _b	15.84 _b	62.64 _a	21.52 _b	140.30 _b	15.63 _b	62.77 _a	21.61 _b	285.1 _b	6.94
	Z ₃	43.61 _a	7.22 _b	45.78 _b	47.01 _a	197.41 _a	9.70 _b	47.53 _b	42.76 _a	293.8 _b	11.18
	SHO	0.6934	2.342	3.362	2.561	7.485	1.988	2.889	2.303	9.747	1.952
	P-değeri	0.000	0.000	0.014	0.000	0.000	0.000	0.007	0.000	0.000	0.183
Tohum x Sıra üzeri	T ₁ x Z ₁	25.91 _d	51.93 _a	43.89 _{ab}	4.18 _d	57.73	57.20 ^a	40.13 _c	2.67	202.2	2.27
	T ₁ x Z ₂	35.44 _c	18.80 _b	61.89 _a	19.31 _{bcd}	131.26	16.99 _{bc}	64.65 _a	18.36	265.7	7.13
	T ₁ x Z ₃	40.19 _b	11.43 _{bc}	54.46 _{ab}	34.11 _b	171.41	14.21 _{bc}	52.30 _{abc}	33.49	272.4	12.87
	T ₂ x Z ₁	33.04 _c	18.97 _b	65.18 _a	15.85 _{cd}	114.57	23.34 _b	61.67 _{ab}	14.99	232.6	9.85
	T ₂ x Z ₂	37.63 _{bc}	12.88 _{bc}	63.38 _a	23.74 _{bc}	149.34	14.26 _{bc}	60.88 _{ab}	24.86	304.2	6.74
	T ₂ x Z ₃	47.03 _a	3.09 _c	37.09 _b	59.90 _a	223.40	5.19 _c	42.77 _{bc}	52.04	315.1	9.49
	SHO	0.9806	3.312	4.784	0.622	10.585	2.812	4.086	3.256	13.785	0.165
	P-değeri	0.047	0.003	0.006	0.035	0.179	0.000	0.006	0.222	0.902	2.761

^{a, b, c} Bir sütundaki farklı üst simgelere sahip ortalamalar istatistiki olarak farklılık gösterir (p<0.05), SHO standart hata ortalaması, T₁ kalibre edilmiş çıplak tohum, T₂ kaplı tohum, Z₁, Z₂ ve Z₃ sıra üzeri ekim mesafeleri

Havuçların ortalama kütle değerleri 57.73 g ile 223.40 g arasında bulunmuştur. Elde edilen kütle değerlerinin, tohum ($p<0.01$) ve sıra üzeri mesafeden ($p<0.01$) istatistiksel olarak etkilendiği belirlenmiş olup, en büyük ortalama kütle değerinin kaplı tohumda (162.44 g) ve Z_3 ekim mesafesinde (197.41 g) elde edildiği görülmektedir. Kırıkhan yerel ekotip siyah havucun kütle değerinin 109 ile 167.4 g arasında olduğu bildirilmektedir ([Anonim, 2022](#)). Bu açıdan değerlendirildiğinde, T_1Z_1 , T_1Z_3 ve T_2Z_3 kombinasyonlarında elde edilen kütle değerlerinin, bu sınırlar dışında olduğunu görülmektedir. Ayrıca Kırıkhan yerel genotipinin ekiminde ortalama olarak 131.4 g havuç kütlesi elde edildiği bildirilmektedir ([Bıyıktaş, 2018](#)). Bu açıdan değerlendirildiğinde, çıplak tohumla (120.13 g) elde edilen kütle değerlerinin düşük, kaplı tohumla (162.44 g) elde edilen değerin ise yüksek olarak bulunduğunu belirtebiliriz.

Siyah havuçların ortalama uzunluk değerleri 202.2 mm ile 315.1 mm arasında bir değişim göstermiş olup, tohum ($p>0.01$) ve sıra üzeri mesafe parametreleri ($p>0.01$) istatistiksel olarak önemli bulunurken, bu parametrelerin etkileşimi istatistiksel olarak anlamlı bulunmamıştır. En büyük ortalama uzunluk değerinin kaplı tohumda (284 mm) ve Z_3 ekim mesafesinde (293.8 mm) elde edilmiştir. İlgili coğrafi işaret belgesinde havuç uzunluğunun 243 mm ile 307 mm arasında değiştiği belirtilmiştir ([Anonim, 2022](#)). Başka bir ifade ile T_1Z_1 ile T_2Z_1 ve T_2Z_3 kombinasyonlarında elde edilen uzunluk değerleri, belirtilen sınırların dışında bulunmuştur. Ereğli popülasyonu siyah havuç tohumlarıyla 2017 üretim yılında yatay ve dik rotovatorlerle hazırlanan tohum yatağında elde edilen, siyah havuçların boy değerlerinin sırasıyla 212.86 mm ile 242.58 mm ve 216.08 mm ile 281.72 mm arasında değiştiği bildirilmektedir ([Bülbül, 2017](#)). Kırıkhan yerel genotip siyah havuçta ise ortalama havuç boyunun 283.1 mm olarak elde edildiği rapor edilmiştir ([Bıyıktaş, 2018](#)).

Havuçlarda çatallanma oranları %2.27 ile %12.87 arasında bir değişim göstermiş olup, en yüksek çatallanma oranı kaplı tohumda ve Z_3 ekim mesafesinde elde edilmesine rağmen, istatistiksel olarak önemli bulunmamıştır. [Bülbül \(2017\)](#), Ereğli yerel popülasyonu siyah havuç tohumları ile yaptığı ekimlerde, çatallanma oranlarını dik ve yatay rotovatorle hazırlanan tohum yatağında ortalama olarak sırasıyla 2015 yılında %12.05 ile %8.30 ve 2016 yılında ise %18.55 ile %16.22 oranlarında bulmuştur. Araştırmada elde edilen çıplak (%7.43) ve kaplı tohumların (%8.69) ortalama çatallanma oranları düşük bulunmuştur. [Yalçın Dokumacı \(2021\)](#), araştırmasında 2018 yılında aynı ekim tekniğinde ve 3, 5 ve 7 cm'lik sıra üzeri mesafelerde ortalama olarak sırasıyla %19.32, %10.01 ve %30.63'lük çatallanma oranları elde etmiştir. [Vural ve ark. \(2000\)](#), havuçların çatallanma yapmasının istenmediğini, bunun havucun silindirik yapısını bozduğunu, yıkama işlemini zorlaştırdığını ve havucun kalitesini düşürdüğünü vurgulamaktadırlar.

Çizelge 4'te verilen çap aralığı yüzdesinin en yüksek T_1Z_2 'de elde edildiği, T_1Z_3 , T_2Z_1 ve T_2Z_2 ile aralarında ise istatistiksel bir fark olmadığı görülmektedir. Çap değerlerinin <24.99 mm'den küçük olanların en yüksek değeri T_1Z_1 'de (%51.93) elde edilmiş ve diğer kombinasyonlara göre aralarında istatistiksel olarak anlamlı bir ilişki bulunmuştur ($p<0.05$). Çap değerlerinin 45.01 mm'den büyük olanların oranı ise en yüksek T_2 tohumunda (%33.16) ($p>0.01$) ve Z_3 ekim mesafesinde (%47.01) elde edilmiş ve istatistiksel olarak anlamlı bulunmuştur ($p>0.01$). Havuç çap değerleri

45.01 mm'den büyük olanların dağılımı en yüksek T_2Z_3 (%59.90) interaksyonunda, en düşük ise T_1Z_1 (%4.18) interaksyonunda elde edilmiş ve diğer interaksyonlarla arasında istatistiksel olarak anlamlı bir farklılık bulunmuştur ($p<0.05$).

TS 1193'deki havuç boylama standardında ekstra sınıfta bulunan ve 50-200 g kütle aralığına giren havuçların yüzde dağılımları incelendiğinde, Z_2 anma ekime mesafesinde (%62.77) ve interaksyonlarda ise T_1Z_2 kombinasyonunun (%64.65) en yüksek oranlar elde edilmiştir ($p<0.01$). Başka bir ifadeyle, T_2Z_1 ve T_2Z_2 interaksyonları arasında istatistiksel bir farklılık belirlenmemiştir. <49.99 g'dan küçük olanların en düşük oranının T_2Z_3 kombinasyonunda istatistiksel olarak farklılık gösterdiği tespit edilmiştir ($p<0.01$). Kütlesi 200.01 g'dan büyük olanların yüzdeleri incelendiğinde, interaksyonlar arasında istatistiki olarak anlamlı bir ilişki görülmemiştir. Çıplak tohumda T_1 (%18.17) ve Z_1 sıra üzeri mesafede (%8.83) ise istatistiksel olarak anlamlı bir ilişki belirlenmiş ve en düşük değerler elde edilmiştir.

Kırıkhan popülasyonu siyah havuç suyunun renk değerlerinin değişimi Çizelge 5'te verilmiştir. L^* , a^* , b^* , C ve h^* değerleri incelendiğinde, tüm interaksyonların istatistiksel olarak anlamlı olduğu görülmektedir. L^* değerleri (parlaklık) genel olarak değerlendirildiğinde değişimin 24.40 ile 25.98 arasında bir değişim gösterdiği ve T_1Z_1 kombinasyonunda ise parlaklık değerinin yüksek olduğu ve diğer interaksyonlar ile arasında anlamlı bir farklılık olduğu bulunmuştur. a^* değerleri incelendiğinde, kırmızı tonun belirgin olduğu, en yüksek ortalama değer T_1 tohumu (7.499) ile T_1Z_1 (8.35), T_1Z_2 (7.940) ve T_2Z_3 (8.430) interaksyonlarında elde edildiği belirlenmiş ve interaksyonlar arasında istatistiki açıdan bir farklılık olmadığı saptanmıştır. b^* değerlerine bakıldığında, genel olarak mavi tonların hakim olduğunu, en yüksek mavi ton değerinin T_1Z_2 interaksyonunda (-1.623) bulunduğu ve istatistiksel olarak da anlamlı olduğu tespit edilmiştir. [Bıyıktaş \(2018\)](#), Kırıkhan genotipinin farklı ekim zamanlarında havuç etindeki L^* , a^* ve b^* değerlerini ortalama olarak sırasıyla 3.38, 0.36 ve 0.32 olarak rapor etmiştir.

Tablo 5. Kırıkhan popülasyonu siyah havuç suyunun renk özellikleri.

Table 5. Color characteristics of Kırıkhan population black carrot juice.

		L^*	a^*	b^*	C	h^*
Tohum	T_1	24.97	7.499 _a	-1.024 _b	7.58 _a	352.2
	T_2	24.80	6.747 _b	-0.824 _a	6.81 _b	352.4
	SHO	0.1878	0.1648	0.0387 _b	0.1622	0.417
	P-değeri	0.529	0.007	0.003	0.006	0.683
Sıra üzeri mesafe	Z_1	25.22	7.013	-0.913 _b	7.09	351.9 _b
	Z_2	24.61	7.038	-1.245 _c	7.15	350.2 _b
	Z_3	24.82	7.317	-0.615 _a	7.35	354.8 _a
	SHO	0.2300	0.2018	0.0474	0.1986	0.5110
	P-değeri	0.208	0.517	0.000	0.636	0.000
Tohum x Sıra üzeri mesafe	$T_1 \times Z_1$	25.98 _a	8.353 _a	-0.683 _{ab}	8.38 _a	355.3 _{ab}
	$T_1 \times Z_2$	24.40 _b	7.940 _a	-1.623 _d	8.11 _a	348.4 _c
	$T_1 \times Z_3$	24.53 _{ab}	6.203 _b	-0.767 _{ab}	6.25 _b	352.8 _b
	$T_2 \times Z_1$	24.46 _{ab}	5.673 _b	-1.143 _c	5.79 _b	348.5 _c
	$T_2 \times Z_2$	24.83 _{ab}	6.137 _b	-0.867 _{bc}	6.19 _b	352.0 _b
	$T_2 \times Z_3$	25.11 _{ab}	8.430 _a	-0.463 _a	8.44 _a	356.9 _a
	SHO	0.3252	0.2854	0.0670	0.2809	0.7227
	P-değeri	0.012	0.000	0.000	0.000	0.000

a, b, c Bir sütundaki farklı üst simgelere sahip ortalamalar istatistiki olarak farklılık gösterir ($p<0.05$), SHO standard hata ortalaması, T_1 kalibre edilmiş çıplak tohum, T_2 kaplı tohum, Z_1 , Z_2 ve Z_3 sıra üzeri ekim mesafeleri

Siyah havuç suyunun Chroma (C) değeri 0-60 arasında bir değer almakta ve bir rengin yoğunluğunu (parlaklığını) veya canlılığını belirtmektedir. Kırıkhan popülasyonu tohumlarda, Chroma değerleri, 5.79 ile 8.44 arasında bir değişim göstermiştir. Bu değerler en yüksek T_1Z_1 , T_1Z_2 ve T_2Z_3 interaksiyonlarında elde edilmiş ve diğer interaksiyonlarla aralarında ise istatistiksel olarak anlamlı bir farklılık bulunmuştur.

Hue değeri (h°), renk tonu açıları veya renkle (renk değişimi) ilgili bir nitelik olup 0° - 360° arasında değişmektedir. Araştırmada elde edilen Hue değerleri 348.5° ile 356.9° arasında bir değişim göstermiş olup, renk düzleminde kırmızı tonlara karşılık geldiği görülmektedir. T_1Z_2 ile T_2Z_1 interaksiyonlarından elde edilen Hue değerleri, diğer interaksiyonlara göre istatistiksel olarak anlamlı bulunmuş olup, T_1Z_2 ile T_2Z_3 interaksiyonlarının ise kırmızı-mor tonlara yakın olduğunu belirtebiliriz. [Bülbül \(2017\)](#), Ereğli popülasyonu çıplak siyah havuç tohumlarıyla ve dik rotovatorle hazırlanan tohum yatağında, ön ile arka baskı tekeri lastik ve ortada üçlü dar lastik bulunan pnömatik sebze ekim makinesiyle 2015 ve 2016 üretim yılında Chroma değerlerini sırasıyla 13.15 ile 14.75 ve 17.44 ile 17.74 arasında, h° değerlerini ise 356.3° ile 357.7° ve 355.8° ile 358.2° arasında bir değişim gösterdiğini bildirmektedir. Araştırma sonuçları bu yerel popülasyon ile karşılaştırıldığında, Kırıkhan popülasyonu siyah havuç suyunun renk yoğunluğunun ve renk tonunun daha düşük olduğunu, başka bir ifade ile havuç suyunun parlaklığının düşük ve rengin kırmızı-mor tona yaklaştığını vurgulayabiliriz.

Kırıkhan popülasyonu siyah havuç suyunun gıda analiz sonuçları Çizelge 6'da verilmiştir. Tohum x sıra üzeri mesafe interaksiyonunun briks, pH, antioksidan aktivitesi ve toplam fenolik içeriğindeki değerlerin değişimleri istatistiksel olarak anlamlı bulunmamıştır.

Analizi yapılan havuçların nem değerleri %82.32 ile %86.43 arasında, briks değerleri ise %7.37 ile %8.70 arasında bir değişim göstermiştir. Kırıkhan ilçesinde üretilen siyah havuç popülasyonunun coğrafi işaret belgesinde briks değerlerinin %9.1 ile %10.7 arasında değiştiği [\(Anonim, 2022\)](#) ve Kırıkhan ilçesinde aynı havuçlar üzerine yapılan başka bir araştırmada, briks değerlerinin ortalama %9.99 olarak elde edildiği [\(Bıyıktaş, 2018\)](#), Ereğli popülasyonu siyah havucun bu lokasyonunda 2016 yılı üretiminde ise ortalama briks değerinin %16.61 ile %17.42 arasında elde edildiği [\(Bülbül, 2017\)](#) bildirilmiştir. Yapılan diğer araştırmalarda, briks değerinin %9.10 [\(Baysal ve ark., 2013\)](#), siyah havuç suyu örneğinde suda çözünür kuru madde başlangıç değerinin %10.5 [\(Lafcı, 2019\)](#) ve Konya yöresinde üç farklı yerde yetiştirilen yerel siyah havuç genotiplerinde 8.90-15.10 arasında elde edildiği bildirmiştir [\(Naeem, 2017\)](#). Elde edilen pH değeri ise 5.47 ile 5.61 arasında değişim göstermiş olup, yine ilgili coğrafi işaret belgesinde bu değer 5.95 ile 6.22 arasında olduğu belirtilmiştir [\(Anonim, 2022\)](#). Araştırmadan elde edilen briks ve pH değerleri, literatürde belirtilen değerlerden daha düşük bulunmuştur.

Çizelge 6. Kırıkhan popülasyonu siyah havuç suyunun gıda analiz sonuçları.**Table 6.** *Nutritional analysis results of Kırıkhan population black carrot juice.*

		Nem içeriği (%)	Briks (%)	pH	Antioksidan Aktivite (%)	Toplam fenolik içeriği mg GAE (100 g) ⁻¹
Tohum	T ₁	84.05	8.29	5.52	79.81	710.2
	T ₂	83.56	7.73	5.59	78.91	665.9
	SHO		0.1918	0.0239	0.4022	23.667
	P-değeri		0.061	0.065	0.057	0.062
Sıra üzeri mesafe	Z ₁	83.29	7.94	5.56	78.74	712.6 _{ab}
	Z ₂	82.28	7.71	5.53	80.03	744.7 _a
	Z ₃	84.21	8.36	5.58	79.30	607.0 _b
	SHO		0.2349	0.0294	0.4925	28.99
	P-değeri		0.181	0.200	0.222	0.007
Tohum x Sıra üzeri mesafe	T ₁ x Z ₁	83.40	8.10	5.54	79.29	742.1
	T ₁ x Z ₂	82.32	8.06	5.47	79.81	803.7
	T ₁ x Z ₃	86.43	8.70	5.56	80.32	585.1
	T ₂ x Z ₁	83.17	7.78	5.59	78.20	683.1
	T ₂ x Z ₂	82.42	7.37	5.58	80.25	685.7
	T ₂ x Z ₃	85.26	8.03	5.61	78.29	629.1
	SHO		0.6482	0.0405	0.6966	40.99
	P-değeri		0.820	0.479	0.243	0.097

a, b, c Bir sütündeki farklı üst simgelere sahip ortalamalar istatistiki olarak farklılık gösterir (p<0.05), SHO standart hata ortalaması, T₁ kalibre edilmiş çıplak tohum, T₂ kaplı tohum, Z₁, Z₂ ve Z₃ sıra üzeri ekim mesafeleri

Antioksidan aktivite değerleri %78.20 ile %80.32 arasında bir değişim göstermiştir. Ereğli popülasyonu tohumlarla 2016 yılında elde edilen antioksidan aktiviteleri ortalama %43.66 ve %42.96 olarak bildirilmiştir (Bülbül, 2017). Ayrıca, sucuk üretiminde kullandıkları siyah havuç konsantresinin antioksidan değerinin %89.71 olduğu rapor edilmiştir (Ekici ve ark., 2015)

Araştırma sonucunda, toplam fenolik içerikleri, 585.1 ile 803.7 mg GAE (100 g)⁻¹ arasında bir değişim gösterdiği bulunmuştur. Bu değerlerin sıra üzeri mesafedeki değişimi istatistiksel olarak anlamlı bulunmuş olup, Z₁, Z₂ ve Z₃ ekim mesafelerine bağlı olarak toplam fenolik içeriklerinin sırasıyla 712.6, 744.7 ve 607.0 mg GAE. (100 g)⁻¹ olarak elde edildiği ve Z₂ ekim mesafesinde ise en yüksek değer elde edildiği Çizelge 6'da görülmektedir. Fenolik madde miktarlarında gözlenen farklılıkların, sıra üzerindeki bitkiler arası mesafelerin artması sonucunda, biyokimyasal reaksiyonların farklılık göstermesinden kaynaklandığı düşünülmektedir. Bu nedenle, kaplı tohumda tarla koşullarında elde edilen bitkiler arası mesafenin çıplak tohuma göre daha büyük olması fenolik içeriklerinin düşük olmasında etkili olmuştur. Yapılan diğer araştırmalarda, Ereğli popülasyonu siyah havucunun 2015 ve 2016 yılı üretiminde ortalama toplam fenolik madde değerlerinin sırasıyla 504.73 ile 487.57 ve 512.3 ile 517.9 mg.(100 g)⁻¹ arasında (Bülbül, 2017), Ereğli popülasyonu havuçlarda fenolik madde miktarının 3051 mg.kg⁻¹ (El, 2008) ve yine Ereğli ilçesinde aynı alanda ve eşit şartlarda yetiştirilen 700 kökün iç renklerine göre 11 farklı grubun örneklerinin fenolik içeriklerinin 516.5-1199.2 µg GAE. g⁻¹ arasında bir değişim gösterdiği bildirilmiştir (Özgen ve Sekerci, 2013). Ereğli bölgesinde üretilen Kırıkhan genotipi ile Ereğli genotipini toplam fenolik madde değerlerini karşılaştırdığımızda, Kırıkhan genotipinde daha yüksek toplam fenolik içerikleri elde edilmiştir. Literatür incelendiğinde, Algarra ve ark. (2014) Antonina ve Purple Haze havuç çeşitlerinde

sırasıyla 187.8 ve 492 mg GAE. (100 g)⁻¹ fenolik madde miktarı elde ettiklerini, ayrıca [Kaur ve Kapoor \(2002\)](#) siyah havuç suyunda 350.5 mg GAE. (100 g)⁻¹ fenolik madde miktarını elde ettiklerini bildirmişlerdir. Örneklerin antioksidan aktivite ve toplam fenolik içeriklerindeki farklılıkların, lokasyon, tarımsal uygulamalar, iklim farklılıkları ve ekstraksiyon metotları gibi faktörlerden kaynaklanabileceği düşünülmektedir.

SONUÇ

Sebzelere yönelik araştırmalar besin kalitesi, görsel çekicilik ve tıbbi olarak hastalıkların önlemesi açısından önemlidir. Diğer taraftan günümüzde yerel genotiplerin önemi ve ıslah programlarının uygulanması, sürdürülebilir bir tarım sistemi için önemli bir yaklaşım olarak düşünülmektedir. Yerel genotiplerin korunması, sadece araştırmacılar için değil, aynı zamanda üreticiler ve bunların değişik işleme prosesleri ile elde edilen farklı çıktılarla tüketicilere sunulmasında önemlidir. Bu nedenle Kırıkhan popülasyonu siyah havuç tohumlarının farklı bir lokasyonda üretimi yapılmıştır. Ereğli İlçesinde çiftçi uygulamasından farklı olarak, tohumların sınıflandırılması yapılmış ve ayrıca tohumlara kaplama uygulaması yapılarak, pnömatik hassas sebze ekim makinesi ile ekimi yapılmıştır. Böylece yüksek bir tarla çıkışının, optimum bitki sayısının ve bitki dağılımının daha homojen olması (düzgün) amaçlanmıştır. Araştırma sonuçları genel olarak değerlendirildiğinde, tarla koşullarında elde edilen ortalama sıra üzeri mesafeler yüksek oranlarda artmış, ancak bu mesafelerin varyasyon katsayısı değerleri ise azalmıştır. Siyah havuç ekiminde istenilen bitki yoğunluğu, her iki tohumda ve Z₁ ekim mesafesinde yüksek değerlerde elde edilmiştir. Kalite kriterleri açısından, 25-45 mm çap aralığında en yüksek değerler, çıplak tohumda Z₂ ve kaplı tohumda Z₁ ile Z₂ ekim mesafelerinde bulunmuştur. 50 ile 200 g arasındaki kütle yüzdeleri ise en yüksek çıplak tohumda Z₂ ekim mesafesinde saptanmıştır. Ayrıca kaplı tohumda Z₂ sıra üzeri mesafede h⁰ değerinin kırmızı-mor tona yakın ve toplam fenolik miktarının yüksek olması nedeniyle, çıplak ve kalibre edilmiş tohumların Z₂ ekim mesafesinde ekim yapılması gerekmektedir. Bölgede siyah havucun ekim mekanizasyonuna yönelik araştırmalara devam edilmesi, ayrıca farklı havuç ekim tekniklerinin ekim düzgünlüğüne ve kalite kriterlerine etkisi konularında, araştırmaların sürdürülmesi gerekmektedir.

ÇIKAR ÇATIŞMASI

Makale yazarları olarak herhangi bir çıkar çatışması olmadığını beyan ederiz.

YAZAR KATKISI

Haydar HACISEFEROĞULLARI: Araştırmanın planlanması, tarla denemelerinin yapılması, verilerin elde edilmesi, verilerin değerlendirilmesi, makalenin yazımı,

Nurhan USLU: Literatür taraması, tarla denemelerinin yapılması, verilerin elde edilmesi, gıda analizlerinin yapılması, verilerin değerlendirilmesi, makalenin kontrolü.

ETİK KURUL KARARI

Bu makale Etik Kurul Kararı gerektirmemektedir.

KAYNAKLAR

- Abdullakasim P, Songchitsomboon S, Techagumpuch M, Balee N, Swatsitang P and Sungpuag P (2007). Antioxidant capacity, total phenolics and sugar content of selected Thai health beverages. *International Journal of Food Sciences and Nutrition*, 58(1): 77-85.
<https://doi.org/10.1080/09637480601140946>
- Algarrá M, Fernandes A, Mateus N, de Freitas V, da Silva JCGE and Casado J (2014). Anthocyanin profile and antioxidant capacity of black carrots (*Daucus carota* L. ssp *sativus* var. *atrorubens* Alef.) from Cuevas Bajas, Spain. *Journal of Food Composition and Analysis*, 33(1): 71-76.
<https://doi.org/10.1016/j.jfca.2013.11.005>
- Alper Özdemir N (2001). *Nar Suyu Üretimi Üzerine Araştırmalar*. Doktora Tezi. Hacettepe Üniversitesi Fen Bilimleri Enstitüsü, Gıda Mühendisliği Ana Bilim Dalı, Ankara-Türkiye.
- Anonim (2017). No.216-Menşe adı Ereğli siyah havucu, Tescil ettiren Ereğli Belediyesi
- Anonim (2020). MGM, Ereğli ilçesi meteorolojik verileri. İstasyon No:17248.
- Anonim (2022). No:1251-Menşe adı Kırıkhan siyah havucu, Tescil Ettiren: Kırıkhan Sanayi ve Ticaret Odası Başkanlığı.
- AOAC (2000). Official methods of analysis of AOAC Int. (17th ed.). *AOAC Int. Suite.*, 481 North Frederick Avenue Gaithersburg, Maryland 20877-2417 USA.
- Baysal T, Demirdöven A ve Ergün AR (2013). Kara havuç suyu üretiminde elektroliz ve mikrodalga uygulamalarının verim ve kalite özellikleri üzerine etkileri. *Gıda Dergisi*, 38(5): 291-298.
- Bıyıktaş İ (2018). *Hatay İli Kırıkhan İlçesinde siyah havuçta farklı ekim zamanlarının verim ve kaliteye etkisi*. Hatay Mustafa Kemal Üniversitesi Fen Bilimleri Enstitüsü, Bahçe Bitkileri Anabilim Dalı, Hatay-Türkiye.
- Blando F, Marchello S, Maiorano G, Durante M, Signore A, Laus MN, Soccio M and Mita G (2021). Bioactive compounds and antioxidant capacity in anthocyanin-rich carrots: A comparison between the black carrot and the Apulian landrace “Polignano” carrot. *Plants*, 10(3): 564.
<https://doi.org/10.3390/plants10030564>
- Brand-Williams W, Cuvelier ME and Berset C (1995). Use of a free radical method to evaluate antioxidant activity. *LWT-Food science and Technology*, 28(1): 25-30.
- Bülbül H and Haciseferoğulları H (2017). The effects of various types of press wheels mounted on pneumatic precise drilling machine on the quality criteria of black carrot. *International Journal of Secondary Metabolite*, 4(3, Special Issue 1): 125-133.
- Bülbül H (2017). *Siyah havucun pnömatik hassas ekim makinesiyle ekiminde farklı baskı tekerlerinin ekim düzgünlüğüne ve bazı kalite kriterlerine etkilerinin belirlenmesi*, Doktora Tezi, Selçuk Üniversitesi Fen Bilimleri Enstitüsü, Tarım Makinaları ve Teknolojileri Mühendisliği Anabilim Dalı, Konya-Türkiye.
- Cemeroğlu B (2013). Gıda analizlerinde genel yöntemler, Gıda Analizleri, Cemeroğlu, BS (Baş Ed.), *Bizim Grup Basımevi*, Ankara, Türkiye.
- Chhetri L, Rizwan M, Munkombwe S, Dorji N and Mutum E (2022). Utilization and characteristics of black carrot (*Daucus carota* L.): Potential health benefits and effect of processing. *Journal of Pharmaceutical Innovation*, 11: 30-41.
- Chihoub W, Dias MI, Barros L, Calhelha RC, Alves MJ, Harzallah-Skhiri F and Ferreira ICFR (2019). Valorisation of the green waste parts from turnip, radish and wild cardoon: Nutritional value, phenolic profile and bioactivity evaluation. *Food Research International*, 126: 108651.
- Düzgüneş O, Kesici T, Kavuncu O ve Gürbüz F (1983). Araştırma deneme metotları (İstatistik metodları II). *Ankara Üniversitesi Ziraat Fakültesi Yayınları* Ders Kitabı: 295
- Ekici L, Ozturk I, Karaman S, Caliskan O, Tornuk F, Sagdic O and Yetim H (2015). Effects of black carrot concentrate on some physicochemical, textural, bioactive, aroma and sensory properties of sucuk, a traditional Turkish dry-fermented sausage. *LWT-Food Science and Technology*, 62(1): 718-726.

- El SN (2008). *Türkiye’de sıklıkla tüketilen bazı gıdaların toplam fenolik madde içerikleri ve antioksidan aktiviteleri*. Türkiye 10. Gıda Kongresi; 21-23 Mayıs 2008, 21-23, Erzurum-Türkiye.
- Hunt M, Acton J, Benedict R, Calkins C, Cornforth D, Jeremiah L, Olson D, Salm C, Savell J and Shivas S (1991). *AMSA guidelines for meat color evaluation*. In: Proceedings 44th Annual Reciprocal Meat Conference (pp 3-17), 9-12 July 1991, Kansas State University, Manhattan, KS Lebensmittel Eier. Fleisch, Buttermilch. Springer-Verlag Berlin- Heidelberg-New York.
- ISO (1984). Sowing equipment-Test methods. Part 1. Single seed drills (precision drills) [7256/1], *In. Geneva, Switzerland*.
- Kaur C and Kapoor HC (2002). Anti-oxidant activity and total phenolic content of some Asian vegetables. *International Journal of Food Science and Technology*, 37(2): 153-161.
<https://doi.org/10.1046/j.1365-2621.2002.00552.x>
- Kaur G, Sharma N, Singh A, Kapoor S and Khatkar SK (2023). Ultrasound-assisted microemulsions of anthocyanins extracted from black carrot pomace and its utilisation as functional component in kulfi: implication on in vitro release, bio-functional components and rheological characteristics. *International Journal of Food Science & Technology*, 58(5): 2744-2753.
- Kotecha P, Desai BB and DL M (1998). Carrot. In S. D.K. & K.S.S. (Eds.), *Handbook of Vegetable Science and Technology: Production, Compostion, Storage, and Processing*. (pp. 119-140). Marcel Dekker, Inc.
- Lafcı B (2019). *Ozmotik destilasyon ve membran destilasyon ile siyah havuç suyu konsantrasyonu*. Yüksek Lisans Tezi, Hitit Üniversitesi Fen Bilimleri Enstitüsü, Gıda Mühendisliği Anabilim Dalı, Çorum-Türkiye.
- Lei X, Hu H, Wu W, Liu H, Liu L, Yang W, Zhou Z and Ren W (2021). Seed motion characteristics and seeding performance of a centralised seed metering system for rapeseed investigated by DEM simulation and bench testing. *Biosystems Engineering*, 203: 22-33.
- Naeem MY (2017). *Investigation of biochemical differences between commercial cultivar deep purple and local genotypes of black carrots*. Niğde Ömer Halisdemir Üniversitesi, Fen Bilimleri Enstitüsü. Niğde-Türkiye.
- Ozgen S ve Sekerci S (2013). Ereğli siyahı havuç çeşidinin fitokimyasal varyasyonu. *Turkish Journal of Agriculture-Food Science and Technology*, 1(2): 86-89.
- Önal İ (1987). Vakum prensibiyle çalışan bir pnömatik hassas ekici düzenin ayçiçeği, mısır ve pamuk tohumu ekim başarısı. *Ege Üniversitesi Ziraat Fakültesi Dergisi*, 24(2): 105-125.
- Önal İ ve Ertuğrul Ö (2011). Üstten akışlı oluklu ekici makarının soğan, havuç ve kanola tohumları için tohum akışı ve sıra üzeri tohum dağılım düzgünlüğü. *Tarım Bilimleri Dergisi*, 17: 10-23.
- Ornek MN, Seflek AY and Haciseferogullari H (2018). Performance of pneumatic precision seed drill in black carrot sowing. *Pakistan Journal of Agricultural Sciences*, 55(3): 645-651.
- Purkiewicz A, Ciborska J, Tańska M, Narwojsz A, Starowicz M, Przybyłowicz KE and Sawicki T (2020). The impact of the method extraction and different carrot variety on the carotenoid profile, total phenolic content and antioxidant properties of juices. *Plants*, 9(12): 1759.
- Sadetaş Önal Ş (2023). *Konya İli Ereğli İlçesinde kaplanmış ve çıplak Kırıkhan yerel popülasyonu siyah havuç tohumlarının ekiminde çimlenme özelliklerinin ve sıra üzeri bitki dağılım düzgünlüğünün belirlenmesi*. Yüksek Lisans Tezi, Selçuk Üniversitesi Fen Bilimleri Enstitüsü, Konya-Türkiye.
- Saranraj P, Behera SS and Ray R C (2019). Chapter 7 - Traditional foods from tropical root and tuber crops: Innovations and challenges. In C. M. Galanakis (Ed.), *Innovations in Traditional Foods* (pp. 159-191). Woodhead Publishing. <https://doi.org/10.1016/B978-0-12-814887-7.00007-1>.
- Seljasen R, Lea P, Torp T, Riley H, Berentsen E, Thomsen M and Bengtsson GB (2012). Effects of genotype, soil type, year and fertilisation on sensory and morphological attributes of carrots (*Daucus carota* L.). *Journal of the Science of Food and Agriculture*, 92(8): 1786-1799.
- Sermenli T (2012). *Önemli Bir Üretim Bölgesi Olan Hatay Kırıkhan’da Havuç (Daucus Carota L.) Yetiştiriciliği*. 9. Sebze Tarımı Sempozyumu (12-14 Eylül 2012) Bildiriler, Konya-Türkiye.
- TSE (2007). Havuç. *Türk Standartları*, TSE 1193.
- Vural H, Eşiyok D ve Duman İ (2000). Kültür sebzeleri (Sebze yetiştirme). *Ege Üniversitesi Basımevi*.
- Yalçın Dokumacı K (2021). *Siyah havucun sırta ekiminde uygulanan farklı ekim tekniklerinin sıra üzeri bitki dağılım düzgünlüğüne ve siyah havucun bazı fiziko-kimyasal özelliklerine etkisi*. Doktora Tezi, Selçuk Üniversitesi Fen Bilimleri Enstitüsü, Tarım Makinaları ve Teknolojileri Mühendisliği Anabilim Dalı, Konya-Türkiye.

- Yılmaz M (2019). *Konya ili Ereğli ve Karapınar ilçelerinde siyah havuç üretimi yapan tarım işletmelerinin mekanizasyon özelliklerinin ve sorunlarının belirlenmesi*. Yüksek Lisans Tezi, Selçuk Üniversitesi Fen Bilimleri Enstitüsü, Tarım Makinaları ve Teknolojileri Mühendisliği Anabilim Dalı, Konya-Türkiye.
- Yousuf B, Gul K, Wani AA and Singh P (2016). Health benefits of anthocyanins and their encapsulation for potential use in food systems: A review. *Critical reviews in Food Science and Nutrition*, 56(13): 2223-2230.



Turkish Journal of
Agricultural
Engineering Research
(Turk J Agr Eng Res)
e-ISSN: 2717-8420



Effects of Using Seed Tube on Seed Distribution Uniformity in Single Seed Planters

Mehdi GÜVEN^a , Nisanur YAKUT^a , Emrah KUŞ^{a*} 

^aIğdır University Faculty of Agriculture Department of Biosystems Engineering, Iğdır, TÜRKİYE

ARTICLE INFO: Research Article

Corresponding Author: Emrah KUŞ, E-mail: emrah.kus@igdir.edu.tr

Received: 19 October 2024 / Accepted: 02 December 2024 / Published: 31 December 2024

Cite this article: Güven, M., Yakut, N., & Kuş, E. (2024). Effects of Using Seed Tube on Seed Distribution Uniformity in Single Seed Planters. Turkish Journal of Agricultural Engineering Research, 5(2), 262-270. <https://doi.org/10.46592/turkager.1570191>

ABSTRACT

In single-seed sowing of small seeds, in addition to seed size and shape, critical problems can be experienced due to the electrostatic force that occurs during seeds adhering to the plate holes. To find a solution to these problems, the effect of using seed tubes in single-seed planters was the subject of the study. For this purpose, the study, designed with two different seed drop heights (115 mm and 200 mm) and without and with seed tube, was carried out at three different forward speeds (0.5 m s⁻¹, 1.0 m s⁻¹, and 1.5 m s⁻¹). According to the analysis results applied to the data, it was determined that the seed distribution uniformity was negatively affected by the increase in seed drop height and progress speed, and the planting quality deteriorated. While it was expected that the use of seed tubes in single-seed planters would have a positive effect on the uniformity of seed distribution intra-rows and inter-rows, it was found that on the contrary, the uniformity of seed distribution deteriorated and there was a high degree of variation. The best values for seed distribution uniformity were obtained with a forward speed of 0.5 m s⁻¹, a seed drop height of 115 mm, and no seed tube.

Keywords: Small seeds, Seed dropping method, Seed drop height, Forward speed

INTRODUCTION

Single-seed planters are machines used to plant large and small seeds that require special care. It is aimed to provide the needs of the plants such as a living space, water, and nutrients during and after the emergence process of the seeds planted through these machines. Single-seed planting of small seeds is relatively more difficult than large seeds. The reasons for this difficulty are the inability of small seeds to adhere well to the seed plate holes due to size, weight, and shape, and the electrostatic force caused by the plate peripheral velocity (Barut, 2008). The coating of small seeds is one of the common methods used to overcome these problems and

to avoid undesirable uniformity of seed distribution. Since the seed coating method provides relative facileness in the planting process, many studies have been carried out so far ([Hacıyusufoğlu *et al.*, 2015](#); [Rocha *et al.*, 2019](#); [Afzal *et al.*, 2020](#)). Another method is to monitor seeds in real-time during planting using sensors. Many of the monitoring devices used in this method are based on piezoelectric, capacitance, radio wave, and photoelectric detection theories ([Liu *et al.*, 2019](#)). In this context, numerous studies have been conducted using advanced systems developed to monitor seed flow rates. Some of these studies include piezoelectric sensors ([Dongyan *et al.*, 2013](#); [Youchun *et al.*, 2017](#); [Youchun *et al.*, 2018](#)), capacitance sensors ([Liming *et al.*, 2010](#); [Yujing *et al.*, 2013](#); [Jakub *et al.*, 2017](#)), high frequency radio wave sensors ([Linco Precision, 2024](#)), photoelectric sensors ([Deividson and Rosane, 2014](#); [Haotun *et al.*, 2018](#); [Marko *et al.*, 2018](#)) and camera systems ([Karayel *et al.*, 2006](#)). The fact that the seed coating method requires an additional cost and that sensor systems are not yet widespread in seed planters shows that simpler solutions for the farmer should be emphasized.

In pneumatic single-seed planters, seed tubes are generally not required since the drop height from the seed cell to the furrow is shorter than in conventional seed drills ([Kuş, 2014](#)). However, the height at which the seed drops into the soil is relatively low and can vary depending on the type of furrow opener used on the planter. Moreover, research suggests that ensuring uniform seed distribution with single-seed planters is quite difficult due to the many factors that can affect planting ([Kuş, 2021a](#); [Kuş, 2021b](#); [Kuş, 2021c](#)). To tackle this challenge, the idea of integrating seed tubes into pneumatic single-seed planters has emerged as a viable solution. The aim of this study was to determine whether the use of a seed tube would make a positive contribution to seed distribution uniformity on small-grained seeds in pneumatic single-seed planters that do not use a seed tube. For this purpose, small-grained seeds were sown without coating, and the performance of the seed device unit was examined under the influence of forward speed, seed-dropping height, and seed-dropping method.

MATERIALS and METHODS

The study was conducted using a sticky band test setup located in the Biosystems Engineering Laboratory of the Faculty of Agriculture at Iğdır University, Türkiye. Mung bean (*Vigna radiata* L.) seeds were used in the experiments. Thousand-grain weight (g), bulk density (kg m⁻³), angle of repose (°), sphericity (%), and laboratory germination degree values of the seeds determined according to [ASAE Standard \(2005\)](#) were 5.0, 87.2, 18.1, 88.3 and 83.3, respectively. Taking into account the practical values commonly used for mung bean seeds, an inter-row spacing of 500 mm and an intra-row spacing of 50 mm were selected.

The experimental stand consists of three parts: a fan unit, a seed metering unit, and a sticky band. The fan unit was employed to generate the vacuum pressure needed for the small seeds to adhere to the holes of the metering disk. For mung beans, 40 perforated discs were used, and following preliminary trials, the optimal disc hole diameter was determined as 2 mm.

The sticky band stand mounted among two rollers, with a diameter of 145 mm, was 10 meters in length and 0.5 meters in width. The sticky band was divided into 400 across strips, each 25 mm wide, using a laser. Furthermore, a continuous line was drawn along the band's longitudinal axis, precisely in the center. This line is called the Band Center Line (BCL) and is used to determine the row deviation amount of the seeds. As it is well known, the inter-row spacing of seeds (i.e. deviation from the row) in field conditions are determined by accounting for the deviations of the seeds to the left and right of the furrow once emergence is completed. The BCL line drawn longitudinally from the center of the band was used to represent the bottom of the furrow in laboratory conditions. To measure the deviation of the seeds from the normal during the experiments, the BCL was positioned to align with the metering disc point where the seeds of mung beans were freely released from the metering unit. While the seeds were falling freely on the sticky band, the amount of grease on the surface of the band was determined by preliminary experiments and examined in each replicate to prevent bounces (Figure 1). The fan, seed metering unit, and sticky band are each powered by separate electric motors and controlled via speed drivers. The electric motor that drives the fan unit adjusted with a speed driver to be equivalent to the 540 rpm PTO of the tractor.

The experiments were carried out with three different band forward speeds (0.5 m s^{-1} , 1.0 m s^{-1} , and 1.5 m s^{-1}) two seed drop heights (115 and 200 mm), and two seed dropping methods (without seed tube and by seed tube), by design a factorial trial layout with three replications. At each repetition, the band is greased, the fan is turned on, and when it reaches the appropriate speed (the speed equivalent to the 540 rpm PTO of the tractor) the seed metering device is started, and finally the electric motor that drives the belt is started. In the closure process, the reverse procedure was applied, and each repetition was completed. Afterward, to determine the uniformity of seed distribution, the spacings between consecutive seeds in rows and the spacings from the right and left to the BCL line were measured by a scale. The measurements were conducted over a 6000 mm section of the sticky band.

Performance indicators were used to determine the sowing quality: if the spacing between consecutive seeds was greater than 1.5 times the target seed spacing (Z), it was evaluated as the miss index ($I_{\text{miss}} > 1.5Z$), if it was equal to or less than half of the target seed spacing, it was evaluated as the multiple index ($I_{\text{mult}} \leq 0.5Z$), and if it was greater than half of the target seed spacing and less than 1.5 times, it was evaluated as the quality of feed index ($0.5Z < I_q \leq 1.5Z$) ([Kachman and Smith 1995](#); [Singh et al., 2005](#)). To determine the impacts of forward speed, seed drop height, and seed dropping method on the planting quality and seed distribution uniformity, analysis of variance (ANOVA) was performed using the SPSS package program. Duncan's Multiple Range was then applied to recognize dissimilarities and similarities among the parameter levels.

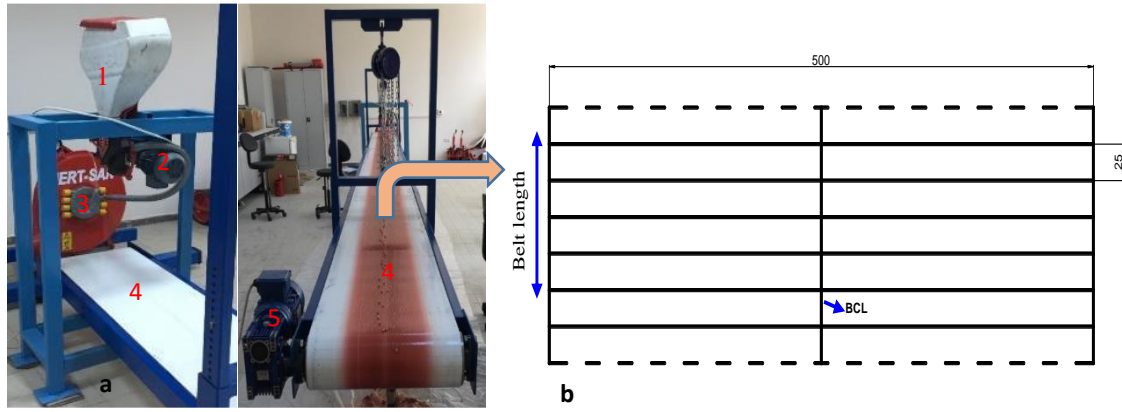


Figure 1. The parts of the sticky band test rig: (a) seed box (1), AC driving (2), vacuum unit (3), sticky band (4), and AC motor (5). The dimensions are measured in millimeters (b), (Kuş, 2021a).

RESULTS AND DISCUSSION

The effects of forward speed, seed dropping height, and seed drop method on the seed distribution uniformity and planting quality of mung beans (*Vigna radiata* L.) using a single-seed planter were determined by applying variance analysis and multiple range tests to the data (Tables 1 and 2). By the outcomes of the ANOVA, although the signification levels of forward speed effects on seed spacing of the intra-row, deviation from the row, miss and multiple indexes, and QFI varied, they were generally found to be significant. The effect of seed drop height was found to be very significant only in the intra-row seed spacing, while the seed dropping method was found to be significant in all other parameters except for the miss index. Additionally, another result to consider in the analyses is the interactive effects of the parameters. While the seed-dropping method does not statistically affect the miss index, the interaction between forward speed and the seed-dropping method was determined to be very significant. As it is known, the increase in forward speed affects the peripheral speed of the seed disc, while the use of a seed tube influences the way the seeds fall. It is assumed that a significant relationship exists between these interactions, which could be a result of the effect of forward speed on the free fall of the seeds and their movement within the seed tube. Furthermore, it has been determined that the three-way interaction significantly influences horizontal seed distribution, particularly in terms of intra-row and inter-row (deviation from row) seed spacing.

Table 1. Significance levels (P values) of variance analysis results.

Sources of Variation	SS	DFR	MI	MU	QFI**
Forward speed (S)	0.000*	0.002	0.040	0.000	0.000
Seed Drop Height (SFH)	0.000	0.766	0.097	0.231	0.779
Seed Drop Method (SFM)	0.000	0.003	0.946	0.000	0.000
S x SFH	0.010	0.019	0.085	0.090	0.028
S x SFM	0.736	0.023	0.000	0.132	0.001
SFH x SFM	0.734	0.001	0.654	0.029	0.041
S x SFH x SFM	0.004	0.030	0.695	0.556	0.644

* : P < 0.01 is greatly significant, P < 0.05 is significant and P > 0.05 is insignificant. **: SS; Intra-Row Seed Spacing, DFR; Deviation from Row, MI; Miss Index, MU; Multiple Index, QFI; Quality of Feed Index

According to the results of the multiple range tests conducted to determine the difference between the forward speed levels, all levels had different effects on the intra-row seed spacing. There was no statistical difference between the first and second levels (0.5 m s⁻¹ and 1.0 m s⁻¹) in deviation from the row and miss index, and between the second and third levels (1.0 m s⁻¹ and 1.5 m s⁻¹) in multiple index and QFI (Table 2).

Table 2. Multiple comparison test results for forward speed.

Forward Speed	SS*	DFR	MI	MU	QFI
0.5 m s ⁻¹	53.03 c**	2.71 b	11.68 b	9.04 b	79.28 a
1.0 m s ⁻¹	56.49 b	2.97 b	12.63 ab	15.63 a	71.17 b
1.5 m s ⁻¹	63.80 a	4.73 a	15.14 a	16.21 a	69.24 b

*: SS; Intra-Row Seed Spacing, DFR; Deviation from Row, MI; Miss Index, MU; Multiple Index, QFI; Quality of Feed Index

** : There is no statistical difference between the averages with the same letter in each column.

The coefficient of variation (CV) values of intra-row seed distribution uniformity are shown in Figure 2. Since the experiments were conducted according to a factorial setting, the value of each column of the forward speed in Figure 2 is the average of 12 replications, and the value of each column of the seed drop height and seed drop method is the average of 18 replications. As they can be seen in Figure 2, the highest CV values were obtained at 1.5 m s⁻¹ forward speed, 200 mm seed drop height, and when the seed tube was used. The CV values were found to be coherent with the results of the ANOVA for intra-row seed spacing given in Table 1. In addition, the average values of actual seed spacing measured intra-row, depending on the effect of forward speed, seed-drop height, and seed-dropping method, were compared with the target seed spacing value in Figure 3. As it can be understood from the figure, the greatest effect of the variation occurring due to the effect of the parameters on the seed spacing intra-row caused an average deviation of approximately 27.6% in forward speed, 19.8% in seed drop height, and 18.9% in seed dropping method.

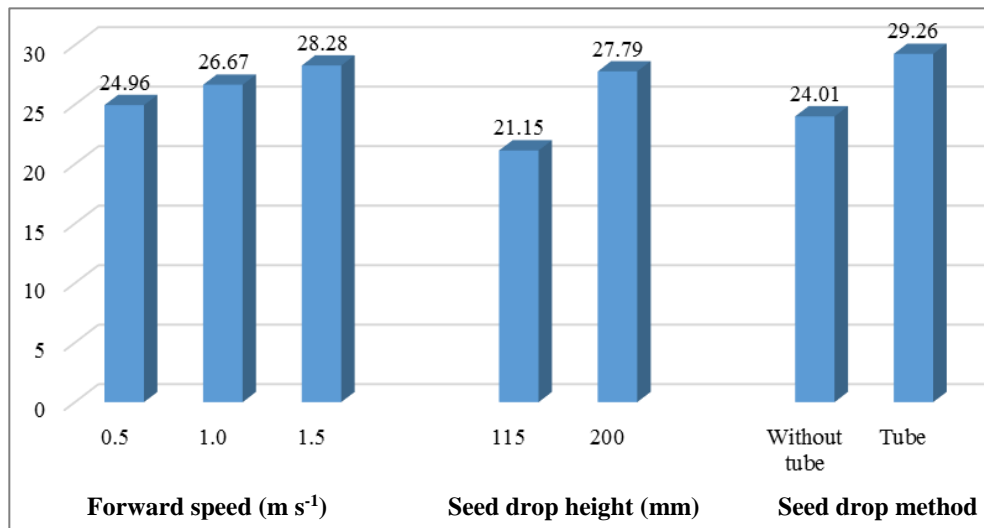


Figure 2. Values in coefficient of variation of seed spacing within the row.

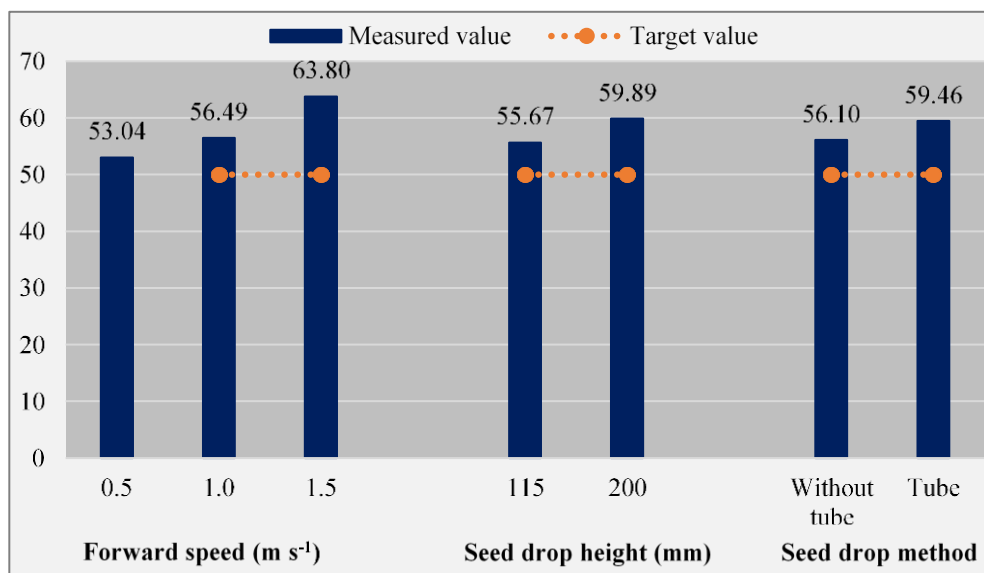


Figure 3. Comparison of seed spacing values measured in row with the theoretical value.

It is understood from the results of the analysis that the seed distribution uniformity of mung bean sown under the influence of three factors was significantly affected. The results of the previous studies with coarse-grain seeds and the effect of forward speed and seed dropping height on seed distribution uniformity were in parallel with the results of the current study with small-grain seeds for the same parameters (Kuş, 2021a; Günal and Kuş, 2021). Another issue that caused a significant worsening in the intra-row seed distribution uniformity was the use of seed tubes. While it was expected that the use of seed tubes would improve the intra-row seed spacing, on the contrary, it caused it to worsen. This distortion in the seed distribution can also be seen in the coefficient of variation values given in Figure 2. We assumed that the reason for this is the movement trajectory of the seed within the seed tube. The reason for this assumption was based on observations made during experiments with the seed tube. In these observations, it was hypothesized

that the seeds would come out of the spout of the tube by bouncing or being scattered, which could be the cause of the irregularity. [Yazgi *et al.* \(2020\)](#) reported that the point at which the seed leaves the metering disc into the seed tube affects the intra-row seed spacing with the effect of the disc's peripheral speed and may cause bouncing and slipping in the seed tube. The information that the seed may be subjected to bouncing and sliding in the seed tube depending on the point of release supports the unevenness detected in the current study.

In addition to the CV, three indexes (the miss, multiple, and QFI indexes) are used as indicators of sowing quality. When the quality indicators of mung bean in Figure 4 were analyzed, the worst result was obtained when the seed tube was used. When the use of the seed tube was evaluated according to the without seed tube condition, it did not cause a difference in the miss index, while it caused an increase of about 3 times in the multiple index. Another noteworthy situation in the graph was that both the miss and multiple indexes increased with the increase in the forward speed. However, according to the effect of seed drop height and seed dropping methods, one of the miss index and the multiple index tended to increase while the other tended to decrease. This indicates that the speed of forward had a more inevitable effect on the deterioration of the intra-row seed distribution uniformity. To understand this effect more clearly, looking at the intra-row mean values given in Figure 4 was sufficient. Figure 4 shows that the forward speed caused the small seeds to be shifted more in the row, increasing both the miss and multiple indexes.

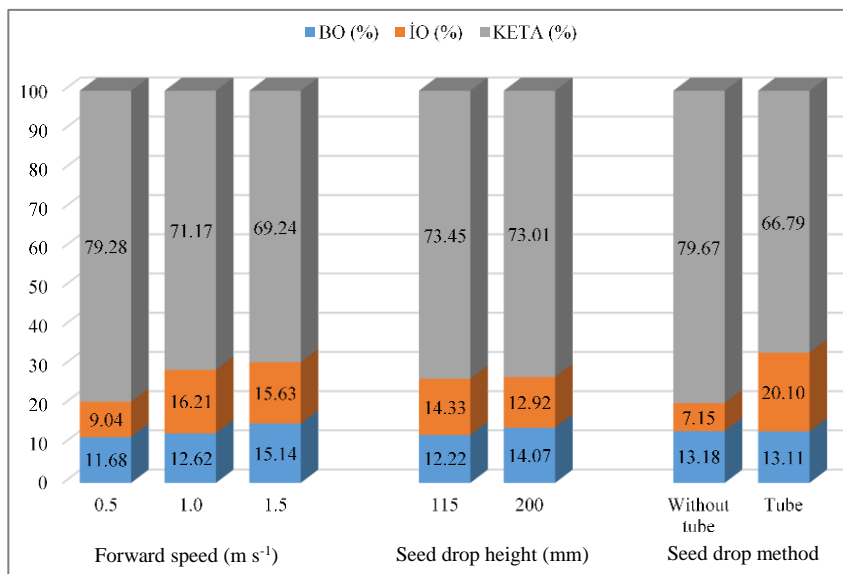


Figure 4. Sowing quality values.

CONCLUSION

The seed distribution uniformity and sowing quality in mung bean planting with a pneumatic single seed planter were affected by all three parameters. The unevenness stated as a percent of the theoretical seed spacing was perhaps affected by the circumferential speed of the seed disc, which increases with the increase of forward speed. Furthermore, the unevenness was the result of the combined effect of three

factors. It shows that although it is desirable to work with high forward speeds in single-seed planters, the forward speed cannot be increased as much as desired while sowing small-grain seeds. In addition, it was determined that certain standards should be taken into consideration since the seed drop height is determined according to the size of the furrow opener and that the use of seed tubes has a negative effect on seed distribution uniformity and sowing quality contrary to what is thought.

DECLARATION OF COMPETING INTEREST

I declare that I have no conflict of interest.

ACKNOWLEDGEMENT

This project was funded within the scope of TUBITAK 2209-A - University Students Research Projects Support Program.

CREDIT AUTHORSHIP CONTRIBUTION STATEMENT

The author declared that the following contributions are correct.

Mehdi Güven: Investigation, experimental studies.

Nisanur Yakut: Investigation, experimental studies.

Emrah Kuş: Investigation, experimental studies, methodology, conceptualization, formal analysis, data curation, validation, writing, review, and editing, visualization.

ETHICS COMMITTEE DECISION

This article does not require any Ethical Committee Decision.

REFERENCES

- Afzal I, Javed T, Amirkhani M and Taylor AG (2020). Modern seed technology: seed coating delivery systems for enhancing seed and crop performance. *Agriculture*, 10(11): 526.
<https://doi.org/10.3390/agriculture10110526>
- ASAE Standard (2005). American Society of Agricultural Engineers (ASAE). Cubes, Pellets, and Crumbles-Definitions and Methods for Determining Density, Durability, and Moisture Content, ASAE S269.4 DEC01. St. Joseph Mich. USA.
- Barut Z (2008). Seed coating and tillage effects on sesame stand establishment and planter performance for single seed sowing. *Applied Engineering in Agriculture*, 24(5): 565-571.
<https://doi.org/10.13031/2013.25268>
- Deividson LO and Rosane F (2014). Usage of the DFRobot RB-DFR-49 Infrared sensor to detect maize seed passage on a conveyor belt. *Computers and Electronics in Agriculture*, 102: 106-111.
<https://doi.org/10.1016/j.compag.2014.01.012>
- Dongyan H, Honglei J, Yue Q, Longtu Z and Honggang L (2013). Seeding monitor system for planter based on polyvinylidene fluoride piezoelectric film. *Transactions of the Chinese Society of Agricultural Engineering*, 23: 15-22.
- Günal ME and Kuş E (2021). Evaluation of parameters effective to performance of vacuum planter in single-seed sowing of the chickpea. *Fresenius Environmental Bulletin*, 11: 12140-12145.

- Hacıyusufoğlu AF, Akbaş T and Şimşek E (2015). Implement of the method of seed coating with pellet on some small-diameter seeds. *Journal of Agricultural Machinery Science*, 11(3): 257-263. (In Turkish).
- Haotun L, Jieyu R, Xin L, Shixiong L, Gang W and Yongjun Z (2018). *Review of the monitoring systems of the machine for precision sowing and fertilization of wheat*. In *Proceedings of the ASABE 2018 Annual International Meeting*, Austin, TX, USA, 29 July-1 August 2018; p. 1800736.
- Jakub L, Václav K, Václav P and František K (2017). Capacitive throughput sensor for plant materials-effects of frequency and moisture content. *Computers and Electronics in Agriculture*, 133: 22-29. <https://doi.org/10.1016/j.compag.2016.12.014>
- Kachman SD and Smith JA (1995). Alternative measures of accuracy in plant spacing for planters using single seed metering. *Transactions of the ASAE*, 38(2): 379-387. <https://doi.org/10.13031/2013.27843>
- Karayel D, Wiesehoff M, Özmerzi A and Müller J (2006). Laboratory measurement of seed drill seed spacing and velocity of fall of seeds using high-speed camera system. *Computers and Electronics in Agriculture*, 50: 89-96. <https://doi.org/10.1016/j.compag.2005.05.005>
- Kuş E (2014). *Determination of effects of drop height of seed and ground speed on sowing qualification for conventional and reduced tillage conditions in precision vacuum seeders*. PhD Thesis, Ataturk University (Unpublished), Turkey.
- Kuş E (2021a). An attempt to evaluate the performance parameters of a precision vacuum seeder in different seed drop height. *Journal of the Institute of Science and Technology*, 11(3): 1846-1853.
- Kuş E (2021b). Evaluation of some operational parameters of a vacuum single-seed planter in maize sowing. *Journal of Agricultural Sciences (Tarim Bilimleri Dergisi)*, 27(3): 327-334.
- Kuş E (2021c). Field-scale evaluation of parameters affecting planter vibration in single seed planting. *Measurement*, 184(3): 109959. <https://doi.org/10.1016/j.measurement.2021.109959>
- Linco Precision (2024). WaveVision Sensors (Precision planting). Available online: <https://www.lincoprecision.com/precision-farming/precisioplanting/wavevision-sensors/> (08/10/2024).
- Liming Z, Xiaochao Z and Yanwei Y (2010). Design of capacitance seed rate sensor of wheat planter. *Transactions of the Chinese Society of Agricultural Engineering*, 10: 99-103.
- Liu W, Hu J, Zhao X, Pan H, Lakhia IA, Wang W and Zhao J (2019). Development and experimental analysis of a seeding quantity sensor for the precision seeding of small seeds. *Sensors (Basel)*, 19(23): 5191. <https://doi.org/10.3390/s19235191>
- Marko K, Dusan R, Dragi R, Lazar S, Nebojsa D, Vladimir C and Natasa L (2018). Corn seeding process fault cause analysis based on a theoretical and experimental approach. *Computers and Electronics in Agriculture*, 151: 207-218. <https://doi.org/10.1016/j.measurement.2021.109959>
- Rocha I, Ma Y, Souza-Alonso P, Vosátka M, Freitas H and Oliveira RS (2019). Seed coating: A tool for delivering beneficial microbes to agricultural crops. *Frontiers in Plant Science*, 10: 1357. <https://doi.org/10.3389/fpls.2019.01357>
- Singh RC, Singh G and Saraswat DC (2005). Optimizing of design and operational parameters of pneumatic seed metering device for planting cottonseeds. *Biosystem Engineering*, 92(4): 429-438. <https://doi.org/10.1016/j.biosystemseng.2005.07.002>
- Yazgı A, Demir V and Değirmencioğlu A (2020). Comparison of computational fluid dynamics based simulations and visualized seed trajectories in different seed tubes. *Turkish Journal of Agriculture and Forestry*, 44(6): 599-611. <https://doi.org/10.3906/tar-1910-15>
- Youchun D, Junqiang Y, Kai Z, Lili Z, Yawen Z and Qingxi L (2017). Design and experiment on seed flow sensing device for rapeseed precision metering device. *Transactions of the Chinese Society of Agricultural Engineering*, 9: 37-44.
- Youchun D, Lili Z, Junqiang Y and Kai Z (2018). Sensing device improvement and communication design on sowing monitoring system of precision planter for rapeseed. *Transactions of the Chinese Society of Agricultural Engineering*, 14: 19-26.
- Yujing S, Honglei J, Deliang R, Jingjing Y and Yang L (2013). Experimental study of capacitance sensors to test seed-flow. *Applied Mechanics and Materials*, 347: 167-170. <https://doi.org/10.4028/www.scientific.net/AMM.347-350.167>



Turkish Journal of
Agricultural
Engineering Research
(Turk J Agr Eng Res)
e-ISSN: 2717-8420



Modeling of Thresher Capacity and Fuel Consumption Equations Using Dimensional's Analysis for Threshing Operation

Tasfaye Aseffa ABEYE^{a*}

^aDepartment of Agricultural Engineering Research, Melkassa Agricultural Research Centre, Ethiopian Institute
Agricultural Research, Addis Ababa, ETHIOPIA

ARTICLE INFO: Research Article

Corresponding Author: Tasfaye Aseffa ABEYE, E-mail: tesfayeaseffa20@gmail.com

Received: 13 September 2024 / **Accepted:** 5 December 2024 / **Published:** 31 December 2024

Cite this article: Abeye, T.A. (2024). Modeling of Thresher Capacity and Fuel Consumption Equations Using Dimensional's Analysis for Threshing Operation. Turkish Journal of Agricultural Engineering Research, 5(2), 271-283. <https://doi.org/10.46592/turkager.1549453>

ABSTRACT

Threshing capacity and fuel consumption in postharvest operations are the main factors in selecting a thresher. The problem was user was not easily understood the relation thresher capacity and fuel consumption. To easily understand the relationship, a model is needed for the independent and dependent factors. The model was developed for threshing capacity, and fuel consumption depends on parameter factors. The purpose of modeling is to select threshers, estimate thresher capacity, and identify direct and indirect factors. There are nine independent variables. These are: cylinder diameter (d), cylinder length (L), concave clearance (Cc), feed rate (Fr), drum speed (S), moisture content (Mc), crop straw ratio (R), spike/peg length (PL), and crop bulk density (ρ) and The Buckingham, pi theorem is used in basic dimensional. The threshing capacity and fuel consumption were developed. The equation was TC is equal to $d^2 v \rho (L * d^{-1}, L * d^{-1}, Fr * d^{-2} V \rho) MC * SR$ and for fuel consumption of stationary thresher was Fc is equal to $d^3 v (L * d^{-1}, L * d^{-1}, Fr * d^{-2} V \rho) MC * SR$ developed. The performance investigation was conducted at three levels of drum speed (1000, 1100, and 1200 rpm) and feed rate (600, 700, and 800 kg h⁻¹) with split-plot experimental design. The maximum threshing capacity is 234.22 kg h⁻¹ at feed rate 800 kg h⁻¹ and a drum speed of 1200 rpm and it consume 2.245 L h⁻¹. The lowest threshing capacity is 223.20 kg h⁻¹ at drum speed is 1000 rpm and the feed rate is 600 kg h⁻¹ with fuel consumption is 2.00 L h⁻¹. The equation developed contributed to research in that it helped researchers and designers easily understand the relation of thresher performance determinants. Consequently, using a model created by dimensional analysis is the most effective method for comprehending thresher-related parameters as result, as the speed of the drum increases, the thresher capacity increases as fuel consumption increases. Therefore, the developed model is a simple and easy way to choose and design the thresher.

Keywords: Thresher capacity, Fuel consumption, Dimensional analysis, Buckingham Pi theorem



INTRODUCTION

Agriculture mechanization can determine the development of a country. Especially, the economy is based on agriculture. It has had significant changes in the growth of domestic products. The effect of mechanization on agricultural implementation leads to sustainable development when using agricultural machinery. According to the suggestions of numerous nations around the world, agricultural mechanization has had a significant effect on the world economy ([Kaumbutho and Takeshima, 2020](#)). The machinery supported crop production agriculture is result economic growth ([Indexed et al., 2017](#)).

The profitability of farming as well as the availability of the farm machines have significantly impacted on the level of mechanization ([Kaumbutho and Takeshima, 2020](#)). The current status of mechanized farming and machinery adoption in developing countries is the main the mains issue especially in Ethiopia. The farming system makes easy way for production and increases the productivity by timelines operation and drudgery reduction. Using machinery makes to easy operate, saves energy, time, and reduces loss is preferred ([Tsegaye et al., 2020](#)). The machinery applications used during the crop production for plowing, planting, harvesting, threshing, storing, and transportation under pre-harvest and post-harvest operations ([Deribe et al., 2022](#)). The main objectives of mechanization technologies for pre-harvest operation and post-harvest production are to increase working quality, efficiently use energy, decrease post-harvest loss, save time, minimize drudgery, improve output quality, and conserve energy. In the mechanical post-harvest operation, multi-crop threshers are used to thresh wheat, barley, and sorghum on a small, medium, and large scale. The threshing operation is performed by a combination of impacting and rubbing to detach the kernels from the ears ([Kumar, 2017](#)).

The threshing performance determinants are design factor, crop factor and operational are the main parameter. Both axial threshing and tangential type threshing technologies are widely used in grain threshing systems ([Deribe et al., 2021](#)). The Stationery thresher for developing country is used to reduce the amount of energy required for crop threshing and minimize drudgery during threshing operations ([Shekhar, 2020](#)). Threshing performance and thresher cost are determined during threshing based on threshing capacity and fuel usage.

Therefore, the primary outcome for design operation is fuel consumption in order to maximize the end-threshing capacity, optimize process design, and estimate cost ([Abich, 2018](#)). Threshing capacity and fuel consumption are the key factors that influence thresher performance and selection. Three factors were taken into consideration when designing the thresher: the crop factor, the design factor, and the human aspect, or feeding factor ([Abich, 2018](#)). The total grain losses, the stationary thresher's threshing and cleaning efficiency, and their combined effects should all be taken into account during the design of the thresher ([Shreen et al., 2016](#)).

According to [Belay and Fetene \(2021\)](#); [Afolabi et al. \(2017\)](#), The thresher performance evaluation was significantly changed by crop moisture content. Additionally, the performance of grain damage is influenced by the pattern of contact between grain crops and threshing components. The grain damage decreased along

with high crop moisture content, while threshing performance decreased. Power usage increased along with the amount of energy used to thresh the crop at higher moisture content. Increasing the drum's diameter, number of beaters, peg beaters, and length all increase the threshing capacity ([Afolabi et al., 2017](#)). The operating time and the amount of grain output for thresher capacity of influenced by its shape and size drum. Threshing efficiency is affected by the number of rows of artificial teeth fixed to the drum, the type of crop, the feeding speed of the threshing chamber, the angle of the thresher concave, and the speed of the drum ([Indexed et al., 2017](#)). The thresher performance depends on the cylinder diameter, concave clearance, concave length, and threshing speed, which are direct relationships. The feed rate influences the seed passing through the concave clearance ([Thet et al., 2019](#)). Also the feed rate had a direct relationship with threshing capacity ([Awgichew, 2019](#)). According to [Ahorbo \(2016\)](#), suggestion the fed rate impact of thresher operation on in terms of energy consumption and threshing capacity which have direct proportional.

According to [Journal and Dula \(2019\)](#), As cylinder speed increases, threshing capacity increases. Increased impact energy from faster speeds increases thresher capacity and increases fuel consumption. Additionally, it relates to the crop variety, human factors, and design factors that affect the thresher performance ([Al-shamiry et al., 2020](#)).

During thresher design, understanding the relation between the thresher factor and design, the testing selection model can be used in a simple way. That models will be needed for thresher selections and designs. The dimensional application is the most effective for modeling and estimation of threshers' parameters identification technique. The goals are to identifications the most effective parameters to minimize the total number of variables and non-dimensional groups of variables. When Dimensional's apply the dependent and independent factor to carefully identify and filtering the important parameters as it is advisable recommended methods. the parameter variables in the groups were frequently organized so that each group had physical relevance ([Garcia-Suarez et al., 2019](#)). The basic dimensional and theorem of Buckingham's were used to generate equations based on the parameter factor. They are different suggestions for studded throughput per unit energy usage and thresher performance. Since the principles of construction and thresher operation are not well defined ([Abich, 2018](#)). The three most significant aspects that impact the thresher's performance are crop variety, feed rate, and cylinder speed ([Ajmal et al., 2017](#)).

The main problem during thresher design was identification parameter relationships. Some are direct relationships, and some are indirect relationships. During the performance evaluation, parameters were also considered, but the relationship was not clearly defined. Due to that, there is different confusion for the design, selection, and evaluation of the thresher. Understand the fundamental design elements that one should anticipate from agricultural engineers or designers in order to design, test, and select the thresher. In order to comprehend thresher performance selection and design equipment parameters, it is necessary to study the thresher factor for determining thresher capacity and optimization by fuel consumption.

So, it is necessary to develop simple model calculations for researchers, designers, and others for easy understanding. To be used to construct and optimize thresher design for threshing capacity and fuel consumption during operation. The aim of this study was the determination of the equation or model for thresher threshing capacity and performance evaluation for simple understanding and estimation. Then, finally, a performance evaluation based on a parameter factor for comparing the practical result with the developed equation. The main purpose was model development for the thresher capacity and fuel consumption equations using dimensional data. Finally, the purpose is to evaluate thresher performance to compare with the developed model.

MATERIALS and METHODS

Description of the studies area

The tests were conducted in the Oromia region, East of Shewa, Awash Melkasa at Wake Tiyo Kebeles. During the performance tests the thresher was obtained from the Melkassa Agricultural Research Center's and Department of agricultural Engineering research.

Techniques of Using Dimensional Analysis to Develop Models for Thresher Capacity and Fuel Consumption Equation

A fuel consumption equation was developed using the theorem of Buckingham based on the basic dimensions of parameters. The thresher capacity based on the thresher parameter factor. In dimension analysis, there are two method of techniques to solve the variables approach to generate modeling ([Program and Plantation, 2022](#)): ([Singla *et al.*, 2022](#)). The Rayleigh and Buckingham pi theorems, which incorporate combinations of mass, length, and time or force, are examples of these methods. Rayleigh's approach is not often used because of its complexity when handling large numbers of variables. In addition, our study makes use of the Buckingham pi theorem. Using the fundamental dimensions are: length, Time and mass applied for the theorem of the Buckingham pi for gradually used to generate the final associated equation.

The step used was one. Enumerate the independent parameters factor or thresher capacity and fuel consumption. There are nine overall quantities (n) for both fuel consumption and thresher capacity. The parameters are cylinder radius (d), length of the cylinder (L), concave clearance (Cc), feed rate (Fr), drum speed (S), moisture content (Mc), crop straw ratio (R), spike/peg length PL, and crop bulk density (ρ). The thresher capacity (TC) and fuel consumption (Fc) are the dependent factors ([Pandey and Stevens, 2016](#)). Next were listed the principal dimensions of all nine factors.

Table 1 represents the dependent and independent factors of thresher performance evaluation, and the basic units listed below for nine based on impact and relation identification are listed below. To model, consider the three basic fundamentals: length with its units, mass with its units, and time with its units, as shown below. Analyzed and noted in similar tendencies are ([Nkakini *et al.*, 2019](#); [Program and Plantation, 2022](#)).

Table 1. The parameter of thresher for performance equation determination.

Variables	Symbols'	Dimension symbols	Units
In depend parameters			
Bulk density	D	$L^{-3} M$	$kg\ m^{-3}$
Drum radius	R	L	m
Drum length	Dl	L	
Concave clearance	Cc	L	m
Peg length	L	L	m
Feed rate	Fr	$M\ T^{-1}$	$kg\ s^{-1}$
Moisture content	Mc	-	
Straw ratio	SR	-	-
Drum speed	V	$L\ T^{-1}$	$m^3\ s^{-1}$
Dependent parameters			
Fuel	F	$L\ T^{-3}$	$m^3\ s^{-1}$
Thresher capacity	TC	$M\ T^{-1}$	$kg\ s^{-1}$

Then, using the determinant and constants parameters, the next procedure was determining the number of primary dimensions (M) based on the reduction. The expected number of IIs, by calculating k, which is the number independent factor minus the number determinant factor, which is nine minus three, equal to six. Where N represents the total amount of performance evaluation parameter factor and M, represents the basic number of fundamental dimensions: time (T), mass (M), and Length (L), then there are six IIs needed to be modelling the equation for thresher capacity and fuel consumption.

The fourth step was to select the repeating parameters (j), and several guidelines have been proposed to select the repeated variables ([Jarolmasjed et al., 2013](#); [Singla et al., 2022](#)). Choose the parameters that repeat (j). A number of recommendations have been made to choose the recurring variables. To ensure that only one pi carries the dimensional value, whenever possible, choose dimensional constants over dimensional variables. Select common parameters as they might show up in all of the IIs. Whenever feasible, choose simple variables over complex ones. Drum radius (R), drum speeds (V), and densities (D) are chosen as repeated parameters based on the aforementioned eight guidelines, and the same pattern is shown in [Jarolmasjed et al. \(2013\)](#); [Program and Plantation \(2022\)](#).

The final steps was construct the "k" IIs and adjust as needed. The following manipulation and construction are applied to the six identified pi terms:

$$TC = f(R, L, Cc, Fr, Mc, SR, V, D) \quad (1)$$

$$F = f(R, L, Cc, Fr, Mc, SR, V, D) \quad (2)$$

$$\pi_1 = (\pi_2, \pi_3, \pi_4, \pi_5, \pi_6) \quad (3)$$

The determination of π_1 is the function of thresher capacity and fuel consumption, drum radius (R), drum speed (v), and crop densities (D). Based on the theorem, it was developed by considering dimensional analysis. $\pi_1 = (TC, r, V, D)$ and $\pi_1 = (F, r, V, D)$ for both threshing capacity and fuel consumption. π_2 is the function of drum radius (R), drum length (L), and bulk density (D). In function form, $\pi_2 = (L, R, V, D)$. For equation development, π_3 is the function of concave clearance (Cc), drum radius (R), drum speed (V), and crop densities (D). The function was $\pi_3 = (Cc, R, V, D)$. For π_4 equation development, it is the function of drum radius (R), feed rate (Fr), and bulk

density (D), where $\pi_4 = (Fr, R, V, D)$. Then for the π_5 equation, it is the function of drum radius (R), moisture content (Mc), speed (V), and bulk density (D), and the function form was $\pi_5 = (Mc, R, V, D)$. Finally, π_6 is the function of drum radius (R), straw ratio (SR), drum speed (V), and crop density (D), and the equation was $\pi_6 = (SR, R, V, D)$ was the Pi function threshing capacity and fuel consumption.

For manipulation of π_1 and the formulation π_1 , is equal to $TC \cdot R^a \cdot V^b \cdot D^c$ & $M^0 L^0 T^0 = MT^{-1} \cdot (L)^a \cdot (LT^{-1})^b \cdot (ML^{-3})^c$ and when we apply basic dimensions for M, = 0, c = -1 and For L, $0=a+b-3c$ solve for T and insert b value in this equation gives; a = -2, and For T, = 0 = -1·b; b=-1, finally, $\pi_1 = TC d^{-2} V^{-1} \rho^{-1}$.

The manipulation of π_1 for threshing capacity and the formulation π_1 are equal to $TC^* V^a \cdot R^b \cdot D^c$ and $L^0 T^0 M^0$. Then, by considering dimensions, application equals $MT^{-1} (LT^{-1})^a (L)^b (ML^{-3})^c$ and then $L^0 T^0 M^0 = MT^{-1} (LT^{-1})^a (L)^b (ML^{-3})^c$ by using the theorem of Buckingham for determination relation as shown below. From the above relation and solving for the values when L = 0, then the exponent relation $a + b = 3c$. The value of T = 0, then the value of an exponent based on the theorem is a = -1. Finally, when the value of M = 0, then C = -1, then y substitution, the value of b = -2. The value of C is -1, then when T is a zero exponent, the value of b is -1, and when we substitute the values in equation π_1 are equal to $TC (V)^{-1} \cdot (R)^{-2} \cdot (D)^{-1}$

$$\pi_1 = \frac{TC}{R^2 V D} \quad \text{dimensionless (for threshing capacity)} \quad (4)$$

For determination of thresher performance with fuel utilization of π_1 modeling formulation shown below and the formulation $\pi_1 = F \cdot (V^a \cdot R^b \cdot D^c)$ and $L^0 M^0 T^0 = L^3 T^{-1} (LT^{-1})^a \cdot (L)^b \cdot (ML^{-3})^c$ based on theorem application and the developed equation when L = 0 then $3 + a + b - c$ and for solved m, is the values c = 0 for T, is =0 For M, = 0, a = -1 and solve for T is zero and insert b value in this equation gives; b = -2. When we substitute

$$\pi_1 = FR^{-2} V^{-1} = \frac{F}{R^2 V} \quad \text{dimensionless (for fuel consumption)} \quad (5)$$

For determination of thresher performance with fuel utilization of π_2 modeling formulation shown below and the formulation $\pi_{12} = L \cdot (R^a \cdot V^b \cdot D^c)$ and $L^0 M^0 T^0 = L (L)^a \cdot (LT^{-1})^b \cdot (L^{-3} M)^c$ based on theorem application and the developed equation when is, M zero, C is zero. Then L, = 0 the apply theorem $-1 = a + b - 3c$. Then when solving for T, side zero the value of result b is zero. Then L is zero, $0=1+a+b-3c$ solve for T and insert b value in this equation gives; a= -1 then substitute in to below equation.

$$\pi_2 = LR^{-1} V^0 D^0, \pi_2 = \frac{L}{R} \quad \text{dimensionless} \quad (6)$$

The equation π_3 and its value of $\pi_3 = Cc \cdot R^a \cdot V^b \cdot D^c$ were used to develop the equation π_2 of $\pi_2 = L \cdot R^a \cdot V^b \cdot D^c$, and $T^0 L^0 M^0 = L (L)^a \cdot (LT^{-1})^b \cdot (L^{-3} M)^c$ then the value of M, zero c is also zero. Then L, is $0=1+a+b-3c$, solve for T is zero b is zero and insert b, which is zero and equals then the value of a is -1. Then equation was shown below.

$$\pi_3 = LR^{-1} V^0 D^0 \quad \pi_3 = \frac{L}{R} \quad \text{dimensionless.} \quad (7)$$

To represent the equation of π_4 s, which is equivalent to = Fr. R^a . V^b . D^c & $T^0 M^0 L^0$ = $MT^{-1} (L)^a (T^{-1}L)^b (L^{-3}M)^c$ and use simple dimensions. For M, $0=1+c$; $c=-1$, then for L, $0=+a+b+3$ Solving for T and inserting b into this equation yields: $a=2$. For T: $0 = -b$, $b = -1$, and lastly, $\pi_4 = Fr R^{-2} V^{-1} D^{-1}$

$$\pi_4 = \frac{Fr}{R^2 V D} \text{ dimensionless} \quad (8)$$

Manipulating π_5 and equal Mc. R^a . V^b . D^c . Then use dimensional analysis. $M^0 L^0 T^0 = (L)^a (L T^{-1})^b (L^{-3} M)^c$ Apply basic dimensions. For M, $0 = +c$ and $c = 0$. For L, $0 = 1 + a + b - 3c$ solve for T and put the b value in this equation provides; $a=0$ and for T, $0 = -b$; $b=0$ and finally, $\pi_5 = Mc V^0 \rho^0 d^0 = Mc$; dimensionless.

$$\text{Modeling for } \pi_5 \text{ and } \pi_6 = SR. R^a. V^b. D^c \quad (9)$$

$T^0 M^0 L^0 = (L)^a (L T^{-1})^b (L^{-3} M)^c$ then apply the basic dimensions. For M, 0 equals +c and c equal 0. For L, $0 = 1 + a + b - 3c$, solve for T and enter b value in this equation provides; $a=0$ and for T, $0 = -b$; $b=0$ and lastly, $\pi_5 = SR d^0 \rho^0 V^0 = SR$, dimensionless. The necessary π groups are successfully identified, verified, and dimensionless.

Step 6: Check your math and write the final functional connection. We can represent fuel consumption as follows as it depends on other factors, as shown in equations 1 and 2. $\pi_1 = (\pi_2, \pi_3, \pi_4, \pi_5, \pi_6)$ was the formula that was created for the threshing capacity and fuel consumption of the thresher. $\frac{TC}{R^2 V D} = (\frac{L}{R}, \frac{L}{R}, \frac{Fr}{R^2 V D}) MC^* SR$ and this is the developed thresher capacity, which is directly proportional to the drum's radius, speed, length, feed rate, straw ratio and moisture content. The final equation developed for threshing capacity is shown below in Equation (10).

$$TC = R^2 v D (\frac{L}{R}, \frac{L}{R}, \frac{Fr}{R^2 V D}) MC^* SR \quad (10)$$

For fuel conception, $\frac{F}{R^2 v} = (\frac{L}{d}, \frac{L}{d}, \frac{Fr}{d^2 v \rho}) MC^* SR$. The model created fuel consumption model for stationary threshers were $F = R^2 v (\frac{L}{R}, \frac{L}{R}, \frac{Fr}{R^2 V D}) MC^* SR$. The testing was conducted to check the relation of model for threshing capacity and fuel consumption of the multi-crop thresher's performance was tested and evaluated. For fuel conception equation the developed equation shown below based on dimension analysis in Equation (11).

$$Fc = d^2 v (\frac{L}{d}, \frac{L}{d}, \frac{Fr}{d^2 v \rho}) MC^* SR \quad (11)$$

When the performance was conducted at Wake Tiyo Awash Melkasa, East Oromia zone, the agronomic data were recorded, such as crop length and speck length, during the thresher testing. The performance investigation was conducted at three levels of drum speed (1000, 1100, and 1200 rpm) and feed rate (600, 700, and 800 kg h⁻¹). Testing parameters and data collected were drum speed, feed rate, concave clearance, fuel consumption, and biomass weight before threshing, and moisture content. Asplit-plot experimental design was used to investigate thresher capacity, with drum speed as the primary factor and feed rate as a sub factor.

Statistical data analysis

Data were collected based on agronomics' for testing and engineering parameters are recorded. Statistics 8 was used to do the analysis. The thresher's data's studies were concentrated on thresher performance and fuel usage, and analysis of variance (ANOVA) was performed to compare treatments. To distinguish statistically significant differences between treatment means at the 5 percent significance level, the least significant difference (LSD) was used (5 percent). To establish the association's significance, an analysis of variance and an F-tests were utilized.

RESULTS AND DISCUSSION

The thresher's performance was tested conducted based on different parameters. After the result was analyzed, the effect of the thresher parameter on thresher capacity and fuel consumption was evaluated. The impact of threshing speed, cleaning efficiency, efficiency, capacity, and percentage of loss achieved. A thresher tested at 12 percent moisture on the Tef Komcho variety. Tef is harvested when the seeds have dried and reached physiological maturity. Throughout testing, information on crop and equipment performance was successively recorded. The data on the crop was recorded both before and after threshing, including plant height, speck height, chaff length, optimal tef moisture content, variety of tef grain, and weight of biomass. To identify the ideal feed rate and speed of thresher capacity assessment, thresher data such as threshing capacity (kg), threshing efficiency, and time feed rate (kg) were closely recorded.

Table 2. Engineering properties of harvested tef (*Boset variety*).

Variable	Mean	Sensitivity to shattering
Plant length (cm)	104±69	Medium
Speck length (cm)	32±94	Medium
Chaff length (cm)	12±8	Medium
Chaff output (kg)	33.12	Medium

During the teff thresher's evaluation, we chose a split plot design with biomass as the treatment during performance evaluation where fed rate of thresher was 600, 700, and 800 kg per hour and drum speeds of 1000 rpm, 1100 rpm and 1200 rpm. These thresher speed trends were used for testing tef on a multi-crop thresher ([Kidanemariam, 2020](#)). All three replications were conducted 27 times. The threshing capacity was significantly impacted by both the feed rate and drum speed ($p < 0.05$) (Table 3). Threshing capacity is also significantly impacted by the interaction between feed rate and drum speed. During performance evaluation, the data collected was based on the parameters and evaluation results. The final result was compared with a developed equation based on dimensional analysis. It was also for food consumption that the evaluation was conducted. Such practical testing strengthened the validity of the developed equations.



Figure 1. Field performance test of tef thresher during testing at Awash Melkassa wake Tiyo.

Table 3. Anova of testing multi-crop thresher result on Tef Komcho variety.

	df	df Sum sq	means sq	fvalues	Pr, (>F)
Feed rate (kg.h ⁻¹)	2	2627.0	313.48	6.4085	0.007913 **
Drum speed revolution per minute	2	23465.8	1732.91	35.4256	5.748e-07 ***
Feed rates (kg.h ⁻¹) x Drum speed (rpm)	4	489.6	22.41	0.4582	0.0765358 **

With a fed rates of the thresher at 800 kg h⁻¹ and a drum speed of 1200 rpm, the maximum threshing capacity is 234.22 kg h⁻¹. The lowest threshing capacity is 223.20 kg h⁻¹ when the drum speed is 1000 rpm and the feed rate is 600 kg h⁻¹ (Table 4). Drum speed and feed rate have a considerable impact on the outcome. These trends, like the feed rate, increase the thresher capacity ([Abagisa et al., 2015](#)).

Table 4. Threshing capacity of multi-crop thresher.

Drum speed (RPM)	Threshing capacity	Fuel consumption
1000	234.22±23 ^a	2.1494 ±3 ^a
1100	232.37±21 ^a	1984.8 ± ^{ab}
1200	223.20±2 ^b	1992.21± ^{ab}

From the Figure 1, the effectiveness of the thresher was assessed at various feed rates and drum speeds. The threshing capacity increases in tandem with the feed. The thresher's performance or capacity increases as the drum speed increases. The threshing capacity was significantly impacted by feds rates and drum spends, as indicated from the developed mathematical model equations. It is accurate based on the testing results. Once more, the model equation shows that fuel usage is directly correlated with threshing capacity.

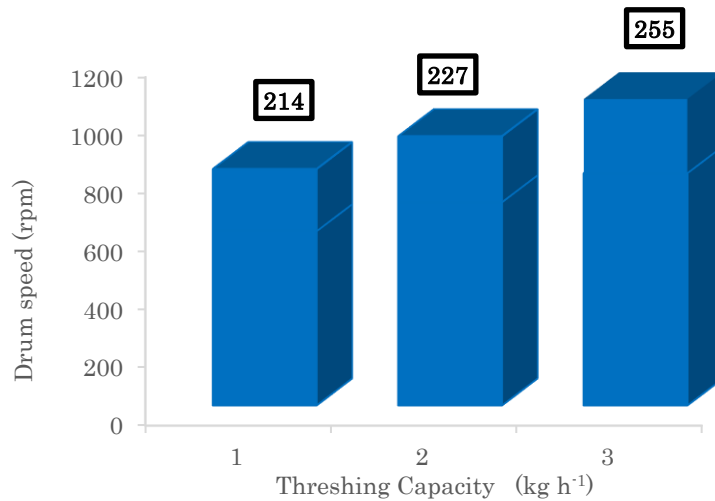


Figure 2. Graph of thresher capacity at different speeds.

As feed rates rise, so does threshing performance increases and fuel consumption also increases. These direct relationships in the model also show direct relationships when practically tested. Figure 2 represents the relationship between drum speed, thresher capacity, and fuel consumption. These three factors had a direct relationship during thresher performance testing. As the model is developed, the real testing is also directly proportional. As drum speed increases, the thresher capacity increases, and fuel consumption increases. These are the results of the relationship with pre evaluated by ([Chaturvedi et al., 2019](#)).

Figure 3 represents the relationship between drum speed, thresher capacity, and fuel consumption. These three factors had a direct relationship during thresher performance testing. As the model is developed, the real testing is also directly proportional. As drum speed increases, the thresher capacity increases, and fuel consumption increases.

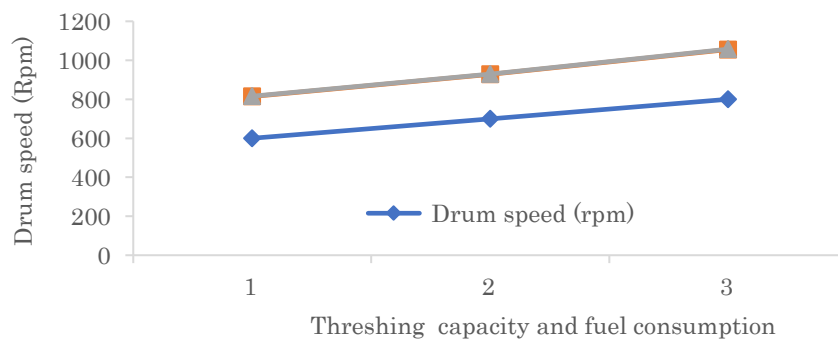


Figure 3. Effect of feed on fuel consumption and threshing capacity.

Table 5. *Threshing capacity of thresher at different drum speeds and feed rates.*

Fed rates (k h ⁻¹)	Drum speeds (rpm)	Capacity (kg h ⁻¹)	Fuel consumption (L h ⁻¹)
800	1200	250.43 ±21 ^a	2.245±12 ^a
700	1200	244.60 ±.4 ^{ab}	2.041±.3 ^{ab}
700	1100	235.02 ±3 ^{bc}	2.021±.8 ^{ab}
800	1100	233.96 ±42 ^{bc}	2.015±13 ^{ab}
600	1200	233.27 ±31 ^{bc}	2.012±.1 ^{ab}
600	1100	226.50 ±5 ^{cd}	2.007±.3 ^b
800	1000	218.26 ±3 ^{de}	2.00±17 ^b
700	1000	217.53 ±42 ^{de}	2.003±.8 ^b
600	1000	209.83 ±32 ^e	2.0023±.4 ^b

From Table 5, at 800 kg h⁻¹ and 1200 rpm, the threshing capacity is 250 kg h⁻¹ and fuel consumption are 2.245 L h⁻¹. At 600 kg hr⁻¹ and 1000 rpm. The threshing capacity is 2.09 kg h⁻¹ and fuel consumption is 2.00 L h⁻¹ is so it had a direct relationship between feed rate, threshing capacity, and fuel consumption. Tef threshing was chosen after assessing the testing performance evaluation metrics. As cylinder speed increased as thresher capacity increased. The drum speeds increase with the space between the cylinder and concave clearance, and the thresher capacity decreases.

CONCLUSION

The study used dimensional analysis and the Buckingham pi theorem for threshers to construct a model for the thresher capacity and the fuel consumption equation. Good quality of thresher should be durable and easily constructed from available materials, should have good threshing capacity, good efficiency, ease to use or handle, efficiently used power, and best safety operation. The thresher capacity and fuel consumption equation take into account independent variables: cylinder radius (R), length of the cylinder (L), concave clearance (Cc), feed rate (Fr), drum speed (S), moisture content (Mc), crop straw ratio (R), spike/peg length PL, and crop bulk density (D). The equation and threshing capacity was (TC) is equal to $R^2v_p \left(\frac{L}{R}, \frac{L}{R}, \frac{Fr}{R^2VD} \right) MC * SR$ and for fuel conception (F) is equal to $\frac{F}{R^2v} = \left(\frac{L}{R}, \frac{L}{R}, \frac{Fr}{R^2VD} \right) MC * SR$ here is the model created for fuel consumption of stationary threshing performance process. $\frac{F}{R^2v} = \left(\frac{L}{R}, \frac{L}{R}, \frac{Fr}{R^2VD} \right) MC * SR$ this is the developed fuel consumption model for stationary thresher operation, $F_c = d^2v \left(\frac{L}{d}, \frac{L}{d}, \frac{Fr}{d^2Vp} \right) MC * SR$. The testing was conducted to check the relationship between the model's threshing capacity and fuel consumption. The multi-crop thresher's performance was tested and evaluated. As the dimensional analysis shows, the practical result has improved. So, to design a machine, understanding the analysis is the best way, with any complexity, to identify the relationship. The testing was conducted to check the relationship between the model's threshing capacity and fuel consumption. The multi-crop

thresher's performance was tested and evaluated. As the dimensional analysis shows, the practical result has improved. So, to design a machine, understanding the analysis is the best way, with any complexity, to identify the relationship.

DECLARATION OF COMPETING INTEREST

The author declares that they have no conflict of interest.

ACKNOWLEDGEMENT

The Ethiopian Institute of Agricultural Research (EIAR) is also greatly appreciated for its sponsorship of the study, provision of research funds and Melkassa Agricultural Engineering research staff and technicians provided support for the work.

CREDIT AUTHORSHIP CONTRIBUTION STATEMENT

The author declared that the following contribution is correct.

Tasfaye Aseffa ABEYE: Investigation, methodology, conceptualization, formal analysis, data curation, validation, writing-original draft, review, and editing, visualization etc.

ETHICS COMMITTEE DECISION

This article does not require any Ethical Committee Decision.

REFERENCES

- Abagisa H, Tesfaye T and Befikadu D (2015). Modification and testing of replaceable drum multi-crop thresher. *International Journal of Sciences: Basic and Applied Research (IJSBAR)*, 23(1): 242-255. <http://gssrr.org/index.php?journal=journalOfBasicAndApplied>
- Abich SO (2018). *Optimization of threshing performance of a spike tooth sorghum threshing unit*. Egerton University, Master Thesis, <http://41.89.96.81:8080/xmlui/handle/123456789/1707>
- Ahorbo GK (2016). Design of A Throw-In Axial Flow Rice Thresher Fitted with Peg and Screw Threshing Mechanism. *International Journal of Scientific Technology Research*, 5(7): 171-177.
- Ajmal UB, Khan MU, Faheem M, Tayyab M, Majeed M, Sarwar A, Khan MR, Shariati MA, Shafeeqe M, Mohamed AM (2017). Modiction and performance evaluation of a wheat thresher. *RJOAS*, 5(65), 261-270. <http://dx.doi.org/10.18551/rjoas.2017-05.34>
- Al-shamiry FMS, Mohammed N and Yahya A (2020). *The performance evaluating of thresher machine attached to the tractor*, 3: 7-16. <https://doi.org/10.53555/ar.v6i3.3533>
- Awgichew A (2019). Aerodynamic properties of tef for separation from chaff. *Civil and Environmental Research*, 11(3): 39-43. <https://doi.org/10.7176/cer/11-3-05>
- Belay D and Fetene M (2021). The Effect of moisture content on the performance of melkassa multicrop thresher in some cereal crops. *Bioprocess Engineering*, 5(1): 1. <http://dx.doi.org/10.11648/j.be.20210501.11>
- Chaturvedi S, Rathore F and Pandey S (2019). Performance evaluation of developed thresher cylinder on millet crop. *International Journal of Current Microbiology and Applied Science, Special Issue*, 8: 102-106.

- Deribe Y, Getnet B, Kang TG and Tesfaye A (2022). Benchmarking the Status of Agricultural Mechanization in Ethiopia. In *SSRN Electronic Journal Research Report* No: 133. <https://doi.org/10.2139/ssrn.3968527>
- Garcia-Suarez J, Kusanovic D and Asimaki D (2019). Dimensional analysis: Overview and applications to problems of soil-structure interaction. <http://dx.doi.org/10.31224/osf.io/m3ycp>
- Kidanemariam G (2020). Tef (*Eragrostis tef* (Zucc) Trotter) on the basis of its engineering (Physical and Mechanical) Properties. June 2020. Addis Ababa University <http://etd.aau.edu.et/handle/12345678/23475>
- Indexed S, Warghane RS, Bhagat VK and Nawale SB (2017). *Review on design and optimization of antennas using machine learning algorithms and techniques*. International Journal of RF and Microwave Computer-Aided Engineering, 8(11): 1020-1028. <http://dx.doi.org/10.1002/mmce.22356>
- Jarolmasjed S, Gundoshmian TM and Ghazvini MA (2013). Mathematical modeling of combine harvester header loss using dimensional analysis. *Efitu Wcca CIGR 2013 Conference*, June 2013, 24-27.
- Journal I and Dula MW (2019). Review on development and performance evaluation of maize sheller. <https://doi.org/10.17577/IJERTV8IS050329>
- Kaumbutho P and Takeshima H (2020). *Mechanization of Agricultural Production in Kenya: Current State and Future Outlook*. 231-256.
- Kumar A (2017). Performance Evaluation of harvesting and threshing methods for wheat crop. *International Journal of Pure & Applied Bioscience*, 5(2): 604-611. <http://dx.doi.org/10.18782/2320-7051.2497>
- Nkakini SO, Ekemube RA and Igoni AH (2019). Modeling fuel consumption rate for harrowing operations in loamy sand soil. *European Journal of Agriculture and Forestry Research*, 7(2): 1-12.
- Pandey A and Stevens RM (2016). Performance evaluation of high capacity multi crop thresher on 'gram' crop. *International Journal of Agricultural Engineering*, 9(1): 94-101.
- Program JI and Plantation M (2022). The use of dimensional analysis for modeling tractor fuel consumption for harrowing operation. *Nigerian Journal of Technology (NIJOTECH)*, 41(5): 913-919.
- Shekhar KS (2020). Design of the components of a stationary power thresher for paddy crop. http://courseware.cutm.ac.in/wp-content/uploads/2020/06/PPT_Design-of-threshher.pdf
- Shreen FA, Badr SE and Morad MM (2016). Maximizing wheat crop yield using a mobile thresher at small holdings. *Agricultural Engineering International: CIGR Journal*, 18(3): 63-73.
- Singla S, Modibbo UM, Mijinyawa M, Malik S, Verma S and Khurana P (2022). Mathematical Model for Analysing Availability of Threshing Combine Machine Under Reduced Capacity. *Yugoslav Journal of Operations Research*, 32(4): 425-437. <https://doi.org/10.2298/YJOR220315019S>
- Thet WW, Kyaw S and Sein MM (2019). Design and stress analysis of threshing cylinder drum for a combine paddy harvester (25HP). *IRE Journals*, 3(4): 185-190.
- Tsegaye W, Chala F, Dandena K, Taye B and Amare S (2020). *Small-scale mechanization options for rural communities in the Ethiopian highlands*. Brief 48, December 2020.



Turkish Journal of
Agricultural
Engineering Research
(Turk J Agr Eng Res)
e-ISSN: 2717-8420



Development of a greenhouse steam-powered, self-propelled soil sterilization device

Ahmed Shawky EL-SAYED^a, Mohamed Mansour Shalaby REFAAY^b

^aDepartment of Agricultural Bioengineering Systems, Agricultural Engineering Research Institute (AENRI),
Agricultural Research Center (ARC), Dokki, Giza, EGYPT

^bDepartment of Agricultural Operations Mechanization Systems, Agricultural Engineering Research Institute
(AEnRI), Agricultural Research Center (ARC), Dokki, Giza, EGYPT

ARTICLE INFO: Research Article

Corresponding Author: Ahmed Shawky EL-SAYED, E-mail: ahmedshawkyelsayed85@gmail.com

Received: 20 October 2024 / **Accepted:** 8 December 2024 / **Published:** 31 December 2024

Cite this article: El-Sayed, A.S., & Refaay, M.M.S. (2024). Development of a Greenhouse Steam-Powered, Self-Propelled Soil Sterilization Device. Turkish Journal of Agricultural Engineering Research, 5(2), 284-302.
<https://doi.org/10.46592/turkager.1570860>

ABSTRACT

*This study aims to develop an eco-friendly, self-propelled device to sterilize greenhouses soils with pressurized, superheated steam. The innovated device sterilizes greenhouse soils directly without removing their structures. The device operates electrically with remote control and is equipped with a smart electronic system to control superheated steam temperatures. The device is an alternative to pollutant chemical and long-term solarization sterilization methods. Three forward speeds (steaming exposure periods) of the steam soil sterilizer were tested: 0.05 m s⁻¹ (7s), 0.12 m s⁻¹ (4s), and 0.19 (3s) m s⁻¹. Three pressurized superheated steam temperatures of 153°C (0.414 MPa), 170°C (0.689 MPa), and 183°C (0.965 MPa) were tested at three heights of the steam distributor above the soil surface: 0, 25, and 50 mm. The efficiency of controlling common fungal pathogens, nematodes, and weed seeds were estimated and compared to solarization control. The performance rates, field efficiency, and operating costs of the steam sterilizer were evaluated. The maximal control efficiencies for fungal pathogens for *Fusarium oxysporum*, *Rhizoctonia solani*, and *Pythium* spp. were 90.90, 92.72, and 91.37%, respectively. The highest value of nematode control efficiency was 97.73%. The maximal specific energy consumption rate was 30.96 kWh ha⁻¹ at a field capacity of 0.05 ha h⁻¹ with an average operational cost of 434.18 USD ha⁻¹. The cucumber yield for experimental greenhouses increases by 3.36% over control. It could be recommended to generalize using the developed sterilizer technique in greenhouses for cultivating organic crops.*

Keywords: Cucumber, Distributor, Pathogens, Remote, Super-heated, Thermal



INTRODUCTION

Agricultural crop disease is one of the main obstacles facing the greenhouse farmers ([Ghani et al., 2019](#)). Using scientific methods prevents the emergence of greenhouse diseases ([Gullini et al., 2022](#)). Numerous infections or fungi within enclosed greenhouses are the cause of seed loss and seedling death ([Singh et al., 2020](#)). *Fusarium*, *Rhizoctonia solani*, and *Pythium* are considered the main fungal infections that cause root rot diseases ([Bodah, 2017](#); [El-Kazzaz et al., 2022](#)). Choosing the right strategy to start controlling fungal diseases depends on preventive treatment ([Daughtrey and Buitenhuis, 2020](#)). Infection with the *Fusarium* fungus manifests as browning of the plant's roots in the first thirty days or less ([Punja, 2021](#)). Symptoms of a *Rhizoctonia solani* infection include sunken brown spots that start between the root and the stem, suffocate the stem, and eventually kill the fruit ([Aghazadeh et al., 2022](#)). The tendency of the stem bearing the plant to fall off after fruiting is one sign of a *Pythium* fungal infestation ([Sarkar et al., 2022](#)). Infections with *Rhizoctonia solani* and *Fusarium oxysporum* can induce wilt and root rot diseases in cucumber crops grown in greenhouses by 67.7% and 71.0%, respectively, at the post-emergence stage, which has a relative impact on productivity ([Farrag and Fotouh 2010](#)).

The results of the development of steam soil sterilization machines were studied. [Gay et al. \(2010\)](#) assembled a prototype of a self-propelled steam injection machine to disinfect open-field tomato crops from *Fusarium*. The generated steam flow rate was 500 kg h⁻¹ at a pressure of 50 kPa. The results included the elimination of the *Fusarium exsporum* fungus at rates ranging from 63 to 100%. [Wang et al. \(2018\)](#) developed a mobile soil rotary steam disinfection machine that generates steam with a pressure of 0.6 MPa and a temperature of 158.86°C with a rotary working speed of 0.035 m s⁻¹ for soil depth of 15 cm and consuming power of 87.78. Also, [Gao et al. \(2023\)](#) developed a vertical rotary soil tilling disinfection combine to sterilize soil using a forward speed of 0.26 m s⁻¹, and the results concluded that the soil disinfection uniformity coefficient reached 85.57%. [Peruzzi et al. \(2011\)](#) developed a self-propelled machine to disinfect the soil using steam and chemicals while using a plastic mulch film. The steam exposure time was increased by reducing the working speed to 60 m h⁻¹. The maximum soil sterilization efficiency was increased at 100 °C for the soil surface temperature. [Nishimura et al. \(2015\)](#) evaluated the performance of a self-propelled machine equipped with a steam generator that generates superheated steam from 150 to 300 °C at a pressure of 0.4 MPa using fuel. The machine was tested at speeds ranging from 0.3 to 1 km h⁻¹. The effectiveness of eliminating weed seeds were reached at a soil temperature of 60 °C. Operating the machine was ineffective in the open field due to the high operating cost. [Raffaelli et al. \(2016\)](#) designed a prototype of soil fumigation from pathogens and weed seeds. A maximum temperature of 63 °C at a depth of 25 mm with a steam dose of 2.87 kg m⁻² was able to significantly reduce soil weed bank in the layer of 0-100 mm soil depth.

The investigated research problem is that greenhouses require periodic sterilization operations due to the frequent fungal and viral soil infections. The use of chemical methods is the most common and harmful

([Daughtrey and Buitenhuis, 2020](#)). Soil chemical sterilization had many environmental and health disadvantages, in addition to its high cost. Applying chemical sterilization to the soil prevents the cultivation of medicinal and aromatic crops ([Namdeo, 2018](#)). Soil solar sterilization requires warm weather for a long period of 6-8 weeks and completely evacuates the greenhouse ([Mormile et al., 2016](#)). Steam sterilization is the most successful method of sterilizing greenhouse soils but is expensive in small greenhouses ([Dietrich et al., 2020](#); [Gullino et al., 2022](#)). Using fuel-powered steam boilers to sterilize greenhouses generates gas emissions that pollute the environment ([Khattak et al., 2016](#); [Srivastava et al., 2020](#)). Therefore, the idea was given to design a self-propelled steam device that runs on electricity to directly sterilize the greenhouse soil. The quick and efficient steaming direct procedure with no chemical residues allows the soil steam sterilizer device to overcome the shortcomings of both chemical and solarization methods ([Gay et al., 2010](#)). The developed steam sterilizer is more cost-effective and environmentally friendly compared to traditional solarization methodology ([Gullino et al., 2022](#)).

This research aims to develop and performance-evaluate an electric self-propelled steam sterilizer device to sterilize soil greenhouses from fungal pathogens and nematodes. On the other hand, reducing yield production costs and maximizing its quality with rationalization of harmful chemical pesticide using were aimed at.

MATERIALS and METHODS

Experimental procedure

The experiments were carried out at Ashmoun, Dakahlia, Egypt (latitude 31° 09' 11" and longitude 31° 64' 60") on cucumber (*Cucumis sativus*) in September 2023. Three plastic tunnel-type greenhouses were steamed, and one greenhouse for control was sterilized by solarization. This site was chosen due to the presence of a history of bacterial and fungal infections. The greenhouse soil was plowed and leveled in preparation for steaming before planting. The area of one greenhouse is 405 m², with dimensions of 9 x 45 m. Each greenhouse was divided into 40 plots; every plot had an area of 9 m² with dimensions of 1×9 m. The total number of experimental plots was 135, with a total area of 1215 m². The experimental greenhouse structures weren't removed, unlike the solarized control greenhouse. Three variables were tested in a completely randomized block design (RCBD) with five replicates. Three levels of forward speeds for the self-propelled steam soil sterilizer in exchange for steaming exposure periods (FS) [0.05 m s⁻¹ (7 sec), 0.12 m s⁻¹ (4 sec), and 0.19 m s⁻¹ (3 sec)] were tested. A delay period of 2 seconds has been added to the forward speeds at an operating distance of 0.25 m using the flashing button within the remote control. Three temperatures of pressurized super-heated steam (ST) were tested: 153°C (0.414 MPa), 170°C (0.689 MPa), and 183°C (0.965 MPa). Three heights (H) of the truss steam distributor above the ground (zero level; 25 and 50 mm) were tested. All experiments were tested using a steam discharge rate of 0.04 L s⁻¹.

General description

The self-propelled device sterilizes the soil with pressurized, superheated steam to eliminate fungal pathogens and nematodes directly. The treated infected greenhouse soil surface layer disinfects due to drying up the pathogens. Solarization requires around two weeks to solarize the soil by covering it with plastic and mulching tools over the top 5 cm of the ground. The temperature can reach 42 to 60°C, though this varies greatly from place to place. The developed device works with electrical energy without any polluting gas emissions. The device's geometric dimensions were designed to suit small and medium greenhouses, as shown in Figures 1 and 2. The developed device generates steam using a pressure steam boiler made of thick steel to withstand high pressures. The boiler is mechanically secured with an overpressure relief valve to avoid explosion. The boiler is electrically secured with an electric pressure sensor to cut off the electric current when the mechanical valve is blocked. The device is well insulated from electric shocks due to the use of wooden insulators in the base of the device and electrical insulating paint. The device generates superheated steam with a maximum temperature of 183°C and pressures up to 0.965 MPa. The total width of the device is 1 m to fit the greenhouse entrance, while the actual operating width is 0.75 m. The height of the device is 1.16 m. The device is self-propelled and operates with a remote control. The sterilizer is a tricycle for easy maneuvering in tight spaces. The device's net weight is 175 kg, which does not affect the soil's compressibility. The steam height above the soil surface can be controlled from 0 to 50 mm. The steam generator was insulated using glass wool fiber lining to prevent heat leakage and minimize consumed power. The device is equipped with a transmission DC motor that runs on a speed control circuit. The device operates using a 220-volt, 50-Hz alternating current. The device also works with a 5-kilowatt diesel electrical generator that is installed outside the greenhouse to avoid polluting with combustion exhaust. The steam soil sterilization device consists of the following parts, as shown in Figures 1 and 2.

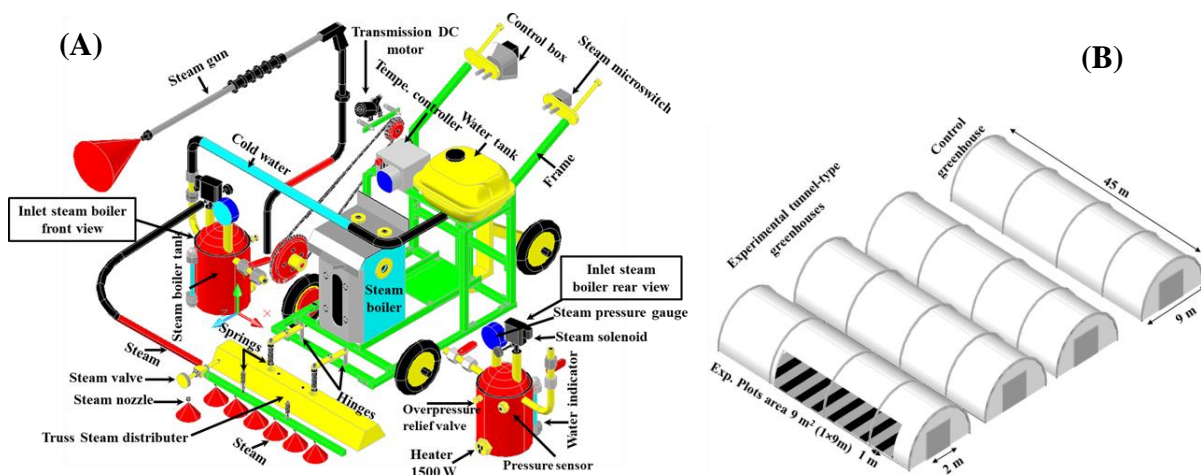


Figure 1. (A) Isometric view of the self-propelled steam soil sterilizer and (B) The experimental plastic tunnel-type greenhouses.

A light frame is designed from 30 mm hollow square-section tubes of 3 mm thick iron, as shown in Figure 1A. The frame is durable to resist shocks and vibrations during operation. The frame was assembled with screws without welding for ease of maintenance. The device is rear-steering to ensure front stability for steaming. A solid wheel type with a diameter of 270 mm was installed axially, as shown in Figure 2A No. 9. The front wheels are installed at a distance of 280 mm from the frame to maintain balance. The right front wheel is equipped with a gear (42 teeth) to front-tow the device (Figure 2 A and C). The rear wheel is mounted on a cylindrical axis 300 mm long and 381 mm in diameter, equipped with an internal shaft to turn the device (Figure 2A, No. 6). The rear wheel is mounted on a U-shaped holder with a 10 mm thickness and 10 mm width to resist shocks (Figure 2C). A pair of solid handles was installed to guide the device (Figure 2A, No. 15). The frame base is lined with a plywood base for electrical insulation, as shown in Figure 1A. Safety factors were taken into account when designing the device, in agreement with [Yonter and Houndomougbo \(2022\)](#); [Alkan and Gugor \(2024\)](#).

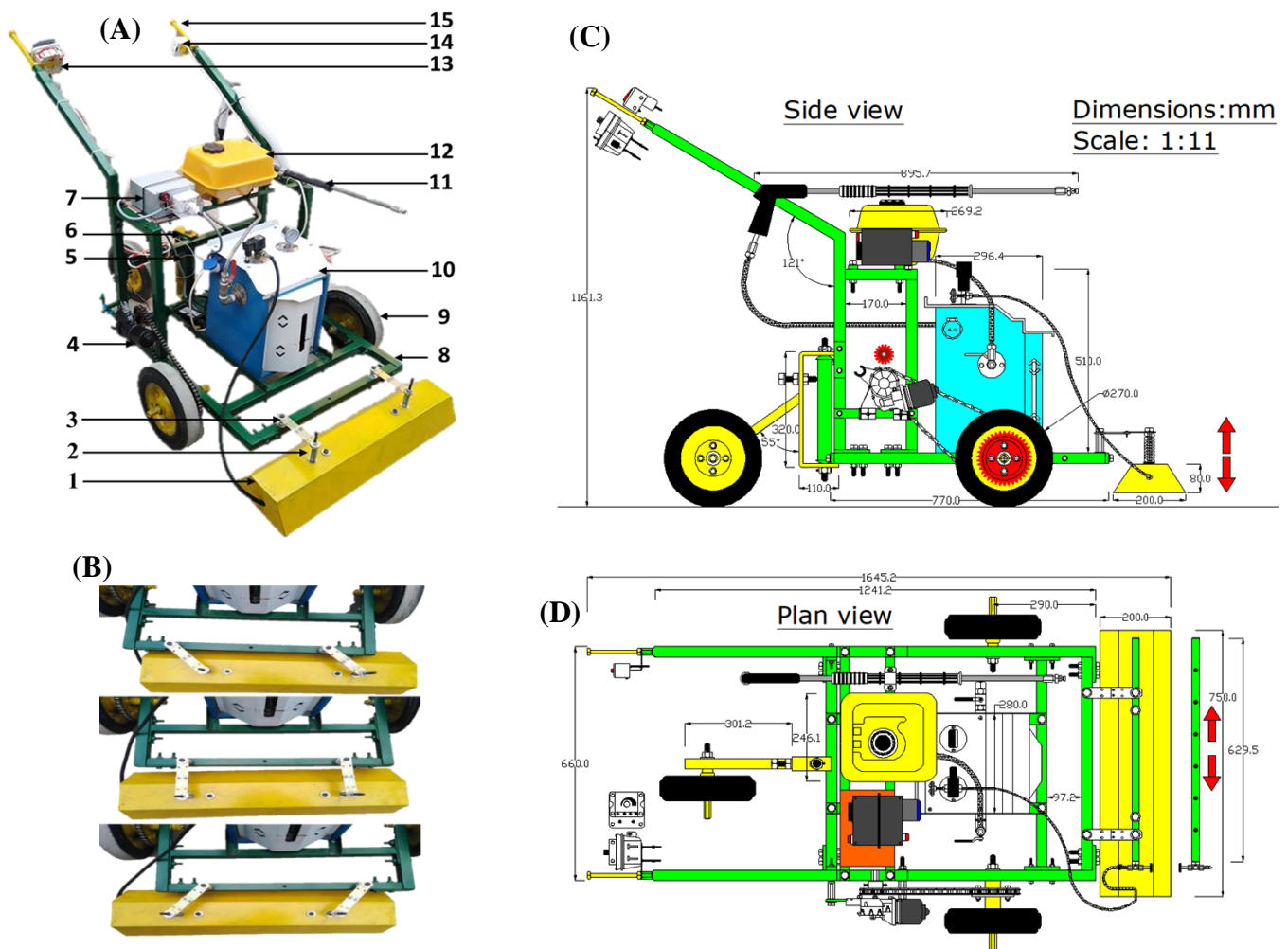


Figure 2. (A) The self-propelled steam soil sterilizer (1-steam distributor; 2-spring holder; 3-rotary hinges; 4-DC transmission motor; 5-thermocouple sensor; 6-rear wheel spindle; 7-thermocontroller; 8-frame; 9-front wheels; 10-steam generator unit; 11-steam gun; 12-water tank; 13-control box; 14-steam microswitch; 15-handle), (B) steam distributor positions, (C) Side view of the 2D geometric of a soil steam sterilizer device and (D) plan view of the 2D geometric of a soil steam sterilizer device.

The pressurized steam generation unit consists of a steam boiler, a water tank, and, as shown in Figure 2A, No. 10 and 12. The water tank is made of rust-resistant galvanized sheet and is provided internally with a filter to trap impurities (Figure 2A, No. 12). The steam boiler is connected to the water tank using a thermal hose with a diameter of 12.7 mm. The steam boiler converts water into pressurized steam and directs it to the steam distributor (Figure 2A, No. 10) (El-Sayed and El-Hameed, 2017). The steam boiler consists of an outer body made of coated, electrical insulating galvanized sheet, as shown in Figure 1A. The steam boiler internally contains a cylindrical tank made of galvanized iron with a thickness of 20 mm to resist large pressures (Figure 1A). The boiler's inner tank is lined with glass wool to insulate the boiler thermally and saves power. The inner diameter of the steam boiler tank is 250 mm, and its height is 330 mm, as shown in Figure 1A. The steam boiler is supplied with a thermo-resistant glass water indicator (Figure 1A). The boiler's inner tank is connected from the right side with a 12.7-mm-diameter pipe connected by a valve to the 7-liter water tank (Figure 1A). The inner tank boiler lefting tube is connected by a valve and connected to the steam gun (Figure 2A, No. 11). The steam gun is used to sterilize narrow places, pots, and the interior walls of the greenhouse. The steam gun is made from galvanized iron tubes with a thickness of 2 mm, a length of 1 meter, and a diameter of 10 mm. The steam gun is equipped with a front nozzle with a diameter of 1.5 mm to distribute the steam in the form of a cone shape (Figure 1A). The steam gun is well thermally insulated with a thick layer of heat-resistant polyethylene to protect operators' hands from overheating. A spiral copper electrical heater with an internal tungsten coil (1.5 kW and 220 V) was inserted in the boiler inner tank base (Figure 1A). An electrical solenoid was used to control the outlet steam from the boiler automatically (Figure 1A). The steam solenoid is operated automatically by a thermo-controller (Figure 2A, No. 7). A mechanical safety valve was used to protect the steam boiler explosion and relieve overpressures up to 0.965 MPa, as shown in Figure 1A. The steam distribution unit directs the pressurized superheated steam directly to the surface of the soil, as shown in Figure 2B. The steam distribution unit consists of a truss shape made of galvanized sheet with a thickness of 1 mm and geometric dimensions (Figure 2 C and D). The operating width of the steam distributor is 750 mm. The steam distributor height over the soil surface ranged from 0 to 50 mm. The steam distributor prevents steam leakage and directs it to a soil area of 0.15 m². A square-section pipe (630 mm in length) that contains six copper nozzles (1 mm in diameter) was used to distribute steam in a cone shape (Figure 1A). The steam square-section pipe is connected axially to a copper valve to control the steam discharge rate, as shown in Figure 1A. A pair of twin hinges was used to direct the steam distributor axially on the right and left sides (Figure 2A, No. 3). Two 130-mm-long spring spiral guides were utilized to adjust the steam distributor's height and absorb shocks (Figure 2A, No. 2). A DC-type electric motor within speed-reducer gears was used to fit the slow process of soil sterilization (Figure 2A, No. 4). Forward speeds were slow to allow the steam to penetrate the surface layer of the soil efficiently, as listed in Table 1. The transmission motor has a large withdraw torque of 29-60 N m, and its specifications are listed in Table 1. The motor is mounted laterally using guides and a tensioner to tighten the transmission chain (Figure 2D).

A driving 14-teeth gear was installed on the transmission motor, versus a 42-teeth gear on the right front wheel axle, as shown in Figure 2C. A control box was used to control the motor speeds (Figure 2A, No. 13). The transmission motor is controlled remotely by an infrared remote control circuit for easy operation of the device, as shown in Figure 3E.

Table 1. Forward speeds for the steam sterilizer device and the used steam specifications.

Transmission motor specifications		Motor speed (14 teeth), rpm	gear (42 teeth), rpm	Wheel speed (42 teeth), rpm	Linear speeds, m s^{-1}	forward Consumed power, Amp.
Rating voltage	12 V	10		3.33	0.05	1
Rating power	50 W	25		8.33	0.12	2.5
Torque	29-60 N m	40		13.33	0.19	4
Net weight	1400 g m	Forward speeds: 0.18, 0.43, and 0.68 km h^{-1}				
Superheated steam Temp., $^{\circ}\text{C}$	Pressure, MPa	Specific enthalpy, kcal kg^{-1}	Specific volume, $\text{m}^3 \text{kg}^{-1}$		Specific heat, $\text{kcal (kg }^{\circ}\text{C)}^{-1}$	Viscosity, mPas
153	0.414	664.008	0.183		0.657	0.014
170	0.689	661.211	0.243		0.621	0.147
183	0.965	664.008	0.183		0.657	0.151

A smart electronic circuit was equipped with the device to automatically control the operation, as shown in Figure 3A. A digital thermo-controller attached to a thermocouple was used to set the steam temperature automatically (Figure 2A, No. 5 and 7). The thermocouple sensor is inserted into the outlet upper pipe attached to the electrical solenoid. The measured temperature is displayed on the thermo-controller digital screen (Figure 3D). The settled temperature of outlet steam is controlled using the touch buttons on the digital thermo-controller LCD screen (Figure 3D). The thermo-controller is connected to a 16-amp contactor to transfer the electrical load of the steam boiler (Figure 3B). The digital thermo-controller unit is supplied with an outer plug connected to the electrical steam solenoid, as shown in Figure 3A. A direct micro-switch is mounted on the left device handle to operate the steam solenoid directly (Figure 3C). A control box was installed on the right handle to control forward speeds (Figure 3E). A dimmer was used as a speed regulator switch with the controlling box (Figure 3E). A triple switch on the right side of the control box is used to disconnect and operate the motor at two speeds: fast (right side) and slow (left side), and a disconnect (middle), as shown in Figure 3E. A left triple switch on the left side was used to operate the changeable speeds from dimmer (Figure 3E). A 12-volt, 16-amp relay is used to connect the control box's electrical loads (Figure 3A). An infrared receiver unit is connected to the relay's magnetic coil terminals to remotely control the device forward (Figure 3E). The positive electrical current is transmitted remotely to the transmission motor through the attached

relay by the remote control, as shown in Figure 3A. To operate the self-propelled sterilizer device, the forward speed is selected using the dimmer in the electrical control box. The forward speed is chosen according to the severity of the injury and the condition of the soil. The left key in the control box is turned to the right. The transmission motor is controlled remotely by pressing the remote control. The electrical steam boiler is operated using a side button installed in it, as shown in Figure 3A. The digital thermo-controller button is switched, and the desired temperature is selected from 100 to 183°C. The solenoid steam socket is connected to the thermo-controller outer plug. Each temperature corresponds to a specific pressure that can be read on the pressure gauge, as shown in Figure 3B. The steam boiler takes a period of preparing time (20 minutes, approximately) to reach the required temperature. The height of the truss steam distributor above the ground is adjusted using the screw guides as needed. Sterilization operations are carried out by passing the device side by side inside the greenhouse.

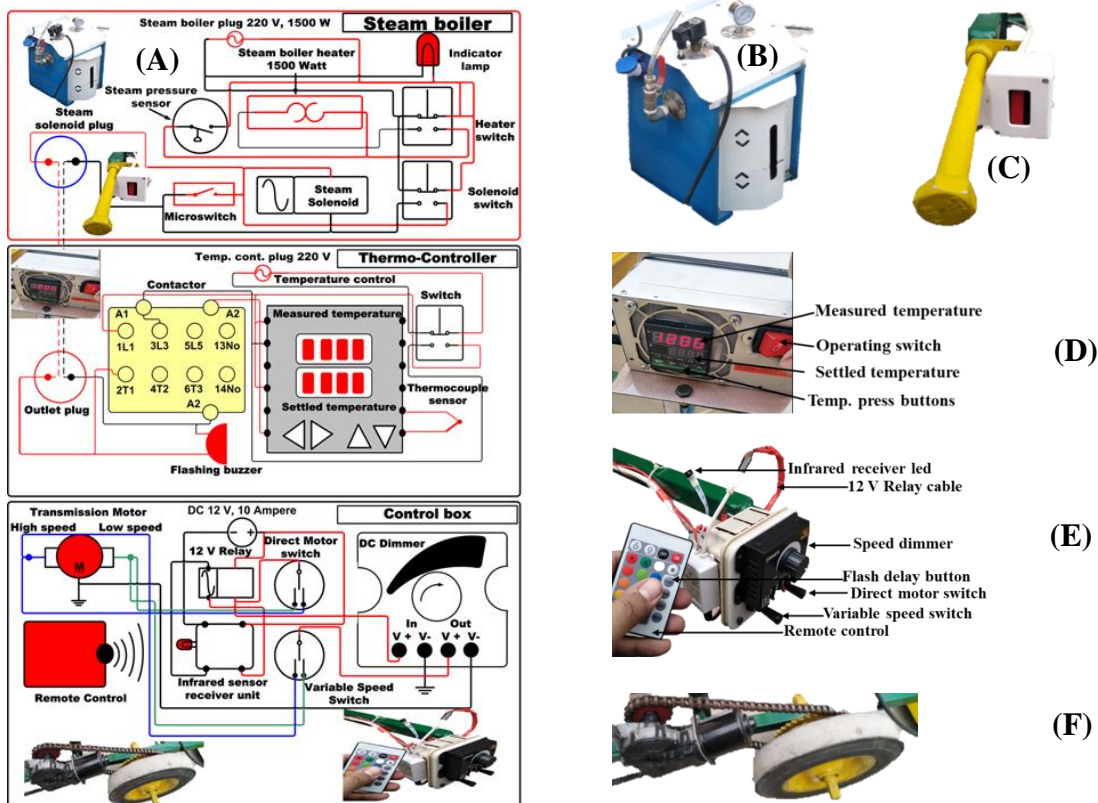


Figure 3. Electrical wiring circuit for the self-propelled steam sterilizer device. (A) Electrical wiring diagram for steam soil sterilizer; (B) Steam generator unit; (C) Steam micro-switch; (D) Thermo-controller; (E) Control box for the self-propelled steam soil sterilizer device; and (F) Transmission motor.

The self-propelled soil steamer sterilizer device evaluation

The soil texture of the experimental greenhouses had been analyzed within a depth of 0-600 mm of the soil surface layer, according to [Carter and Gregorich \(2007\)](#). The testing location had a clay-loam soil structure that consisted of 22.14% sand, 45.05%

silt, and 32.81% clay. To determine the soil surface temperatures (SST, °C) after treatment directly, three thermo-sensors connected to a data logger were used. Each thermal sensor is installed inside a vertical tube and implanted in the soil at a depth of 200 mm. The temperature sensors were distributed evenly along the operating width of the steam sterilizer to measure the soil temperature. Five random samples were collected from each experimental plot at depths of 0-100 and 100-200 mm and placed in plastic bags 24 hours after steaming treatments. The fungal pathogen CFU (colony-forming unit) and nematode populations were estimated before and after the sterilization procedure. To determine the sterilizer device efficiency, a comparison was made between the solarized control greenhouse and the steamed experimental greenhouse. One gram of soil was taken from the treated random samples before and after steaming treatment. A soil suspension was made and diluted, and then 1 ml of the solution was transferred to petri dishes. The samples were inserted in petri dishes with agar medium (NA) and incubated at a temperature of 25 ± 2 °C for 72 hours. A dilution percentage was chosen according to the colonies forming the unit's appearance. The colonies forming unit (Cfu g⁻¹) for the main common pathogen infections (*Fusarium Oxysporum*, *Rhizoctonia Solani*, and *Phytium spp.*) were recorded according to the methodology of [Masago et al. \(1977\)](#). To estimate the number of nematode populations (NP) per 100 g of soil, the samples were ground and sieved, then diluted with water. The soil suspensions were filtered with fine sieves (< 2 mm) according to the methodology of [Seinhorst \(1962\)](#). The control efficiency (C_η) for fungal pathogens (FC_η) and nematode infections (FC_η) was determined according to Equation (1) ([Mao et al., 2016](#)).

$$C_{\eta} = \frac{X_1 - X_2}{X_1} \times 100 \quad (1)$$

Where; C_η: control efficiency, %; X₁: the pathogens forming colonies CFU g⁻¹ or the nematode population number in untreated plots; %; and X₂: the pathogens forming colonies CFU g⁻¹ or the nematode population number in the treated plots.

The soil weed seed bank (SB) was determined according to [Chejara et al. \(2019\)](#). Samples were taken from experimental plots at depths of 0-100 and 100-200 mm to estimate SB by sieving before and after treatments. The cucumber crop yield was estimated for the experimental greenhouses compared to the control. Cucumber was planted directly in mid-September after the steaming sterilization for the experimental greenhouses until harvested in mid-February. Cucumber was planted in the control greenhouse at the end of October after the solarization sterilization and harvested at the end of April. The chemical and physical properties of soil samples before and after sterilization were estimated at depths of 0-200 mm, according to [Ngakou et al. \(2008\)](#). Soil-steaming self-propelled sterilizer device performance was estimated. The field efficiency and actual field capacity were estimated according to [Kepner et al. \(1978\)](#). The specific energy consumption rate (SE) was determined as presented in Equation (2), according to [Culpin \(1986\)](#). Operating costs (OC) for operating the steam sterilizer were estimated in Equation (3), according to [Hunt \(1983\)](#).

$$SE, kWh\ ha^{-1} = \frac{\text{Consumed power } kW\ h}{\text{Actual field capacity, } ha\ h^{-1}} \quad (2)$$

$$OC, USD\ ha^{-1} = \frac{\text{Device hourly cost } USD\ h^{-1}}{\text{Actual field capacity, } ha\ h^{-1}} \quad (3)$$

Statistical analysis

The statistical analysis programs COSTAT (version 2019) and IBM SPSS (version 2020) were used. The mean average values and standard deviation of the measurements for the tested variables were statistically analyzed. Significance tests were conducted at a level of $P \leq 0.05$ for the tested variables. The ANOVA analysis was conducted to assess the difference between the means of the tested factor levels. Linear-type regression analysis was performed to study the association between a continuous outcome variable and a continuous covariate.

RESULTS AND DISCUSSION

Soil surface temperatures

The experiments were conducted in September, when the average daily temperature was 25.60°C and the relative humidity was 0.65%, according to the Meteorological Unit Data. As listed in Table 3, the average measured soil surface temperatures (SST) for the experimental plots after treatment were recorded. Solar sterilization temperatures do not exceed 60°C when covered with plastic at maximum solar radiation at noon, which is less than half the temperature measured by exposure to steam, 140°C, which leads to the elimination of fungal pathogens. Figure 4A illustrates, the sterilizer device forward speeds (FS) increment is comparatively opposite to the SST. The maximum measured soil surface temperature (SST) was 155.69°C at the lowest forward speed (FS) of 0.05 m s⁻¹, and the highest temperature of superheated steam used (ST) was 183°C. The lowest value of SST was 93.50°C recorded at the maximum level of FS of 0.19 m s⁻¹, and the lowest ST was 153°C, as shown in Figure 4A. As shown in Figure 4B, there is a directly proportional relationship between ST and SST at different levels of superheated steam heights (H). The highest value of SST was 137.17°C at H of 0 mm, and ST was 183°C. The minimal value of SST was 107.48°C at H of 50 mm, and ST was 153°C. The measured SST decreased by 25.04 and 29.75%, respectively, at the maximum ST of 183°C and the lowest H of 0.0 mm, and vice versa, at the lowest ST of 153°C and the highest H of 50 mm, as shown in Figure 4B. As mentioned in Table 3, there is a high significant probability at the $P \leq 0.05$ level for the SST measurement, the main factors, and the interaction between them. Statistically, a linear regression Equation of SST was obtained, as illustrated in Equation 4.

$$SST, ^\circ C = -249.229\ FS\ (m\ s^{-1}) + 0.913\ ST\ (^\circ C) - 0.0384\ H\ (mm)\ (R^2 = 0.899) \quad (4)$$

In order to anticipate the required measurement result and determine the performance rate of the developed device, the regression equation is applied with varying levels of coefficients based on the fungal infection state and varying levels of device adjustment.

The measured soil surface temperature after treatment decreased by 14.92 and 38.89%, respectively, at the maximum ST of 183°C and the lowest FS of 0.05 m s⁻¹, and vice versa, at the lowest ST of 153°C and the highest FS of 0.19 m s⁻¹. The percentage decrease in measured soil surface degrees was relatively small at low forward speeds compared to high speeds. Soil temperature fluctuations are due to the fact that the steam flow rate coincides inversely with the increase in the forward speed of the steam sterilizer, in accordance with [Runia and Greenberger \(2004\)](#). The steam penetration ratio into the interstitial soil pores increases in direct proportion to the soil surface temperature, in accordance with [Raffaelli et al. \(2016\)](#). The rate of transferred heat quantity increases with a lower height of emitted steam to the soil surface, in agreement with [Mormile et al. \(2016\)](#).

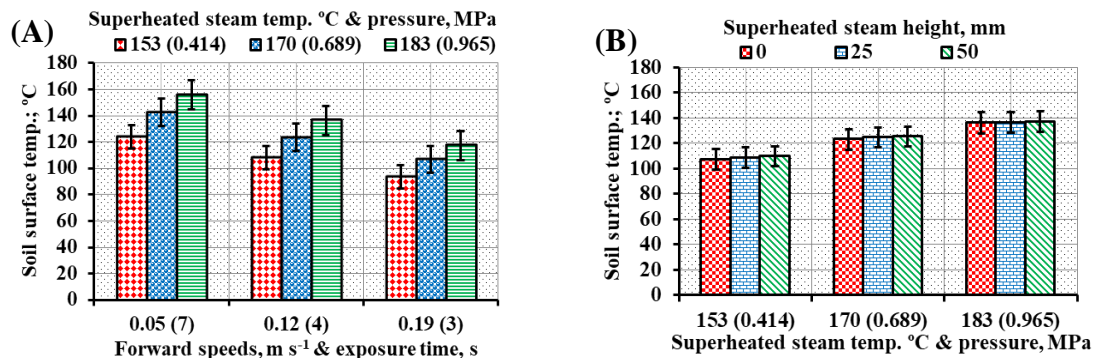


Figure. 4. The soil surface temperatures at the effect of (A) forward speeds (exposure times) and the superheated steam temperatures; and (B) superheated steam temperatures and the steam heights.

Fungal pathogens control efficiency

Figure 5A displays an inversely proportional correlation between sterilizer forward speeds (FS) and the efficiency of controlling fungal pathogens (FC_η) with the steam temperatures (ST). The highest values for controlling fungal pathogen efficiencies FC_η were (90.90, 92.72, and 91.37%), respectively, for *Fusarium oxysporum* (*Fus. Ox.*), *Rhizoctonia solani* (*Rhiz. S.*), and *Pythium* spp. (*Pyt. spp.*), at the lowest FS of 0.05 m s⁻¹ and the highest ST of 183°C, as shown in Figure 5A. Figure 5A illustrates the FC_η lowest values of (66.11, 79.42, and 75.61%), respectively, for *Fus. Ox.*, *Rhiz. S.*, and *Pyt. spp.*, at the maximum FS of 0.19 m s⁻¹ and the lowest ST of 153°C. The FC_η values for control greenhouse were (47.11, 49.55, and 45.53%), respectively, as shown in Figure 5A. Figure 5B illustrates an inversely proportional correlation between the ST and FC_η at the different levels of H. The maximum values for FC_η were (84.01, 88.64, and 85.70%), respectively, for *Fus. Ox.*, *Rhiz. S.*, and *Pyt. spp.*, at the minimum H of 0 mm and the highest ST of 183°C, as shown in Figure 5B. The minimal values for FC_η were (75.97, 84.58, and 80.31%) for *Fus. Ox.*, *Rhiz. S.*, and *Pyt. spp.*, respectively, at the maximum H of 50 mm and the lowest ST of 153°C, as shown in Figure 5B. The FC_η values for the control greenhouse were (47.11, 49.55, and 45.53%), respectively, as shown in Figure 5B. The average mean values and the standard deviation for soil fungal pathogen infections before and after steam treatment are indexed in Table 2. Statistically, there is a high significance effect at a probability of $P \leq 0.05$ for the FC_η, the main factors, and the interaction

between them, as listed in Table 2. The linear regression formulas for fungal pathogen efficiencies for the steam sterilizer were obtained and illustrated in Equations 5 to 7.

$$Fus. Ox FC\eta, \% = -128.373 FS + 0.568 ST - 0.0219 H \quad (R^2 = 0.897) \quad (5)$$

$$Rhiz. S. FC\eta, \% = -56.184 FS + 0.552 ST + 0.0460 H \quad (R^2 = 0.896) \quad (6)$$

$$Pyt. spp. FC\eta, \% = -67.889 FS + 0.540 ST - 0.0038 H \quad (R^2 = 0.897) \quad (7)$$

Table 2 displays the CFU of the different fungal pathogens before and after the thermal treatment with steam and the solarized control. There are highly significant differences that confirm the efficiency of the steam sterilizer device compared to solar sterilization. The efficiency of controlling fungal pathogens in the soil for the control decreased by rates of (43.79, 43.17, and 45.84%) and (36.9, 39.09, and 40.17%), respectively, from the maximum control values for *Fus. ox.*, *Rhiz. s.*, and *Pyt. spp.* for the experimental greenhouses, as shown in Figures 5A and B. The efficiency of controlling fungal pathogens in experimental greenhouses increased at the highest steam exposure time (lower forward speeds) of the steam soil sterilizer device. The superheated steam was used oppositely to the saturated steam despite the higher heat transfer capacity than superheated steam due to it easily penetrating the soil pores using superheated steam and being free of water, which can raise soil humidity when the temperature drops due to condensation, creating an active environment for fungal pathogens. The efficiency of fungal pathogen control increases proportionally with an increase in the duration of soil steaming exposure. Superheated steam eliminates fungal pathogens and disinfects the soil directly in a quick, safe, and economical manner, with the agreement of [Raffaelli et al. \(2016\)](#). Increasing the exposure time and temperature of the steam increases the sterilization efficiency. Reducing steam height increases the penetration of dynamically pressurized superheated steam into the fungal-infected soils. There were significant differences between the control and experimental greenhouses. This significant effect is due to raising the treated soil temperatures above the lethal range for pathogens thermal potential range, 70°C, in agreement with [Gay et al. \(2010\)](#), [Aghazadeh et al. \(2022\)](#), and [El-Kazzaz et al. \(2022\)](#).

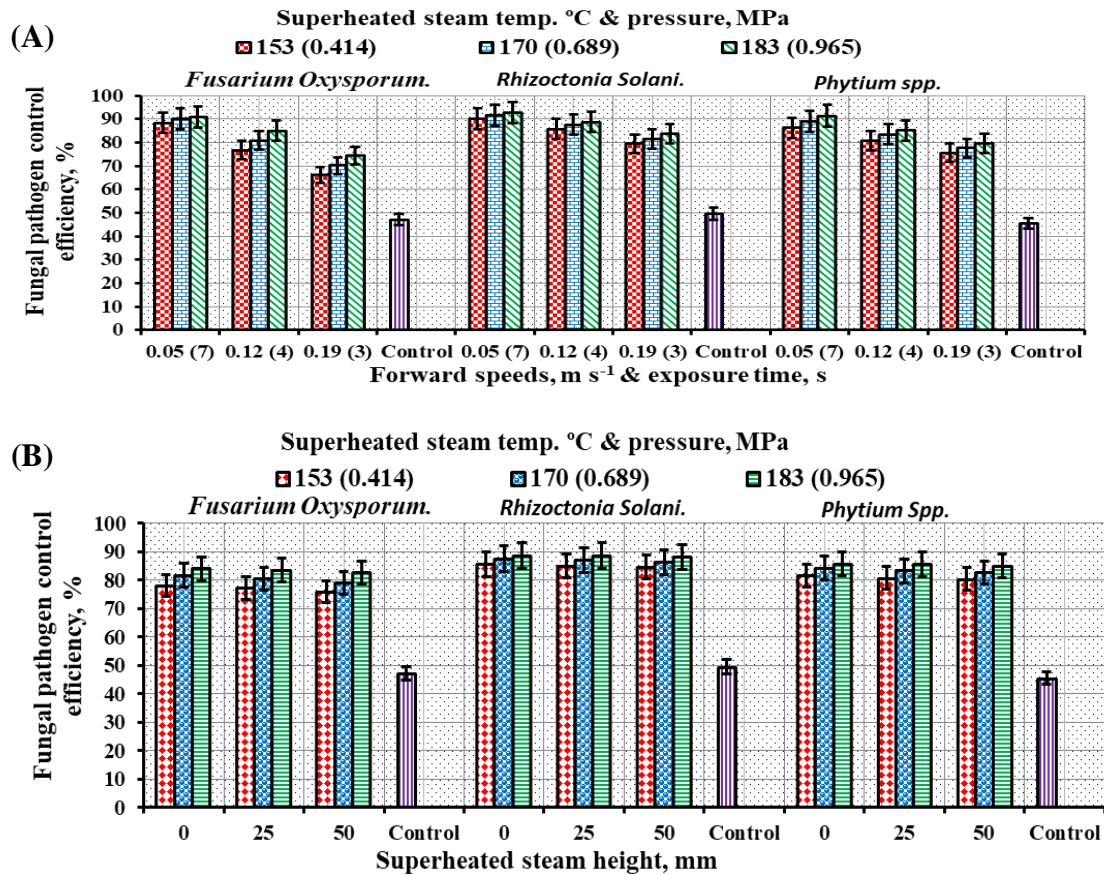


Figure 5. The fungal pathogen control efficiency at the effect of (A) forward speeds (exposure times) and superheated steam temperatures and (B) superheated steam heights and steam temperatures.

Table 2. Mean values and standard deviations of the fungal pathogen CFU of soil samples and the fungal control efficiencies before and after soil thermal treatments.

Samples and the fungal control inoculants before and after soil thermal treatments.										
Factors		Fus. ox.1, CFU g ⁻¹	Fus. ox.2, CFU g ⁻¹	Rhiz. s 1, CFU g ⁻¹	Rhiz. s 2, CFU g ⁻¹	Pyt. spp 1, CFU g ⁻¹	Pyt. spp. 2, CFU g-1	Fus. Ox., FC η %	Rhiz. S., FC η %	Pyt. Spp., FC η %
FS, m s ⁻¹	0.05	216±36 ^a	22±5 ^a	210±16 ^a	18±2 ^a	839±112 ^a	93±23 ^a	89.77	91.48	88.88
	0.12	228±36 ^a	44±12 ^b	217±24 ^a	28±4 ^b	849±61 ^a	143±17 ^b	80.83	87.31	83.11
	0.19	236±31 ^b	70±13 ^c	212±12 ^a	39±4 ^c	848±91 ^a	190±26 ^c	70.15	81.59	77.58
ST,°C	153	237±34 ^a	56±26 ^a	204±12 ^a	31±10 ^a	848±80 ^a	163±42 ^a	77.04	85.06	80.85
	170	214±28 ^a	42±17 ^b	220±25 ^a	29±9 ^b	830±93 ^a	138±42 ^b	80.33	86.89	83.36
	183	229±39 ^b	39±20 ^c	214±11 ^b	25±8 ^c	859±95 ^a	126±46 ^c	83.37	88.42	85.35
H, mm	0	232±32 ^a	44±20 ^a	214±24 ^a	28±10 ^a	811±87 ^a	132±44 ^a	81.22	87.24	83.81
	50	220±37 ^a	45±24 ^b	211±15 ^a	28±9 ^b	861±99 ^a	144±44 ^b	80.36	86.84	83.17
	25	228±36 ^a	48±23 ^b	213±14 ^a	29±10 ^b	864±73 ^b	151±48 ^c	79.16	86.29	82.58
Control		230±30	108±44	219±24	109±29	833±96	379±54	47.11	49.55	45.53
LSD 0.05		11.487	2.154	9.358	1.229	41.191	7.201	0.259	0.134	0.172
P value		0.0007***	0.0013**	0.00***	0.0001***	0.00***	0.00***	0.001**	0.00***	0.0031**
R ²		0.754	0.879	0.394	0.860	0.517	0.843	0.898	0.798	0.797

Where: FS: forward speeds, m s⁻¹; ST: superheated steam temp., °C; H: steam height, mm; *Fus. ox.*, *Rhiz. S.*, and *Pyt. spp. 1&2*: *Fusarium oxysporum*, *Rhizoctonia solani*, and *Pythium* spp. pathogens in soil before and after treatment, CFU g⁻¹; FCη: fungal control efficiencies for the pathogens, %; R²: determination factor; P: probability at (P ≤ 0.05). ^{a,d} the means with no common subscript within each column differed significantly (P ≤ 0.05).

Nematode control efficiency in greenhouse

As demonstrated in Table 3, the average nematode population decreased significantly after treatment with a steam soil sterilizer. As shown in Figure 6 A and B, the highest values of nematode control efficiency $NC\eta$ using steam sterilization were 97.73 and 92.12%, respectively, at the lowest FS of 0.05 m s^{-1} , the lowest H of 0 mm, and the highest ST of 183°C . Also, the lowest values of $NC\eta$ using steam sterilization were 75.88 and 85.28%, respectively, at the highest FS of 0.19 m s^{-1} , the highest H of 50 mm, and the lowest ST of 153°C . Nematode control efficiency is inversely proportional to the sterilizer forward speeds and steam height at various steam temperatures. The nematode control efficiency for the control greenhouse decreased to 49.13%, as shown in Figures 6A and B. The linear regression analysis for $NC\eta$ was determined as presented in Equation 8.

$$NC\eta, \% = -100.204 \text{ FS} + 0.596 \text{ ST} - 0.0095 \text{ H} \quad (R^2 = 0.896) \quad (8)$$

As listed in Table 3, there is a high significant effect at a probability of $P \leq 0.05$ for the nematode control efficiency. Nematode knot aggregations are eliminated significantly due to direct exposure to the lethal heat using pressurized superheated steam (Mao *et al.*, 2016). The nematode elimination ratio in control decreased due to the heat is not being enough to affect them (39°C) in the solar sterilization, in agreement with Runia and Greenberger (2004).

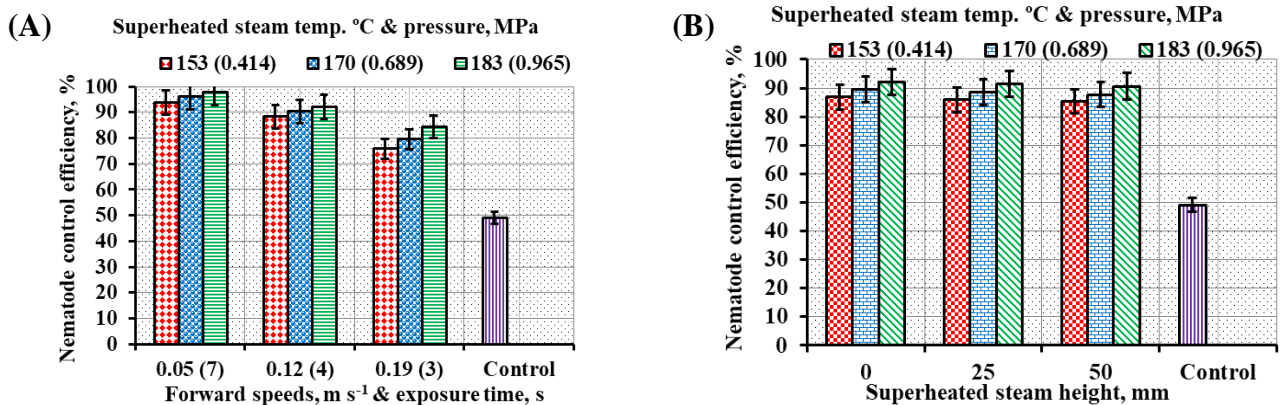


Figure 6. The nematode control efficiency at the effect of (A) forward speeds and superheated steam temperatures and (B) superheated steam heights and superheated steam temperatures.

Table 3. Mean values and standard deviations of the measured soil surface temperatures and the nematode populations before and after soil thermal treatment.

Factors		SST, °C	NP1, No./100g soil	NP2, No./100g soil	NC η %
FS, m s ⁻¹	0.05	140.8±13.25 ^a	293±35 ^a	12±5 ^a	95.87
	0.12	122.76±11.74 ^b	281±31 ^{ab}	55±14 ^b	79.93
	0.19	105.98±10.06 ^b	276±40 ^b	28±5 ^c	90.26
ST, °C	153	108.63±12.76 ^a	287±31 ^a	40±23 ^a	86
	170	124.36±14.91 ^b	281±40 ^a	32±19 ^b	88.62
	183	136.55±15.88 ^c	281±37 ^a	24±16 ^c	91.44
H, mm	0	124.09±18.57 ^a	285±29 ^a	30±21 ^a	89.49
	50	122.22±18.79 ^b	281±38 ^a	32±20 ^{ab}	88.68
	25	123.23±18.57 ^c	283±40 ^a	34±21 ^b	87.89
Control		33± 2.5	280±39	138±22	49.13
LSD 0.05		0.242	16.874	2.702	0.191
P value		0.00***	0.0005***	0.00***	0.013*
R ²		0.899	0.495	0.860	0.898

Where: FS: forward speeds, m s⁻¹; ST: superheated steam temperature, °C; H: steam height, mm; SST: soil surface temperature, °C; NP1&2: nematode populations in soil before and after treatment, No. /100g soil; NC η: nematode control efficiency, %; R²: determination factor; P: probability at (P ≤0.05). ^{a-d} the means with no common subscript within each column differed significantly (P≤ 0.05).

Weed seed bank

As demonstrated in Table 4, the soil seed weed bank reduction ratio for the experimental greenhouses increased significantly compared to the control greenhouse. The overall mean average of the variables interaction was determined. The most infested Experimental plots with weeds were selected to estimate the weed seed bank reduction ratio. The superheated steam usage led to the atrophy of weed seeds present in the surface layer of the soil, in agreement with [Peruzzi et al. \(2011\)](#). Reducing the soil weed seed bank leads to reducing weed control costs, in agreement with [Daughtrey and Buitenhuis \(2020\)](#). Using a steam sterilizer makes it possible to dispense with the need for mulching plants in the greenhouse, which saves production costs and increases quality, in agreement with [Nishimura et al. \(2015\)](#) and [Raffaelli et al. \(2016\)](#).

Table 4. Weed seed classification before and after three weeks of treatment.

Weeds classification	Narrow-leaved weeds No. m ⁻²			Broad-leaved weeds, No. m ⁻²		
	<i>Phalaris minor</i> L.	<i>Lolium temulentum</i> L.	<i>Poa annua</i> L.	<i>Lathyrus hirsutus</i> L.	<i>Medicago polymorpha</i> L.	<i>Cichorium endivia</i> L.
Exp. 1	211	119	88	68	57	42
Exp. 2	37	27	15	19	17	11
Con. 1	215	120	75	55	63	44
Con. 2	89	44	31	23	26	19
SB Exp. RT, %	82.46	77.31	82.95	72.06	70.18	73.81
SB Con. RT %	58.60	63.33	58.67	58.18	58.73	56.82

Where: Exp.; Con. 1&2: total main average of experimental and control greenhouses seed bank before and after 3 weeks from treatment; SB Exp. RT: experimental greenhouse weed seed bank reduction ratio, %; SB Con. RT: Control greenhouse weed seed bank reduction ratio, %.

Crop yield

The crop yield of the *Belgino* cucumber variety was collected after the end of the loop for the experimental and control greenhouses. The average productivity of the three experimental greenhouses was 4 tons. Each greenhouse contained 800 plants, with an average productivity of 5 kg per plant. The yield of the control greenhouse decreased to 3.87 tons as a result of the delay in the planting date and the emanation of *Fusarium* wilt and root rot diseases. The cost of fungal disease control in the control greenhouse increased to 200 USD as a result of the use of chemical fungicides. Solar sterilization was not sufficient to disinfect the soil. The cost of plastic mulching for soil solarization was 203 USD. The cost of steaming a single greenhouse using the new device was 32.25 USD. The use of sterilizer devices led to a saving of 88.50% on the cost of solar sterilization. Steam sterilization led to an increase in crop yield of 3.36% compared to the control treatment.

Soil chemical properties

The device can be used in a variety of settings, and because of the moderate fall temperatures, it is best to utilize it around September. When the treatment is applied throughout the winter at low temperatures, the steam temperature can be regulated. Given that clay soil is particularly vulnerable to fungal infections, the treatment was applied to it. The soil chemical analysis before and after steam and solar sterilization treatments for testing greenhouses is listed in Table 5. The percentage of available nutrients in the steam-treated soil increased relatively as a result of increasing soil moisture content, in accordance with [Dietrich et al. \(2020\)](#). The relative increase in available soil nutrients reduced fertilizer requirements for minerals by 2% for steam sterilization and 1% for solar sterilization, in the agreement with [Ngakou et al. \(2008\)](#).

Table 5. Chemical analysis for the experimental and control greenhouses before and after sterilization.

Chemical analysis	EC, dSm ⁻¹	OM, g kg ⁻¹	pH	N, %	P, ppm	K, ppm	Fe, ppm	Mn, ppm	Zn, ppm
Experimental before	1.17	13.43	7.44	0.09	27.03	280.14	30.55	18.39	7.03
Experimental After	1.98	14.55	7.47	0.11	28.09	285.05	31.15	19.05	7.55
Control before	1.15	12.95	7.34	0.08	28.13	280.22	30.28	18.78	6.98
Control after	1.23	13.22	7.39	0.12	27.15	282.33	31.15	18.98	7.01

Where: EC: Electrical Conductivity; OM: Organic Matter.

Self-propelled steam sterilizer evaluation performance

The field efficiency of the self-propelled steam soil sterilizer increased to 0.95% as a result of less time lost due to malfunctions. The actual field capacities of the soil steam sterilizer were 0.013, 0.03, and 0.05 ha h⁻¹, respectively, at the different forward speeds of the device. Field capacity decreased due to the long time required for sterilization. Specific energy consumption rates reached 77.85, 42.67, and 30.96 kWh ha⁻¹, respectively, at the device forward speeds. The operating cost of the

self-propelled soil sterilizer is 769.23, 333.33, and 200 USD ha⁻¹, respectively, at the sterilizer device forward speeds.

CONCLUSION

Utilizing the self-propelled steam soil sterilizer device in greenhouses was highly significant compared to solar sterilization. Optimum sterilization levels were achieved at the lowest device forward speed of 0.18 km h⁻¹ at a steam exposure time of 7 sec. Setting the steam distributor height to zero and the steam temperature to 183°C (0.965 MPa) achieved the maximum results for disinfecting soil fungal pathogens. Fusarium wilt diseases were eliminated up to 90.90% using the developed sterilizer. The highest fungal control efficiencies for *Rhizoctonia solani* and *Pythium* spp. fungi were 92.72 and 91.37%, respectively. The root rot infections were significantly decreased. The nematode infestation rate decreased to 2.27% by using the developed sterilizer. The soil bank of weed seeds decreased significantly for experimental greenhouses over control. Soil properties improved positively, and the availability of soil nutrients increased. The experimental greenhouse yield increased by 3.36% over the control. The quality of cucumber yield was significantly improved by using the device. The device's average power consumption was 50.49 kWh ha⁻¹ at an average field capacity of 0.031 ha h⁻¹. The average operating cost was 434.18 USD ha⁻¹. The new device can be recommended for small greenhouse owners to save on production costs and maintain crop quality.

DECLARATION OF COMPETING INTEREST

The authors declare that they have no conflict of interest.

ACKNOWLEDGEMENT

The authors of this manuscript extend their thanks to the Agricultural Engineering Research Institute and the Egyptian Agricultural Research Center for their technical and scientific support.

CREDIT AUTHORSHIP CONTRIBUTION STATEMENT

This research work was conducted in cooperation with all authors equally in terms of the idea, conducting experiments, writing the research, and reviewing it in its final form.

ETHICS COMMITTEE DECISION

This article does not require any Ethical Committee Decision.

REFERENCES

- Aghazadeh Naeini SS, Maleki M, Gholamnezhad J, and Shirmardi M (2022). Evaluation of the effect of some plant extracts in controlling Rhizoctonia rot in the greenhouse cucumber. *BioControl in Plant Protection*, 9(2): 87-113. <https://doi.org/10.22092/bcpp.2022.128595>
- Alkan U and Gungor C (2024). Health and safety sign knowledge levels of tractor operators in agricultural production. *Journal of Agriculture Faculty of Ege University*, 60(4): 581-593. <https://doi.org/10.20289/zfdergi.1349654>
- Bodah ET (2017). Root rot diseases in plants: a review of common causal agents and management strategies. *Agric. Res. Technol. Open Access J*, 5, 555661. <https://doi.org/10.19080/artoaj.2017.05.555661>
- Carter MR and Gregorich EG (2007). Soil sampling and methods of analysis. 2nd Edition, CRC press. pp: 950-1022. <https://doi.org/10.1201/9781420005271>
- Chejara VK, Kristiansen P, Whalley RW, Sindel BM and Nadolny C (2019). The role of seed banks in invasions by *Hyparrhenia hirta* (L.) Stapf in Australia. *The Rangeland Journal*, 41(5): 383-392. <https://doi.org/10.1071/rj19039>
- Culpin C (1986). Farm Machinery-The English Language. *Book Society. Collins*, 276-285.
- Daughtrey M and Buitenhuis R (2020). Integrated pest and disease management in greenhouse ornamentals. *Integrated pest and disease management in greenhouse crops*, 625-679. https://doi.org/10.1007/978-3-030-22304-5_22
- Dietrich P, Cesarz S, Eisenhauer N and Roscher C (2020). Effects of steam sterilization on soil abiotic and biotic properties. *Soil Organisms*, 92(2), 99-108. <https://doi.org/10.25674/so92iss2pp99>
- El-Kazzaz MK, Ghoneim KE, Agha MKM, Helmy A, Behiry SI, Abdelkhalek A and Elsharkawy MM (2022). Suppression of pepper root rot and wilt diseases caused by *Rhizoctonia solani* and *Fusarium oxysporum*. *Life*, 12(4): 587. <https://doi.org/10.3390/life12040587>
- El-Sayed AS and El-Hameed GM (2017). *Development of a weed control device using water steam. 5th International Conference of Agricultural& Bio- Engineering. Egyptian Journal of Agricultural Research*, 2(9): 413-442.
- Farrag ES and Fotouh YO (2010). Solarization as a method for producing fungal-free container soil and controlling wilt and root-rot diseases on cucumber plants under greenhouse conditions. *Archives of Phytopathology and Plant Protection*, 43(6), 519-526. <https://doi.org/10.1080/03235400701875679>
- Gao J, Shen Y and Ma B (2023). Optimized design of touching parts of soil disinfection machine based on strain sensing and discrete element simulation. *Sensors*, 23(14): 6369. <https://doi.org/10.3390/s23146369>
- Gay P, Piccarolo P, Aimonino DR and Tortia C (2010). A high efficacy steam soil disinfestation system, Part II: Design and testing. *Biosystems Engineering*, 107(3): 194-201. <https://doi.org/10.1016/j.biosystemseng.2010.07.008>
- Ghani S, Bakochristou F, ElBialy EMAA, Gamaledin SMA, Rashwan MM, Abdelhalim AM and Ismail SM (2019). Design challenges of agricultural greenhouses in hot and arid environments *A review. Engineering in Agriculture, Environment and Food*, 12(1): 48-70. <https://doi.org/10.1016/j.eaef.2018.09.004>
- Gullino ML, Garibaldi A, Gamliel A and Katan J (2022). Soil disinfestation: From soil treatment to soil and plant health. *Plant Disease*, 106(6): 1541-1554. <https://doi.org/10.1094/pdis-09-21-2023-fe>
- Hunt D (1983). Farm power and machinery management 8th Ed. *Iowa State Univ., Ames, USA*.pp 180-185.
- Kepner RA, Bainer R and Barger EL (1978). Principles of farm machinery. 3rd Edition. *West part, Connecticut, USA: AVI, pub.*
- Khattak MA, Ashraf MA, Ikmal M, Syafiq A and Hazritz M (2016). Common types of fuels in steam power plant: a review. *Journal of Advanced Research in Fluid Mechanics and Thermal Sciences*, 23(1): 1-24. <https://semarakilmu.com>
- Mao L, Wang Q, Yan D, Li Y, Ouyang C, Guo M and Cao A (2016). Flame soil disinfestation: A novel, promising, non-chemical method to control soil borne nematodes, fungal and bacterial pathogens in China. *Crop Protection*, 83: 90-94. <https://doi.org/10.1016/j.cropro.2016.02.002>
- Masago H, Yoshikawa M, Fukada M and Nakanishi N (1977). Selective inhibition of *Pythium* spp. on a medium for direct isolation of *Phytophthora* spp. from soils and plants. *Techniques*, 67: 425-429.

- Mormile P, Rippa M, Petti L, Immirzi B, Malinconico M, Lahoz E and Morra L (2016). Improvement of soil solarization through a hybrid system simulating a solar hot water panel. *Journal of Advanced Agricultural Technologies*, 3(3). <https://doi.org/10.18178/joaat.3.3.226-230>
- Namdeo AG (2018). *Cultivation of medicinal and aromatic plants*. In Natural products and drug discovery, *Natural Products and Drug Discovery, Elsevier. pp. 525-553*. <https://doi.org/10.1016/b978-0-08-102081-4.00020-4>
- Ngakou A, Megueni C, Makalao MM, Nwaga D, Taine J and Ndjouenkeu R (2008). Changes in the physico-chemical properties of soil and harvested soybean seeds in response to soil solarization and bradyrhizobial inoculation. *Archives of Agronomy and Soil Science*, 54(2): 189-202. <https://doi.org/10.1080/03650340701793579>
- Nishimura A, Asai M, Shibuya T, Kurokawa S and Nakamura H (2015). A steaming method for killing weed seeds produced in the current year under untilled conditions. *Crop Protection*, 71: 125-131. <https://doi.org/10.1016/j.cropro.2015.02.015>
- Peruzzi A, Raffaelli M, Ginanni M, Fontanelli M and Frascioni C (2011). An innovative self-propelled machine for soil disinfection using steam and chemicals in an exothermic reaction. *Biosystems Engineering*, 110(4): 434-442. <https://doi.org/10.1016/j.biosystemseng.2011.09.008>
- Punja ZK (2021). Epidemiology of Fusarium oxysporum causing root and crown rot of cannabis (*Cannabis sativa* L., marijuana) plants in commercial greenhouse production. *Canadian Journal of Plant Pathology*, 43(2): 216-235. <https://doi.org/10.1080/07060661.2020.1788165>
- Raffaelli M, Martelloni L, Frascioni C, Fontanelli M, Carlesi S and Peruzzi A (2016). A prototype band-steaming machine: Design and field application. *Biosystems Engineering*, 144: 61-71. <https://doi.org/10.1016/j.biosystemseng.2016.02.001>
- Runia WT and Greenberger A (2004). Preliminary results of physical soil disinfestation by hot air. In VI *International Symposium on Chemical and non-Chemical Soil and Substrate Disinfestation-SD2004* 698 (pp. 251-256). <https://doi.org/10.17660/ActaHortic.2005.698.33>
- Sarkar M, Chakraborty B and Srivastava JN (2022). Key Diseases of Cucurbits and Their Management. *Diseases of Horticultural Crops: Diagnosis and Management: Volume 2: Vegetable Crops*, 153. <https://doi.org/10.1201/9781003160427>
- Seinhorst JW (1962). Modifications of the elutriation method for extracting nematodes from soil. *Nematologica*, 8(2): 117-128.
- Singh RP, Tiwari S, Singh M, Singh A and Singh AK (2020). Important diseases of greenhouse crops and their integrated management: a review. *Journal of Entomology and Zoology Studies*, 8(1): 962-970. <http://www.entomoljournal.com>
- Srivastava RK, Shetti NP, Reddy KR and Aminabhavi TM (2020). Biofuels, biodiesel and biohydrogen production using bioprocesses. A review. *Environmental Chemistry Letters*, 18: 1049-1072. <https://doi.org/10.1007/s10311-020-00999-7>
- Wang KW Li C, Yang Z, Sun G, Shi and Zhao B (2018). Development of mobile soil rotary steam disinfection machine. *Transactions of the Chinese Society of Agricultural Engineering*, 34(2): 18-24. <http://www.tcsae.org/nvgcxben/ch/index.aspx>
- Yonter G and Houndonougbo HM (2022). A study on the comparison of kinetic energies calculated with some formulas using Fulljet nozzle. *Ege Üniversitesi Ziraat Fakültesi Dergisi*, 59(3): 397-408. <https://doi.org/10.20289/zfdergi.950402>



Turkish Journal of
Agricultural
Engineering Research
(Turk J Agr Eng Res)
e-ISSN: 2717-8420



Air injection in Subsurface Drip Irrigation as an Efficient Method for Zucchini Production

Nermin HUSSEIN^a, Shereen SAAD^b, Khaled REFAIE^c, Wael SULTAN^a,
Mohamed GHONIMY^{d*}, Ahmed ALZOHEIRY^e

^aAgricultural Engineering Research Institute, Agricultural Research Center, Dokki, Giza, EGYPT

^bPhysics and Chemistry Dept., Soils, Water and Environment Research Institute, Agricultural Research Center, Giza, EGYPT

^cApplication Dept., Central Laboratory for Agricultural Climate, Agricultural Research Center, Dokki, Giza, EGYPT

^dDepartment of Agricultural and Biosystems Engineering, College of Agriculture and Food, Qassim University, P.O.Box 6622, Buraydah, Al-Qassim 51452, Saudi Arabia; Agricultural Engineering Dept., Faculty of Agriculture, Cairo University, Giza, EGYPT

^eDepartment of Agricultural and Biosystems Engineering, College of Agriculture and Food, Qassim University, P.O.Box 6622, Buraydah, Al-Qassim 51452, Saudi Arabia; Department of Natural Resources and Agricultural Engineering, Faculty of Agriculture, Damanshour University, Damanshour, EGYPT

ARTICLE INFO: Research Article

Corresponding Author: Mohamed GHONIMY, E-mail: mohamed.ghonimy@agr.cu.edu.eg

Received: 28 October 2024 / **Accepted:** 11 December 2024 / **Published:** 31 December 2024

Cite this article: Hussein, N., Saad, S., Refaie, K., Sultan, W., Ghonimy, M., & Alzoheiry, A. (2024). Air Injection in Subsurface Drip Irrigation as an Efficient Method for Zucchini Production. Turkish Journal of Agricultural Engineering Research, 5(2), 303-318. <https://doi.org/10.46592/turkager.1574644>

ABSTRACT

Agriculture is a key pillar of the economy, constantly facing challenges due to population growth and climate change. Enhancing the sustainability and efficiency of crop production and improving water use efficiency are essential to evaluate air injection into subsurface drip irrigation system for zucchini production as efficient method for subsurface drip irrigation systems to improve water use efficiency (WUE), and zucchini production in heavy clay soils. Results showed that injecting air through built-in emitters using a compressor during the last third of the irrigation time maintained acceptable system performance, as measured by indicators like CV, qvar, and EU%. It also improved the physical properties of dry sieved aggregates and enhanced the availability of macronutrients, significantly improving and maintaining heavy clay soil, leading to a 27% increase in zucchini crop yields and 22% water savings compared to the control. Economic analysis indicated that air injection was a feasible option, increasing gross returns by 21% compared to the control, with a benefit-cost ratio of 2.3% for air injection versus 1.8% for the control.

Keywords: Subsurface drip irrigation, Air-injection, Crop production, Water use efficiency



INTRODUCTION

Subsurface drip irrigation (*SSDI*) is recognized as one of the most efficient irrigation methods for enhancing water use efficiency (*WUE*). By delivering small amounts of water at frequent intervals, *SSDI* minimizes water loss due to deep percolation, runoff, and soil evaporation, leading to better water and nutrient absorption by plants and improved *WUE*. However, temporary waterlogging within the root zone during and after irrigation can negatively impact root respiration, water and nutrient uptake, and overall plant growth. Irrigating with hyper-aerated or oxygenated water could help alleviate the adverse effects of waterlogging in the rhizosphere. Aerating soil by injecting atmospheric air through a subsurface drip irrigation system is believed to speed up water depletion from macropores and increase oxygen levels in the soil air. Oxygation is a technique designed to improve the efficiency of subsurface drip irrigation systems by injecting air directly into the crop root zone. This approach helps to balance aerobic and aquatic conditions in soils, particularly in heavy clay soils, to mitigate the adverse effects of inadequate soil aeration. Additionally, oxygation can boost crop yield and quality, especially for crops grown in heavier soils. The advantages are linked to the abundance of air in the rhizosphere and the higher level of dissolved oxygen in the water, which improves the absorption of nutrients by the roots. In addition, there are positive results in the irrigation system itself, such as a reduction in the formation of algae in the tubing due to the oxygen, and the suspension of solids due to micro bubbles, which reduces the possibility of emitter clogging ([Essah and Holm, 2020](#)). Achieving a harmonious equilibrium among the three soil phases, solid, liquid, and gas, is paramount for successful crop cultivation. The introduction of air through injection enhances the hydro-aerobic balance, particularly under conditions of frequent irrigation. Aerated *SSDI* has been shown to enhance yields and overall crop quality across various crops, including bell pepper ([Goorahoo et al., 2001](#)), soybean ([Bhattarai et al., 2004](#)), strawberry ([Goorahoo et al., 2007](#); [Goorahoo et al., 2008](#)), melon ([Goorahoo et al., 2007](#); [Goorahoo et al., 2008](#)), edamame ([Bhattarai et al., 2008](#)), tomato ([Goorahoo et al., 2007](#)), cotton ([Bhattarai et al., 2004](#); [Pendergast et al., 2014](#)), pineapple ([Dhungel et al., 2012](#)), sugar beet ([Vyrlas et al., 2014](#)), potato ([Shahien et al., 2014](#)), pumpkin, and lettuce ([D'Alessio et al., 2020](#)). Continuous saturation of the root zone hampers effective root functioning due to the restricted diffusion of oxygen. It is postulated that the diminished oxygen concentration in the rhizosphere, particularly at the wetting front, significantly constrains the performance of *SSDI* crops under higher irrigation rates. [Goorahoo et al. \(2001\)](#) found that the average weights of aerated and non-aerated peppers were 103.7 grams and 99.4 grams, respectively. The aerated plants exhibited a 39% increase in weight compared to the non-aerated plants. Additionally, the aerated plants demonstrated a root weight increase of 17.53 grams, corresponding to a 54% rise over the plants receiving water only. Furthermore, the aerated plants displayed a stem and leaf weight increase of 68.98 grams. When sufficient water and food availability are given for both aerated and non-aerated plants, the air injection may be responsible for a larger percentage of the root mass in the aerated plants. [Hussein \(2015\)](#) observed that the injection of air through the Subsurface Drip Irrigation system during the

final third of the irrigation period maintained all hydraulic parameters for the emitter within an acceptable range, resulting in an efficient system for crop yield, water conservation, and water use efficiency (*WUE*). [Refaie et al. \(2019\)](#) indicated that air injection in irrigation systems can enhance aeration in the root zone, thereby enhancing the value of grower investments in subsurface drip irrigation techniques. Moreover, they noted that the increased yields and potential enhancement in soil quality associated with root zone aeration suggest that adopting subsurface drip irrigation-air injection technology primarily serves as a means to enhance carrot productivity. [Dissanayake \(2020\)](#) discovered that the aerated zone at a soil depth of 45 cm contained an equal or even higher level of soil oxygen than the non-aerated zone at a depth of 25 cm. Additionally, air injection reduced soil moisture content, likely attributable to increased root water intake due to enhanced root and soil respiration. Furthermore, it was found that air injection through *SSDI* positively influenced the growth parameters of corn and sugar beet crops. The drip irrigation system also exhibited more efficient water usage and conservation across various summer and winter crops ([Essah and Holm, 2020](#)).

Cultivating zucchini holds significant importance in Egypt, both culturally and economically. This versatile crop is vital in Egyptian cuisine, featuring prominently in traditional dishes such as stuffed zucchini and vegetable stews. Beyond its culinary value, zucchini cultivation contributes to the country's agricultural sector, providing income for farmers and supporting local economies. Its export potential further enhances its economic significance as Egypt leverages its agricultural resources to generate revenue from international markets. Additionally, zucchini's resilience to drought conditions makes it a valuable crop in regions with limited water resources, contributing to food security and agricultural sustainability ([Seleim et al., 2015](#)). Thus, the main objective of this research work was to evaluate air injection into subsurface drip irrigation system for zucchini production as efficient method for subsurface drip irrigation systems to improve water use efficiency (*WUE*), and zucchini production in heavy clay soils. This objective was planned to be realized through the following stages:

- Evaluating the impact of air injection through subsurface drip irrigation system on the hydraulic performance and system distribution uniformity.
- Evaluating the enhancement of soil properties with air injection.
- Effecting of air injection on the *WUE* and zucchini crop production in heavy clay soil.
- Assessing the Economic return of adding air injection in *SSDI* systems.

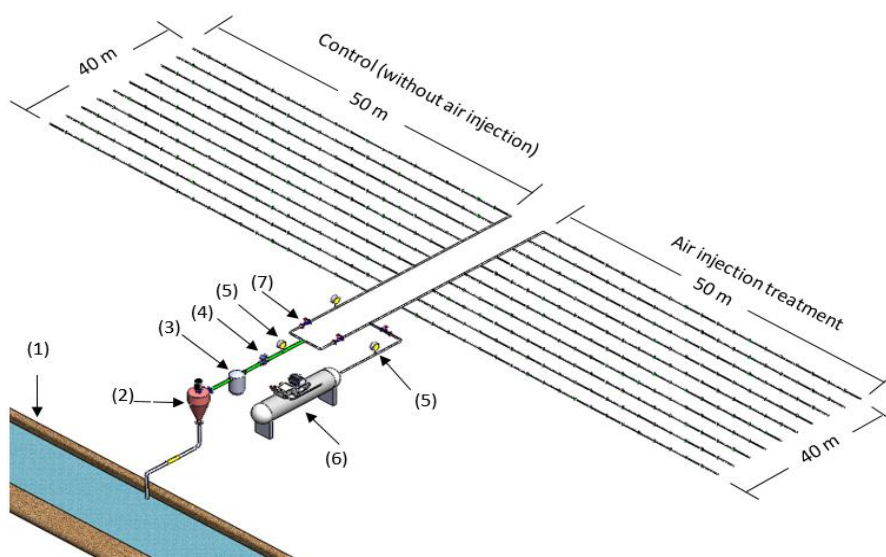
MATERIALS and METHODS

Field experiments were performed during two summer seasons of 2022 and 2023, laboratory experiments at the National Irrigation Laboratory of Agricultural Engineering Research Institute (AENRI), Dokki, Giza, Egypt, field experiment was at special farm in Menoufia Governorate. Zucchini plants (Anglia variety) were sown between August 10 and 15. The plants were spaced 1 m apart between rows and 0.5 m apart within rows. They were planted in heavy clay soil (59.2% clay, 6.4% silt,

and 34.4% sand) on a 4000 m² plot designated for crop cultivation. The planting was conducted manually to ensure proper placement and spacing of the seeds. Harvesting was performed manually between September 22 and October 15, at the optimal maturity stage, when the fruits reached the desired size and quality. The agricultural treatments for zucchini were based on the guidelines provided by [Abdel Aal et al. \(2019\)](#), which served as the reference for the crop management practices applied in the study. The subsurface drip line was installed at a 15 cm depth during the growing season. Fertilization and pest control operations were carried out on zucchini plants using the recommended doses of the Ministry of Agriculture and Land Reclamation. The daily irrigation requirements for the zucchini crop were determined based on data from the Central Laboratory for Agricultural Climate (C.L.A.C) under the Ministry of Agriculture and Land Reclamation for the study location, using the Penman-Monteith equation. The average estimated evapotranspiration (ET_o) was used to calculate the daily water consumption. A compressor was used to deliver air through water in the built-in emitters. The compressor injects ambient air at the last third of irrigation duration, and the aerated water is injected into the plant root zone through the built-in emitters.

Components of Subsurface Drip Irrigation System

The experimental field's subsurface drip irrigation system (Figure 1) consisted of a pumping and control unit, including a water source supply, pumping unit, pressure gauge, non-return valve, media filter, control valves, pressure regulators, and an air injector unit. Water flows from the pumping unit to the main line made of UPVC with a diameter of 63 mm, and from there to a PVC sub-main line with a diameter of 32 mm. Then the water flows into the Lateral lines. The Lateral lines were 16 mm diameter low-density polyethylene (LDPE), with a 4 lph (at 1 bar operating pressure) built-in emitters, the distance between emitters 50 cm (Figure 2).



(1) Water source (2) Pump (3) Media filter (4) Pressure regulator (5) Pressure gauge
(6) Air compressor (7) Valve

Figure 1. Experiment design of subsurface drip irrigation system for control and air injection.


Specification of emitter	
Average flow rates 8 lph /m at 1 bar	

Figure 2. Built-in emitter.

Hydraulic test bench

Figure (3) illustrates the components of the hydraulic test bench, used to assess the emitters hydraulic performance.

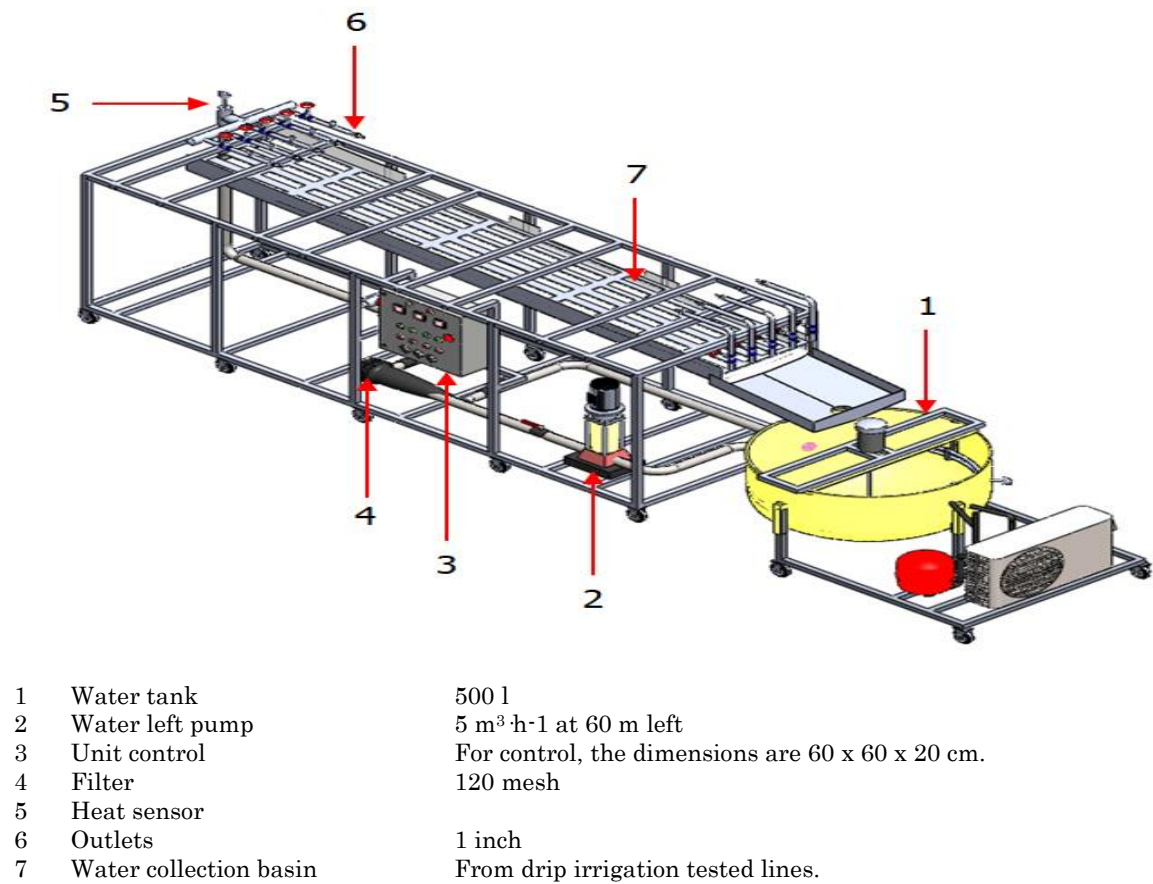


Figure 3. Trickle hydraulic test bench.

Experimental design and treatments

Evaluating the performance of built-in emitter

The flow rates of the emitters were measured across six operating pressures ranging from 0.6 to 2 bar. Flow rates were determined by weighing the water collected in a plastic cylinder over 6 minutes, timed using a stopwatch. All emitter flow rates versus pressure were evaluated via coefficient of variation (*CV*), discharge variation (*q_{var}*), and emission uniformity (*EU*) according to [ASAE \(1996\)](#) and [MSAE \(2005\)](#) Standards.

Determining the effect of air injection on emitter hydraulic performance

The experiment included evaluating and comparing the hydraulic performance between the control (without air injection) and the air injection treatment using the above criteria. The treatment included air injection in the last third of irrigation.

Field experiment

To study the effect of air injection in heavy clay soil on crop production, water use efficiency *WUE*, and economic evaluation many variables, including, crop yield, total seasonal irrigation water, total annual costs were recorded for with each treatment. *WUE*, financial analysis measures of benefit-cost ratio (*BCR*), and net return (*NR*) values were estimated. This data was then analyzed and compared to determine the economic return of air injection in subsurface drip irrigation.

Measurements and Calculation**Evaluation of the built-in emitters***Pressure-flow relationships*

The emitter flow rate is typically defined by the relationship among flow rate, pressure, and an emitter flow rate exponent. The flow rate equation, widely used by researchers ([Keller and Karmeli, 1974](#); [MSAE, 2005](#)), is derived from Equation (1):

$$q = kp^x \quad (1)$$

Where; q is emitter flow rate, lph; k is constant of proportionality that characterizes each emitter and compensates for units; p is the operating pressure, bar; and x is emitter flow rate exponent that characterizes the flow regime.

Equation (2) can be used to express the pressure influence on emitter flow rate variation (q_{var}) either directly as the average of the emitter flow rate or as a percentage of the flow rate change that takes place at the actual operating pressure and pressure of 1 bar with the same water temperature, divided by the flow rate at pressure of 1 bar.

$$q_{var} = \frac{q_{max} - q_{min}}{q_{max}} \times 100 \quad (2)$$

Where; q_{var} is the emitter flow variation, %; q_{max} is the maximum emitter flow, lph; and q_{min} is the minimum emitter flow, lph.

In general, the acceptable values of q_{var} were about from 10 to 20 %; and greater than 20% is not acceptable according to [ASAE \(1996\)](#).

Emitter manufacture's coefficient of variations (CV)

The manufacture's coefficient of variation (*CV*) indicates the unit-to-unit variation in flow rate for a given emitter. The emitter manufacture's coefficient, Equation 3, was calculated by measuring the flow rate from a sample of the new emitters as follows:

$$CV = s/q_a \quad (3)$$

Where; CV is manufacturer's coefficient of emitter variation; s is standard deviation of emitter flow rate rates at a reference pressure head, lph; and q_a is the average flow rate, lph.

Emission uniformity (EU)

Emission Uniformity (EU) is a measure of how evenly water is applied throughout a specified area. This measurement is essential for scheduling irrigations efficiently. EU is used to indicate performance for emitters. EU was calculated from Equation (4) according to [Keller and Karmeli \(1974\)](#).

$$EU = (q_n/q_a)100 \quad (4)$$

Where; EU is the emission uniformity, %; q_n is average of the lowest 1/4 of the emitter flow rate, lph; and q_a is average of all emitter flow rate, lph.

Calculation of irrigation time

The irrigation time was determined based on the evapotranspiration (ET) data from the AENRI Weather Station. The following equations were used to calculate the irrigation time:

$$ET_c = K_c \times ET_o \quad (5)$$

Where; ET_c represents the evapotranspiration for the crop, mm day⁻¹; K_c is the crop coefficient values; and ET_o is the evapotranspiration, mm day⁻¹. All the ET_o calculation and the K_c values and the length of the growth periods were taken from the FAO 56 ([Allen et al., 1998](#)).

$$App. Irri. Rate = \frac{Q}{S_m \times S_L} \quad (6)$$

Where; $App. Irri. Rate$ is the applied irrigation rate, mm h⁻¹; Q is the emitter flow rate, lph; S_m is the distance between emitters, m; and S_L is the distance between lateral, m.

$$Irri. Duration = \frac{ET_c}{App. Irri. Rate} \quad (7)$$

Where; $Irri. Duration$ is the duration irrigation rate, h day⁻¹.

The total yield per Fadden was calculated as follows:

$$Total\ yield\ per\ Feddan(kg/fed) = \frac{yield\ weight\ (kg) \times 4200}{sample\ area\ (m^2)} \quad (8)$$

Irrigation requirements were carefully calculated and applied to ensure efficient water usage, soil moisture within the active root zone was continuously monitored using a portable TDR device, ensuring optimal water management throughout the growing season.

Water Use Efficiency (*WUE*)

The *WUE* in this work was calculated for each treatment ([Tolossa, 2021](#)). This parameter can be used to compare between the studied treatment and control. The *WUE* for the tested treatments was calculated from Equation (8)

$$WUE = \frac{Y}{IRR} \quad (9)$$

Where; *WUE* is the water use efficiency, kg m⁻³; *Y* is the total yield, kg ha⁻¹; and *IRR* is total amount of irrigation applied, m³ ha⁻¹.

Soil physical and chemical properties evaluation

The physical and chemical properties of the soil were evaluated at the end of the experimental periods as follows:

Soil physical properties (Soil dry sieved aggregates)

Soil dry sieved aggregates were separated, using a sieve shaker with stacked and classify using equation (10) according to [Richards \(1954\)](#).

$$\text{Dry sieved aggregates (\%)} = \frac{\text{Weight of each aggregate size fraction (g)}}{\text{Weight of soil (g)}} \times 100 \quad (10)$$

Soil chemical properties

The available soil macro nutrients were measured; Nitrogen determined using Kjeldahl method described by [FAO \(1980\)](#), Phosphorus determined by a spectrophotometer according to [Watanabe and Olsen \(1965\)](#), and Potassium was using flame photometer, according to [Page et al. \(1982\)](#).

Economic return

Total annual costs

Total annual costs equal to renting farm for season, fertilizer, other chemicals, irrigation system cost installation divided into 5 years of use (construction elements of the subsurface drip irrigation system include outlets, regulators, laterals, manifolds, mainlines, fittings, and pumps), energy, workers salary through germination period and cultivation.

Net returns

Net returns are calculated by subtracting the estimated average annual costs (*C*) from the average annual gross returns (*B*). To achieve the economic objective of maximizing net return, the system with the highest net return (*B – C*) is considered the most effective based on the economic analysis.

Benefit-cost ratio (B/C ratio)

The Benefit/Cost ratio is calculated by dividing the annual benefits by the annual costs. When aiming to maximize return on investment, the system with the highest *B/C* ratio is considered the best choice according to economic analysis. It is common for one system to yield the highest net return while another achieves the highest *B/C* ratio ([Khalifa, 2020](#)).

$$\text{Gross return } (B)(\$) = \text{Crop yield}(\text{ton/ha}) \times \text{Area}(\text{ha}) \times \text{Price}(\$ / \text{ton}) \quad (11)$$

$$\text{Net return } (B - C)(\$) = \text{Gross return} - \text{Total annual costs} \quad (12)$$

$$B/C \text{ Ratio } (\%) = \text{Gross return} / \text{Total annual costs} \quad (13)$$

RESULTS AND DISCUSSION

Performance and Evaluation of the Built-In Emitters

It is necessary to evaluate the hydraulic performance of subsurface drip irrigation system. Thus, a test was run to evaluate the hydraulics of pressure-compensating emitter 4 lph flow rate with pressure rating of 0.6 to 2.0 bar. Figure (4) shows the average values of emitter flow rate for each pressure. The results clearly indicated that as the operating pressure increased, discharge of emitters is fixed. It's also clear that the flow rate coefficient (k) and emitter flow rate exponent (x) were 3.97, and 0.07 respectively.

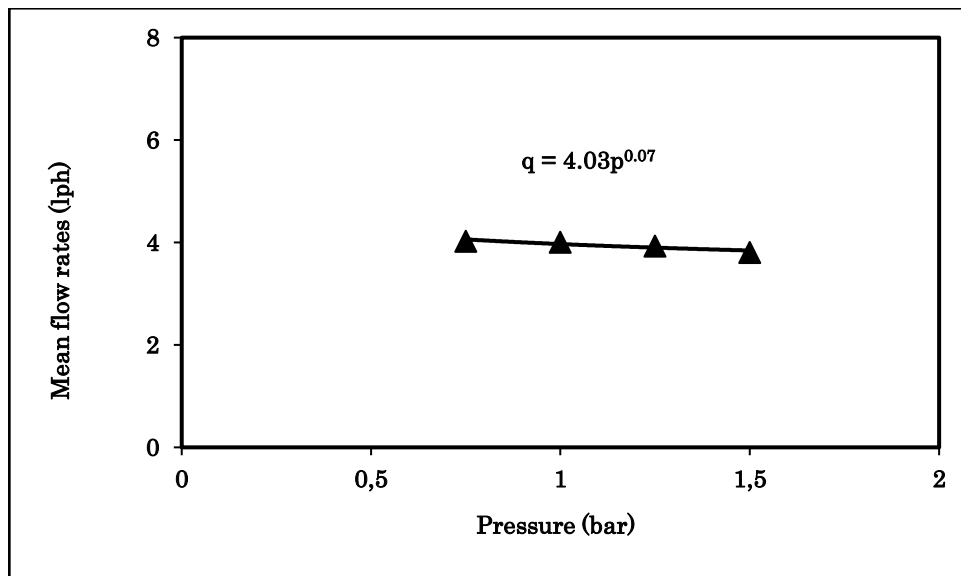


Figure 4. Performance curves of the experimental emitter sample (built-in 4 lph-50 cm).

Evaluation of the impact air injection in the last third of the Irrigation through subsurface drip irrigation system on the hydraulic performance and system distribution uniformity and comparison with control.

Figure (4) and Table (1) show that there is a close relationship between emitter flow rates and pressure. By comparing the evaluation results with the results of the control, the results showed that there is no significant difference between the injection treatment in the last third of the irrigation time and the control, because the points maintain all their acceptable hydraulic properties without being negatively affected by the air injection. The values of all parameters injecting air in the last third of irrigation duration $q = 3.91$ lph, $CV = 2.26\%$ were excellent according to ASAE standard, $EU = 97.44\%$ were excellent according to ASAE standard. $q_{var} = 10.71\%$ was acceptable according to ASAE standard. This result agrees with of

[Hussein \(2015\)](#). Thus, adding air during the subsurface drip irrigation system has a positive effect in maximizing the benefit from the subsurface drip irrigation system, especially for crops that depend for their growth on aerobic bacteria, as well as in flooded lands that need to change and improve the structure and increase the amount of oxygen in them, thus improving the management of the system.

Table 1. The impact of air injection by air compressor through subsurface drip irrigation system on the hydraulic performance and uniformity distribution.

Treatments	Water flow rate, lph	CV, %, at 1 bar		EU, %		q_{var} , %	
	Mean	Value	ASAE standard	Value	ASAE standard	Value	classification
Control	4.03	2.26	Excellent	97.18	Excellent	11.15	Acceptable
Air injection	3.91	2.26	Excellent	97.44	Excellent	10.71	Acceptable

CV= Manufacture's coefficient of variation, EU= Emission uniformity, q_{var} = Emitter flow variation

The effect of air injection on the water use efficiency and plant performance in a heavy clay soil

The average results of two seasons of zucchini crop that were grown using air injection in subsurface drip irrigation showed a significant increase in yield compared to the control found that air injection in the last third of the irrigation increased the zucchini yield by 27% compared with control. Total yield (ton ha⁻¹) was 19.05 with air injection and 15 ton ha⁻¹ with control. The applied water (m³ ha⁻¹) with air injection was 1152.4 in comparison Control which was 1476.2 m³ ha⁻¹. This means that there was water saving in case of using this method of 22%. The water use efficiency (Table 2) under air injection resulted in 16.53 kg m⁻³, but with Control, it was 10.16 kg m⁻³. This result agrees with [Goorahoo et al. \(2001\)](#); [Bhattarai et al. \(2008\)](#); [Shahien et al. \(2014\)](#); [Refaie et al. \(2019\)](#).

Table 2. Average water use efficiency and Zucchini yield under air injection and control treatments.

Treatments	IRR, m ³ ha ⁻¹	Y, ton ha ⁻¹	WUE, kg m ⁻³	Increasing in WUE, %
Control	1476.2	15.00	10.16	38.54
Air injection	1152.4	19.05	16.53	

Y= Zucchini yield, IRR= total amount of irrigation applied, WUE = water use efficiency.

Effect of air injection on physical and chemical properties of heavy clay soil:

Soil physical properties (Soil dry sieved aggregates)

The results of the soil dry sieved aggregates at the end of the experimental practices with and without air injection show a change in the aggregates distribution by air injection indicate to an improvement of heavy clay soil physical properties by changing the arrangement of soil aggregates which improves soil structure. While Table (3) shows, there was a decrease in the large macro-aggregates that have diameters from 2 to 10 mm which distributed to a small macro-aggregate (2 to1, 1 to 0.5 and 0.5 to 0.25 mm) resulted in relative increase of these aggregates diameters,

also micro-aggregates that less than 0.25 mm were decreased comparing to the absence of air injection. That can contribute in alleviating compaction impacts create pathways for air, water, nutrients and allow roots elongation to reach its need while, air, water, earthworms, microbes, roots and seeding have trouble moving through heavy clay soil, so crop yields suffer.

Table 3. Air injection techniques effect on distribution fraction (%) of soil dry sieved aggregates.

Treatments	Dry aggregates diameter, mm						
	10-2	2-1	1-0.5	0.5-0.25	0.25-0.125	0.125-0.063	<0.063
Control	43.16	18.56	19.34	11.72	4.47	2.55	016
Air injection	58.41	11.94	12.16	8.85	5.85	2.62	0.17

Soil chemical properties

Figure (5) shows an increase in available macronutrients N, P and K with air injection. The amount of available nitrogen increased from 94.1 ppm for the control treatment to 116.4 for the air injection treatment, K values increased from 60.8 ppm for the control treatment to 80.2 ppm for the air injection treatment, and P values increased from 4.1 ppm for the control treatment to 6.2 ppm for the air injection while that avoid the loss of N converted to gases by the denitrification and also oxygen has a dramatic impact on microbial activity and rate of decomposition of nutrients, releasing K on exchange sites of the clay and P from its unavailable compounds while, many nutrients can be in soluble form and easy to plant uptake by roots of crops in case of air condition ([Refaie et al., 2019](#)).

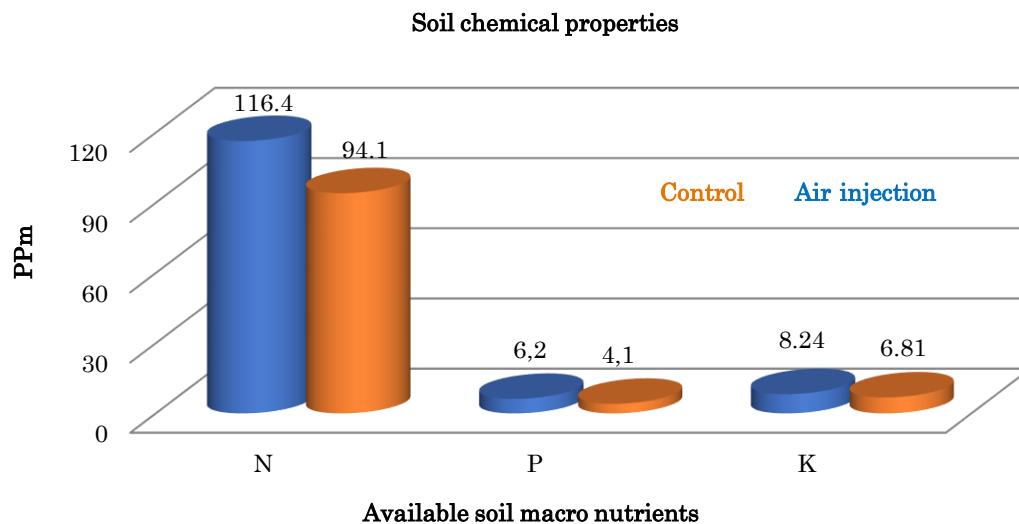


Figure 5. Air injection techniques performance on available soil macronutrients.

Economic return of air injection through subsurface drip irrigation system

The following parameters were taken as an economical evaluation in case injecting air through drip irrigation system the following items were the major item in economic analysis:

1. Gross return LE and \$,
2. Net return LE and \$ and,
3. Benefit-cost ratio (B/C ratio).

Table (4) shows the gross return, net return, and benefit-cost ratio (B/C ratio). It's clear that the gross return of air injecting treatment was 72000 LE (4161.9 \$) compared with the control treatment (without air injecting) which was 56700 LE (3277.5 \$). The gross return of air injection increased by 21% compared with control treatment (without air injecting). While the net return of air injecting was 40695 LE (2352.3 \$) compared with the control treatment (without air injecting) which was 25395 LE (1467.9 \$). Furthermore, the benefit-cost ratio of air injection stood at 2.3%, surpassing the 1.8% of the control treatment. Economic analysis, which included criteria such as the benefit-cost ratio (B/C) and net return values ($B-C$), indicated that air injection represented a viable economic option.

Table 4. *Economic return of air injection and control treatments through subsurface drip irrigation system.*

Treatments	Gross return, LE (\$)	Net return, LE (\$)	B/C ratio, %
Control	56700 (3277.4 \$)	25395 (1467.9 \$)	1.8
Air injection	72000 (4161.9 \$)	40695 (2352.3 \$)	2.3

B/C = benefit-cost ratio

The findings of this study revealed that introducing air into the drip line did not impact the hydraulic performance of the emitters. The T-test analysis indicated no significant differences between the air injection treatment and the control group. This lack of distinction could be attributed to the similar behaviour of the air injected into the lines compared to water flowing in the lines, particularly considering the pressure-compensating type of the emitter used. While the results showed a slight reduction in emitter flow rate with air injection treatments, this was likely due to a less dense water-air mixture in these instances rather than a change in emitter performance. The reduced density of the water-air mixture led to less water accumulation from the same volume passing through the emitter compared to the control treatment, resulting in a lower emitter flow rate. The method of determining emitter flow rate by collecting and weighing the flow mass over time is what caused the observed differences in flow rate between treatments. This is consistent with the findings of [Li et al. \(2023\)](#). The results of the crop yield and the total seasonal irrigation water (SIW) shows a decrease in the SIW while increasing the yield for the air injected treatment when compared to the control treatment. The decrease of the SIW is due to the slight decrease in the emitter flow rate and the increase in yield may be due to the fact that the heavy clay soils induces hypoxia in the rhizosphere through air purge, which limits root respiration and growth as well as microbial

respiration ([Chen et al., 2010](#)), particularly in heavy clay soils ([Midmore et al., 2007](#)). Airiation was proposed as a promising method that can alleviate hypoxia effects on a variety of crops to improve their performance ([Bhattarai et al., 2006](#); [Bhattarai et al., 2008](#)). Airiation can improve and maintain heavy clay soil to enjoy benefits clay offers for healthy plants while air can effect positively on soil reactions and in turn many soil properties as enhancing biodegradation of organic practices within the aggregates which the vital cementing agent for micro- aggregates to become macro-aggregates contribute to improving soil structure and lead to better water infiltration, better aeration and better nutrition ([Zhang et al., 2022](#)). Airiation improved soil oxygen content and soil respiration in root zone, which was beneficial for plant growth and yield in wheat, rice, and pineapple ([Chen et al., 2010](#)). Plant growth and development necessitate the presence of oxygen in the rhizosphere; it is involved in several processes, including carbohydrate metabolism and nutrient uptake by roots ([Makita et al., 2015](#)). Because of the treatment's increased yield and decreased water supply, the *WUE* of the air injection treatment was significantly higher than that of the control treatment. The results are in accordance with [Abuarab et al. \(2013\)](#) how reported moer leaf area faster grain filling and less maturation time for corn plant when using ariation in subsurface drip irrigation lines. [Zhang et al. \(2023\)](#) also reported a higher *WUE* for tomato plants under oxygenated drip irrigation in heavy clay soils. The availability of soil nutrients increased with the air injection treatment. Soil airiation impacted microbial activity and nutrient decomposition rate, releasing from its unavailable compounds on exchange sites of the clay. This agrees with [Refaie et al. \(2019\)](#) who concluded that many nutrients can be in soluble form and easy to plant uptake by roots in case of airiation condition. The economic analysis shows that even though the cost of aeration was higher because of the need to an air compressor and the extra cost of energy required for its' operation the extra revenue added by the increase in the crop productivity covered the extra costs and allowed for more profit as shown from the increase of the net return and the higher benefit-cost ratio of the air injection treatment.

CONCLUSION

Integrating air injection into subsurface drip irrigation (*SSDI*) systems has proven to be a cost-effective method for enhancing vegetable production, particularly in heavy clay soils. This approach offers several advantages, including improved water use efficiency, increased crop yields, and enhanced soil properties compared to conventional irrigation methods. By introducing atmospheric air into the soil through *SSDI* systems, issues such as waterlogging in the root zone are mitigated, resulting in better root respiration, improved nutrient uptake, and overall enhanced plant growth. The benefits of air injection were especially evident in zucchini cultivation, where significant increases in yield and water conservation were achieved. Furthermore, from an economic standpoint, the use of air injection systems contributed to higher gross and net returns for farmers, along with a favorable benefit-cost ratio. These results highlight the effectiveness and sustainability of air injection in modern agricultural practices.

DECLARATION OF COMPETING INTEREST

The authors declare that they have no conflict of interest.

CREDIT AUTHORSHIP CONTRIBUTION STATEMENT

The authors declare that the following contributions are correct.

Nermin Hussein: Contributed equally to various roles including setting research goals, development of methodology, performing the experiments, analyzing data, and writing the artical.

Shereen Saad: Contributed equally in various roles including setting research goals, development of methodology, performing the experiments, analyzing data, and writing the artical.

Khaled Refaie: Contributed equally in various roles including setting research goals, development of methodology, performing the experiments, analyzing data, and writing the artical.

Wael Sultan: Contributed equally in various roles including setting research goals, development of methodology, performing the experiments, analyzing data, and writing the artical.

Mohamed Ghonimy: Contributed equally in various roles including setting research goals, development of methodology, performing the experiments, analyzing data, and writing the artical and also coordinated the activities with the co-author.

Ahmed Alzoheiry: Contributed equally in various roles including setting research goals, development of methodology, performing the experiments, analyzing data, and writing the artical.

ETHICS COMMITTEE DECISION

This article does not require any Ethical Committee Decision.

REFERENCES

- Abdel Aal HM, Farag RM and Kamel SMH (2019). Zucchini cultivation and production. *Central Administration for Agricultural Extension, Agricultural Research Center (ARC), Ministry of Agriculture and Land Reclamation*, Egypt. Arabic reference.
- Abuarab M, Mostafa E, Ibrahim M (2013). Effect of air injection under subsurface drip irrigation on yield and water use efficiency of corn in a sandy clay loam soil. *Journal of Advanced Research*, 4(6): 493-499. <https://doi.org/10.1016/j.jare.2012.08.009>
- Allen RG, Pereira LS, Raes D and Smith M (1998). Crop evapotranspiration-Guidelines for computing crop water requirements-FAO Irrigation and drainage paper 56. *FAO, Rome*, 300(9), D05109.
- ASAE (1996). Design and installation of micro irrigation systems. *EP405*.
- Bhattarai SP, Huber S and Midmore DJ (2004). Aerated subsurface irrigation water gives growth and yield benefits to zucchini, vegetable soybean, and cotton in heavy clay soils. *Association of Applied Biologists*, 144: 285-298. <https://doi.org/10.1111/j.1744-7348.2004.tb00344.x>
- Bhattarai SP, Pendergast L and Midmore DJ (2006). Root aeration improves yield and water use efficiency of tomato in heavy clay and saline soils. *Scientia Horticulturae*, 108: 278-288. <https://doi.org/10.1016/j.scienta.2006.02.011>

- Bhattarai SP, Midmore DJ and Pendergast L (2008). Yield, water-use efficiencies, and root distribution of soybean, chickpea, and pumpkin under different subsurface drip irrigation depths and oxygation treatments in vertisols. *Irrigation Science*, 26(5): 439. <https://doi.org/10.1007/s00271-008-0112-5>
- Chen X, Dhungel J, Bhattarai SP, Torabi M, Pendergast L and Midmore DJ (2010). Impact of oxygation on soil respiration, yield and water use efficiency of three crop species. *Journal of Plant Ecology*, 4(4): 236-248. [https://doi.org/10.1016/S2095-3119\(19\)62618-3](https://doi.org/10.1016/S2095-3119(19)62618-3)
- D'Alessio M, Durso LM, Williams C, Olson CA, Ray C and Paparozzi ET (2020). Applied injected air into subsurface drip irrigation: Plant uptake of pharmaceuticals and soil microbial communities. *Journal of Environmental Engineering*, 146(2): 06019008. [https://doi.org/10.1061/\(ASCE\)EE.1943-7870.0001655](https://doi.org/10.1061/(ASCE)EE.1943-7870.0001655)
- Dhungel J, Bhattarai SP and Midmore DJ (2012). Aerated water irrigation (oxygation) benefits to pineapple yield, water use efficiency, and crop health. *Advanced Horticulture*, 23(1): 3-16. <https://doi.org/10.13128/ahs-12746>
- Dissanayake D (2020). *Beneficial effect of injected air into Subsurface Drip Irrigation (SDI) on plant growth using runoff from a feedlot*. M.Sc. Thesis in Natural Resource Sciences, University of Nebraska, USA.
- Essah SY and Holm DG (2020). Air injection of subsurface drip irrigation water improves tuber yield and quality of russet potato. *American Journal of Potato Research*, 97: 432-438. <https://doi.org/10.1007/s12230-020-09792-2>
- FAO (1980). Soil and Plant Analysis. Soils Bulletin, 38, 242-250.
- Goorahoo D, Carstensen G and Mazzei A (2001). A pilot study on the impact of air injected into water delivered through subsurface drip irrigation tape on the growth and yield of bell peppers. *California Agricultural Technology Institute (CATI) Publication*, 10201.
- Goorahoo D, Adhikari D, Zoldoske D, Mazzei A, Fanucchi R (2007). *Application of airjection irrigation to cropping systems in California*. In International Water Technology and Ozone V Conference, Fresno.
- Goorahoo D, Adhikari D, Reddy N, Cassel F, Zoldoske D, Mazzei A and Fannuchi R (2008). Optimizing crop water use efficiency with AirJection® irrigation. *Fresno, CA: California State University*.
- Hussein NS (2015). *Effect of air addition through subsurface trickle irrigation for improving plant-use efficiency in heavy soils*, Ph.D. Thesis, Faculty of Agricultural, Ain Shams University.
- Keller J and Karmeli D (1974). Trickle irrigation design parameters. *Transaction of ASAE*, 17(4): 678-684.
- Khalifa WM (2020). An Economic analysis of crops production using a trickle irrigation system. *International Transaction Journal of Engineering, Management, & Applied Sciences & Technologies*, 11(8): 1-13. <https://doi.org/10.14456/ITJEMAST.2020.151>
- Li H, Ma Z, Zhang G, Chen J, Lu Y and Li P (2023). Performance of a Drip Irrigation System under the Co-Application of Water, Fertilizer, and Air. *Horticulturae*, 10(1): 6. <https://doi.org/10.3390/horticulturae10010006>
- Makita N, Hirano Y, Sugimoto T, Tanikawa T and Ishii H (2015). Intraspecific variation in fine root respiration and morphology in response to in situ soil nitrogen fertility in a 100-year-old *Chamaecyparis obtusa* forest. *Oecologia*, 179: 959-967. <https://doi.org/10.1007/s00442-015-3413-4>
- Midmore D, Bhattarai S, Pendergast L and Torabi M (2007). *Oxygation: aeration of subsurface drip irrigation water and its advantages for crop production*. In: Proceedings of the ANCID Conference 2007.
- MSAE (2005). Drip-line testing standard; *ir/dr/p/dr/p-in05*, *Misr Society of Agricultural Engineering*, 7 p.
- Page AL, Miller RH and Keeny DR (1982). Methods of soil analysis Part² Chemical and Biological Properties. *Amer. Soc. Agron. Inc. Masecon*, Wisconsin USA.
- Pendergast L, Bhattarai SP and Midmore DJ (2014). Benefits of oxygation of subsurface drip-irrigation water for cotton in a Vertosol. *Crop and Pasture Science*, 64(12): 1171-1181. <https://doi.org/10.1071/CP13348>
- Refaie KM, Sultan WMM and Saad SAH (2019). Feasibility of air injection into subsurface drip irrigation system. *Current Science International*, 8(3): 549-564.
- Richards AL (1954). Diagnosis and improvement of saline and alkali soils. U.S. Dept. Agric. HandBook. No 60, *U.S. Govt. Print Office*, Washington. D.C.

- Seleim MA, Hassan MA and Saleh ASM (2015). Changes in nutritional quality of zucchini (*Cucurbita pepo* L.) vegetables during the maturity. *Journal of Food and Dairy Sciences*, 6(10): 613-624. <https://www.doi.org/10.21608/JFDS.2015.50079>
- Shahien MM, Abuarab ME and Magdy E (2014). Root aeration improves yield and water use efficiency of irrigated potato in sandy clay loam soil. *International Journal of Advanced Research*, 2(10): 310-320.
- Tolossa TT (2021). Onion yield response to irrigation level during low and high sensitive growth stages and bulb quality under semi-arid climate conditions of Western Ethiopia. *Cogent Food & Agriculture*, 7(1): 1859665. <https://doi.org/10.1080/23311932.2020.1859665>
- Vyrlas P, Sakellariou-Makrantonaki M and Kalfountzos D (2014). Aerogation: Crop root-zone aeration through a subsurface drip irrigation system. *WSEAS Transactions on Environment and Development*, 10: 446-451.
- Watanabe FS and Olsen SR (1965). Test of an ascorbic acid method for determining phosphorus in water and NaHCO₃ extracts from soil. *Soil Science Society America Proceedings*, 29: 677-678. <https://doi.org/10.2136/sssaj1965.03615995002900060025x>
- Zhang Y, Li P, Liu X and Xiao L (2022). Fractions, stability and associated organic carbon and nitrogen in different land use types in the loess plateau, China. *Sustainability Journal*, 14(7): 3963. <https://doi.org/10.3390/su14073963>
- Zhang Z, Yang R, Zhang Z, Geng Y, Zhu J and Sun J (2023). Effects of oxygenated irrigation on root morphology, fruit yield, and water–nitrogen use efficiency of tomato (*Solanum lycopersicum* L.). *Journal of Soil Science and Plant Nutrition*, 23(4): 5582-5593. <https://doi.org/10.1007/s42729-023-01423-z>

TURKISH JOURNAL OF AGRICULTURAL ENGINEERING RESEARCH



TURKAGER

2024

e-ISSN:2717 - 8420

<https://dergipark.org.tr/tr/pub/turkager>

